Julius-Maximilians-Universität Würzburg

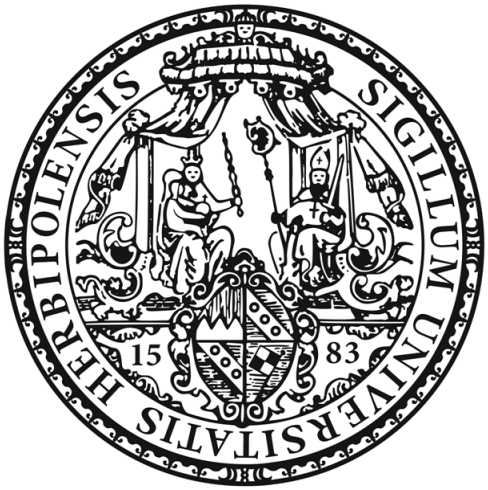

Studies on receptor signaling and regulation in platelets and T cells from genetically modified mice

Studien zur Signaltransduktion und Regulierung von Rezeptoren in Thrombozyten und T-Zellen genetisch veränderter Mäuse

Doctoral thesis for a doctoral degree
at the Graduate School of Life Sciences,
Section Biomedicine

submitted by

Timo Vögtle
from
Pforzheim

Würzburg, 2014

Submitted on: ……

Members of the *Promotionskomitee*:

Chairperson: Prof. Dr. Manfred Gessler

Primary Supervisor: Prof. Dr. Bernhard Nieswandt

Supervisor (Second): Prof. Dr. Stephan Kissler

Supervisor (Third): Prof. Dr. Thomas Dandekar

Date of Public Defence: ……

Date of Receipt of Certificates: ……...

Summary

Receptors with tyrosine-based signaling motifs control essential functions of hematopoietic cells, including lymphocytes and platelets. Downstream of the platelet receptor *glycoprotein* (GP) VI and the *T cell receptor* (TCR) the *immunoreceptor tyrosine-based activation motif* (ITAM) initiates a signaling cascade that involves kinases, adapter and effector proteins and finally leads to cellular activation. This thesis summarizes the results of three studies investigating different aspects of receptor signaling and regulation in platelets and T cells.

In the first part, the impact of constitutive Ca^{2+} influx on TCR signaling and T cell physiology was investigated using a transgenic mouse line with a mutation in the Ca^{2+} sensor *stromal interaction molecule 1* (STIM1). The elevated cytoplasmic Ca^{2+} level resulted in an altered phosphorylation pattern of the key enzyme *phospholipase* (PL) Cγ1 in response to TCR stimulation, but without affecting its enzymatic activity. Withdrawal of extracellular Ca^{2+} or inhibition of the phosphatase calcineurin restored the normal phosphorylation pattern. In addition, there was a decrease in the release of Th2-type cytokines interleukin 4, 5 and 13 upon stimulation *in vitro*.

The second part of the thesis deals with the role of the adapter protein *growth factor receptor-bound protein 2* (Grb2) in platelets using a megakaryocyte/platelet-specific knockout mouse line. Loss of Grb2 severely impaired signaling of GPVI and *C-type lectin-like receptor 2* (CLEC-2), a related hemITAM receptor. This was attributed to defective stabilization of the *linker for activation of T cells* (LAT) signalosome and resulted in reduced adhesion, aggregation, Ca^{2+} mobilization and procoagulant activity downstream of (hem)ITAM-coupled receptors *in vitro*. In contrast, the signaling pathways of *G protein-coupled receptors* (GPCRs) and the integrin αIIbβ3, which do not utilize the LAT signalosome, were unaffected. *In vivo*, the defective (hem)ITAM signaling caused prolonged bleeding times, however, thrombus formation was only affected under conditions where GPCR signaling was impaired (upon acetylsalicylic acid treatment). These results establish Grb2 as an important adapter protein in the propagation of GPVI- and CLEC-2-induced signals.

Finally, the proteolytic regulation of the *immunoreceptor tyrosine-based switch motif* (ITSM)-bearing receptor CD84 in platelets was investigated. This study demonstrated that in mice CD84 is cleaved by two distinct and independent proteolytic mechanisms upon platelet activation: shedding of the extracellular part, which is exclusively mediated by *a disintegrin and metalloproteinase* (ADAM) 10 and cleavage of the intracellular C-terminus by the protease calpain. Finally, the analysis of soluble CD84 levels in the plasma of transgenic mice revealed that shedding of CD84 by ADAM10 occurs constitutively *in vivo*.

Zusammenfassung

Rezeptoren mit Tyrosin-basierten Signaltransduktionsmotiven sind von fundamentaler Bedeutung für die Funktion hematopoietischer Zellen wie Lymphozyten und Thrombozyten. Unterhalb des *Glykoproteins* (GP) VI auf Thrombozyten und des *T-Zell Rezeptors* (TZR) auf T-Zellen initiiert das *immunoreceptor tyrosine-based activation motif* (ITAM) eine Signalkaskade, die Kinasen, Adapter- und Effektorproteine mit einbezieht und schlussendlich zur Aktivierung der Zelle führt. Die hier vorgelegte Arbeit fasst die Ergebnisse dreier Studien zusammen, die sich mit verschiedenen Aspekten der Signaltransduktion und Regulation von Rezeptoren in Thrombozyten und T-Zellen befasst.

Im ersten Teil wurde der Einfluss eines konstitutiven Ca^{2+}-Einstroms auf die TZR Signalkaskade und T-Zell Funktion untersucht. Hierzu wurde eine transgene Mauslinie mit einer Mutation im Ca^{2+}-Sensor *stromal interaction molecule 1* (STIM1) verwendet. Die erhöhte zytoplasmatische Ca^{2+}-Konzentration veränderte das Phosphorylierungsmuster der *Phospholipase* (PL) Cγ1, ein Schlüsselenzym der Signalkaskade, nach Stimulation des TZRs. Die enzymatische Aktivität der PLCγ1 blieb hierbei jedoch unverändert. In der Abwesenheit von extrazellulärem Ca^{2+} oder bei Inhibition der Phosphatase Calcineurin war das Phosphorylierungsmuster hingegen wieder normal. Darüber hinaus zeigten die T-Zellen nach Stimulation *in vitro* eine verringerte Produktion von Interleukinen des Th2-Typs (Interleukin-4, 5 und 13).

Der zweite Teil der Arbeit befasst sich mit der Funktion des Adapterproteins *growth factor receptor-bound protein 2* (Grb2) in Thrombozyten, die unter Zuhilfenahme einer Megakaryozyten- und Thrombozyten-spezifischen *Knockout* Mauslinie untersucht wurde. Hierbei zeigte es sich, dass der Verlust von Grb2 die Signaltransduktion von GPVI und des verwandten hemITAM-Rezeptors *C-type lectin-like receptor 2* (CLEC-2) schwer beeinträchtigt. Dies konnte auf eine mangelnde Stabilisierung des *linker for activation of T cells* (LAT) Signalosoms zurückgeführt werden und resultierte in einer verminderten Adhäsion, Aggregation, Ca^{2+}-Mobilisierung und prokoagulatorischen Aktivität nach Aktivierung (hem)ITAM gekoppelter Rezeptoren *in vitro*. Im Gegensatz hierzu blieben die Signaltransduktionswege *G-protein-gekoppelter Rezeptoren* (GPCRs) und des Integrins αIIbβ3, die das LAT Signalosom nicht nutzen, unbeeinflusst. In *in vivo* Studien verursachte die beeinträchtigte (hem)ITAM Signaltransduktion eine verlängerte Blutungszeit der Mäuse, während die Entstehung von Thromben nur bei gleichzeitiger Hemmung von GPCR-Signalwegen (durch Acetylsalicylsäuregabe) vermindert war. Diese Ergebnisse etablieren Grb2 als ein wichtiges Adapterprotein in der Signaltransduktionskaskade von GPVI und CLEC-2.

Schließlich wurde im dritten Teil dieser Arbeit die proteolytische Regulation des Rezeptors CD84, der ein *immunoreceptor tyrosine-based switch motif* (ITSM) enthält, untersucht. In dieser Studie konnte gezeigt werden, dass CD84 in Mausthrombozyten durch zwei verschiedene und unabhängige proteolytische Mechanismen geschnitten wird: Zum einen durch *Shedding* des extrazellulären Teils, was ausschließlich durch die *a disintegrin and metalloproteinase* (ADAM) 10 bewerkstelligt wird, und zum anderen durch das Schneiden des intrazellulären C-Terminus durch die Protease Calpain. Des Weiteren zeigte eine Untersuchung von Plasmaproben transgener Mäuse, dass das *Shedding* von CD84 durch ADAM10 konstitutiv *in vivo* erfolgt.

Table of contents

1 Introduction 1
1.1 Platelets 1
1.1.1 Platelets and thrombus formation 1
1.2 Signaling events during thrombus formation 3
1.3 (hem)ITAM receptor signaling in platelets 4
1.3.1 GPVI 4
1.3.2 CLEC-2 6
1.3.3 Attenuation of ITAM signaling by ITIM receptors 8
1.4 T cells 8
1.5 T cell receptor signaling of $CD4^+$ T cells 10
1.6 Adapter proteins in platelet and T cell receptor signaling 13
1.6.1 LAT, SLP-76 and Gads 13
1.6.2 Grb2 14
1.7 Store-operated Ca^{2+} entry (SOCE) 16
1.7.1 The history of SOCE 16
1.7.2 The mediators of SOCE – STIM and Orai 17
1.7.3 Physiological consequences of mutations in STIM1 and Orai1 19
1.8 CD84: an ITSM-bearing receptor of the hematopoietic system 21
1.9 Receptor proteolysis 22
1.10 Aims of this thesis 24
2 Materials and Methods 25
2.1 Materials 25
2.1.1 Chemicals and reagents 25
2.1.2 Cell culture materials 27
2.1.3 Kits 27
2.1.4 Antibodies 28
2.1.5 Mice 32

2.1.6 Buffers and media 32
2.2 Methods 37
2.2.1 Mouse genotyping 37
2.2.2 Biochemistry 39
2.2.3 Generation of plasma and serum samples 40
2.2.4 *In vitro* analyses of platelet function 41
2.2.5 *In vivo* analyses of platelet function 46
2.2.6 Isolation and analyses of immune cells 48
2.2.7 Statistical analysis 51
3 Results 53
3.1 Investigation of T cell receptor signaling in *Stim1*$^{Sax/+}$ mice 53
3.1.1 Normal T cell development in *Stim1*$^{Sax/+}$ mice 53
3.1.2 NFAT resides in the nucleus of *Stim1*$^{Sax/+}$ CD4^{+} T cells in the absence of stimulation 53
3.1.3 Altered phosphorylation of PLCγ1 in *Stim1*$^{Sax/+}$ CD4^{+} T cells due to calcineurin activity 56
3.1.4 Despite alterations in the phosphorylation pattern, the enzymatic activity of PLCγ1 in *Stim1*$^{Sax/+}$ CD4^{+} T cells is unaltered 58
3.1.5 Impaired Th2-type cytokine production of *Stim1*$^{Sax/+}$ T cells 60
3.1.6 High prevalence of regulatory T cells in the spleen of *Stim1*$^{Sax/+}$ mice 61
3.2 Analysis of Grb2-deficiency in platelets 63
3.2.1 Grb2 is dispensable for platelet generation 63
3.2.2 Diminished responses to GPVI and CLEC-2 stimulation, but unaltered integrin outside-in signaling in *Grb2*$^{-/-}$ platelets 64
3.2.3 Defective Ca^{2+} mobilization in *Grb2*$^{-/-}$ platelets in response to the GPVI agonist CRP 68
3.2.4 *Grb2*$^{-/-}$ platelets exhibit impaired procoagulant activity and defective aggregate formation on collagen under flow 70
3.2.5 Impaired hemostasis and partially defective arterial thrombus formation in *Grb2*$^{-/-}$ mice 71

3.2.6 Grb2 stabilizes the LAT signalosome 78
3.3 Studies on the proteolytic regulation of CD84 receptor levels in platelets 83
3.3.1 CD84 is cleaved from the surface of human and mouse platelets 83
3.3.2 Dual regulation of CD84 by calpain and metalloproteinases 86
3.3.3 ADAM10 is critical for CD84 ectodomain cleavage in murine platelets 90
3.3.4 High concentrations of sCD84 in mouse plasma 93
4 Discussion 94
4.1 Constitutive Ca^{2+} influx alters phosphorylation, but not activation of PLCγ1 94
4.2 Grb2 stabilizes the LAT signalosome 97
4.3 Dual regulation of platelet CD84 by ADAM10 and calpain 103
4.4 Concluding remarks 108
4.5 Perspective 109
5 References 110
6 Appendix 129
6.1 Abbreviations 129
6.2 Acknowledgements 132
6.3 Curriculum vitae 134
6.4 Publications 135
6.4.1 Original articles 135
6.4.2 Reviews 136
6.4.3 Talks 136
6.4.4 Poster 136
6.5 Affidavit 137
6.6 Eidesstattliche Erklärung 137

1 Introduction

1.1 Platelets

Platelets are small anucleated blood cells which originate from the cytoplasm of *megakaryocytes* (MKs) in the bone marrow. The platelet count in the blood of healthy humans ranges from 150,000 – 450,000 platelets/µl and averages at about 250,000 platelets/µl. Mice, which represent an important model system in thrombosis research, exhibit a platelet count of approximately 1,000,000 platelets/µl. The lifespan of platelets is about 10 days in humans and about 5 days in mice.

Since platelets lack a nucleus, their protein *de novo* synthesis is limited. However, several other cell organelles and structures are present in platelets like mitochondria, the open canalicular and dense tubular system, glycogen stores and three major types of granules (α-granules, dense granules and lysosomes) which have different contents.

Platelets play an essential role in hemostasis, as they survey the vascular integrity while circulating through the blood stream. In an intact vasculature, most platelets never undergo firm adhesion to the vessel wall and are cleared by the reticuloendothelial system in the spleen and liver at the end of their life time. Upon disruption of the endothelial cell layer, however, platelets rapidly adhere to the exposed components of the subendothelial *extracellular matrix* (ECM). This leads to subsequent platelet activation and initiates a self-amplifying loop that results in the recruitment of additional platelets that interact with each other to form a plug that seals the wound. This process, called primary hemostasis, is a prerequisite to limit blood loss after injury. On the other hand, under pathological conditions, such as rupture of an atherosclerotic plaque, thrombus formation may result in irreversible occlusion of the vessel. In the worst case, the obstruction of blood flow with the accompanying loss of oxygen supply results in irreversible damage of vital organs.[1,2] Myocardial infarction, triggered by occlusion of coronary arteries, and stroke, elicited by thrombus embolization to the brain, are two of the leading causes of disability and mortality worldwide.[3] Therefore, a detailed understanding of platelet physiology and the mechanisms underlying thrombus formation is essential to develop novel therapeutic strategies.[2,4]

1.1.1 Platelets and thrombus formation

Platelet activation and subsequent thrombus formation at sites of vascular injury involve multiple interactions of platelet receptors with immobilized ligands and soluble agonists and can be divided into three major steps (Figure 1-1): (i) tethering and adhesion of platelets, (ii) platelet activation and finally (iii) platelet aggregation and thrombus growth.

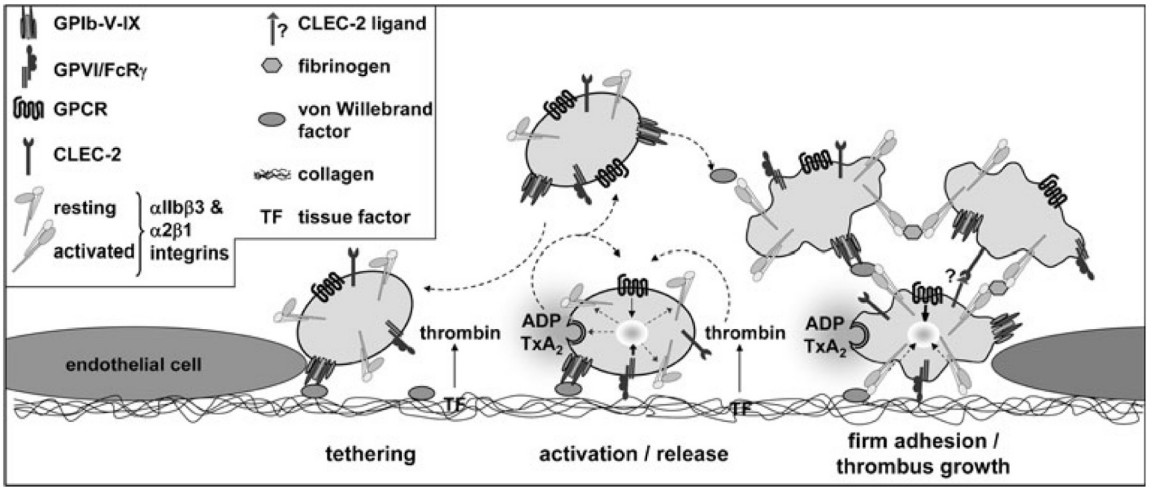

Figure 1-1 Simplified model of platelet adhesion and aggregation on the ECM. Platelet tethering on the wounded vessel wall is mediated by GPIb-vWF interaction, which mediates platelet deceleration and enables the platelet to stay in close contact with the ECM. In the next step, GPVI-collagen interactions initiate cellular activation, followed by a shift of integrins from a low to a high affinity state. The release of second wave mediators like ADP and TxA_2 by activated platelets, as well as the locally produced thrombin further enhance platelet activation and mediate thrombus growth. Finally, the thrombus is stabilized by signaling through CLEC-2; the underlying mechanism remains to be identified. Activated integrins mediate firm adhesion of platelets to the ECM as well as platelet-platelet interactions via binding to vWF and fibrinogen. (Picture is taken from: Stegner and Nieswandt, *J Mol Med,* 2011)[5]

In the first step, platelets are tethered to ECM components, like collagen, laminin or fibronectin, and "roll" along the side of injury in a stop-and-go manner. Under high shear conditions, such as those prevailing in arteriols or stenosed arteries, this initial adhesion is mediated by the interaction of platelet receptor complex *glycoprotein* (GP) Ib/V/IX with *von Willebrand factor* (vWF), which becomes immobilized on collagen.[6] This interaction is characterized by a fast dissociation rate and therefore does not allow firm platelet adhesion by itself, but induces the rapid deceleration of the platelets, thereby enabling the interaction of collagen with the immunoglobulin-like receptor GPVI, the major platelet collagen receptor.[7,8] Through an *immunoreceptor tyrosine-based activation motif* (ITAM) in the associated *Fc receptor* (FcR) γ-chain, GPVI induces intracellular signaling processes. These lead to cellular activation and the release of second wave mediators, most notably *adenosine diphosphate* (ADP), secreted by dense granules, and *thromboxane* A_2 (TxA_2), synthesized by cyclooxygenase-1. Additionally, platelet activation results in scramblase-mediated exposure of negatively charged *phosphatidylserine* (PS) on the platelet surface, providing a platform for the assembly of two major coagulation factor complexes and subsequent thrombin production.[9] In parallel, exposed *tissue factor* (TF) triggers local thrombin generation. ADP, thrombin and TxA_2 further reinforce and sustain cellular activation by initiating different pathways via *G protein-coupled receptors* (GPCRs),[10] and recruit additional platelets from the blood stream into the growing thrombus. In addition, platelet activation can also be

triggered through the hemITAM receptor *C-type lectin-like receptor 2* (CLEC-2),[11] but the receptor ligand in this process remains to be identified.

All these signaling pathways finally converge in the "final common pathway" of platelet activation: the functional upregulaton of adhesion receptors of the integrin class which shift from a low to a high affinity state, allowing firm ligand binding. Platelets express three β1 integrins, α2β1, α5β1 and α6β1, which mediate binding to collagen, fibronectin and laminin, respectively, and two β3 integrins, αvβ3 (binds to vitronectin) and αIIbβ3. The latter one is the most abundantly expressed integrin in platelets and plays an essential role in aggregation, since its binding of multiple ligands, most notably fibrinogen, fibrin and vWF, bridges adjacent platelets and also mediates stable platelet adhesion to the ECM.[2,12] Ligand occupied integrins in turn transduce "outside-in" signals, which promote platelet cytoskeletal rearrangements, spreading and clot retraction.[12,13]

1.2 Signaling events during thrombus formation

Platelets express a variety of receptors that induce or contribute to platelet activation. Based on the underlying signaling pathways, two major routes can be distinguished.[5] Both culminate in the activation of *phospholipase C* (PLC) isoforms and subsequent elevation of *intracellular calcium (Ca^{2+}) levels* ($[Ca^{2+}]_i$), a central step in platelet activation, and a prerequisite for granule release, integrin activation and procoagulant activity.[14]

One pathway is initiated by engagement of the GPVI-FcR γ-chain complex or CLEC-2 and requires the phosphorylation of critical tyrosine residues in the ITAM or (hem)ITAM, respectively, and is similar to signaling cascades used by immunoreceptors. Signal propagation is mediated by tyrosine kinases of the *spleen tyrosine kinase* (Syk) and Src families, as well as downstream adapter proteins and effector proteins and finally culminates in activation of PLCγ2.[12,15] Details of this signaling pathway are discussed in the next capter.

The other major pathway is triggered by GPCRs which are stimulated by soluble platelet agonists, such as thrombin, ADP and TxA_2. Three different types of heterotrimeric G proteins are found downstream of GPCRs in platelets: G_q, $G_{12/13}$ and G_i. The G proteins induce multiple signaling events, like stimulation of Rho-GTPases (via $G_{12/13}$), *phosphoinositide-3-kinase* (PI3K)/Akt (via G_i) signaling and activation of PLCβ (via G_q).[10]

In GPCR as well as in (hem)ITAM signaling, the activated PLC isoforms hydrolyze the membrane phospholipid *phosphatidylinositol-4,5-biphosphate* (PIP_2) to *inositol-1,4,5-trisphosphate* (IP_3) and *diacylglycerol* (DAG). DAG activates *protein kinase C* (PKC) and induces moderate Ca^{2+} influx via *transient receptor potential channel* (TRPC) 6.[16] IP_3 binds to

IP_3 sensitive Ca^{2+} channels in the membrane of intracellular Ca^{2+} stores, thereby inducing store depletion. The decrease in the Ca^{2+} store content subsequently triggers the opening of Ca^{2+} channels in the plasma membrane, resulting in pronounced elevations of $[Ca^{2+}]_i$. This process is known as *store-operated Ca^{2+} entry* (SOCE) and represents the main Ca^{2+} influx mechanism in non-excitable cells, including platelets (see chapter 1.7).[14,17,18]

1.3 (hem)ITAM receptor signaling in platelets

The ITAM is a conserved sequence motif involved in the signaling of a number of hematopoietic immunoglobulin receptors, like the *T and B cell receptor* (TCR and BCR), Fc receptors and activating natural killer cell receptors. The ITAM was described in the late 1980's[19] and consists of two copies of the sequence YxxL/I separated by 6-*12 amino acids* (aa) ($YxxL/I(x)_{6-12}YxxL/I$; in which x is an unspecified aa). The two tyrosine residues within the motif become phosphorylated upon receptor engagement and are the starting point for complex downstream signaling cascades.

Platelets express three receptors that signal via ITAM or hemITAM: GPVI, CLEC-2 and FcγRIIa. Since the latter one is present in human, but not in mouse platelets, and the experiments presented in this thesis were almost entirely performed with mouse platelets, only GPVI and CLEC-2 will be discussed here. ITAM-signaling of the TCR is described in chapter 1.5.

1.3.1 GPVI

Two receptors capable of binding collagens are expressed in platelets: GPVI and integrin $\alpha2\beta1$.[8] While $\alpha2\beta1$ has been considered to be the main collagen receptor in platelets for long time, it is now well established that this role applies to GPVI[7,8,20] and that $\alpha2\beta1$ has a supportive role for the initial collagen-platelet interaction.[21]

GPVI is a 62 kDa type transmembrane protein belonging to the *immunoglobulin* (Ig) superfamily of surface receptors. It has a structure similar to the natural killer cell receptor and to the Fcα receptor[22] and is exclusively expressed in platelets and MKs. GPVI consists of two IgG domains bearing the collagen binding site, followed by a mucin-rich stalk, containing O-glycosylation sites, a transmembrane domain and a cytoplasmic tail.[8,23] The cytoplasmic tail is short, comprising only 27 aa in mice (51 aa in humans),[8] and contains a basic and a proline-rich region which allow binding of calmodulin[24] and Src-family tyrosine kinases,[25] respectively.

The most important ligand for GPVI is fibrillar collagen, with type I and III representing the major components of the ECM in blood vessels. The *glycine-proline-hydroxyproline* (GPO) repeats within the collagen represents the specific GPVI recognition motif.[8] Powerful platelet activation via GPVI can also be induced by the GPVI specific agonists *collagen-related peptide* (CRP), made up of GPO repeats, and the snake venom toxin *convulxin* (CVX). CVX is a powerful activator of GPVI,[26] since it is tetrameric and therefore capable of clustering 4 GPVI proteins.[27]

The GPVI receptor is noncovalently associated with an FcR γ-chain homodimer which represents the signaling subunit of GPVI.[28,29] Each FcR γ-chain contains one ITAM and functionally resembles the CD3 and ζ chains in T cells and Igα and Igβ in B cells (see below and Figure 1-3).

Crosslinking of GPVI by ligand binding leads to the activation of the Src-kinase family members Fyn and Lyn which are associated to the cytoplasmic tail of GPVI (Figure 1-2; reviewed in [12]). How GPVI clustering activates Fyn and Lyn is not established, but a favoured model suggests that their activity is regulated by GPVI translocation to lipid rafts, tyrosine phosphatases and *immunoreceptor tyrosine-based inhibition motif* (ITIM) receptors.[30] Src kinases phosphorylate the conserved tyrosine residues within the ITAMs of the FcR γ-chain, leading to recruitment of the tyrosine kinase Syk which binds these phosphorylated tyrosine residues by its tandem Src homology 2 (SH2) domain. Subsequently, Syk undergoes autophosphorylation and phosphorylation by Src kinases and becomes activated. In the next step, Syk initiates a signaling cascade that resembles the one of the TCR (see chapter 1.5). A central step is the phosphorylation of the adapter protein *linker for activation of T cells* (LAT) that builds the core for the formation of a signalosome. This LAT signalosome is composed of a series of adapter and effector proteins. To the first group belong, besides LAT, *Grb2-related adapter downstream of Shc* (Gads) and *SH2 domain-containing leukocyte protein of 76 kDa* (SLP-76),[12] but also the adapter *growth factor receptor-bound protein 2* (Grb2) has been reported to associate to LAT upon platelet stimulation of human platelets with GPVI agonists.[26,31] These proteins form a scaffold for the binding of numerous signaling molecules that are targeted to the cell plasma membrane close to their molecular substrates. Among these signaling molecules are the Tec family kinases Tec and Btk, the *guanine nucleotide exchange factors* (GEFs) Vav1 and Vav3, PI3K and the small GTPase Rac1.[12] All these complex interactions orchestrate the regulation of the major effector enzyme in the GPVI signaling pathway, PLCγ2 (see above and chapter 1.7.2).

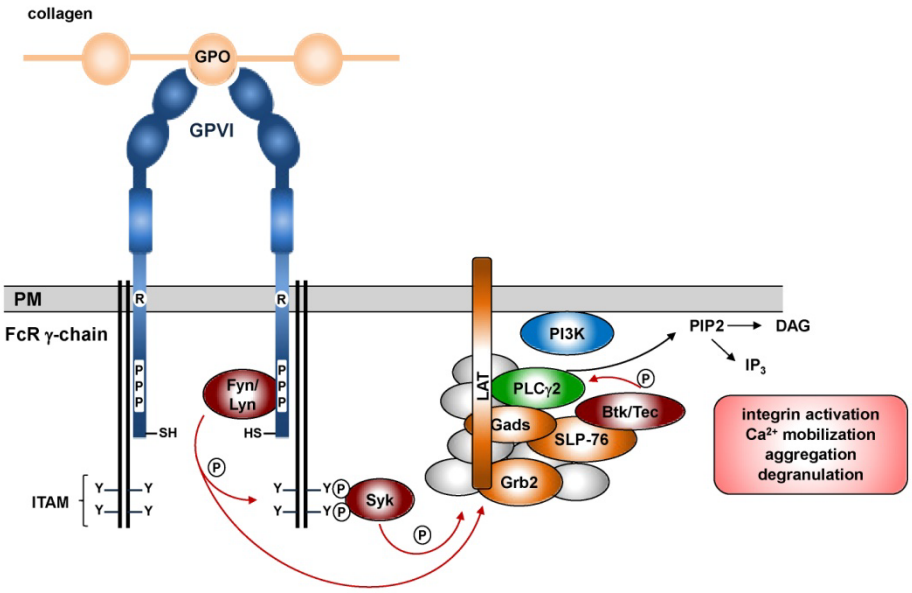

Figure 1-2 Signaling of the GPVI/FcR γ-chain complex. Crosslinking of GPVI results in the activation of the Src-kinases Fyn and Lyn initiating a Syk-dependent signaling pathway. For details see text. Src, Syk and Tec kinases are depicted in dark red, adapter proteins in orange. Grey circles denote additional proteins involved in the LAT signalosome. For overview reason, not every phosphorylation event and interaction is highlighted herein. (Image modified from Dütting *et al.*, *Trends Pharmacol Sci*, 2012)[23]

This signaling pathway is of great importance for platelet physiology. The absence or inhibition of components of this signaling pathway like Rac1,[32] the GEFs Vav1 and Vav3,[33] Syk[34] and the Src kinases Fyn and Lyn[35] has been reported to impair or to abolish platelet responses to collagen and to interfere with thrombus formation *in vivo*.[32,36] The importance of adapter proteins in GPVI signaling is separately discussed in chapter 1.6. In addition, GPVI can be cleaved from the cell surface by metalloproteinases, generating a soluble GPVI fragment and a small transmembrane remnant.[37] This process is called ectodomain-shedding and is supposed to downregulate platelet reactivity (see chapter 1.9).[38]

GPVI is a promising antithrombotic target as in mice, GPVI deficiency, either by antibody-mediated depletion or genetic approaches, results in protection from arterial thrombosis accompanied by only mildly prolonged tail bleeding times. Similarly, human patients with GPVI deficiency show no major bleeding diathesis (reviewed in [23]).

1.3.2 CLEC-2

In 2006, CLEC-2 was identified as a novel platelet receptor that mediates strong cellular activation in response to the snake venom toxin rhodocytin.[39] CLEC-2 is a type II transmembrane protein with one extracellular *C-type lectin-like domain* (CLTD) mediating

binding to non-carbohydrate ligands, and a cytoplasmic tail of 31 amino acids. CLEC-2 is one of the most megakaryocyte-specific and most abundantly expressed genes in MKs,[40] but is also expressed in liver sinusoidal cells and some immune cells.[15]

Within its intracellular N-terminus CLEC-2 contains a conserved YXXL sequence which mediates downstream signaling.[15] This motif is similar to the ITAM with the important difference, that only one copy of this sequence is present within the protein. Hence, this motif is called hemITAM. This feature requires CLEC-2 dimerization to induce platelet activation,[41,42] thereby bringing together two hemITAMs, which serve as a binding site for the two SH2 domains of the kinase Syk upon phosphorylation. The signaling pathways downstream of the CLEC-2 receptor strongly resemble the pathway downstream of GPVI,[15,43] involving Syk and the Src-family kinases, the adapters LAT and SLP-76, Vav1, the Tec kinase Btk, PI3K and Rac1.[32,39,44] Strikingly, the sequence of phosphorylation at the proximal end differs between CLEC-2 and the ITAM-coupled receptor GPVI: while the ITAM becomes phosphorylated by the Src-family kinases Fyn and Lyn, followed by the recruitment of Syk, the hemITAM within CLEC-2 is phosphorylated by Syk itself, while Src-family kinases are important for downstream signaling.[45,46]

So far the only known physiological CLEC-2 ligand is podoplanin which is expressed in various tissues, including lymphatic endothelial cells, alveolar cells and kidney podocytes, but is also present on tumor cells.[39,47] Importantly, the interaction of CLEC-2 with podoplanin and the subsequent platelet activation are essential for proper separation of lymphatic and blood vessels during development, as demonstrated by the appearance of blood filled lymphatics and edema in various mouse models deficient in one of those proteins (reviewed in [47]). More recently, it has been shown that the interaction of podoplanin with platelet CLEC-2 maintains the integrity of high endothelial venules.[48]

In addition, CLEC-2 plays an important role in the stabilization of platelet thrombi: CLEC-2-deficient platelets exhibit impaired stable aggregate formation in whole blood perfusion assays *in vitro*, and thrombus formation in CLEC-2 depleted or CLEC-2-deficient *bone marrow chimeric* (BMc) mice was abolished *in vivo*.[11,49] Since podoplanin is not expressed in blood vessels and hematopoietic cells, the mechanism by which CLEC-2 contributes to thrombus stabilization may involve a novel, yet not identifed CLEC-2 ligand, or alternatively homophilic interactions of CLEC-2 receptors.[49] Similar to the outcome of GPVI deficiency, mice lacking CLEC-2 in the hematopoietic system show no[49-51] or only moderately prolonged tail bleeding times,[11] and therefore CLEC-2 has been proposed to be a promising antithrombotic target. Of note, the combined deficiency of CLEC-2 and GPVI resulted in a

dramatic hemostatic defect, indicating a functional redundancy of these two (hem)ITAM receptors.[50]

1.3.3 Attenuation of ITAM signaling by ITIM receptors

Platelet activation by the (hem)ITAM receptors GPVI and CLEC-2 can be attenuated by receptors bearing an ITAM variant termed ITIM (consensus sequence: (S/I/V/L)xYxx(I/V/L)). Phosphorylated ITIMs serve as docking site for *SH2 domain-containing protein-tyrosine phosphatases* (SHP) 1 and 2 and the *SH2 domain-containing inositol-5-phosphatase-1* (SHIP-1) which dephosphorylate key components of activation pathways.[52] Platelets express four ITIM-containing receptors: *platelet-endothelial cell adhesion molecule-1* (PECAM-1), *carcinoembryonic antigen-related cell adhesion molecule 1* (CEACAM1), *triggering receptor expressed on myeloid cell-like transcript-1* (TLT-1) and G6b-B.[30] PECAM-1 has been reported to mediate weak inhibition of platelet activation by GPVI and CLEC-2, similar observations were made for CEACAM1 against platelet activation by GPVI.[53,54] The physiological significance of this inhibition for platelet physiology remains to be established.[30] Strikingly, mice deficient in G6b-B exhibited a severe macrothrombocytopenia and increased platelet turnover, clearly establishing this ITIM receptor as an essential mediator of platelet function and production.[55]

Receptors bearing a second variant of the ITAM, the *immunoreceptor tyrosine based switch motif* (ITSM), are discussed in chapter 1.8.

1.4 T cells

Lymphocytes are the effector cells of the adaptive immune system which specifically recognizes and responds to foreign antigens. B lymphocytes are responsible for antibody production and hence form the humoral part of the adaptive immune response, while T lymphocytes (also termed T cells) are the mediators of cellular immune response. The characteristic feature of T cells is the expression of a TCR which is encoded by a somatically rearranged gene and clonally distributed among T cells, thus enabling them to detect a very large spectrum of antigens. Most T cells express a TCR that constitutes of an α and β chain ($\alpha\beta$ receptor), while only a small portion expresses a $\gamma\delta$ TCR. T cells with an $\alpha\beta$ TCR can be further divided in two major T cell subsets, depending on which co-receptor they express. $CD8^+$ T cells can recognize peptides associated with class I *major histocompatibility complexes* (MHC) and subsequently kill infected cells or tumor cells that display foreign antigens; hence they are also called cytotoxic T cells. $CD4^+$ T cells are restricted to class II

MHC complexes present on antigen-presenting cells, such as dendritic cells and macrophages. This T cell subset has been termed T helper cells, since their support of B cell differentiation is essential for proper antibody production.

T cells originate from precursors that arise in the bone marrow and migrate to the thymus. These cells are called thymocytes and undergo various stages of maturation within the thymus to give rise to $CD4^+$ or $CD8^+$ T cells. Central steps of this maturation are positive and negative selection processes. Positive selection ensures the expression of a functional TCR that is capable of interacting with peptide/MHC complexes and also finally assigns the thymocytes to the $CD4^+$ or $CD8^+$ lineage. During negative selection, potentially harmful cells recognizing self antigens with high affinity are eliminated to prevent autoimmune reaction. This process is called central tolerance. Of note, proper receptor signaling is required for T cell maturation, since absence of critical signaling molecules can result in the absence of mature T cells.[56]

Because of their central role in adaptive immunity, $CD4^+$ T cells are extensively studied. $CD4^+$ T cells are a heterogeneous cell population in which different subsets or lineages can be distinguished. *Regulatory T cells* (Tregs) make up about 10 - 20% of the $CD4^+$ T cells in mouse lymph nodes and spleen. This cell population is characterized by strong expression of the α-chain of the high-affinity IL-2 receptor (CD25) and the transcription factor *forkhead box P3* (Foxp3), which is critical for their development and function.[57] Tregs are produced in the thymus (*natural Tregs*; nTregs), but can also be induced from naïve T cells in the periphery (*inducible Tregs*, iTregs). Tregs play an essential role in maintaining immunological unresponsiveness to self-antigens (peripheral tolerance) and in suppressing excessive immune responses. This is illustrated by mouse models with mutated *Foxp3* gene which lack regulatory T cells and develop an aggressive lymphoproliferative autoimmune syndrome.[57]

Upon TCR activation, naïve CD4 T cells may differentiate into one of several lineages of *T helper* (Th) cells, as defined by their pattern of cytokine production and function.[58] Th1 cells secrete *interferon* (IFN)γ and stimulate the phagocyte-mediated immunity by promoting the intracellular destruction of phagocytosed bacteria. The signature cytokines of Th2 cells are *interleukin* (IL) 4, 5 and 13. These cells contribute to the defence against extracellular parasites, including helminthes, by promoting IgE- and eosinophil/mast cell-mediated immune reactions. This polarization into distinct Th subsets is primarily controlled by the particular cytokine milieu,[58] and also the strength of TCR signaling, with weak signaling favoring Th2 differentiation and stronger signals promoting Th1 differentiation. [59] A third type of effector Th cells, Th17, was identified in 2003, and is characterized by secretion of IL-17.

The principal role of Th17 cells appears to be the protection against bacterial and fungal infections, but the lineage came into the focus of intense research due to their participation in inflammatory and autoimmune diseases.[60] As mentioned above, naïve T cells can also differentiate into iTregs. This process is controlled by *transforming growth factor* (TGF)-β, IL-2 and retinoic acid.[57]

1.5 T cell receptor signaling of CD4⁺ T cells

The TCR of CD4⁺ T cells consists of a heterodimer of two transmembrane polypeptide chains, termed α and β, covalently linked by a disulfide bridge. Like GPVI, the α and β chain of the TCR belong to the Ig superfamily and comprise one N-terminal variable and one constant Ig-like domain in their extracellular part, a hydrophobic transmembrane region and a short cytoplasmic region.[61] The TCR is accompanied by a CD4 co-receptor, which is involved in the binding of the TCR to peptide/class II MHC complexes.

Signaling through the TCR controls key events in T cell physiology: It is required during T cell development in the thymus (see above), the survival of naïve T cells in the periphery,[62] and, of course, for the clonal expansion and activation of T cells after encountering their specific antigen. The proximal signaling events downstream of the TCR have many similarities to the signaling pathway of the BCR and the platelet collagen receptor GPVI, involving ITAM-bearing receptor subunits, kinases of the Src, Tec and Syk/ZAP-70 families, PLCγ and adapter proteins (Figure 1-3).[12,63,64]

	T cell	Platelet	B cell
Ligand binding	TCR	GPVI	BCR
ITAM-containing signaling molecule	CD3 γ, δ, ε and ζ chains	FcR γ-chain	Igα and Igβ
Src family kinases	Lck (Fyn)	Fyn, Lyn	Fyn, Lyn, Blk
Syk/ZAP70 family kinase	ZAP-70	Syk	Syk
Main adapter proteins	LAT	LAT	SLP-65
	SLP-76	SLP-76	
	Grb2	Grb2	Grb2
	Gads	Gads	Gads
PLC isoform	PLCγ1	PLCγ2	PLCγ2
Tec family kinases	Itk, Rlk, Tec	Btk, Tec, (Itk)	Btk

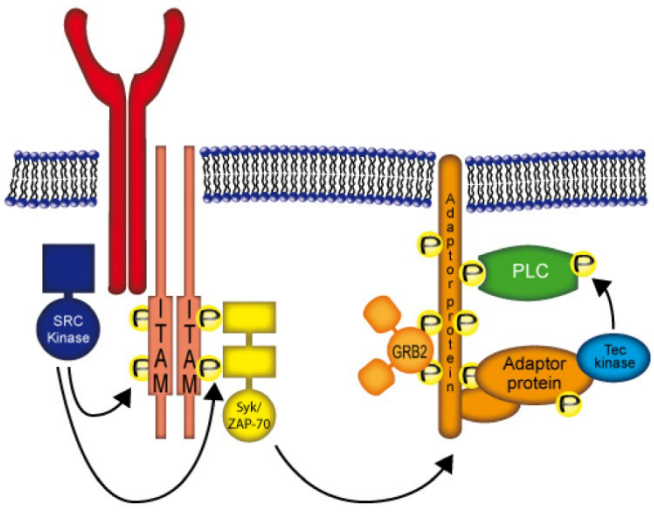

Figure 1-3 Comparison of BCR, TCR and GPVI signaling. Please note: This is a simplified overview of the complex signaling pathways of B cells, T cells and platelets, emphasizing general similarities in the signaling cascades. Therefore, biochemical details may not apply to the individual signaling pathways.

Like GPVI, the TCR itself does not have intrinsic enzymatic activity, but is associated with multiple signaling subunits: the CD3 γ,δ and ε proteins and ζ chains. Each αβ dimer forms a complex with one CD3 γβ heterodimer, one CD3 δε heterodimer and one covalent ζζ homodimer. Like the FcR γ-chain, these molecules contain ITAMs in their cytoplasmic tails which initiate downstream signaling pathways. One ITAM is present in each CD3 protein, and three in each ζ chain, adding up to 10 ITAMs per TCR complex.[61] Of note, antibodies directed against CD3ε can trigger T cell activation.

Physiological TCR signaling in $CD4^+$ T cells is induced by binding of the TCR to its specific peptide antigen presented on class II MHC complexes. The first proximal event is the activation of the Src family kinase tyrosine kinase Lck which is associated with the cytoplasmic tail of CD4. The active Lck subsequently phosphorylates the ITAM within the CD3 and ζ chains. This is followed by the recruitment of ZAP-70, which binds to phosphotyrosines and becomes phosphorylated by Lck (Figure 1-4). As a result, ZAP-70 acquires its own kinase activity and, similarly to its family member Syk in platelets, orchestrates the following signaling steps by phosphorylation of numerous downstream targets. Among the most important ZAP-70 substrates are the adapter proteins LAT and SLP-76 that form the backbone of a multiprotein complex which organizes adapter and effector molecules to allow the activation of multiple signaling pathways. The composition of this T cell LAT signalosome shares many similarities to the LAT signalosome present in the GPVI signaling pathway, including the adapters SLP-76, Gads and Grb2- the GEF Vav1, PI3K and the Tec kinase *IL-2-induced tyrosine kinase* (Itk). It is thought, that the complex interactions of different molecules stabilize the signalosome to facilitate optimal activation of the key enzyme PLCγ1.[64]

These proximal signaling events finally lead to cytoskeletal changes with Vav1 as an important mediator of actin remodeling,[65] and the induction of transcriptional activity. There are three major transcription factors in T cells which are activated by distinct signaling pathways: *nuclear factor of activated T cells* (NFAT), *activator protein 1* (AP-1, a dimer of Fos/Jun) and NF-κB (Figure 1-4; reviewed in [63,64]).

The two metabolites generated from PLCγ1 activity, IP_3 and DAG, have essential roles in the activation of these pathways. DAG recruits the GEF *Ras guanyl nucleotide-releasing protein* (RasGRP) to the plasma membrane where it becomes activated. RasGRP catalyzes the GTP for GDP exchange on the guanine nucleotide-binding protein Ras, thereby converting the protein into its activated form. This process of Ras activation is further enhanced by a second GEF, *son of sevenless homolog 1* (Sos1), which is recruited to the LAT signalosome by the adapter protein Grb2. Ras in turn initiates a phosphorylation cascade that results in

the activation of the *mitogen-activated protein* (MAP) kinase *extracellular-signal-regulated kinase* (ERK). ERK translocates into the nucleus where it triggers the transcription of AP-1. Two other members of the MAP kinase family, *c-Jun N-terminal kinase* (JNK) and p38, are activated in a similar manner by a pathway involving the GEF Vav1, as well as Rac and Cdc42 (Figure 1-4).[63,64] The second important signaling pathway regulated by DAG is mediated by its activation of PKCθ. PKCθ induces a signaling pathway that finally liberates the transcription factor NF-kB from its inhibitory subunits allowing its translocation into the nucleus where it activates different genes required for T cell function (Figure 1-4).[64,66]

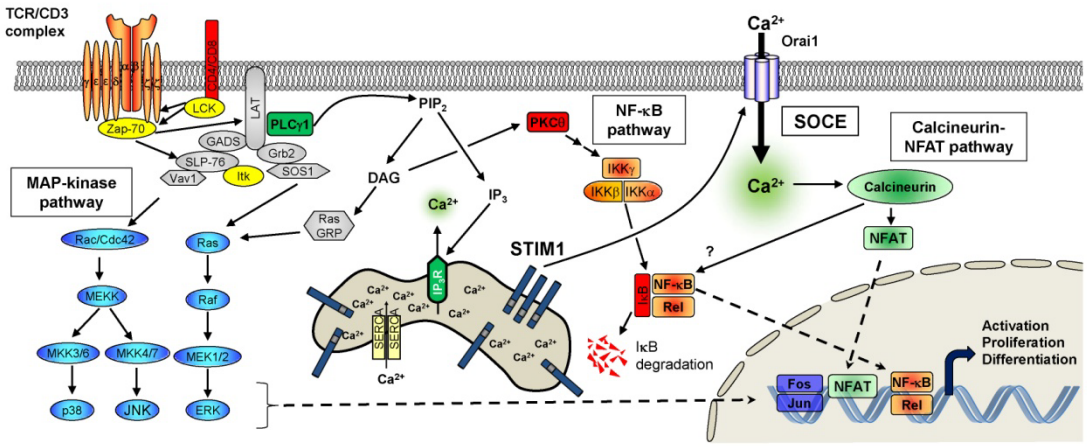

Figure 1-4 Summary of the TCR-induced signaling pathways. Ligand binding of the TCR induces a signaling cascade involving the formation of a LAT signalosome which is the origin of the three major signaling pathways: the MAP-kinase pathway (blue), resulting in the transcription of AP-1 (Fos and Jun), the NF-κB pathway (red) and the calcineurin-NFAT pathway (green), triggered by elevation of $[Ca^{2+}]_i$. For details, see text. Please note: In this simplified overview not all signaling events and interactions are depicted.

IP_3, the second metabolite generated by PLCγ1, induces a robust Ca^{2+} influx by a mechanism termed SOCE (see chapter 1.7). Ca^{2+} is a universal second messenger essential for activation of T cells.[67] TCR-induced elevation of $[Ca^{2+}]_i$ results in binding of Ca^{2+} to calmodulin which in turn binds to and activates the phosphatase calcineurin. This protein dephosphorylates the NFAT protein, thereby unmasking the nuclear localization sequence resulting in the translocation of NFAT into the nucleus (Figure 1-4). The activity of calcineurin is counterbalanced by the nucleus-resident *glycogen synthase kinase 3* (GSK3) which promotes the extracellular export of NFAT. In the nucleus, NFAT can form cooperative complexes with a variety of other transcription factors, most notably AP-1, thereby integrating signaling pathways, resulting in distinct specific gene expression patterns. The importance of the calcineurin-NFAT pathway for T cell activation is illustrated by the fact that the most potent immunosuppressants FK506 and cyclosporin A directly target this pathway[68,69] Of

note, transcriptional activity of NFAT in the absence of AP-1 activation has been reported to induce a pattern of gene expression that results in T cell anergy, a state of unresponsiveness to re-stimulation of the TCR that can be induced e.g. by TCR stimulation in the absence of ligation of the CD28 co-receptor.[70,71]

In addition to NFAT, Ca^{2+} influx also regulates other signaling pathways including the transcription factors *myocyte-enhancing factor 2* (MEF2) and *downstream regulatory element antagonist modulatror* (DREAM), as well as *Ca^{2+}-calmodulin-dependent kinase II* (CamKII).[69,72] In addition, Ca^{2+} also participates in the regulation of NF-κb.[73]

1.6 Adapter proteins in platelet and T cell receptor signaling

Adapters are proteins that lack enzymatic activity, but contain multiple protein-interaction sites and serve as intracellular scaffolds that organize effector molecules and their substrates in the correct spatiotemporal manner, thereby allowing the activation of multiple signaling pathways.[74] The most prominent adapter molecules in platelets and T cells include LAT, SLP-76, Grb2 and Gads.

1.6.1 LAT, SLP-76 and Gads

LAT and SLP-76 are among the most important targets of ZAP-70/Syk kinases in T cells and platelets [75-78] and form the backbone of a multimolecular signaling complex in close proximity to the plasma membrane, referred to as the LAT signalosome (see above and [12,79]).

Upon receptor stimulation, the transmembrane protein LAT is phosphorylated at five tyrosine residues which subsequently serve as binding sites for several SH2 domain containing proteins, e.g. PLCγ, Grb2 and Gads.[79] SLP-76 becomes phosphorylated at three tyrosine residues which facilitate binding of Vav and Nck.[80] Of note, LAT and SLP-76 do not directly bind to each other, but are linked to each other by a third adapter protein, Gads. Gads, like PLCγ, is constitutively bound to the proline rich region of SLP-76, and, upon receptor stimulation, recruits SLP-76 to LAT by way of the interaction of its SH2 domain with phospho-LAT.[81] An additional adapter protein within this complex is Grb2, which is discussed below. Although LAT and SLP-76 nucleate the signalosome, several other effector and adapter proteins are required to stabilize this protein complex and a current model proposes that the numerous interactions cooperatively regulate the optimal recruitment and activation of the key enzyme PLCγ.[64,79]

The T cell and platelet phenotypes of mice lacking LAT, SLP-76 and Gads have been described. Strikingly, the absence of LAT or SLP-76 results in a complete inhibition of pre-TCR signaling of thymocytes and subsequently in a block in T cell development and the lack of peripheral T cells.[56,82-84] Platelets from *Slp76*$^{-/-}$ and *Lat*$^{-/-}$ mice exhibit defective responses to agonists of the (hem)ITAM receptors GPVI and CLEC-2, however, to a different extent: *SLP76*$^{-/-}$ platelets show severe defects in aggregation and Ca^{2+} mobilization, even in response to high doses of CVX and CRP. Phosphorylation of PLCγ2 is dramatically reduced and only detectable at residual levels at high agonist concentrations, clearly demonstrating that SLP-76 is essential to couple GPVI to PLCγ2 activation.[76,85,86] In contrast, the GPVI signaling defect of LAT-deficient platelets can be overcome at high agonist concentrations as demonstrated by the full aggregation response and robust PLCγ2 phosphorylation.[31,77,86] Nevertheless, LAT-deficient platelets fail to form three-dimensional thrombi under flow,[31] show decreased PS exposure[87] and *Lat*$^{-/-}$ mice are protected in a thrombosis model of laser induced injury.[88] Absence of SLP-76 also impairs CLEC-2 signaling: mice with a platelet-specific deletion of SLP-76 show a defect in lymphatic/blood vessel separation, similar to mice deficient in CLEC-2 or its ligand podoplanin.[47,89] Distinct from GPVI, however, CLEC-2 is able to induce a partial activation of PLCγ2 and platelet aggregation at high rhodocytin concentrations in the absence of SLP-76 *in vitro*.[39,44] LAT deficiency also results in aggregation defects in response to rhodocytin,[31,39] but *Lat*$^{-/-}$ mice, in contrast to *Slp76*$^{-/-}$ mice, are born at normal Mendelian ratios and neither show fetal hemorrhage nor blood filled lymphatics,[56,85,90] indicating that LAT function downstream of CLEC-2 can be bypassed *in vivo*. Of note, SLP-76 is also involved in the activation of PLCγ2 downstream of integrin αIIbβ3 and is required for platelet spreading, while LAT is dispensable for this process.[31,86,91]

In addition, *Gads*$^{-/-}$ mice have been described. Studies with these animals revealed a less prominent role of this adapter protein in TCR and GPVI signaling as compared to LAT and SLP-76. *Gads*$^{-/-}$ thymocytes show several developmental defects, but still differentiated into mature T cells, indicative of residual signaling activity of the pre-TCR.[92] Platelets lacking Gads are grossly normal and only exhibit mild aggregation defects in response to weak activation of GPVI or CLEC-2.[31]

1.6.2 Grb2

Grb2 was the first adapter protein to be described[93] and is the prototype of the Grb2 family of adapters which also comprises Gads and *Grb2-related adapter protein* (Grap). The Grb2 protein is composed of a central SH2 domain flanked by two SH3 domains and has molecular weight of about 25 kDa (Figure 1-5).[93,94] SH3 domains bind to prolin-rich

recognition sites with a PxxP core, SH2 domains bind to short consensus motifs bearing phosphorylated tyrosine residues.[95,96] Grb2 was initially identified as an essential mediator of Ras activation downstream of growth factor receptors.[94] A number of seminal publications in 1993 ultimately unraveled the underlying mechanism how Grb2 couples receptor signaling to Ras activation (summarized in [97]): Ligand induced crosslinking of the surface receptor induces kinase activity and trans-phosphorylation of tyrosine residues in the cytoplasmic receptor domains leading to the recruitment of Grb2 which binds to these residues with its SH2 domain. Grb2 itself is constitutively bound to Sos1, a GEF, which becomes localized into the vicinity of its substrate Ras. Sos1 provokes a GTP/GDP exchange in Ras, triggering a signaling cascade of serine-threonine kinases.

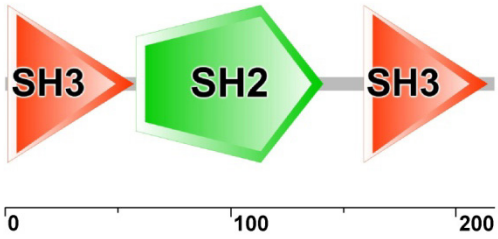

Figure 1-5 Domain structure of the mouse Grb2 protein. The ruler designates the amino acids.
(Source: *http://smart.embl-heidelberg.de*)

Grb2 is ubiquitously expressed and therefore also found in lymphocytes, where it can interact with several components involved in antigen receptor signaling,[74,96,98] and platelets (see below). One of the most prominent Grb2 interaction partners present in T cells and platelets is LAT.[78] This interaction has been extensively studied[79] and it is now established that Grb2, via its SH2 domain, binds to phosphorylated LAT at the distal three tyrosines.[99,100] Similar to its recruitment to growth factor receptors, Sos1 is also recruited via Grb2 to LAT upon TCR stimulation.[78,101] Importantly, it has been shown that Grb2 and Sos1 form 2:1 complexes in Jurkat cells which oligomerize with LAT into large signaling clusters to enhance TCR signaling.[102] In contrast, the role of Sos1 in Ras activation and downstream ERK activation upon TCR stimulation seems to be of minor importance, since Ras activation is mainly triggered by the GEF Ras-GRP.[64] Similar to Gads, it has been shown that Grb2 is also able to couple Lat and SLP-76 in DT40 B cells, but it has lower binding affinity to SLP-76 and thus does this coupling less efficiently.[103,104]

Because of the pivotal role of Grb2 in growth factor receptor signaling, Grb2-deficient mice die early in embryogenesis, making the analysis of lymphocytes and platelets impossible.[105] Therefore, heterozygous Grb2 knockout mice (*Grb2*$^{+/-}$) were used as a model for the investigation of Grb2 function in T cell development. In response to TCR stimulation, *Grb2*$^{+/-}$ thymocytes show weakened activation of the MAP kinases p38 and JNK, but unaltered

activation of ERK, resulting in a decreased ability to undergo negative selection.[106] Meanwhile, these findings have been confirmed in mice with a conditional deletion of Grb2 in the T cell lineage. These Grb2-deficient thymocytes additionally show attenuated Ca^{2+} influx in response to TCR stimulation, which is attributed to a marked impairment of Lck activation at the top end of the signaling cascade.[107] Recently, two independent studies described the role Grb2 in B cells using B cell-specific Grb2-deficient mouse lines.[108,109] In contrast to T cells, enhanced BCR-induced Ca^{2+} influx was observed in both studies, while conflicting results on the impact of Grb2 on MAP kinase activation were reported. Grb2-deficiency also affects several other signaling pathways resulting in impaired germinal center formation and decreased survival.[108,109]

Grb2 is also expressed in platelets and MKs where it interacts with a plethora of proteins (http://plateletweb.bioapps.biozentrum.uni-wuerzburg.de/plateletweb.php[110]). *In vitro* studies proposed that the Grb2/SOS/Ras/Raf-1/*mitogen-activated protein kinase/ERK kinase* (MEK) pathway is critical for MK differentiation.[111,112] Furthermore, biochemical experiments demonstrated the interaction of Grb2 with critical components of the GPVI signaling pathway, namely LAT, Syk and FcR γ-chain, in CVX stimulated platelets, implicating a role for Grb2 in the LAT signalosome downstream of GPVI.[26] This is further supported by tyrosine phosphorylation of Grb2 in response to GPVI stimulation.[113] Interestingly, immunoprecipitations in human platelets revealed that Grb2 associates much stronger with LAT after GPVI stimulation than the Grb2 related adapter Gads, which has a minor role in supporting GPVI signaling.[31] Additionally, Grb2 may also be involved in integrin outside-in signaling, since it shows increased interaction with the adapter protein *downstream of tyrosine kinase* (Dok)-1 and Dok-3 in human platelets upon activation of integrin αIIbβ3.[114] However, due to the lack of an appropriate animal model, the exact role of Grb2 in platelet physiology and in distinct signaling pathways has remained elusive.

1.7 Store-operated Ca^{2+} entry (SOCE)

1.7.1 The history of SOCE

Ca^{2+} is a ubiquitous second messenger in eukaryotic cells which controls a variety of cellular functions and therefore its spatial and temporal dynamics are tightly regulated.[115] The concept of SOCE, initially termed capacitative Ca^{2+} entry, was established in 1986 by Putney.[116] He proposed a Ca^{2+} influx mechanism where the depletion of the intracellular stores triggers the opening of Ca^{2+} channels (termed SOC channels) in the plasma membrane.[18,116] Direct evidence in support of this model was provided by patch-clamp

studies that identified a SOC current which was named *Ca^{2+}-release-activated Ca^{2+}(CRAC) current* (I_{CRAC}) in mast cells[117] and Jurkat leukemic T cells.[118,119]

Subsequent studies revealed that SOCE does more than just provide Ca^{2+} for refilling stores, but is itself the main Ca^{2+} entry mechanism in virtually all non-excitable cells,[17,120] including platelets[121-123] and immune cells.[67] This is exemplified by humans suffering from severe immunodeficiency due to defective SOCE in T cells.[124-128] However, the molecular mechanisms mediating this process, including the CRAC channels identity, remained elusive for two decades and different models have been proposed.[18,120]

1.7.2 The mediators of SOCE – STIM and Orai

In 2005, the first breakthrough was achieved by the identification of stromal interaction molecules as essential regulators of SOCE by two different *RNA interference* (RNAi) screens.[129,130] STIM1 is a type I transmembrane molecule that resides predominantly in the *endoplasmic reticulum* (ER) membrane.[129,131] In its intraluminal N-terminus, STIM1 possesses a *sterile α motif* (SAM) and a canonical EF-hand motif which binds Ca^{2+}, thereby sensing the store content. In the cytoplasmic C-terminal part, three *coiled-coil* (CC) domains and a lysine-rich and a serine-proline rich region have been identified (Figure 1-6 A).[132,133]

In parallel with STIM1, its homolog STIM2 was also described as a regulator of SOCE.[129] STIM1 and STIM2 share 53% amino acid identity and exhibit a similar domain structure, but diverge significantly in their C-terminus.[133] As STIM2 has a lower Ca^{2+} affinity than STIM1, and therefore can be active at small fluctuations of ER Ca^{2+} levels, it has been supposed that STIM2 maintains basal $[Ca^{2+}]_i$ in resting cells.[134] The majority of the studies, however, focused on STIM1, since this is the dominant STIM isoform in many cell types, including most immune cells[67] and platelets.[14]

Only one year later, the second milestone in revealing the mechanism of SOCE was the discovery of a new class of Ca^{2+} channels, the Orai proteins. Orai1 (also called *CRAC modulator 1* - CRACM1) was identified by the use of genome wide RNAi screens in *Drosophila* S2 cells for inhibitors of SOCE and NFAT translocalization as well as by linkage analysis in human patients whose T cells lack functional SOCE.[135-137]

Also two homologs of Orai1 were identified in mammals and named Orai2 (CRACM2) and Orai3 (CRACM3).[135] All Orai isoforms can contribute to STIM1-mediated SOCE and may form heteromultimeric complexes.[138] Orai1 is by far the best studied family member and critical for CRAC channel function in different immune cells[67] and platelets (see below).[14] Orai1 is a type IV-A plasma membrane protein with four transmembrane domains, a CC

domain at the intracellular C-terminus and does not bear homology to any known channel.[139] By subsequent mutational analysis of critical amino acids, it was proven that this protein is not just a regulator of the CRAC, but indeed represents the pore-forming subunit.[140-142]

The identification of STIM and Orai sparked a large number of studies describing SOCE and substantial advances in understanding the molecular regulation of SOCE were made (reviewed e.g. in [132], see also Figure 1-6 B). In the current model SOCE is initiated by binding of agonists to different kinds of receptors, like ITAM-coupled receptors or GPCRs which mediate the activation of PLCs (see above). PLC generates IP_3 which in turn binds to IP_3-sensitive Ca^{2+} channels in the membrane of intracellular Ca^{2+} stores (the dense tubular system in platelets, the ER in most other cell types). The subsequent release of Ca^{2+} from the stores into the cytosol[143] results in a decrease in Ca^{2+} store content and dissociation of the Ca^{2+} from the EF-hand motif of STIM. Subsequently, STIM multimerizes[144,145] and translocates into puncta at ER-plasma membrane junctions.[131,146] Here, STIM binds to CRAC channels formed by four Orai proteins[147] in the plasma membrane, resulting in opening of the channel and subsequent Ca^{2+} influx (SOCE).

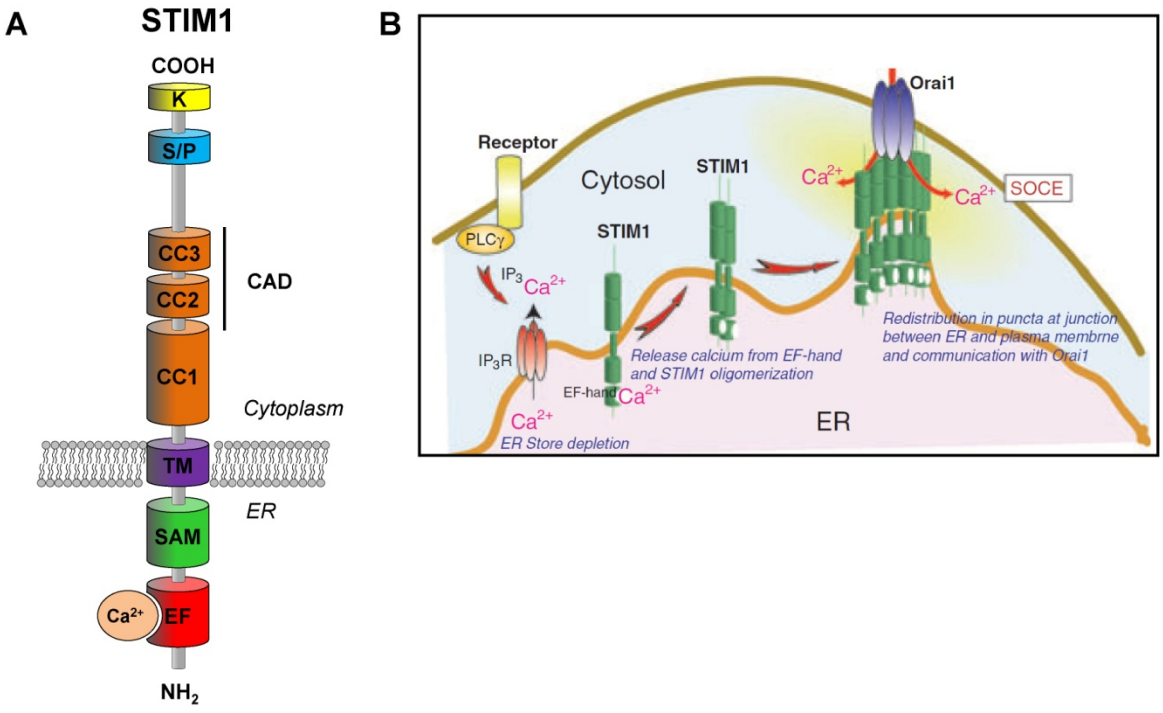

Figure 1-6 STIM1 and store operated Ca^{2+} entry. (A) Molecular structure of STIM1. The N-terminal part of the protein is located in the *endoplasmic reticulum* (ER) lumen and comprises an *EF-hand motif* (EF) responsible for Ca^{2+} sensing. CAD indicates *CRAC channel activation domain* which directly binds to Orai and is required for CRAC channel activation. CC, coiled coil; K, lysine-rich; S/P serine/proline-rich; TM, transmembrane; **(B)** Simplified model of SOCE. For details see text. (Figure in B is taken from Baba and Kruosaki, *Immunol Rev,* 2009)[148]

Of pivotal importance in this process are aspartate and glutamate residues within the Ca^{2+} EF-hand motif of STIM1 which coordinate Ca^{2+} binding. Mutation of either D76, D84 or E87 mimics the Ca^{2+} dissociated state of STIM1 and thus empty Ca^{2+} stores.[129,149,150] This results in stimulus-independent STIM1 activation and constitutive Ca^{2+} influx. The *in vivo* consequences of such a mutation are discussed in the next section.

1.7.3 Physiological consequences of mutations in STIM1 and Orai1

The discovery of STIM and Orai proteins as essential mediators of SOCE has allowed the generation of genetic mouse models and the identification of mutations in human patients. Deficiency of STIM1 and Orai1 has been shown to affect many different cell types,[151] including platelets[14] and immune cells.[67]

Intracellular Ca^{2+} measurements in platelets from STIM1-deficient mice and from mice lacking functional Orai1 revealed severely defective Ca^{2+} responses to all major agonists and towards the SOCE-inducer *thapsigargin* (TG) which induces passive store depletion by blocking ER resident *sarco-endoplasmic Ca^{2+} ATPases* (SERCA).[152-155] These results established SOCE as the major route of Ca^{2+} entry in platelets and STIM1 and Orai1 as critical mediators of this process. On the functional level, *Stim1*$^{-/-}$ and *Orai1*$^{-/-}$ platelets display a selective defect of GPVI-ITAM signaling that is less pronounced in *Orai1*$^{-/-}$ platelets,[154,155] reduced procoagulant activity,[152,153,156] and a protection in collagen-driven thrombosis models, as well as in the *transient middle cerebral artery occlusion model* (tMCAO) of ischemic stroke.[154,155]

The importance of CRAC channel function for $CD4^+$ T cells function becomes apparent in patients with mutations in the *ORAI1* gene which interfere with protein function or expression. These patients harbor normal numbers of T cells which, however, lack SOCE and show a reduced proliferative response to TCR stimulation. As a consequence, the patients suffer from severe immunodeficiency associated with recurrent life-threatening bacterial, fungal and viral infections. Without hematopoietic stem cell transplantation, patients die within the first year of life[125,127,128,157] (reviewed in [158]). $CD4^+$ T cells from Orai1-deficient or Orai1 mutant mice also show impaired SOCE, cytokine production and effector functions, but the defects are milder compared to the human situation, especially in naïve $CD4^+$ T cells, which was explained by expression of Orai2 and Orai3 in mouse $CD4^+$ T cells.[159-161]

$CD4^+$ T cells derived from *Stim1*$^{-/-}$ mice show abolished SOCE and impaired cytokine production, clearly establishing STIM1 as the major isoform in $CD4^+$ T cells, while STIM2 has a supporting function.[162,163] Unexpectedly, *Stim1*$^{-/-}$ BMc mice develop a lymphoproliferative

phenotype with enlarged lymph nodes and splenomegaly and this phenotype is even more pronounced in mice with a T cell-specific deletion of both STIM isoforms (*Stim1*$^{fl/fl}$ *Stim2*$^{fl/fl}$ *CD4-cre*$^{+/-}$).[163] In the latter case, this observation is attributed to severely defective Treg development and function.[163] In contrast, Treg cell frequencies and suppressive activity are normal in mice lacking STIM1 only, suggesting a T cell intrinsic defect and a SOCE-dependent negative feedback loop to constrain excessive proliferation was proposed.[162] Despite the described defects, STIM1-deficient BMc mice are still able to mount T cell dependent antibody responses and the ability of T cells from these mice to induce graft-versus-host disease is only slightly impaired compared to wildtype controls.[162] In contrast, STIM1 BMc mice or mice with a T cell-specific loss of STIM1 are protected from inflammatory bowel disease[157] and experimental autoimmune encephalitis,[164,165] a model of multiple sclerosis, suggesting that SOCE may be of pivotal importance in these settings. A slight protection in the latter model was also observed upon STIM2 deficiency demonstrating a role in T cell physiology which may be of special importance in Th17 polarization.[164,165]

Human patients lacking STIM1 show an almost identical clinical disease spectrum as Orai1-deficient patients, including severe immunodeficiency[166-168] (reviewed in [158]). In addition, and partially comparable to mice, these patients exhibit lymphoproliferation and autoimmune cytopenias.[166-168]

Of particular interest is the *Stim1*^{Sax} mouse which was analyzed in 2007 in our laboratory. This mouse line carries an activating mutation (D84G) in the Ca^{2+}-binding EF-hand motif of STIM1, abolishing Ca^{2+} binding and thus mimicking empty stores.[149] Hence, this mouse model provides one of the rare examples how enhanced CRAC channel activation affects cell functions. Homozygous (*Stim1*$^{Sax/Sax}$) mice are embryonically lethal with severe diffuse hemorrhages in different regions of the body, indicating hemostatic and/or vascular defects. Heterozygous (*Stim1*$^{Sax/+}$) mice are born at normal Mendelian ratios, but exhibit splenomegaly and a pronounced macrothrombocytopenia. The latter is a consequence of increased $[Ca^{2+}]_i$ in platelets which results in a preactivation state and subsequently leads to increased platelet clearance from the circulation. In addition, a selective unresponsiveness towards ITAM-coupled receptor agonists was observed. *Stim1*$^{Sax/+}$ T cells exhibit spontaneous Ca^{2+} influx with elevated basal $[Ca^{2+}]_i$ and enhanced Ca^{2+} mobilization in response to TG, but normal SOCE in response to TCR stimulation. Importantly, T cell development, proliferation and cytotoxic T cell function are normal in *Stim1*$^{Sax/+}$ mice and – surprising to experts in the field[132] – no signs of autoimmunity despite constitutive CRAC channel activity were observed.

1.8 CD84: an ITSM-bearing receptor of the hematopoietic system

The *signaling lymphocytic activation molecule* (SLAM) receptors are recognized as important immunodulatory receptors and are expressed on the surface of a wide variety of hematopoietic cells.[169] The SLAM family belongs to the group of immunoglobulin receptors and comprises 9 members, with SLAM (CD150) as their prototypical eponym. The family members are type I transmembrane proteins and share a common N-terminal ectodomain structure, featuring a membrane-distal Ig-like *variable* (V) domain, lacking disulfide bridges, and a membrane proximal Ig-like *constant 2-type* (C2) domain, stabilized by disulfide bonds.[169]

A key feature of the SLAM receptor family is the presence of one or more *immunoreceptor tyrosine-based switch motif* (ITSM) in the cytoplasmic domains.[169] The ITSM (consensus sequence: TxYxxI/V) differs from the ITAM, which consists of two YxxL/I sequences, but shows similarities to the ITIM (see above).[170] ITSMs appear to be phosphorylated by Src kinases upon activation of the receptor by ligand binding or *antibody* (Ab)-mediated crosslinking.[171,172] Similar to ITIMs, the phosphorylated ITSM can recruit SH2 containing molecules, such as the phosphatases SHP-1, SHP-2 and SHIP. Notably, unlike ITIMs, ITSMs also bind the adapters *SLAM-associated protein* (SAP also termed SH2D1A), *Ewing's sarcoma activated transcript 2* (EAT-2), *Eat-2-related transducer* (ERT) and the p85 regulatory subunit of PI3K. Whether an ITSM transduces activating or inhibitory signals depends on the cell type and the cellular context of stimulation.[169,170]

The SLAM receptor family has attracted much attention because inactivating mutations in *Sh2d1a*, encoding SAP, underlie most cases of *X-linked lymphoproliferative syndrome* (XLP).[173] This immune disease is characterized by a profoundly abnormal response to infection with Epstein-Barr virus, the development of a lymphoproliferative disorder and dysgammaglobulinemia.[169]

At least two SLAM family members are expressed in platelets: SLAM and CD84.[174,175] SLAM becomes tyrosine phosphorylated in an aggregation dependent manner and SLAM-deficient platelets exhibit defective platelet aggregation *in vitro* and delayed arterial thrombus formation *in vivo*.[175]

CD84 is a type I transmembrane glycoprotein comprising an N-terminal ectodomain, bearing one IgV and IgC2 domain (199 aa in mice), a transmembrane domain (25 aa) and a C-terminal intracellular region (87 aa) containing two ITSMs.[169,176] Interestingly, CD84 also contains an additional tyrosine residue which is located between the ITSMs and becomes phosphorylated upon platelet aggregation.[175] Besides platelets, CD84 is also expressed in different immune cell populations, including B and T lymphocytes, granulocytes and dendritic

cells.[169,174,177] Like most SLAM family members, CD84 can undergo homophilic interactions.[178] Importantly, ligation of CD84 with *monoclonal Ab* (mAb) or recombinant CD84 enhances IFNγ production and proliferation in T cells stimulated with low doses of anti-CD3 mAb.[172,178]

The signaling pathway downstream of CD84 has not been examined in detail. Ab-mediated crosslinking of CD84 results in phosphorylation of the ITSMs and the recruitment of the adapter SAP.[172,175] In T cells, it has been demonstrated that the Src family kinase Lck mediates CD84 phosphorylation.[172] It is presumed that, similar to CD150, SAP facilitates the recruitment of Fyn to the CD84/SAP complex, and additionally may also positively influence signaling by interfering with the binding of the phosphatase SHP-2.[169,179] Interestingly, CD84 can be tyrosine phosphorylated in SAP-deficient T cells from XLP patients,[172] raising the possibility that CD84 phosphorylation does not require Fyn recruitment, while SAP itself may be still required for signaling transduction.[180] Ab-mediated crosslinking of CD84 also induces receptor phosphorylation in B cells,[181] and biochemical studies in transfected cell lines suggest that this may result in the recruitment of the SAP homolog EAT-2.[181,182]

A functional role for CD84 has been described in a study using of CD84-deficient mice. It was demonstrated that CD84 is required for prolonged B cell and T cell interaction and its loss results in impaired germinal center formation.[180] The platelet phenotype of CD84 deficient mice has not been described yet, however, two findings implicate that CD84 and CD84 receptor signaling may be of relevance in platelets: (i) the cytoplasmic tail of CD84 becomes phosphorylated in response to platelet aggregation, and (ii) wildtype platelets, but not SAP deficient platelets, are able to spread on immobilized CD84. Therefore, CD84 has been proposed to mediate contact dependent signaling and contribute to thrombus stabilization, similar to CD150.[175] However, the role of CD84 in platelet aggregation and thrombus formation as well as the regulation of its surface regulation, remain elusive.

1.9 Receptor proteolysis

One way to downregulate platelet reactivity is to remove activatory receptors from the platelet surface by internalization[183] or proteolytic cleavage.[38] The extracellular cleavage of platelet receptors by (metallo)proteinases is termed ectodomain shedding and has been described for a number of major receptors, including GPIbα,[184] GPVI,[185,186] GPV,[187,188] semaphorin 4D,[189] P-Selectin,[190] and CD40L.[191]

Two proteinases of the *a disintegrin and metalloproteinase* (ADAM) family have been identified to be involved in the extracellular cleavage of platelet receptors: ADAM10 and

ADAM17. The latter is the principal sheddase of GPIbα,[184] whereas cleavage of GPV or GPVI can occur through either ADAM10 or ADAM17, depending on the shedding-inducing stimulus.[37,192]

Shedding of GPIb[184,185,193] and GPV[37,188] from the platelet surface can be induced by activating human or mouse platelets with receptor agonists, while metalloproteinase-dependent downregulation of GPVI in response to stimulation with GPVI agonists has been observed in human,[186] but not in mouse platelets.[185] However, GPVI can be released from the platelet surface in circulating murine platelets by *in vivo* administration of monoclonal anti-GPVI antibodies.[20,183] Recently, a proteomic approach demonstrated that many platelet receptors, including CD84 (see previous chapter), might be cleaved from the surface of human platelets in a metalloproteinase-dependent manner, but details of this process remained elusive.[194]

To study platelet receptor regulation *in vitro*, platelets can be treated with different agents that induce shedding of multiple platelet membrane receptors by distinct mechanisms (see Figure 1-7 and [38]): The calmodulin inhibitor W7 induces the disruption of calmodulin from receptors, thereby facilitating ectodomain shedding, e.g. of GPIbα[37,192] and GPV[188] by ADAM17 and GPVI by ADAM10.[186,192] In addition, W7 may also act in part by activating ADAMs themselves.[38] *N-ethylmaleimide* (NEM) is a thiol-modifying reagent which directly activates ADAM10 and ADAM17 by acting on a cysteine-switch within the proteases. Like W7, NEM induces the loss of platelet receptor without accompanying platelet activation.[38] *Carbonyl cyanide m-chlorophenylhydrazone* (CCCP) induces mitochondrial injury by

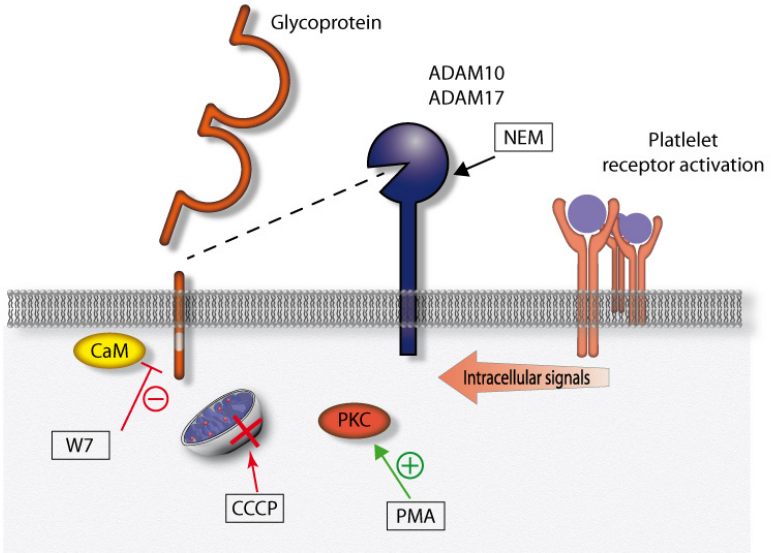

Figure 1-7 Different ways leading to receptor shedding. Platelet activation by receptor agonists results in intracellular signaling events, which are involved in inside-out activation of metalloproteinases. *In vitro*, shedding can be induced by reagents acting in distinct manners and independently of platelet receptor stimulation. For details see text.

uncoupling oxidative phosphorylation and triggers receptor shedding mainly in an ADAM17-dependent manner.[184,192] The phorbol ester *phorbol 12-myristate 13-acetate* (PMA) is an activator of PKC thereby inducing ectodomain shedding, e.g. of GPV and GPIb, mainly by ADAM17.[184,188]

Another mechanism to modulate platelet receptor signaling is proteolytic cleavage of the receptor by intracellular proteases like calpain. Calpain is a cysteinyl protease, in part regulated by Ca^{2+}, and cleaves a number of proteins, many of them involved in the regulation of the cytoskeleton.[195] Studies in platelets have demonstrated that calpain cleaves the intracellular part of β3 integrin,[196] FcγRIIa,[197] and PECAM-1[198] which results in degradation or modification of the signal transducing cytoplasmic receptor tail.[197,199] Of note, activation of signaling pathways leading to extracellular shedding is concomitant with activation of calpain (e.g. in response to calmodulin inhibitors),[38,197] suggesting that intra- and extracellular cleavage events might be simultaneously operative in the downregulation of receptor signaling in platelets.

1.10 Aims of this thesis

The aim of this thesis was to investigate different aspects of receptor signaling and receptor regulation in cells of the hematopoietic system:

The *Stim1*$^{Sax/+}$ mouse provides a unique model to investigate the impact of constitutive Ca^{2+} influx on the physiology and function of different cell types. While deleterious to platelet function, T cells with *Stim1*^{Sax} mutation have been found to behave surprisingly normal. Since the underlying mechanisms remained elusive, the first aim of the thesis was to examine the TCR signaling pathway and function of *Stim1*$^{Sax/+}$ T cells by biochemical approaches.

The formation of signaling complex called LAT signalosome is of central importance for proper signal transduction of (hem)ITAM receptors, such as the TCR as well as GPVI and CLEC-2 in platelets. Previous studies have shown that Grb2 is part of the LAT signalosome, but the exact function of this protein in platelets is unknown. Therefore, mice with MK/platelet-specific deletion of Grb2 were analyzed.

Besides modulation of intracellular signaling pathways, regulation of receptor levels, either by internalization or intra- or extracellular proteolytic cleavage, is another important mechanism to modulate cell function. A proteomic approach provided first evidence for metalloproteinase-dependent cleavage of CD84 from the surface of human platelets. The object of this study was a detailed description of the mechanisms underlying the downregulation of CD84 receptor levels.

2 Materials and Methods

2.1 Materials

2.1.1 Chemicals and reagents

Reagent	Company
3,3,5,5-tetramethylbenzidine (TMB)	BD Biosciences (Heidelberg, Germany)
Adenosine diphosphate (ADP)	Sigma-Aldrich (Schnelldorf, Germany)
Agarose	Roth (Karlsruhe, Germany)
ALLN	Calbiochem (Bad Soden, Germany)
Amersham Hyperfilm ECL	GE Healthcare (Little Chalfont, UK)
Ammonium peroxodisulfate (APS)	Roth (Karlsruhe, Germany)
Apyrase (grade III)	Sigma-Aldrich (Schnelldorf, Germany)
Aspirin® i.v. 500 mg	Bayer (Wuppertal, Germany)
Avertin® (2,2,2-tribromoethanol)	Sigma-Aldrich (Schnelldorf, Germany)
Bovine serum albumin (BSA)	AppliChem (Darmstadt, Germany)
Calcium chloride	Roth (Karlsruhe, Germany)
Carbonyl cyanide m-chlorophenylhydrazone (CCCP)	Sigma (Schnelldorf, Germany)
Complete mini protease inhibitors (+EDTA)	Roche Diagnostics (Mannheim, Germany)
Convulxin (CVX)	Enzo Lifesciences (Lörrach, Germany)
Cyclosporin A	Calbiochem (Bad Soden, Germany)
dNTP mix	Fermentas (St. Leon-Rot, Germany)
EDTA	AppliChem (Darmstadt, Germany)
Ethidium bromide	Roth (Karlsruhe, Germany)
Fat-free dry milk	AppliChem (Darmstadt, Germany)
Fentanyl	Janssen-Cilag (Neuss, Germany)
Fibrillar type I collagen (Horm)	Nycomed (Munich, Germany)
Flumazenil	Delta Select (Dreieich, Germany)
Isofluran CP®	cp-pharma (Burgdorf, Germany)
Fura-2 acetoxymethyl ester (AM)	Invitrogen (Karlsruhe, Germany)
GeneRuler 1kb DNA Ladder	Fermentas (St. Leon-Rot, Germany)
GM6001	Calbiochem (Bad Soden, Germany)
Heparin sodium	Ratiopharm (Ulm, Germany)

Reagent	Company
Human fibrinogen	Sigma-Aldrich (Schnelldorf, Germany)
IGEPAL® CA-630	Sigma-Aldrich (Schnelldorf, Germany)
Immobilon-P transfer membrane	Millipore (Schwalbach, Germany)
Indomethacin	Alfa Aesar (Karlsruhe, Germany)
MDL 28170	Calbiochem (Bad Soden, Germany)
Medetomidine (Dormitor)	Pfizer (Karlsruhe, Germany)
Midazolam (Dormicum)	Roche (Grenzach-Wyhlen, Germany)
Midori Green Advanced DNA stain	Nippon Genetics Europe (Düren, Germany)
Naloxon	Delta Select (Dreieich, Germany)
N-ethylmaleimide (NEM)	Calbiochem (Bad Soden, Germany)
PageRuler prestained protein ladder	Fermentas (St. Leon-Rot, Germany)
Phenol/chloroform/isoamyl alcohol	Roth (Karlsruhe, Germany)
Phorbol 12-myristate 13-acetate (PMA)	Sigma (Schnelldorf, Germany)
Pluronic F-127	Invitrogen (Karlsruhe, Germany)
Prostacyclin (PGI_2)	Sigma (Schnelldorf, Germany)
Protease inhibitor cocktail (100x)	Sigma-Aldrich (Schnelldorf, Germany)
Proteinase K	Fermentas (St. Leon-Rot, Germany)
Protein G Sepharose 4 Fast Flow	GE Healthcare (Freiburg, Germany)
Rotiphorese gel 30 acrylamide	Roth (Karlsruhe, Germany)
Sodium orthovanadate	Sigma (Schnelldorf, Germany)
Triton X-100	AppliChem (Darmstadt, Germany)
Taq polymerase	Fermentas (St. Leon-Rot, Germany)
Taq polymerase buffer (10x)	Fermentas (St. Leon-Rot, Germany)
Tetramethylethylenediamine (TEMED)	Roth (Karlsruhe, Germany)
Thapsigargin (TG)	Invitrogen (Karlsruhe, Germany)
Thrombin (20 U/ml)	Roche Diagnostics (Mannheim)
Thrombin (100 U/ml)	Sigma (Schnelldorf, Germany)
Tween 20	Roth (Karlsruhe, Germany)
U46619	Enzo Lifesciences (Lörrach, Germany)
Western lightning chemiluminescence (ECL)	PerkinElmer LAS (Boston, USA)

Collagen-related peptide (CRP) was kindly provided by Prof. Dr. S.P. Watson (University of Birmingham, UK). Rhodocytin was a generous gift from Prof. Dr. J. Eble (University Hospital Frankfurt, Germany). All other non-listed chemicals were obtained from AppliChem (Darmstadt, Germany), Sigma (Schnelldorf, Germany) or Roth (Karlsruhe, Germany).

2.1.2 Cell culture materials

70 µm nylon cell strainer	BD Falcon (Heidelberg, Germany)
β-mercaptoethanol	Roth (Karlsruhe, Germany)
Fetal calf serum (FCS)	Gibco (Karlsruhe, Germany)
L-glutamine	Gibco (Karlsruhe, Germany)
Non-essential amino acids	Gibco (Karlsruhe, Germany)
Phosphate buffered saline (PBS)	Gibco (Karlsruhe, Germany)
Penicillin/streptomycin	Gibco (Karlsruhe, Germany)
RPMI medium	Gibco (Karlsruhe, Germany)
Sodium pyruvate	Gibco (Karlsruhe, Germany)
Well plates (6-well, 12-well, 24-well or 96-well)	Greiner (Frickenhausen, Germany)

2.1.3 Kits

ELISA kits:

Mouse IFNγ ELISA Set	BD Biosciences (Heidelberg, Germany)
Mouse IL-1α ELISA MAX™ Standard	Biolegend (Fell,Germany)
Mouse IL-10 ELISA Ready-SET-Go!®	eBioscience (Frankfurt, Germany)
Mouse IL-13 ELISA Ready-SET-Go!®	eBioscience (Frankfurt, Germany)
Mouse IL-2 ELISA Set	BD Biosciences (Heidelberg, Germany)
Mouse IL-3 ELISA MAX™ Standard	Biolegend (Fell,Germany)
Mouse IL-4 ELISA Set	BD Biosciences (Heidelberg, Germany)
Mouse IL-5 ELISA MAX™ Standard	Biolegend (Fell,Germany)
Mouse IL-6 ELISA MAX™ Deluxe	Biolegend (Fell,Germany)
Mouse TNF-α ELISA MAX™ Deluxe	Biolegend (Fell,Germany)
IP-ONE ELISA assay	Cisbio (Codolet, France)

Fixation and permeabilization of cells:

Foxp3/transcription factor staining buffer set	eBioscience (Frankfurt, Germany)

$CD4^+$ T cell isolation:

Dynal® Mouse CD4 negative isolation kit	Invitrogen (Karlsruhe, Germany)

NuPAGE® Pre-cast gel system for electrophoresis:

NuPAGE® Bis-Tris 4 - 12% Gel, 1.0 mm	Invitrogen (Karlsruhe, Germany)
NuPAGE® LDS Sample Buffer (4x)	Invitrogen (Karlsruhe, Germany)
SeeBlue® Plus2 Pre-Stained Standard	Invitrogen (Karlsruhe, Germany)

2.1.4 Antibodies

2.1.4.1 Antibodies and reagents used for flow cytometry

Antibodies and reagents used for analyses of immune cells:

Antibodies were purchased from eBioscience (Frankfurt, Germany), Biolegend (Fell, Germany), BD Biosciences (Heidelberg, Germany) or Miltenyi Biotec (Bergisch Gladbach, Germany), as indicated.

Antibodies are directed against the mouse protein, if not indicated otherwise.

Antibody (anti-)	Clone	Species, isotype	Company	Dilution
B220/Alexa647	RA3-6B2	rat, IgG2a, κ	BD Biosciences	1:400
CD3/PE-Cy5	145-2C11	hamster, IgG1, κ	BD Biosciences	1:100
CD4/PE	GK1.5	rat, IgG2b, κ	BD Biosciences	1:500
CD4/Alexa647	RM4-5	rat, IgG2a, κ	BD Biosciences	1:250
CD4/APC-Cy7	L3T4	rat, IgG2b, κ	BD Biosciences	1:400
CD8/PE	53-6.7	rat, IgG2a, κ	BD Biosciences	1:200
CD8/PE-Cy5	53-6.7	rat, IgG2a, κ	BD Biosciences	1:200
CD8/PE-Cy7	53-6.7	rat, IgG2a, κ	BD Biosciences	1:300
CD11b/PE	M1/70	rat, IgG2b, κ	BD Biosciences	1:200
CD25/PerCP-Cy5.5	PC61.5	rat, IgG1, λ	eBioscience	1:100
CTLA-4/biotin	UC10-4B9	hamster, IgG	eBioscience	1:50
Foxp3/PE	FJK-16s	rat, IgG2a, κ	eBioscience	1:50

Gr-1/FITC	RB6-8C5	rat, IgG2b, κ	BD Biosciences	1:1500
Helios/FITC	22F6	Hamster, IgG	Biolegend	1:20
Ki67/FITC	B56	mouse, IgG1, κ	BD Biosciences	1:20
human-CD84/FITC	MZ18-21F6	mouse, IgG1	Miltenyi Biotec	1:11
Isotype control/FITC	MOPC-21	mouse, IgG1, κ	BD Biosciences	1:20
Isotype control/ PerCP-Cy5.5	eBRG1	rat, IgG1	eBioscience	1:100

Streptavidine/FITC was purchased from DAKO (Hamburg, Germany).

Antibodies and reagents used for platelet analyses:

If not indicated otherwise, antibodies were purified in our laboratory.

Antibody	**Clone**	**Species, isotype**	**Antigen**	**Description/source**
p0p4	15E2	Rat, IgG2b	GPIbα	[193]
p0p6	56F8	Rat, IgG2b	GPIX	[200]
DOM 2	89H11	Rat, IgG2a	GPV	[200]
-	96H10	Rat, IgG2a	CD9	unpublished
JAQ1	98A3	Rat, IgG2a	GPVI	[201]
JON6	14A3	Rat, IgG2b	αIIbβ3	unpublished
INU1	-	Rat, IgG1	CLEC-2	[11]
JER1	10B6	Rat, IgG2a	CD84	[202]
-	2.4G2	Rat, IgG2b	FcγRIIb/RIII (CD16/32)	hybridoma HB-197 purchased from ATCC[203]
JON/A	4H5	Rat, IgG2b	αIIbβ3	[204]
WUG 1.9	5C8	Rat, IgG1	P-selectin	unpublished
-	12C6	Rat, IgG2b	Integrin α2	unpublished
Anti-integrin β1 chain (CD29)/FITC	9EG7	Rat, IgG2a	Integrin β1	BD Biosciences

The antibodies were labeled with *fluorescein isothiocyanate* (FITC) or with *phycoerythrin* (PE) by standard methods, as described previously.[204]

Annexin V was purified in our lab and coupled to DyLight 488 by standard methods.

2.1.4.2 Antibodies and reagents used for *in vitro* assays, Western blotting and ELISA

Western blotting and immunoprecipitation:

Antibody	Company/Description
Rabbit anti-actin (no. A2066)	Sigma-Aldrich (Deisenhofen, Germany)
Rat anti-β3 integrin-HRP (clone 57B10)	[200]
anti-Btk	Kindly provided by Dr. M. Tomlinson
anti-CLEC-2	Kindly provided by Dr. D. Mourão Sá
Rabbit anti-CD84 (product M130)	Santa Cruz Biotechnology (Heidelberg, Germany)
Rat anti-CD84-HRP (clone 10B6)	[202]
Rabbit anti-GAPDH (14C10)	Cell Signaling (Danvers, MA, USA)
Mouse anti-Grb2 (clone 3F2)	Millipore (Schwalbach, Germany)
Rabbit anti-Grb2 (product C23)	Santa Cruz Biotechnology (Heidelberg, Germany)
Rabbit anti-LAT (no. 9166)	Cell Signaling (Danvers, MA, USA)
Rabbit anti-LAT (no. 06-807) (for IP)	Millipore (Schwalbach, Germany)
Rabbit anti-phospho-LAT (Y191) (no. 3584)	Cell Signaling (Danvers, MA, USA)
Rabbit anti-phospho-LAT (Y132) (no. ab4476)	Abcam (Cambridge, UK)
Rabbit anti-phospho-Lck (Y505) (no. 2751)	Cell Signaling (Danvers, MA, USA)
Rabbit anti-LSD1 (clone C69G12)	Cell Signaling (Danvers, MA, USA)
anti-NFAT	Kindly provided by Prof. Dr. E. Serfling
Rabbit anti-p38 MAPK (no. 9212)	Cell Signaling (Danvers, MA, USA)
Rabbit anti-phospho-p38 MAPK (T180/Y182) XP® (clone D3F9)	Cell Signaling (Danvers, MA, USA)
Rabbit anti-p44/42 MAPK (ERK1/2) (no. 9102)	Cell Signaling (Danvers, MA, USA)
Mouse anti-phospho-p44/42 MAPK (ERK1/2) (T202/Y204) (clone E10)	Cell Signaling (Danvers, MA, USA)
Rabbit anti-PLCγ1 (no. 2822)	Cell Signaling (Danvers, MA, USA)
Rabbit anti-phospho-PLCγ1 (Y783) (no. 2821)	Cell Signaling (Danvers, MA, USA)
Rabbit anti-phospho-PLCγ1 (Y771) (no. 2350-1)	Epitomics (Burlingame, CA, USA)
Rabbit anti-PLCγ2 (product Q20)	Santa Cruz Biotechnology (Heidelberg, Germany)

Rabbit anti-phospho-PLCγ2 (Y759) (no.3874)	Cell Signaling (Danvers, MA, USA)
Mouse anti-phosphotyrosine (clone 4G10)	Millipore (Schwalbach, Germany)
Rabbit anti-SAPK/JNK (clone 56G8)	Cell Signaling (Danvers, MA, USA)
Rabbit anti-phospho-SAPK/JNK (T183/Y185) (no. 9251)	Cell Signaling (Danvers, MA, USA)
Sheep anti-SLP-76 (no. 06-548)	Millipore (Schwalbach, Germany)
Rabbit anti-phospho-Syk (Y525/526) (clone C87C1)	Cell Signaling (Danvers, MA, USA)
Rabbit anti-Syk (clone D1I5Q)	Cell Signaling (Danvers, MA, USA)
Mouse anti-α-tubulin (clone B-5-1-2)	Sigma-Aldrich (Deisenhofen, Germany)
Rabbit anti-Vav1 (product C-14)	Santa Cruz Biotechnology (Heidelberg, Germany)
Rabbit anti-Vav3 (no. 07-465)	Millipore (Schwalbach, Germany)
Rabbit anti-ZAP-70 XP® (clone D1C10E)	Cell Signaling (Danvers, MA, USA)
Rabbit anti-pZAP-70 (Y319)/pSyk (Y352) (clone 65E4)	Cell Signaling (Danvers, MA, USA)
Rabbit anti-mouse IgG HRP (no. P0260)	DAKO (Hamburg, Germany)
Donkey anti-sheep IgG HRP (no. HAF016)	R+D Systems (Abingdon, UK)
Goat anti-rabbit IgG (H&L) HRP (no. 7074)	Cell Signaling (Danvers, MA, USA)
Donkey anti-rat IgG HRP (no. 712-034-153)	Jackson ImmunoResearch (West Grove, PA, USA)
Biotinylated Protein Ladder Detection Pack	Cell Signaling (Danvers, MA, USA)

ELISA:

Mouse anti-human CD84 (clone MAX.3)	[174,205]
Mouse anti-human CD84 biotin (clone 2.G7)	eBioscience (Frankfurt, Germany)
Rat anti-CD84 (clone 10B6)	[202]
Hamster anti-CD84 biotin (clone CD84.7)	Biolegend (Fell, Germany)
Streptavidin-HRP (no. 016-030-084)	Jackson ImmunoResearch (West Grove, PA, USA)
Goat anti-mouse IgG (H+L) (no. 115-005-062)	Jackson ImmunoResearch (West Grove, PA, USA)
Nunc MaxiSorp™, F96-Wells	Thermo Scientific (Braunschweig, Germany)

In vitro assays:

Hamster anti-mouse CD3ε, functional grade purified	eBioscience (Frankfurt, Germany)
Goat anti-armenian hamster IgG (no. 127-005-160)	Jackson ImmunoResearch (West Grove, PA, USA)
Dynabeads® Mouse T-Activator CD3/CD28	Invitrogen (Karlsruhe, Germany)

2.1.5 Mice

Mice carrying the *Grb2* gene with exon 2 flanked by loxP sites (*Grb2*^{fl})[108] were kindly provided by Prof. Dr. Lars Nitschke (Division of Genetics, Department of Biology, University of Erlangen). To generate mice lacking Grb2 specifically in MKs and platelets, these mice were crossed with mice carrying the *platelet factor 4* (Pf4)–cre transgene (*Pf4-cre*$^{+/-}$)[206] and the offspring was genotyped by PCR as described below. Absence of Grb2 protein in platelets of *Grb2*$^{fl/fl}$*/Pf4-cre*$^{+/-}$ mice was confirmed by Western blot analysis (see results section). Littermates (*Grb2*$^{fl/fl}$*/Pf4-cre*$^{-/-}$) served as controls. The mice used for the experiments were on a C57Bl/6J background (F5).

Stim1^{Sax} mice (C3H background) were described previously[149] and genotyped as described below. The generation of CD84-deficient animals has been described in the thesis “Studies on the function and regulation of CD84, GPVI and Orai2 in genetically modified mice” by Dr. Sebastian Hofmann (University of Würzburg, 2013). Mice deficient in ADAM10 were generated in our lab and provided by Dr. Markus Bender.[192] *Adam17* transgenic mice (ADAM17$^{ex/ex}$)[207] were received from Prof. Dr. Stefan Rose-John (Kiel, Germany). ADAM17$^{ex/ex}$ bone marrow chimeras were generated by irradiation (10 Gray) of 5 - 6 week old C57Bl/6J mice (Janvier Labs, Saint Berthevin, France) and transfer of 4x10^6 bone marrow donor cells. LAT-[56] and Talin1-deficient[208] mice have also been described. Animal studies were approved by the district government of Lower Franconia (Bezirksregierung Unterfranken).

2.1.6 Buffers and media

All buffers were prepared in deionized water obtained from a MilliQ Water Purification System (Millipore, Schwalbach, Germany). pH was adjusted with HCl or NaOH.

- **ACK Lysing Buffer of erythrocyte lysis, pH 7.2 - 7.4**

NH_4Cl	150 mM
$KHCO_3$	10 mM
Na_2EDTA	0.1 mM

- **Blocking solution for immunoblotting**

Washing buffer (TBS-T, see below)	
BSA or fat-free dry milk	5%

- **Cell culture medium**

RPMI	
FCS	10%
Sodium pyruvate (100 mM)	1%
L-Glutamine (200 mM)	1%
Non-essential amino acids	1%
β-mercaptoethanol	30 µM
Penicillin/streptomycin	100 U/ml (each)

- **Coating buffer, pH 9.6**

Na_2CO_3	15 mM
$NaHCO_3$	85 mM

- **FACS buffer**

PBS (1x)	
FCS	1%
NaN_3	0.02%

- **Laemmli buffer for SDS-PAGE**

TRIS	40 mM
Glycine	0.95 mM
SDS	0.5%

- **Lysis buffer (for DNA isolation), pH 7.2**

TRIS base	100 mM
EDTA	5 mM
NaCl	200 mM
SDS	0.2%
Proteinase K (to be added directly before use)	100 µg/ml

- **Lysis buffer 2x (for tyrosine phosphorylation assay), pH 7.5**

TRIS base	20 mM
NaCl	300 mM
EDTA	2 mM
EGTA	2 mM
IGEPAL CA-630	2%
NaF	10 mM
to be added directly before use:	
Na_3VO_4	2 mM
Complete mini protease inhibitor *or*	1 tablet/10 ml
protease inhibitor cocktail (100x)	2%

- **Lysis buffer 1x (for T cell experiments), pH 7.5**

TrisHCl	20 mM
NaCl	150 mM
NaF	10 mM
Triton X-100	1%
to be added directly before use:	
Pepstatin	3 µg/ml
Leupeptin	5 µg/ml
Aprotonin	10 µg/ml
PMSF	1 mM
Na_3VO_4	1 mM

- **MOPS-Buffer, 20x**

MOPS	1 M
TRIS base	1 M
SDS	69.3 mM
EDTA	20.5 mM

- **Phosphate buffered saline (PBS), pH 7.14**

NaCl	137 mM
KCl	2.7 mM
KH_2PO_4	1.5 mM
Na_2HPO_4	8 mM

- **Sample buffer for agarose gels, 6x**

Tris buffer (150 mM)	33%
Glycerine	60%
Bromophenol blue (3',3",5',5"-tetrabromophenol-sulfonphthalein)	0.04%

- **SDS sample buffer, 4x**

β-mercaptoethanol (for reducing conditions)	20%
TRIS buffer (1 M), pH 6.8	20%
Glycerine	40%
SDS	4%
Bromophenol blue	0.04%

- **Separating gel buffer (Western Blot), pH 8.8**

TRIS/HCl	1.5 M

- **Stacking gel buffer (Western Blot), pH 6.8**

TRIS/HCl	0.5 M

- **Stripping buffer (Western Blot), pH 2.0**

PBS (1x)	
Glycine	25 mM
SDS	1%

- **TAE buffer, 50x, pH 8.0**

TRIS	0.2 M
Acetic acid	5.7%
EDTA	50 mM

- **T cell isolation buffer**

PBS (1x)	
FCS	0.2%
EDTA	2 mM

- **TE buffer, pH 8.0**

TRIS base	10 mM
EDTA	1 mM

- **Transfer buffer**

Tris Ultra	50 mM
Glycine	40 mM
Methanol	20%

- **Tris-buffered saline (TBS), pH 7.3**

NaCl	137 mM
TRIS/HCl	20 mM

- **Tyrode's buffer, pH 7.3**

NaCl	137 mM
KCl	2.7 mM
$NaHCO_3$	12 mM
NaH_2PO_4	0.43 mM
$CaCl_2$	0 or 2 mM
$MgCl_2$	1 mM
HEPES (4-(2-hydroxyethyl)-1-piperazineethanesulfonic acid)	5 mM
to be added directly before use:	
BSA	0.35%
Glucose	1%

- **Washing buffer for immunoblotting (TBS-T)**

TBS (1x)	
Tween 20	0.1%

- **Washing buffer for ELISA (PBS-T)**

PBS (1x)	
Tween 20	0.1%

2.2 Methods

2.2.1 Mouse genotyping

2.2.1.1 Isolation of genomic DNA from mouse tissue

Approximately one third of a mouse ear was dissolved in 500 µl lysis buffer at 55°C under shaking conditions (900 rpm) in a Thermomixer comfort (Eppendorf, Hamburg, Germany) 500 µl of phenol/chloroform/isoamyl alcohol were added and, after vigorous shaking, samples were centrifuged at 10,000 rpm for 10 min at *room temperature* (RT). The upper phase was carefully transferred to a new tube containing 500 µl isopropanol. After vigorous shaking, the samples were centrifuged at 14,000 rpm for 10 min at 4°C. Subsequently, the supernatant was removed and the DNA pellet was washed with 500 µl of 70% ethanol and centrifuged again at 14,000 rpm for 10 min at 4°C. Next, all the ethanol was removed and the pellet was dried for approximately 30 min at 37°C. Finally, the pellet was dissolved by adding 75 µl TE buffer and shaking (300 rpm) for 30 min at 37°C, followed by short vortexing. Usually, 1 - 2 µl DNA solution were used for a PCR reaction.

2.2.1.2 Detection of the PF4-Cre transgene by PCR

Primers:

PF4-Cre_fwd 5' CCC ATA CAG CAC ACC TTT G 3'
PF4-Cre_rev 5' TGC ACA GTC AGC AGG TT 3'

Pipetting scheme:

2 µl	genomic DNA
5 µl	Taq-buffer (10x)
5 µl	$MgCl_2$ (25 mM)
2 µl	dNTPs (10 mM)
2 µl	PF4-Cre_fwd primer (1:10 in H_2O, stock 1 µg/ml)
2 µl	PF4-Cre_rev primer (1:10 in H_2O, stock 1 µg/ml)
0.5 µl	Taq-Polymerase (5 U/µl)
31.5 µl	H_2O

PCR-Program:

95°C	5:00 min	
95°C	0:30 min	35x
58°C	0:30 min	
72°C	0:45 min	
72°C	5:00 min	
4°C	stop	

Results (expected band sizes):

wt: no PCR product

PF4-cre^{+}: 450 bp

2.2.1.3 Detection of the *Grb2* floxed allele by PCR

Primers:

Grb2_LoxP fwd	5' CCA GCA CAC ATG TCC TGC CTT C 3'
Grb2_LoxP rev	5' GGT GGC TCA CAA CCA CCT ATA AC 3'

Pipetting scheme:

1.2 µl	genomic DNA
5 µl	Taq-buffer (10x)
5 µl	$MgCl_2$ (25 mM)
1 µl	dNTPs (10 mM)
1.5 µl	Grb2_LoxP fwd primer (1:10 in H_2O, stock 100 µM)
1.5 µl	Grb2_LoxP rev primer (1:10 in H_2O, stock 100 µM)
0.5 µl	DMSO
0.2 µl	Taq-Polymerase (0.5 U/µl)
34.1 µl	H_2O

PCR-Program:

94°C	4:00 min	
95°C	0:20 min	35x
58°C	0:20 min	
72°C	0:30 min	
72°C	10:00 min	
4°C	stop	

Results (expected band sizes):

wt/wt: 241 bp

floxed/floxed: 209 bp

wt/floxed: 241 and 209 bp; 1 additional upper band

2.2.1.4 Agarose gel electrophoresis

Agarose was dissolved in 1x TAE buffer by heating it in a microwave. Depending on the length of DNA fragments to be separated, different amounts of agarose were used (1 - 2%). When the temperature had decreased to approx. 60°C, 5 µl ethidiumbromide (2 mg/ml) or Midori green per 100 ml were added and the fluid was poured into a tray with a comb. After solidification of the gel, the tray was positioned in an electrophoresis chamber containing 1x TAE buffer and the comb was removed. PCR reactions were mixed with 6x sample loading buffer and 20 µl were loaded into the slots of the gel. For size-separation DNA samples were run for approximately 45 min at about 100 -160 V, depending on the gel size. A 1 kb DNA ladder was used to determine the size of the DNA bands under UV light later on.

2.2.1.5 Genotyping of *Stim1^{Sax}* mice by Sysmex-analysis

Alterations in *mean platelet volume* (MPV) and platelet count have previously been shown to reveal the genotype of *Stim1^{Sax}* mice with 100% accuracy.[149] Therefore, to genotype *Stim1^{Sax}* mice, 50 µl blood were drawn from the retroorbital plexus of anesthetized mice using heparinized microcapillaries and collected into a 1.5 ml reaction tube containing 300 µl heparin in TBS (20 U/ml, pH 7.3). Platelet count and size were determined using a Sysmex KX-21N automated hematology analyzer (Sysmex Corp., Kobe, Japan). Mice with a platelet count of less than 30x10^3 platelets/µl diluted blood (approx. less than 30% of *wildtype* (wt) levels) and a MPV bigger than 7.0 fl (approx. 30% increase compared to wt) were regarded as carrier of the *Stim1^{Sax}* mutation (*Stim1$^{Sax/+}$* mutant mice).

2.2.2 Biochemistry

2.2.2.1 Western blotting (immunoblotting)

For Western blot analysis of the phosphorylation status of proteins, cell lysates were obtained as described in sections 2.2.4.6 and 2.2.6.4. Alternatively, for determination of Grb2 expression levels, platelets or splenocytes were centrifuged at 2,800 rpm for 5 min and resuspended in lysis buffer containing 1.5% IGEPAL and protease inhibitors. After incubation for 20 min on ice and centrifugation at 14,000 rpm for 10 min at 4°C, the supernatant was obtained.

Cell lysates were mixed with the respective amount of 4x SDS sample buffer and boiled for 5 min at 95°C. For SDS-PAGE, 15 - 25 µl per sample were loaded onto a gel with a 4% stacking part and a 10 or 12% separating part, provided in a gel chamber filled with Laemmli

buffer. Alternatively, a NuPAGE® Pre-cast gel system for electrophoresis with 4 - 12% Bis-Tris gradient gel was used.

After separation, the stacking part of the gel was removed and the gel was put into transfer buffer and subjected to immunoblotting. Transfer of proteins onto a *polyvinylidene difluoride* (PVDF) membrane was performed with a semi-dry blotting system for 70 min with 0.85 mA per cm^2 membrane at RT. To avoid non-specific binding of antibodies, the membrane was blocked for at least 40 min in blocking buffer at RT. Subsequently, the membrane was incubated with the primary antibody, diluted in blocking buffer, at 4°C overnight with gentle shaking. Afterwards, the membrane was washed at least three times for 10 min at RT. Next, the membranes were incubated with the appropriate secondary HRP-labeled antibody for 1 h at RT. Finally, the membranes were washed several times and proteins were visualized by ECL using X-ray developing films or digitally by the use of the Fluorchem™ Q system (Protein Simple, Santa Clara, CA, USA).

For stripping, membranes were incubated with stripping buffer for 20 - 25 min at RT under rotation. Afterwards, membranes were washed briefly several times in TBS-T to remove residual stripping buffer. Then, the membranes were blocked again and probed with antibodies as described.

2.2.2.2 Immunoprecipitation

For immunoprecipitation of individual proteins, platelet lysates were precleared with Protein G Sepharose for 1 h at 4°C under rotating conditions. The respective antibody and prewashed Protein G Sepharose were added to the resultant supernatant and rotated at 4°C for 2 h or overnight. The sepharose pellet was washed in a 1:1 mixture of 2x lysis buffer and Ca^{2+}-free Tyrode's buffer, containing 0.2% IGEPAL and protease inhibitors. Finally, 2x NuPAGE® LDS Sample Buffer was added to the sepharose pellet and the sample was boiled for 5 min at 95°C. Precipitated proteins were separated by SDS-PAGE and subjected to Western blotting.

2.2.3 Generation of plasma and serum samples

For generation of mouse plasma samples, blood was drawn with heparinized microcapillaries from the retroorbital plexus and collected in 1.5 ml reaction tubes containing heparin and GM6001. Samples were centrifuged at 2,800 rpm for 5 min at RT, then the supernatant was collected and centrifuged at 14,000 rpm for 10 min at RT. Finally, the supernatant was taken off and used for experiments.

Serum was prepared by drawing blood with non-heparinized microcapillaries and collected in 1.5 ml reaction tubes without heparin. In some experiments, Tyrode's buffer was provided in the reaction tube to achieve equal dilution like plasma samples, which required heparin. Clotting occurred at RT for 1 h. The samples were centrifuged for 10 min at 5,000 rpm, the supernatant was collected and centrifuged one more time as in the step before. Finally, the supernatant was used for experiments or frozen at -20°C for later use.

2.2.4 *In vitro* analyses of platelet function

2.2.4.1 Platelet preparation and washing

Mice were bled under isoflurane anesthesia from the retroorbital plexus. 700 µl blood were collected into an 1.5 ml reaction tube containing 300 µl heparin in TBS (20 U/ml, pH 7.3). 200 µl heparin were added and blood was centrifuged at 800 rpm (Eppendorf Centrifuge 5415C) for 5 min at RT. Supernatant and buffy coat were transferred into a new tube containing 200 µl heparin and centrifuged at 800 rpm for 5 min at RT to obtain *platelet rich plasma* (prp). To prepare washed platelets, prp was centrifuged at 2800 rpm for 5 min at RT in the presence of *prostacyclin* (PGI_2) (0.1 µg/ml) and apyrase (0.02 U/ml) and the pellet was resuspended in 1 ml Ca^{2+}-free Tyrode's buffer containing PGI_2 and apyrase (0.02 U/ml). After 5 min incubation at 37°C, the sample was centrifuged at 2,800 rpm for 5 min. After resuspending the platelets once more in 1 ml Ca^{2+}-free Tyrode's buffer, the platelet numbers were determined by taking a 1:1 dilution of the platelet solution and the platelet count was measured in a Sysmex KX-21N automated hematology analyzer. Finally, the pellet was resuspended in the appropriate volume of Tyrode's buffer containing apyrase (0.02 U/ml) to reach the required platelet concentration for experimenets.

For preparation of human platelets, blood (9 volumes) from healthy volunteers was collected in sodium citrate (1 volume). EDTA was added to a final concentration of 5 mM and prp was obtained by centrifugation at 300 g for 20 min. Prp was mixed 1:1 with PBS containing 5 mM EDTA and was centrifuged at 380 g in the presence of PGI_2 (0.1 µg/ml) and apyrase (0.02 U/ml) for 20 min at RT. After two washing steps (Tyrode's buffer with PGI_2 and apyrase), pelleted platelets were resuspended in Tyrode's buffer containing 2 mM Ca^{2+} and 0.02 U/ml apyrase.

2.2.4.2 Platelet counting

For determination of platelet count and size, 50 µl blood were obtained from the retroorbital plexus of anesthetized mice using heparinized microcapillaries and collected into an 1.5 ml

reaction tube containing 300 µl heparin in TBS (20 U/ml, pH 7.3). PBS was added to receive a final 1:20 dilution and the sample was analyzed with a Sysmex KX-21N automated hematology analyzer.

2.2.4.3 Flow cytometric analysis of platelets

50 µl of blood were collected in 300 µl heparin in TBS (20 U/ml, pH 7.3) and 1 ml Tyrode's buffer without Ca^{2+} was added. 50 µl of diluted blood were stained for 15 min at RT with saturating amounts of fluorophore-conjugated antibodies and analyzed directly after addition of 500 µl PBS.

To analyze platelet activation responses, blood samples were washed twice (2,800 rpm, 5 min, RT) in Tyrode's buffer without Ca^{2+} and finally resuspended in Tyrode's buffer containing 2 mM Ca^{2+}. Platelets were activated with appropriately diluted agonists for 7 min at 37°C followed by 7 min at RT in the presence of saturating amounts of PE-coupled JON/A (4H5) and FITC-coupled anti-P-selectin (5C8) antibodies. The reaction was stopped by addition of 500 µl PBS and samples were analyzed with a FACSCalibur flow cytometer using Cell Quest™ software (BD Biosciences, Heidelberg, Germany). Platelets were identified by their *forward/side scatter* (FSC/SSC) characteristics. Obtained data was analyzed using FlowJo v7 (TreeStar, Ashland, OR, USA).

2.2.4.4 Determination of phosphatidylserine exposure

Washed platelets were adjusted to a concentration of $5x10^4$/µl in Tyrode's buffer containing 2 mM Ca^{2+}. 50 µl of this suspension was used for activation with agonists for 15 min at 37°C in the presence of DyLight-488 coupled annexin V. The reaction was stopped by addition of Tyrode's buffer with 2 mM Ca^{2+} and the samples were immediately analyzed with a FACSCalibur flow cytometer.

2.2.4.5 Aggregometry

50 µl washed platelet suspension or heparinized prp (for measurements with ADP) at a concentration of $0.5x10^6$ platelets/µl were transferred into a cuvette containing 110 µl Tyrode's buffer with 2 mM Ca^{2+}. For all measurements with washed platelets, except those with thrombin as agonist, Tyrode's buffer containing 100 µg/ml human fibrinogen was used. Agonists were added as 100-fold concentrates and light transmission was recorded over 10 - 15 min with an Apact 4-channel optical aggregation system (APACT, Hamburg, Germany).

For calibration of each measurement, Tyrode's buffer (for washed platelets) or plasma (for prp) was set as 100% aggregation and washed platelet suspension or prp was set as 0% aggregation, before the agonist was added.

2.2.4.6 Protein phosphorylation studies

For platelet signaling studies using phospho-specific antibodies, washed platelets were prepared as described in 2.2.4.1, but without BSA supplementation in the Tyrode's buffer in the last washing step. Platelets were adjusted to a concentration of $0.7x10^6$/µl in BSA- and Ca^{2+}-free Tyrode's buffer and supplemented with EDTA (5 mM *final concentration* (f.c.)), apyrase (2 mM f.c.) and indomethacin (10 µM f.c.) to avoid effects of second wave mediators and to block aggregation. Platelets were stimulated with 0.5 µg/ml CVX under stirring conditions in an aggregometer at 37°C and the stimulation was stopped by mixing the platelet suspension with an equal volume of ice-cold 2x lysis buffer. Afterwards, platelet lysates were centrifuged at 14,000 rpm for 10 min at 4°C and the supernatant was mixed with 4x SDS sample buffer and subjected to Western blot analysis as described above.

For global tyrosine phosphorylation studies, using the 4G10 antibody, platelet lysates were mixed with 4x NuPAGE® LDS Sample Buffer and incubated at 70°C for 5 min. Samples were separated by SDS-PAGE using the *NuPAGE* Pre-cast gel system for electrophoresis with 4 - 12% Bis-Tris gradient gels in a MOPS-buffered system, followed by transfer onto a PVDF membrane. Membranes were blocked for 1 h in 5% milk in TBS-T and then incubated overnight with the anti-phosphotyrosine antibody 4G10, diluted in 5% BSA. Further steps were performed as described in 2.2.2.1.

2.2.4.7 Spreading assay

Glass coverslips (24x60 mm) were coated with 100 µg human fibrinogen under humid conditions at 4°C overnight and blocked for at least 1 h at RT with 1% BSA in sterile PBS. The coverslips were rinsed with Tyrode's buffer and 30 - 60 µl washed platelets (300,000 cells/µl in Tyrode's containing 2 mM Ca^{2+}) were stimulated with thrombin (0.01 U/ml) and immediately added to the fibrinogen surface. Platelets were allowed to spread at RT for the indicated time points, and then the process was stopped by addition of 300 µl 4% PFA/PBS. Excessive liquid was removed and platelets were visualized by *differential interference contrast* (DIC) microscopy with a Zeiss Axiovert 200 inverted microscope (100x/1.4 oil objective). Representative images were taken using a CoolSNAP-EZ camera (Visitron, Munich, Germany) and evaluated according to different platelet

spreading stages with ImageJ (National Institutes of Health, Bethesda, MD, USA). Spreading stages were defined as follows: 1: round, no filopodia, no lamellipodia. 2: only filopodia. 3: filopodia and lamellipodia. 4: full spreading

2.2.4.8 Adhesion under flow

Coverslips (24x60 mm) were coated with 200 µg/ml fibrillar type-I collagen (Horm) overnight at 37°C and blocked for 1 h with 1% BSA at RT. Blood (700 µl) was collected into 300 µl heparin in TBS (20 U/ml, pH 7.3) and two parts of blood were diluted with one part Tyrode's buffer with 2 mM Ca^{2+}. Platelets were labeled with a DyLight-488 conjugated anti-GPIX Ig derivative (0.2 µg/ml) for 5 min at 37°C. The diluted blood was filled into a 1 ml syringe and connected to a transparent flow chamber with a slit depth of 50 µm, equipped with the coated coverslips. Perfusion was performed using a pulse-free pump under high shear stress equivalent to a wall shear rate of 1,000 s^{-1} for 4 min. Thereafter, coverslips were washed by a 2 min perfusion with Tyrode's buffer at the same shear rate and phase-contrast and fluorescent images were recorded from at least five different microscope fields (40x objective) using a Zeiss Axiovert 200 microscope equipped with a CoolSNAP-EZ camera. Image analysis was performed off-line using MetaMorph® software (Molecular Devices, Biberach an der Riss, Germany). Thrombus formation was expressed as the mean percentage of the total area covered by thrombi (= surface coverage) and as the mean integrated fluorescence intensity per mm^2 (= thrombus size).

2.2.4.9 Measurements of intracellular Ca^{2+} levels

Washed platelets were adjusted to a concentration of approximately $0.4x10^6$/µl in Ca^{2+}-free Tyrode's buffer. 100 µl of this suspension were loaded with 5 µM fura-2-AM in the presence of 0.2 µg/ml Pluronic F-127 for 25 min at 37°C. After labeling, the platelets were washed once and resuspended either in 500 µl Tyrode's buffer containing 1 mM Ca^{2+} (for measurement of Ca^{2+} influx) of 2 mM EGTA (for measurements of store release). This cell suspension was transferred into a cuvette, which had been blocked for 30 min with 1% BSA in water at RT, and fluorescence was measured with a PerkinElmer LS 55 fluorimeter (Perkin Elmer, Waltham, MA, USA) under stirring conditions. Excitation was alternated between 340 and 380 nm and emission was measured at 509 nm. Basal Ca^{2+} levels were recorded for 50 s before the indicated reagent or agonist was added. Each measurement was calibrated using 1% Triton X-100 and EGTA.

2.2.4.10 Clot retraction

Mice were bled from the retroorbital plexus under isoflurane anesthesia and up to 1 ml blood was collected into a 1.5 ml reaction tube containing 70 µl citrate. Platelets were isolated, washed once in Ca^{2+}-free tyrode's buffer and adjusted to a concentration of $3x10^5$/µl in the pooled platelet poor plasma which was obtained during platelet isolation. 250 µl of the platelet suspension were mixed with 1 µl erythrocyte suspension in an aggregometry cuvette and supplemented with 20 mM $CaCl_2$ (f.c.) for recalcification. Clot formation was induced by adding high concentrations of thrombin (5 U/ml f.c.). Clot retraction was recorded with a digital camera over a time span of 4.5 hours after activation.

2.2.4.11 Shedding of glycoproteins from the platelet surface

Washed platelets resuspended at a concentration of approximately $3x10^5$/µL in Tyrode's buffer containing 2 mM Ca^{2+} and 0.02 U/ml apyrase were treated for 1 h with CCCP (100 µM), W7 (150 µM), DMSO (vehicle control), for 20 min with NEM (2 mM) or for 15 min with PMA (50 ng/ml) at 37°C. Where indicated, platelets were pretreated with the calpain inhibitors calpeptin (5 µg/ml), ALLN (50 µM) or MDL 28170 (50 µM) and/or the broad range metalloproteinase inhibitor GM6001 (100 µM) for 15 min at 37°C, or with DMSO as a vehicle control. Alternatively, platelets were treated for 1 h with the platelet agonists CVX, CRP, rhodocytin or thrombin. Where indicated, aggregation of mouse platelets was inhibited with saturating concentrations of the integrin αIIbβ3 blocking antibody JON/A $F(ab)_2$.[204]

For flow cytometric analysis, a small sample volume was diluted 1:15 in PBS, stained with FITC-labeled antibodies and analyzed as described in 2.2.4.3.

For detection of *soluble CD84* (sCD84), samples were centrifuged at 2,800 rpm for 5 min at RT and the supernatants were analyzed using the CD84 ELISA system, as described below.

For Western blot analysis, platelets were lysed by addition of a 4:1 mixture of 4x SDS sample buffer (non reducing) and 10% IGEPAL directly into the platelet suspension. Samples were boiled for 5 min at 95°C and subjected to Western blot analysis, as described in 2.2.2.1.

2.2.4.12 Detection of cleaved soluble CD84 by ELISA

Detection of soluble mouse CD84

Nunc MaxiSorp™ plates were coated overnight with 50 µl of 10 µg/ml JER1 antibody, diluted in coating buffer. On the next day, the plates were washed 3 times with PBS-T and blocked for at least 1 h with 10% fat free milk in PBS. After one washing step, 50 µl of the

supernatant from platelets treated with different shedding inducing agents or agonists (see above), plasma or serum samples were transferred to the wells and incubated for 2 h at RT under slight agitation. After five washing steps, plates were incubated with biotinylated mCD84.7 antibody (10 µg/ml), diluted in 10% fat-free milk in PBS-T, for 1 h at RT (50 µl/well). Plates were washed five times and incubated for 45 min with HRP-labeled streptavidin, diluted 1:3000 in 1% fat-free milk in PBS-T (50 µl/well). After five washing steps, plates were developed using *3,3,5,5-tetramethylbenzidine* (TMB). The reaction was stopped by addition of 2 M H_2SO_4 (50 µl/well) and absorbance at 450 nm and 620 nm (background) was measured with a Multiskan Ascent Plate Reader (Thermo Scientific).

Detection of soluble human CD84

The ELISA was performed in a similar way as the mouse sCD84 ELISA. MAX.3 antibody (10 µg/ml) was used for coating the plates, biotinylated 2G7 (5 µg/ml) served as the detection antibody.

2.2.5 *In vivo* analyses of platelet function

2.2.5.1 Intravital microscopy of $FeCl_3$-injured mesenteric arterioles

Mice (15 - 18 g body weight) were anesthetized and the mesentery was exteriorized through a midline abdominal incision. Arterioles with a diameter of 35 - 60 µm were visualized using a Zeiss Axiovert 200 inverted microscope (10x/0.25 air objective) equipped with a 100 W HBO fluorescent lamp and a CoolSNAP-EZ camera. Injury was induced by topical application of a 3 mm^2 filter paper saturated with 20% $FeCl_3$. Adhesion and aggregation of fluorescently labeled platelets (achieved by previous intravenous injection of a DyLight-488 conjugated anti-GPIX Ig derivative) in arterioles was monitored for 40 min or until complete occlusion occurred (blood flow stopped for >1 min). When indicated, acetylsalicylic acid (Aspirin® i.v.; 1 mg/kg body weight) was injected intravenously 10 min prior to the experiment.

Digital images were recorded and analyzed using MetaMorph software. All $FeCl_3$-injury experiments shown in this study were performed and evaluated by Martina Morowski in our research group.

2.2.5.2 Mechanical injury of the abdominal aorta

The abdominal cavity of anesthetized mice (20 - 26 g body weight) was opened by a longitudinal midline incision and the abdominal aorta was carefully exposed. A Doppler ultrasonic flow probe (Transonic Systems, New York, USA) was placed around the aorta and

mechanical injury was induced by firm compression with a forceps and blood flow was monitored for 30 min or until full occlusion. When indicated, acetylsalicylic acid (1 mg/kg body weight) was injected intravenously 10 min prior to the experiment. All aorta injury experiments shown in this study were performed by Martina Morowski in our research group.

2.2.5.3 Bleeding time assay

Mice were anesthetized using triple anesthesia (dormitor, dormicum and fentanyl) and a 1 mm segment of the tail tip was cut off using a scalpel. Blood drops were gently absorbed every 20 s using a filter paper without touching the wound site. When no blood was observed on the paper, bleeding was determined to have ceased. Experiments were stopped after 20 min by cauterization. When indicated, acetylsalicylic acid (1 mg/kg body weight) was injected intravenously 10 min prior to the experiment.

2.2.5.4 *Transient middle cerebral artery occlusion* (tMCAO) model

Experiments were conducted on 8 - 12 week old mice by Dr. Peter Kraft and colleagues in the group of Prof. Dr. Guido Stoll (Department of Neurology, University Hospital, Würzburg) according to the recommendations for research in mechanism-driven basic stroke studies.[209] tMCAO was induced under inhalation anesthesia with the intraluminal technique.[210] Briefly, a midline neck incision was made and a standardized silicon rubber–coated 6.0 nylon monofilament (6021PK10, Doccol, Redlands, CA, USA) was inserted into the right common carotid artery and advanced via the internal carotid artery to occlude the origin of the middle cerebral artery. After 60 min, the filament was withdrawn to allow reperfusion.

24 h after tMCAO the global neurological status was assessed by the Bederson score.[211] Motor function and coordination were graded with the grip test.[212]

For determination of the ischemic brain infarct volume, mice were euthanized 24 h after induction of tMCAO and brain sections were stained with 2% *2,3,5-triphenyltetrazolium chloride* (TTC; Sigma-Aldrich). Planimetric measurements were performed using ImageJ software and used to calculate lesion volumes, which were corrected for brain edema as described.[213]

2.2.6 Isolation and analyses of immune cells

2.2.6.1 Isolation and processing of lymphoid tissues and blood cells

Mice were sacrificed and spleen, thymus and lymph nodes (inguinal, brachial, axillary, superficial cervical, mesenteric and lumbal) were dissected and placed in PBS/ 1% FCS on ice. After collection of all tissues, organs were rubbed through 70 μm cell strainers with a plunger of a syringe to receive a single cell suspension. The suspensions were centrifuged in 15 or 50 ml Falcon tubes at 480 g for 5 min at 4°C (Heraeus Multifugen3S-R). Next, lymph node and thymus cell pellets were resuspended in an appropriate volume (≈ 5 ml) of cell medium or PBS/ 1% FCS for counting. Cell pellets from spleen cells were depleted from red blood cells by resuspension 5 ml ACK buffer (hypo-osmotic shock). Supernatant was then rinsed through a 70 μm cell strainer into a 15 or 50 ml Falcon tube and, after refilling with PBS/ 1% FCS, centrifuged as before. Finally, cell pellets were resuspended in an appropriate volume for counting (5 - 10 ml).

Cell counts were determined with a Sysmex KX-21N automated hematology analyzer or with a counting chamber, using trypan blue staining to exclude dead cells.

To isolate immune cells from the blood compartment, blood was drawn from the retroorbital plexus with heparinized microcapillaries and collected in 1.5 ml reaction tubes containing heparin. Samples were centrifuged at 2,800 rpm for 5 min at RT and the blood cell pellet was resuspended in ACK buffer (resuspension volume: 1.5 ml for samples up to 100 μl and 10 ml for samples of 700 μl blood). Samples were centrifuged at 2,800 rpm for 5 min and the supernatant and red blood cell debris was aspirated. Cell pellets were resuspended in PBS/ 1% FCS.

2.2.6.2 Flow cytometric analysis of immune cells

Usually, the volumes for $1x10^6$ cells of single cell suspensions were transferred into a v-bottomed 96-well plate, filled with FACS buffer and washed by centrifugation for 3 min at 480 g. The supernatant was discarded and the Fc-receptors were blocked by resuspension of cells in 25 μl FACS buffer containing 2.4G2 antibody (10 μg/ml f.c.) and incubation for at least 15 min on ice. Next, appropriately diluted antibodies were added in a volume of 25 μl FACS buffer, resulting in a total staining volume of 50 μl. After a minimum incubation time of 15 min on ice in the dark, cells were washed in FACS buffer, resuspended and transferred into an appropriate tube for FACS analysis and measured in a total volume of about 300 μl FACS buffer.

For intracellular staining of Ki-67, Foxp3 and *cytotoxic T lymphocyte antigen 4* (CTLA-4) expression, the cells were first blocked and then stained with antibodies directed against surface antigens, as described above. For fixation and permeabilization, cells were washed once with FACS buffer and resuspended in 100 µl of freshly prepared Foxp3 fixation/ permeabilization buffer, and then incubated for at least 30 min at RT in the dark. Then the fixation reagent was removed by washing the cells with permeabilization buffer. The cells were blocked for 30 min on ice in 25 µl of a 1:50 dilution of rat serum in permeabilization buffer. Next, antibodies, appropriately diluted in 25 µl permeabilization buffer, were added and allowed to bind for at least 30 min on ice. After two washing steps (the first one in permeabilization buffer, the second one in FACS buffer), the cells were ready for flow cytometric analysis as described above.

Measurements of immune cells were carried out on a FACSCalibur™ flow cytometer using Cell Quest™ software or on a FACSCanto™ II operating with FACSDiva™ software (BD Biosciences, Heidelberg, Germany). Compensation was performed prior to each experiment. Obtained data was analyzed using FlowJo v7. Dot plots and histograms are shown as $\log_{10}$ fluorescence intensities on a four-decade scale.

2.2.6.3 Isolation of CD4$^+$ T cells

CD4$^+$ T cells were purified from lymph node cell suspensions and red blood cell depleted spleen cell suspensions of wt or *Stim1*$^{Sax/+}$ mice by magnetic depletion of cells positive for CD8, CD45R (B220), CD11b (Mac1), Ter-119 or CD16/CD32 using the Dynal® Mouse CD4 negative isolation kit and the MACSiMAG™ Separator (Miltenyi Biotec, Bergisch Gladbach, Germany). When cells were isolated from pure lymph node suspensions, the amount of beads was reduced to 1/3 of the manufacturer's recommendation. Cell count of the purified cells was determined as described above. The cell purity of CD4$^+$ T cells, as assessed by flow cytometry (CD4$^+$CD3$^+$ cells), was 93% or higher.

2.2.6.4 *In vitro* stimulation of T cells for signaling studies (anti-CD3 crosslinking)

Either lymph node cells or purified CD4$^+$ T cells (see above) were used for these experiments. When lymph node cells were used, comparable frequencies of B and T cells between wt and *Stim1*$^{Sax/+}$ samples were confirmed by flow cytometry.

Freshly isolated CD4$^+$ T cells were allowed to rest for at least 1 h at a cell concentration of about 5x10^6/ml in cell culture medium at 37°C in the incubator before being subjected to the

next steps. When indicated, cyclosporin A (10 µg/ml f.c.) or DMSO, as vehicle control, was added to the media.

The cells were centrifuged at 480 g for 5 min and adjusted to a concentration of $1x10^6$/ml in ice cold PBS containing either 0 or 2 mM Ca^{2+}. When indicated, cyclosporin A (10 µg/ml f.c.) or DMSO, as vehicle control, was added to the buffer. Hamster anti-mouse CD3ε antibody was added at a final concentration of 10 µg/ml and cells were incubated for 15 - 20 min on ice. To remove unbound antibody, additional buffer was added and the cells were centrifuged at 480 g at 4°C for 5 min. Next, cells were resuspended at a concentration of $1x10^6$/ml in their respective buffer (at RT), spread into four 1.5 ml reaction tubes and briefly incubated at 37°C in a Thermomixer. Stimulation was initiated by addition of 10 µl prediluted goat anti-armenian hamster IgG (110 µg/ml) per 100 µl cell suspension resulting in a final antibody concentration of 10 µg/ml. Incubation was stopped by addition of ice cold PBS and centrifugation at 14,000 rpm for 5 min at 4°C. Finally, the supernatant was removed and the cell pellets were either frozen or directly lysed in lysis buffer.

2.2.6.5 Cell fractionation for determination of NFAT localization

$CD4^+$ T cells were stimulated as described above. Cell pellets were washed twice in PBS and then resuspended in hypotonic lysis-buffer (10 mM Tris-HCl, 10 mM NaCl, 3 mM $MgCl_2$, pH 7.5; 60 µl for $1x10^6$ cells). After 15 min incubation on ice, cells were transferred onto a QiaShredder Column (Qiagen, Hilden, Germany) and centrifuged at 14,000 rpm for 2 min at 4°C. To separate the nuclear from the cytosolic fraction, the flowthrough was centrifuged for 15 min at 800 rpm at 4°C. The supernatant (= cytosolic fraction) was collected and the remaining nuclei were washed twice in hypotonic wash buffer (10 mM Tris-HCl, 10 mM NaCl, 3 mM $MgCl_2$, 0.5% IGEPAL; pH 7.5). Finally, the purified nuclei were lysed with hypertonic lysis buffer (20 mM Tris-HCl, 280 mM NaCl, 10 mM NaF, 2% Triton X 100; pH 7.5; 60 µl for $1x10^6$ cells) and centrifuged at 12,500 rpm for 10 min at 4°C. The supernatant was collected for Western blotting. The cell fractionation of $CD4^+$ T cells depicted in this thesis was performed by Dr. Christoph Hintzen.

2.2.6.6 Measurement of IP_3 production

$8x10^6$ lymph node cells were centrifuged in an 1.5 ml reaction tube and adjusted to a concentration of $1x10^6$ cells/ml (800 µl) in a modified phosphate-free Tyrode's buffer, containing 0.2% BSA, 50 mM $LiCl_2$ and either 0 or 2 mM $CaCl_2$. Hamster anti-mouse CD3ε antibody was added at a final concentration of 10 µg/ml and cells were incubated for

15 - 20 min on ice. To remove unbound antibody, additional buffer was added and the cells were centrifuged at 2,800 rpm at 4°C for 5 min. Next, cells were resuspended at a concentration of $1x10^6$/ml (800 µl) in their respective buffer (at RT) and briefly incubated at 37°C in a Thermomixer. The cells were activated by addition of 80 µl prediluted goat anti-armenian hamster IgG (110 µg/ml), resulting in a final antibody concentration of 10 µg/ml for 15 min at 37°C (300 rpm). After stimulation, the cells were centrifuged at 2,800 rpm for 5 min at RT and the pellet was lysed in 133 µl lysis buffer provided within the IP-ONE ELISA kit.

50 µl of lysed lymph node cells were used for the IP_1 ELISA assay which was used with the following modifications: Standard, IP_1-conjugate and the monoclonal antibody were diluted 1:1 in assay dilutent and instead of the kit's plate, a Nunc MaxiSorp™ plate, coated with 10µg/ml goat-anti mouse antibody, was used for the experiments.

The T cell and B cell frequencies were determined for each sample by flow cytometry to ensure comparability between wt and *Stim1*$^{Sax/+}$ samples.

2.2.6.7 Determination of cytokine levels

For *in vitro* stimulation of T cells, 24-well plates were coated with 300 µl of hamster anti-mouse CD3ε antibody (10 µg/ml in PBS) and incubated at 4°C overnight. The next day, wells were washed twice with PBS, before $2x10^6$ splenocytes, in a volume of 1 ml cell culture medium, were transferred into each well. Untreated plates served as negative control. After 48 h of incubation, the cell supernatants were transferred into 1.5 ml reaction tubes and centrifuged at 14,000 rpm for 5 min. Supernatants were frozen at -20°C for later analysis. Alternatively, $1x10^6$ splenocytes in 1 ml cell culture medium were stimulated with 25 µl Dynabeads® Mouse T-Activator CD3/CD28 beads, according to the manufacturer's instruction.

Cytokine levels in cell culture supernatants were determined with the ELISA kits listed in the "Materials" section in combination with Nunc MaxiSorp™ plates, according to the manufacturer's instruction.

2.2.7 Statistical analysis

If not stated otherwise, the results shown are mean ± SD. When applicable, a modified t-test (Welch's test) was used to analyze differences between two groups. The Fischer's exact test was applied to assess variance in occurrence of occlusion. For analysis of more than two groups, one-way Anova and the Bonferroni multiple comparison post-hoc test were applied.

For analysis of the Bederson score and the grip test analysis, the Mann-Whitney-U-test was applied. p-values <0.05 were considered as statistically significant (*), p<0.01 (**) and p<0.001 (***).

3 Results

3.1 Investigation of T cell receptor signaling in *Stim1$^{Sax/+}$* mice

STIM1 is established as an essential mediator of SOCE in lymphocytes[67] and platelets.[14] Substitution of critical aspartate and glutamate residues within the EF-hand motif of STIM1 has been previously shown to abolish Ca^{2+} binding and to render the protein constitutively active *in vitro*[129,150] and *in vivo,*[149] resulting in continuous Ca^{2+} influx and elevated *intracellular Ca^{2+} levels* ($[Ca^{2+}]_i$) (see introduction). T cells from mice with such a STIM1-activating mutation (D84G, *Stim1$^{Sax/+}$* mice) exhibited no obvious overt phenotype, but were not studied in detail so far. Therefore, one aim of this thesis was to investigate the impact of elevated $[Ca^{2+}]_i$ on TCR signaling and T cell function using *Stim1$^{Sax/+}$* mice. These signaling studies were performed in collaboration with the group of Dr. Heike Hermanns (Rudolf Virchow Center for Experimental Biomedicine, Würzburg).

3.1.1 Normal T cell development in *Stim1$^{Sax/+}$* mice

To confirm the previous observation of unaltered T cell development and distribution in *Stim1$^{Sax/+}$* mice,[149] lymphocyte frequencies in lymphoid organs were determined by flow cytometry. In line with the previous results, thymocyte subset composition based on CD4 and CD8 expression was indistinguishable between *wildtype* (wt) and *Stim1$^{Sax/+}$* mice, indicating normal T cell development (Figure 3-1 A). Likewise, the prevalence of $CD4^+$ and $CD8^+$ cells ($CD4^+$ and $CD8^+$) and B cells ($B220^+$) in lymph nodes and spleen did not differ significantly. In spleen a slight tendency towards lower lymphocytes frequencies was observed (Figure 3-1 A), which most likely originates from the disproportionately high expansion of non-lymphoid cells ([149] and data not shown). Similar to lymph node and spleen, the blood cell composition of *Stim1$^{Sax/+}$* mice was comparable to wt mice, except for a slight, but significant increase in Gr-$1^{low}$$CD11b^+$ myelomonocytic cells (Figure 3-1 B). *Stim1$^{Sax/+}$* mice developed a pronounced splenomegaly, and, in contrast to the observation of *Grosse et al.*,[149] an elevation of total spleen cell numbers was observed (Figure 3-1 C).

3.1.2 NFAT resides in the nucleus of *Stim1$^{Sax/+}$* $CD4^+$ T cells in the absence of stimulation

One of the major effects of Ca^{2+} influx into T cells is the activation of the Ca^{2+}/calmodulin-dependent phosphatase calcineurin, which dephosphorylates *nuclear factor of activated T*

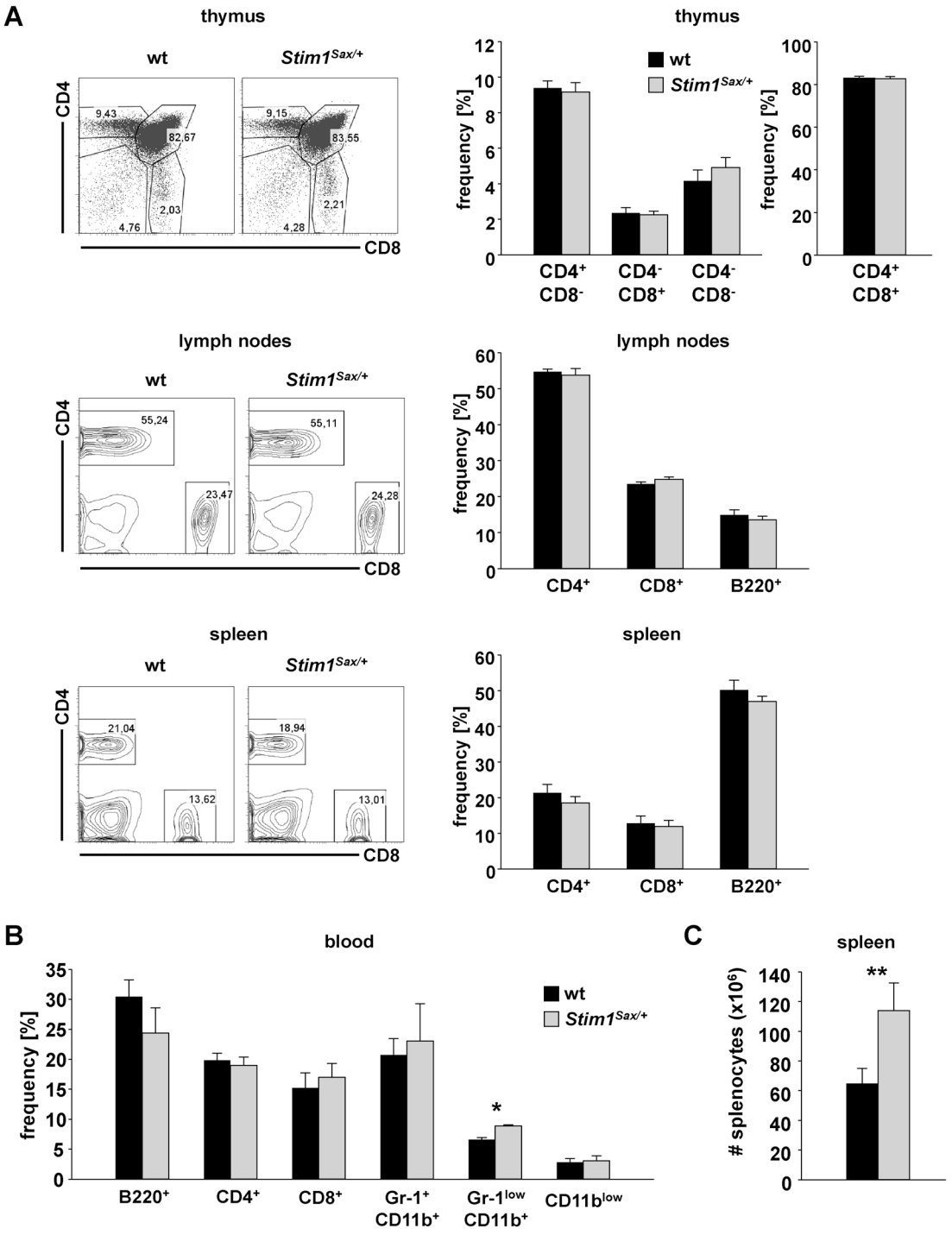

Figure 3-1 Unaltered T cell development and lymphocyte subsets in *Stim1*$^{Sax/+}$ mice. (A) Thymocyte subsets (upper panel) and lymphocyte subsets in lymph nodes and spleen (middle and lower panel) of wt and *Stim1*$^{Sax/+}$ were analyzed by flow cytometry. Representative dot plots are shown on the left, bar graphs depict the mean population frequencies ± SD. **(B)** Flow cytometric analysis of blood immune cell composition. **(C)** Total spleen cell numbers in wt and *Stim1*$^{Sax/+}$ mice. (n≥3 per group); * $p<0.05$ and ** $p<0.01$

cells (NFAT), thereby facilitating its transfer from the cytoplasm into the nucleus (Figure 3-2 A).[68] Therefore, it was investigated whether the elevation in $[Ca^{2+}]_i$ which had previously been observed in *Stim1*$^{Sax/+}$ T cells[149] is sufficient to induce the translocation of NFAT into the nucleus. To this aim, $CD4^+$ T cells isolated from wt and *Stim1*$^{Sax/+}$ animals were stimulated by antibody-mediated crosslinking of the CD3 receptor (further on also termed anti-CD3 crosslinking), mimicking TCR-dependent activation. The lysates of these cells were separated into a nuclear and cytoplasmic fraction and NFAT levels in each fraction were determined by Western blotting (Figure 3-2 B). In the presence of extracellular Ca^{2+}, NFAT was found to be localized almost exclusively in the cytoplasmic fraction in non-stimulated wt $CD4^+$ T cells, but rapidly shifted into the nucleus within 2 minutes after stimulation. This translocation was transient since NFAT was equally distributed between the two fractions after 5 minutes of stimulation and finally, 15 minutes after the stimulus, the initial cytoplasmic localization was re-established. In sharp contrast, NFAT was found to be localized in the nucleus of *Stim1*$^{Sax/+}$ $CD4^+$ T cells at every time point examined, even in the absence of stimulation.

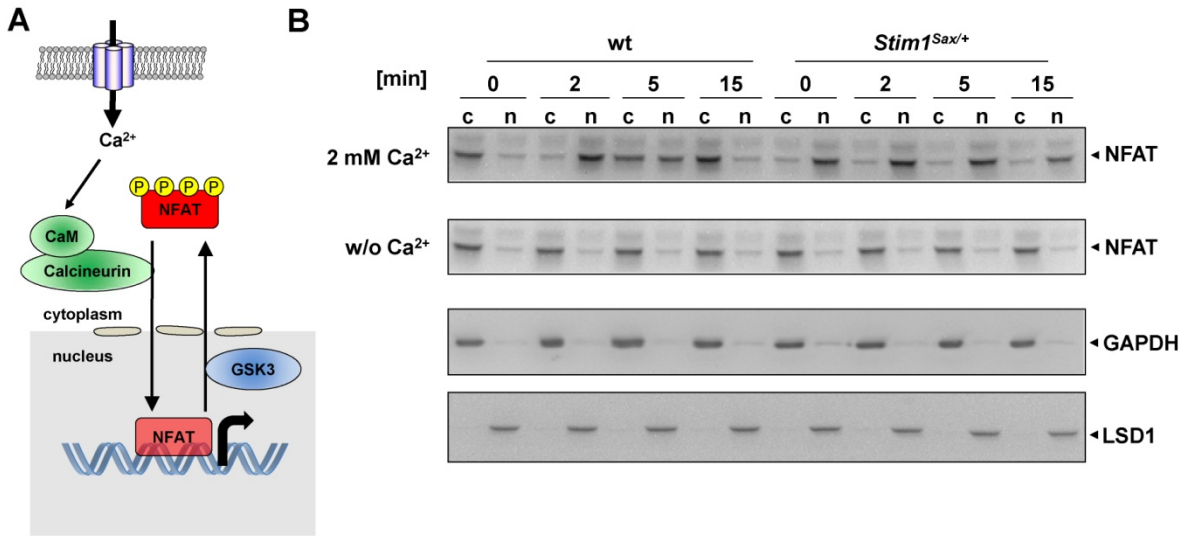

Figure 3-2 NFAT always resides in the nucleus in *Stim1*$^{Sax/+}$ $CD4^+$ T cells in the presence of extracellular Ca^{2+}. (A) Schematic representation of the NFAT shuttling mechanism between cytoplasm and nucleus; CaM, calmodulin; GSK3, glycogen synthase kinase 3 **(B)** Analysis of NFAT localization. $CD4^+$ T cells were preincubated with anti-CD3 antibody, followed by crosslinking with a secondary antibody for the indicated time points in the presence or absence of extracellular Ca^{2+}.The cell lysates were fractionated into the cytoplasmic (c) and the nuclear (n) fraction and samples were subjected to Western blotting and stained with an anti-NFAT antibody. GAPDH and LSD1 were used to control the purity of the cytoplasmic and nuclear fraction, respectively.

In the absence of extracellular Ca^{2+}, both the stimulation-induced NFAT translocation in wt $CD4^+$ T cells as well as constitutive localization of NFAT in the nucleus of *Stim1*$^{Sax/+}$ $CD4^+$ T cells were abolished, highlighting the importance of extracellular Ca^{2+} influx in this process. These data clearly indicated that the continuous Ca^{2+} influx triggered by the *Stim1*^{Sax} mutation results in intracellular Ca^{2+} levels sufficient to activate the phosphatase calcineurin and to promote NFAT translocation.

3.1.3 Altered phosphorylation of PLCγ1 in *Stim1*$^{Sax/+}$ CD4$^+$ T cells due to calcineurin activity

In the next experiment, the impact of elevated $[Ca^{2+}]_i$ on the TCR proximal signaling steps was investigated. For this, the phosphorylation status of essential proteins in the TCR-signaling pathway was analyzed by Western blotting. Stimulation of wt and *Stim1*$^{Sax/+}$ $CD4^+$ T cells by anti-CD3 crosslinking resulted in a comparable and transient phosphorylation of Lck, a member of the Src kinase family which initiates TCR signaling by phosphorylation of the ITAMs within the TCR-associated CD3 chains (Figure 3-3). Similarly, ZAP-70, a kinase binding to phosphorylated ITAMs and a substrate of Lck, became phosphorylated 2 minutes after stimulation to a similar extent in $CD4^+$ T cells of wt and *Stim1*$^{Sax/+}$ mice. Moreover, phosphorylation patterns were not affected by the withdrawal of extracellular Ca^{2+} (Figure 3-3), indicating that extracellular Ca^{2+} influx does not affect these signaling events at the proximal end of the TCR signaling cascade.

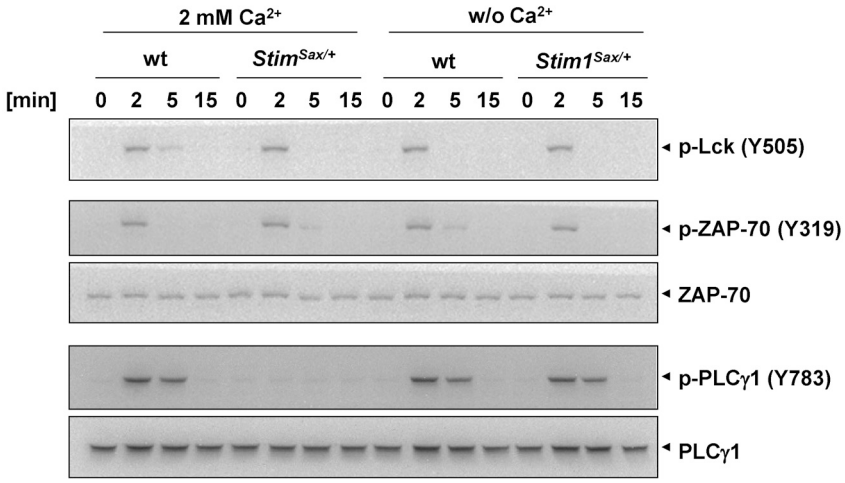

Figure 3-3 Impaired PLCγ1 phosphorylation in the presence, but not in the absence of extracellular Ca^{2+} in *Stim1*$^{Sax/+}$ CD4$^+$ T cells. Wt and *Stim1*$^{Sax/+}$ $CD4^+$ T cells were stimulated by antibody-crosslinking of the CD3 receptor for the indicated time points in the presence (2 mM) or absence (w/o) of extracellular Ca^{2+}. Cell lysates were subjected to Western blotting and the membrane was probed with the indicated antibodies.

To investigate downstream signaling events, the phosphorylation status of PLCγ1 was analyzed using a phospho-specific antibody directed against tyrosine 783 (Y783). Phosphorylation of PLCγ1 at this site has been reported to be required for the enzyme's activity.[214,215] Strikingly, while in wt CD4$^+$ T cells phosphorylation of PLCγ1 became clearly visible 2 and 5 minutes after activation, phosphorylation of PLCγ1 at Y783 was completely abolished in *Stim1*$^{Sax/+}$ CD4$^+$ T cells. However, this was only observed in the presence of extracellular Ca^{2+}, since phosphorylation of PLCγ1 at Y783 was completely restored upon withdrawal of Ca^{2+} from the medium (Figure 3-3). Hence, it can be concluded that the continuous Ca^{2+} influx, triggered by the *Stim1*^{Sax} mutation, interferes with proper phosphorylation of PLCγ1 in CD4$^+$ T cells.

The permanent localization of NFAT inside the nucleus of *Stim1*$^{Sax/+}$ CD4$^+$ T cells implicated constitutive calcineurin activity. To investigate a possible impact of calcineurin on the phosphorylation status of PLCγ1, CD4$^+$ T cells were pretreated with the calcineurin inhibitor *cyclosporin A* (CsA) in Ca^{2+} containing buffer. In wt CD4$^+$ T cells, CsA treatment had virtually no effect on PLCγ1 phosphorylation (Figure 3-4, upper panel). In marked contrast, CsA rescued the phosphorylation of PLCγ1 at Y783 in *Stim1*$^{Sax/+}$ CD4$^+$ T cells, resulting in a comparable phosphorylation pattern as observed under Ca^{2+}-free conditions (Figure 3-4, lower panel). Therefore, calcineurin activity is involved in the translation of elevated $[Ca^{2+}]_i$ into impaired PLCγ1 phosphorylation in *Stim1*$^{Sax/+}$ CD4$^+$ T cells.

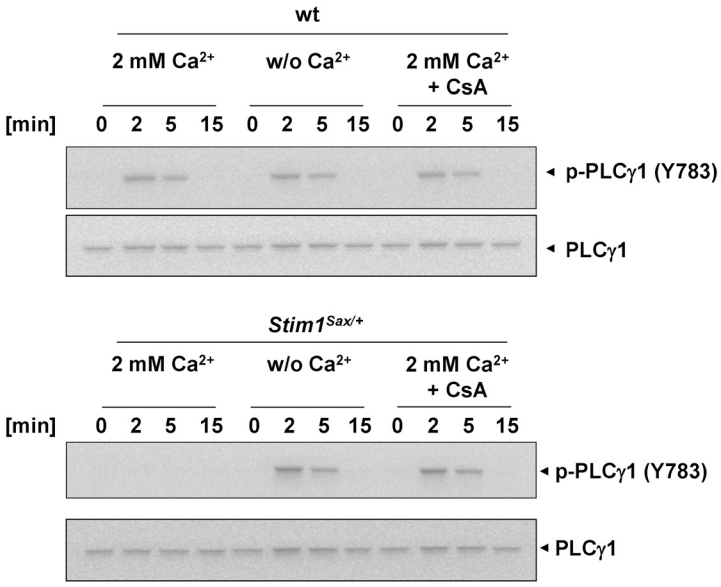

Figure 3-4 Impaired phosphorylation of PLCγ1 in *Stim1*$^{Sax/+}$ CD4$^+$ T cells can be rescued by CsA. CD4$^+$ T cells were stimulated by antibody-crosslinking of the CD3 receptor for the indicated time points in the presence (2 mM) or absence (w/o) of extracellular Ca^{2+}. When indicated, cells were pretreated with CsA. Cell lysates were subjected to Western blotting and stained with anti-p-PLCγ1 (Y783) antibody and reprobed with anti-PLCγ1 antibody.

3.1.4 Despite alterations in the phosphorylation pattern, the enzymatic activity of PLCγ1 in *Stim1*$^{Sax/+}$ CD4^{+} T cells is unaltered

Phospho-specific antibodies directed against critical residues are a powerful and easy to use tool to directly visualize the phosphorylation status of distinct amino acids. However, the drawback of this technique is that phosphorylation of a single residue may not reflect the protein's catalytic activity, especially when a protein possesses various phosphorylation sites. To address this issue, PLCγ1 was immunoprecipitated, transferred onto a membrane, and its overall tyrosine phosphorylation status was analyzed using the pan anti-phospho-tyrosine antibody 4G10. T cells from *Stim1*$^{Sax/+}$ mice clearly exhibited PLCγ1 phosphorylation upon stimulation in the presence of extracellular Ca^{2+} despite the loss of phosphorylation at Y783, however, to a slightly lesser extent than wt T cells (Figure 3-5). This indicated that other tyrosine residues than Y783 become phosphorylated at PLCγ1 in *Stim1*$^{Sax/+}$ T cells. To show this directly, a phospho-specific antibody against the activation-induced phosphorylation site Y771[216,217] was tested. Surprisingly, this antibody revealed elevated phosphorylation of PLCγ1 at this tyrosine residue in *Stim1*$^{Sax/+}$ T cells when extracellular Ca^{2+} was present. Analogous to phosphorylation at Y783, but with opposing effect, withdrawal of extracellular Ca^{2+} abolished the enhanced phosphorylation at Y771 in *Stim1*$^{Sax/+}$ T cells,

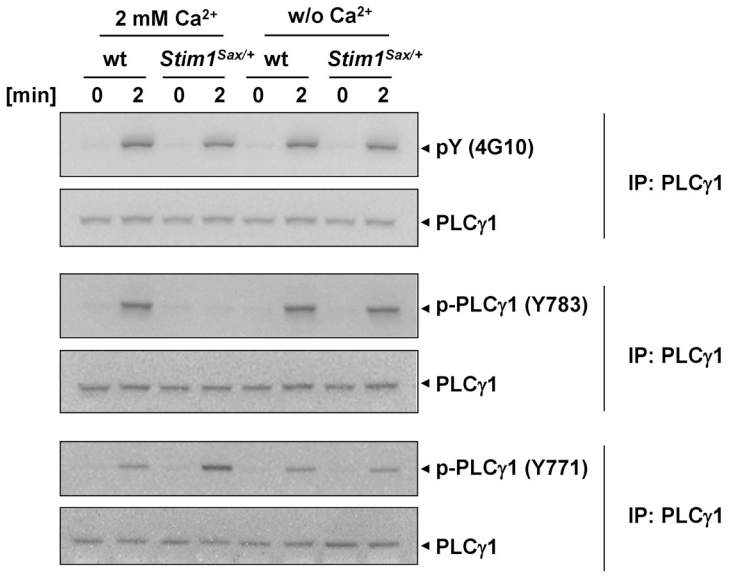

Figure 3-5 Altered phosphorylation pattern of PLCγ1 in *Stim1*$^{Sax/+}$ T cells. Wt and *Stim1*$^{Sax/+}$ lymph node cells were stimulated by anti-CD3 crosslink for 2 min or left untreated, in the presence (2 mM) or absence (w/o) of extracellular Ca^{2+}. PLCγ1 was immunoprecipitated and the samples were blotted and stained with 4G10 (total pY) or anti-p-PLCγ1 antibodies (either specific for Y771 or Y783). Membranes were reprobed with anti-PLCγ1 antibody as a loading control.

resulting in a signal similar to wt cells. In summary, this data shows that the continuous Ca^{2+} influx, triggered by the *Stim1*^{Sax} mutation, leads to changes in the phosphorylation pattern of PLCγ1 on at least two different tyrosine residues, where both, abolished (Y783) as well as elevated (Y771) phosphorylation can be observed.

To investigate the consquences of these alterations of PLCγ1 phosphorylation on the enzyme's activity, indirect measurements of *inositol-1,4,5-trisphosphate* (IP_3) production were performed using an IP_1 ELISA (Figure 3-6). The intracellular half life of IP_3 is very short before it is transformed to IP_2 and IP_1. Addition of LiCl (50 mM) to the cell medium blocks IP_1 degradation leading to its accumulation. Therefore, wt and *Stim1*$^{Sax/+}$ T cells were stimulated by anti-CD3 crosslinking for 15 minutes and the IP_1 production was quantified.

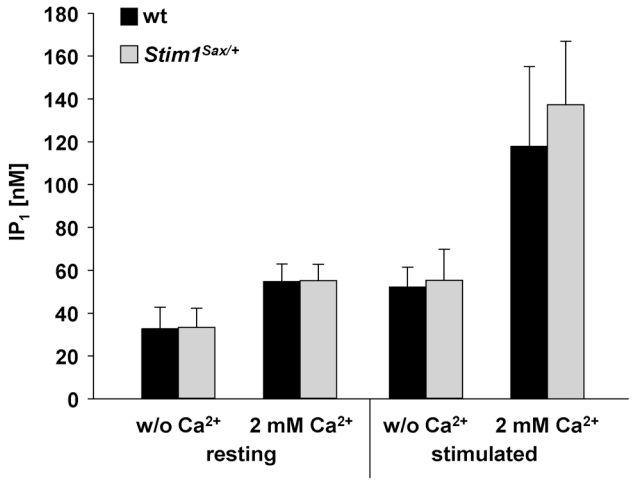

Figure 3-6 Unaltered PLCγ1 activity in *Stim1*$^{Sax/+}$ mice. Quantification of produced IP_1 upon stimulation. Lymph node cell suspensions from wt and *Stim1*$^{Sax/+}$ mice were left untreated or stimulated by anti-CD3 crosslink for a time frame of 15 min. Cells were lysed and IP_1, a specific metabolite of IP_3, was quantified using an ELISA assay. Results are given as the mean IP_1 concentration (nM) ± SD (n=3 per group).

Neither in the presence (corresponding to an altered phosphorylation pattern of *Stim1*$^{Sax/+}$ PLCγ1), nor in the absence of extracellular Ca^{2+}, differences in IP_1 production between wt and *Stim1*$^{Sax/+}$ T cells were measured, implicating normal catalytic activity of PLCγ1 in mutant cells. Of note, withdrawal of extracellular Ca^{2+} resulted in generally decreased IP_1 production in wt and *Stim1*$^{Sax/+}$ samples, when compared to the respective counterparts that had been stimulated in the presence of Ca^{2+} (Figure 3-6). To conclude, the alterations in PLCγ1 phosphorylation induced by continuous Ca^{2+} influx did not translate into functional changes of PLCγ1 activity.

3.1.5 Impaired Th2-type cytokine production of *Stim1*$^{Sax/+}$ T cells

So far, the immediate impact of the *Stim1*^{Sax} mutation and accompanying Ca^{2+} influx on signaling proteins downstream of the TCR in the first minutes after stimulation had been described. To gain insight into the functional, long-term consequences of elevated $[Ca^{2+}]_i$ and the constitutive nuclear NFAT localization, the ability of *Stim1*$^{Sax/+}$ T cells to control cytokine production was investigated. T cells in spleen cell suspensions were stimulated with plate-bound anti-CD3 antibody and the levels of various cytokines in the cell supernatant were determined 48 h later. Proliferation of both wt and *Stim1*$^{Sax/+}$ T cells became apparent by a change in color of the cell medium and increased size of T cells (data not shown). A robust and comparable production of the Th1-type cytokines IFNγ, IL-2 and TNFα, as well as of IL-3 and IL-6 was measured, while IL1α was not detectable in the supernatants of cells from both mouse lines (Figure 3-7). In sharp contrast, *Stim1*$^{Sax/+}$ T cells produced significantly less Th2-type cytokines, namely IL-4, IL-5 and IL-13 (IL-4: 380 ± 168 vs. 102 ± 36 ng/ml; $p<0.05$; IL-5: 250 ± 86 vs. 60 ± 56 ng/ml $p<0.01$; IL-13: 4398 ± 638 vs. 1278 ± 417 ng/ml; $p<0.001$) and also exhibited a tendency towards less IL-10 (4720 ± 1733 vs. 2623 ± 1112 ng/ml; $p=0.058$).

Similar results were observed when splenocytes were stimulated with beads coated with anti-CD3 and anti-CD28 antibodies (data not shown). Furthermore, comparable changes in the cytokine profile of *Stim1*$^{Sax/+}$ T cells were observed on the mRNA level by RT-PCR after anti-CD3/CD28 bead-stimulation of purified $CD4^+$ T cells for 3 or 6 hours (Christoph Hintzen, personal communication). Of note, control samples of wt and *Stim1*$^{Sax/+}$ splenocytes that had been cultured in the absence of stimulation, did not show any signs of proliferation and released no cytokines into the supernatant. Likewise, no or negligibly low cytokine levels were observed in plasma of either mice (data not shown).

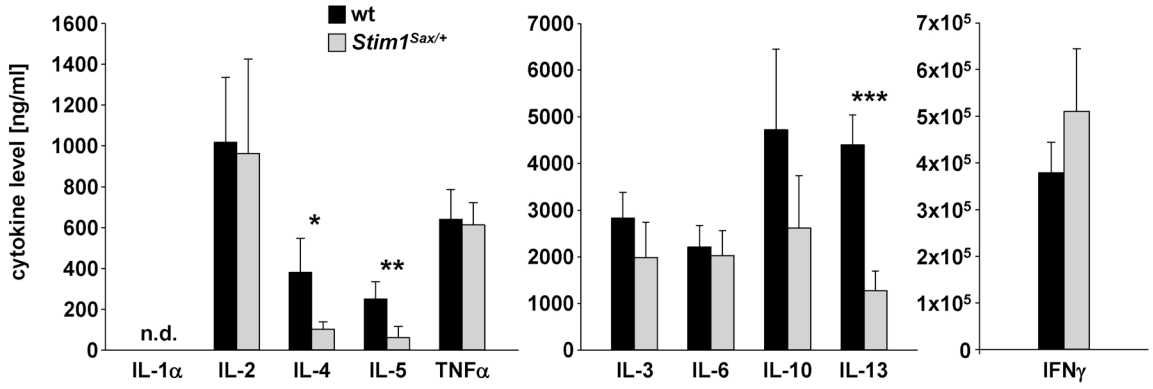

Figure 3-7 Impaired production of IL-4, IL-5 and IL-13 in *Stim1*$^{Sax/+}$ mice. Freshly isolated splenocytes from wt or *Stim1*$^{Sax/+}$ mice were cultured at $2x10^6$ cells/ml with 10 µg/ml of plate-bound anti-CD3 for 48 h. Cytokine levels were determined in the supernatant by ELISA. Bars represent means ± SD (n≥4 per group); * $p<0.05$; ** $p<0.01$; *** $p<0.001$. n.d., not detectable

In summary, T cells from *Stim1*$^{Sax/+}$ mice showed impaired production of Th2-type cytokines, but despite permanent nuclear NFAT localization, did not exhibit spontaneous proliferation or cytokine production in the absence of a stimulus.

3.1.6 High prevalence of regulatory T cells in the spleen of *Stim1*$^{Sax/+}$ mice

Since it has previously been shown that the absence of STIM1 and STIM2 in T cells results in abolished Ca^{2+} influx and defective development and function of Tregs,[163] the impact of continuous Ca^{2+} influx on Tregs was analyzed. Interestingly, *Stim1*$^{Sax/+}$ mice exhibited a pronounced elevation of Treg ($CD4^+$ $Foxp3^+$) frequencies in spleen (wt: 11.03 ± 1.50% vs. *Stim1*$^{Sax/+}$: 18.02 + 2.76% of $CD4^+$ cells; $p<0.01$), but not in blood or lymph nodes, where normal or only slightly increased frequencies were found, respectively (Figure 3-8 A and B). The increase in Treg population was already observed in spleens of 6-week old *Stim1*$^{Sax/+}$ mice (data not shown). Corrected for the increased splenic cell numbers (Figure 3-1 C), the elevation in Treg frequencies resulted in an approximately 2-fold increase

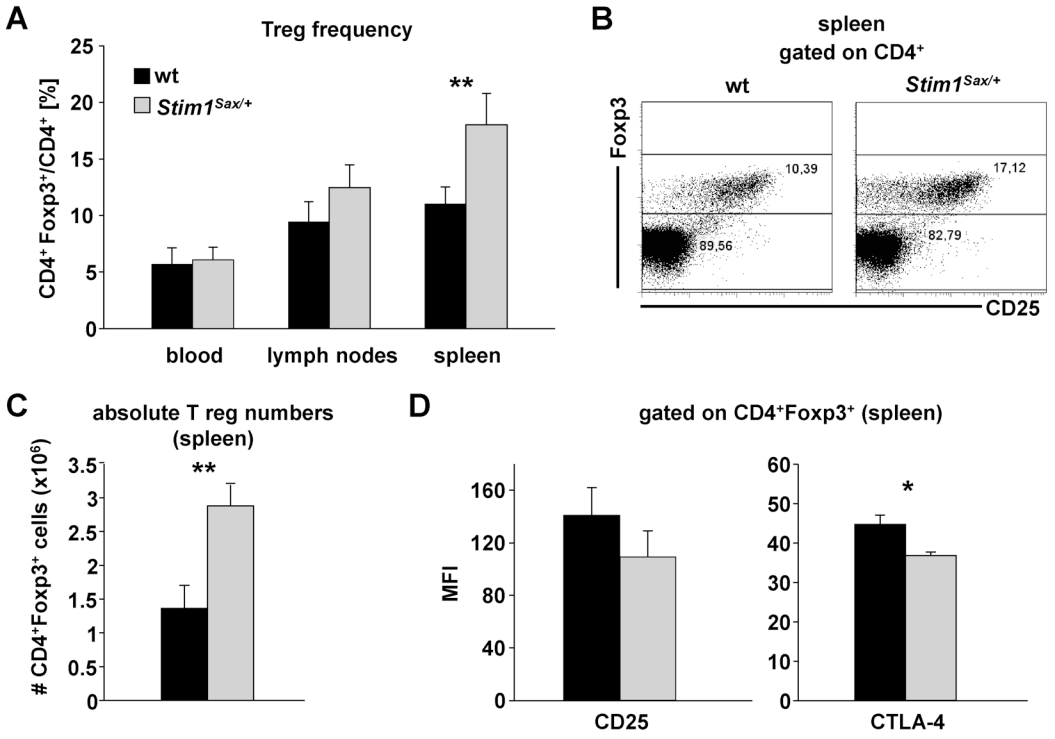

Figure 3-8 Elevated Treg numbers in *Stim1*$^{Sax/+}$ spleens. (A) Treg frequencies were determined in blood, lymph nodes and spleen by flow cytometry (% of $Foxp3^+$ events within the $CD4^+$ cell population). **(B)** Representative dot plots depicting Treg populations in spleen of wt and *Stim1*$^{Sax/+}$ mice. **(C)** Absolute numbers of Tregs in spleen of wt and *Stim1*$^{Sax/+}$ mice. **(D)** CD25 and CTLA-4 expression of splenic Tregs, as determined by flow cytometry. Bars represent means ± SD (n≥3 per group); * $p<0.05$; ** $p<0.01$

of the Treg numbers in *Stim1*$^{Sax/+}$ spleens compared to wt controls (wt: 1.36 ± 0.34 x10^6 vs. *Stim1*$^{Sax/+}$: 2.88 ± 0.31 x10^6 cells; p<0.01, Figure 3-8 C). Flow cytometric analysis of receptor surface expression detected a tendency to decreased levels of the α-chain of the high-affinity IL-2 receptor, CD25, and a significantly reduced expression of CTLA-4 (*mean fluorescence intensity* (MFI) wt: 44.81 ± 2.24 vs. *Stim1*$^{Sax/+}$ 36.85 ± 0.89; p<0.05) of splenic *Stim1*$^{Sax/+}$ Tregs (Figure 3-8 D). Of note, no alterations in CTLA-4 or CD25 expression were observed on lymph node Tregs (data not shown).

Regulatory T cells can either be generated in the thymus or extrathymically by proliferation or peripheral conversion. To test whether the elevated Treg cell numbers originated from enhanced Treg generation in the thymus, the frequency of Tregs in the CD4$^+$ CD8$^-$ thymocyte population was determined. As depicted in Figure 3-9 A, the frequencies of Tregs were comparable between wt and *Stim1*$^{Sax/+}$ mice, indicating unaltered Treg development. This is in accordance with the expression of Helios, a proposed marker for thymus-derived Tregs,[218] which was similar in wt and *Stim1*$^{Sax/+}$ splenic Tregs (Figure 3-9 B).

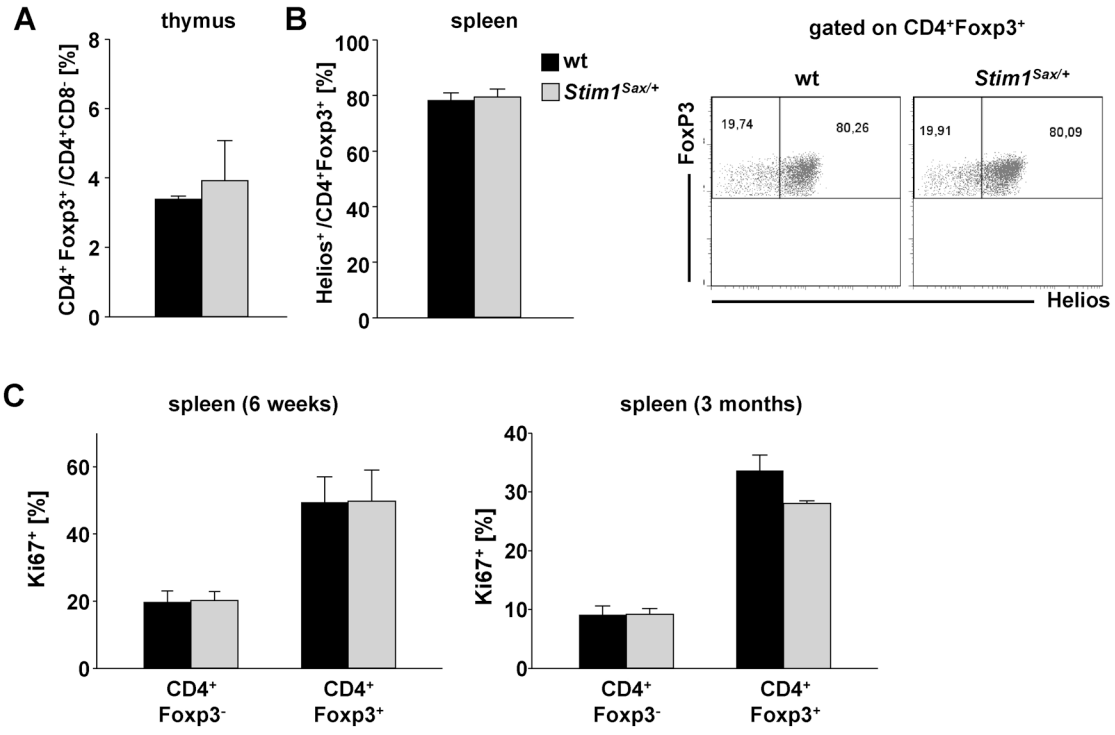

Figure 3-9 Unaltered Treg generation and proliferation in *Stim1*$^{Sax/+}$ mice. (A) Treg frequencies in thymus (% of Foxp3$^+$ events within the CD4$^+$CD8$^-$ cell population) and **(B)** frequency of Helios$^+$ Tregs in spleen were determined by flow cytometry. Right to the bar graphs, representative dot plots are depicted. **(C)** Populations of Ki67$^+$ Treg (CD4$^+$ Foxp3$^+$) and conventional (CD4$^+$ Foxp3$^-$) T cells were determined by flow cytometry. Bars represent means ± SD (n≥3 per group).

Next, the proliferation of Tregs was assessed by the use of an antibody against Ki-67, a protein exclusively expressed in dividing, but not in resting cells.[219] The frequency of proliferating (Ki-67$^+$) Tregs was similar in spleens of 6-week-old mice and not significantly decreased in 3-month-old mice, when compared to the respective wt littermates (Figure 3-9 C). Of note, proliferation of conventional T cells (non-Treg; CD4$^+$ Foxp3$^-$) was also comparable between wt and *Stim1*$^{Sax/+}$ animals, excluding non-proportional proliferation of different cell type subsets as the origin of elevated Treg frequencies.

Hence, neither enhanced generation of Tregs in the thymus nor exaggerated proliferation in the periphery appear to be the sole cause for the elevated Treg numbers in the spleen of *Stim1*$^{Sax/+}$ animals.

3.2 Analysis of Grb2-deficiency in platelets

Grb2 is an ubiquitously expressed adapter protein involved in growth factor receptor and ITAM-coupled receptor signaling.[94,98] In B cells[108,109] and thymocytes,[107] Grb2-deficiency resulted in opposing effects on signaling of the BCR and pre-TCR, respectively. Although it has been shown that Grb2 becomes phosphorylated upon GPVI/ITAM signaling and upon spreading, its role in platelet development and physiology remains unclear. Therefore, this part of the thesis investigates the role of Grb2 in platelet activation and development, with a special focus on (hem)ITAM receptor signaling. These experiments were performed together with Dr. Sebastian Dütting in our research group.

3.2.1 Grb2 is dispensable for platelet generation

To analyze the role of Grb2 in platelet physiology and development *in vivo*, mice with a MK- and platelet-specific deletion were generated, since constitutive Grb2-deficiency results in early embryonic lethality due to defective endoderm differentiation.[105] Therefore, mice carrying two loxP sites flanking exon 2 of the *Grb2* gene (*Grb2*^{fl})[108] were intercrossed with transgenic mice expressing Cre-recombinase under the control of the platelet/MK-specific *platelet factor 4* (PF4) promoter (*Pf4-cre*$^{+/-}$).[206] In the resulting *Grb2*$^{fl/fl}$*/Pf4-Cre*$^{+/-}$ mice (further on referred to as *Grb2*$^{-/-}$ mice) absence of Grb2 in platelets was confirmed by Western blot analysis, whereas the protein was still present in splenocytes (Figure 3-10 A). *Grb2*$^{fl/fl}$*/Pf4-Cre*$^{-/-}$ littermates (further on referred to as *Grb2*$^{+/+}$ or wt) served as wt controls in the experiments.

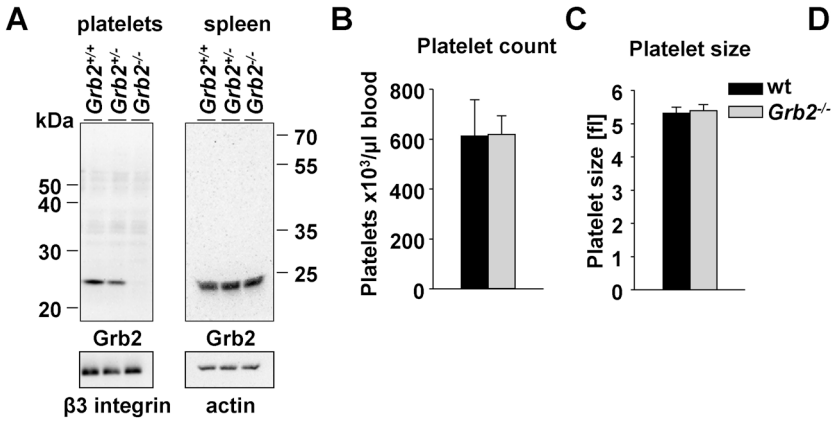

D

	wt	*Grb2*$^{-/-}$
GPIb	376 ± 12	371 ± 13
GPIX	430 ± 7	416 ± 18
GPV	306 ± 7	297 ± 11
CD9	1242 ± 21	1282 ± 22
GPVI	43 ± 3	40 ± 1
CLEC-2	136 ± 6	140 ± 1
αIIbβ3	513 ± 8	496 ± 31
α2	50 ± 2	49 ± 1
β1	146 ± 5	145 ± 4

Figure 3-10 Specific deletion of Grb2 in platelets does not impair platelet production. (A) Analysis of Grb2 expression in wt (*Grb2*$^{+/+}$), *Grb2*$^{+/-}$ and *Grb2*$^{-/-}$ platelets and splenocytes by Western blot analysis. Expression of β3 integrin (GPIIIa) and actin were used as loading controls. **(B)** Peripheral platelet counts and **(C)** platelet volume of wt and *Grb2*$^{-/-}$ mice measured with a blood cell counter are depicted. Results are mean ± SD of 7 mice per group. **(D)** Expression of glycoproteins on the platelet surface was determined by flow cytometry. Data are expressed as MFI ± SD (n=4) and are representative of 3 individual experiments. (Dütting,* Vögtle* *et al.*, *Circ Res* 2013)[220]

Grb2$^{-/-}$ mice were born in Mendelian ratios, appeared healthy and did not show any signs of spontaneous bleeding (Table 3-1 and data not shown). Platelet count and platelet size, as determined with an automated blood cell counter, as well as the surface expression of major platelet glycoproteins, did not differ from wt controls (Figure 3-10 B - D). This data indicated that Grb2 is dispensable for platelet formation.

Table 3-1 Offspring from matings of *Grb2*$^{fl/fl}$*/Pf4-cre*$^{-/-}$ with *Grb2*$^{fl/fl}$*/Pf4-cre*$^{+/-}$ mice.

Genotype	number of mice	frequency	expected frequency
***Grb2*$^{fl/fl}$*/Pf4-cre*$^{-/-}$**	283	51.8%	50%
***Grb2*$^{fl/fl}$*/Pf4-cre*$^{+/-}$**	263	48.2%	50%
total	546	100%	100%

3.2.2 Diminished responses to GPVI and CLEC-2 stimulation, but unaltered integrin outside-in signaling in *Grb2*$^{-/-}$ platelets

To determine whether the lack of Grb2 had functional consequences on platelet activation, platelets were stimulated with different agonists inducing ITAM-coupled or *G protein-coupled receptor* (GPCR) signaling and analyzed by flow cytometry. Two markers for platelet activation were used: Activation of the αIIbβ3 integrin was assessed with the JON/A-PE antibody, which specifically binds the activated conformation of the integrin,[204] and

degranulation was measured by surface expression of P-selectin, which is stored in α-granules in resting platelets and becomes exposed to the platelet surface upon activation-induced granule fusion with the plasma membrane.

Grb2-deficient platelets showed normal responses to the GPCR agonists thrombin, ADP and the stable TxA_2 analogue U46619 (Figure 3-11). In contrast, integrin activation and P-selectin exposure upon stimulation of the ITAM-coupled collagen receptor GPVI, either with *collagen-related peptide* (CRP) or the snake venom toxin CVX were severely reduced in Grb2-deficient platelets. This defect was apparent at high as well as at low agonist concentrations.

Moreover, impaired platelet activation was also observed in response to rhodocytin, a snake venom toxin that activates platelets via the hemITAM receptor CLEC-2. This defect was, however, less pronounced than the one observed for GPVI, since the reduction in integrin activation became apparent only at low, but not at high agonist concentrations (Figure 3-11).

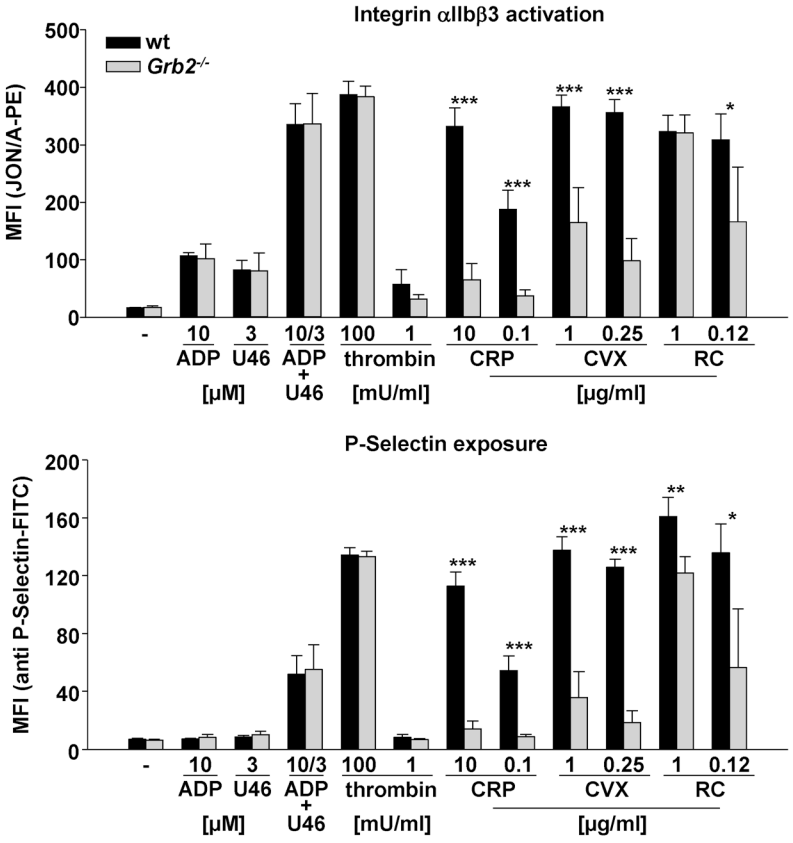

Figure 3-11 Impaired αIIbβ3 integrin activation and degranulation in response to (hem)ITAM-coupled receptor agonists. Flow cytometric analysis of integrin αIIbβ3 activation (upper panel) and degranulation-dependent P-selectin exposure (lower panel) in response to the indicated agonists in wt and *Grb2*$^{-/-}$ platelets. Results are MFI ± SD of 4 mice per group and representative of 4 individual experiments. RC, rhodocytin; U46, U46619; * p<0.05, ** p<0.01 and *** p<0.001. (Dütting,* Vögtle* *et al.*, *Circ Res* 2013)[220]

Platelets of mice heterozygous for the deletion of the *Grb2* gene (*Grb2*$^{fl/+}$*/Pf4-Cre*$^{+/-}$; Grb2$^{+/-}$), had reduced levels of Grb2 (Figure 3-10). In flow cytometry, these platelets exhibited an intermediate phenotype when stimulated with GPVI agonists, indicating that Grb2 regulates GPVI signaling in a quantitative manner (Figure 3-12 A).

Furthermore, the integrin activation response was compared to mice deficient in LAT, another adapter protein that has been shown to be involved in platelet (hem)ITAM receptor signaling and to interact with Grb2 in different cell types.[31,79] Like in *Grb2*$^{-/-}$ platelets, no defects in response GPCR agonists was observed in platelets of LAT-deficient mice. However, the (hem)ITAM receptor signaling defect was more pronounced in *Lat*$^{-/-}$ platelets as compared to *Grb2*$^{-/-}$ platelets, especially for CLEC-2 (Figure 3-12 B).

In summary, Grb2-deficiency resulted in defects of (hem)ITAM receptor signaling, with the strongest effects observed for GPVI, while leaving GPCR signaling fully intact.

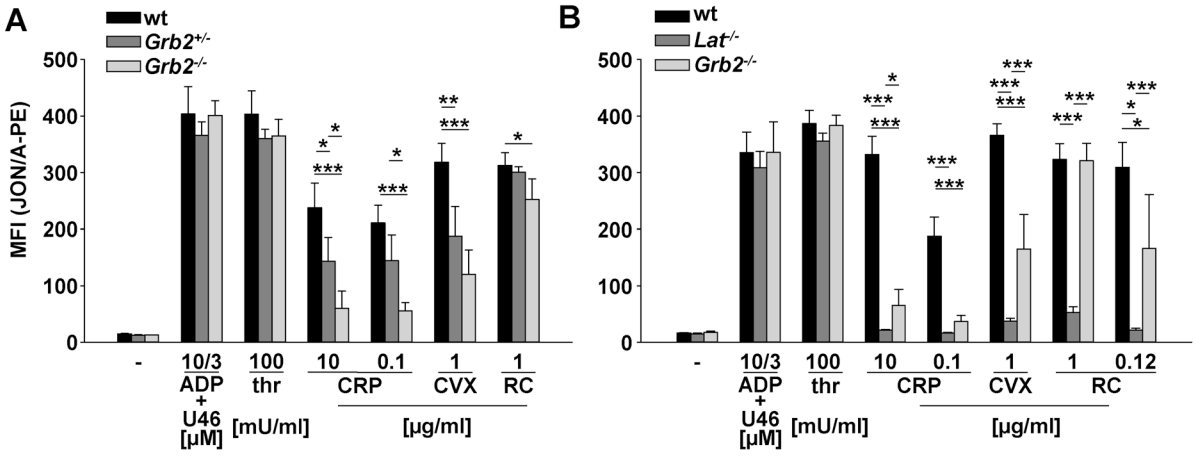

Figure 3-12 Grb2-deficiency produces a milder phenotype than LAT deficiency. Flow cytometric analysis of integrin αIIbβ3 activation in response to the indicated agonists in **(A)** wt, *Grb2*$^{+/-}$ and *Grb2*$^{-/-}$ platelets and **(B)** wt, *Lat*$^{-/-}$ and *Grb2*$^{-/-}$ platelets. Results are MFI ± SD of 4 mice per group and representative of 2 individual experiments. RC, rhodocytin; U46, U46619; * p<0.05, ** p<0.01 and *** p<0.001 as compared to the respective group.

To investigate how these defects in integrin activation and degranulation affected the ability of *Grb2*$^{-/-}$ platelets to aggregate, *ex vivo* aggregation studies were performed. In line with the data from the flow cytometry studies, platelets from *Grb2*$^{-/-}$ animals aggregated normally upon stimulation with the GPCR agonists thrombin, U46619 and ADP at every agonist concentration tested (Figure 3-13). In contrast, the response to the GPVI agonists CRP and collagen was partially impaired at intermediate and abrogated at low agonist concentrations in Grb2-deficient platelets. Similarly, no aggregation of *Grb2*$^{-/-}$ platelets was observed at low doses of the CLEC-2 agonist rhodocytin. The observed defects, however, were overcome at high agonist concentrations, where light transmission traces of *Grb2*$^{-/-}$ platelets reached

similar maximal aggregation rates as wt platelets, but showed a slightly delayed aggregation onset.

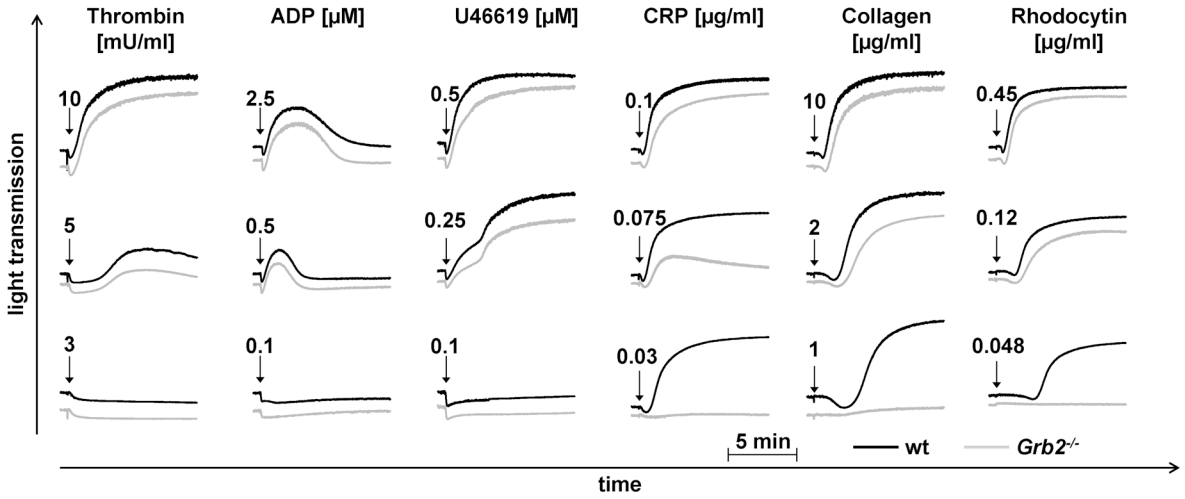

Figure 3-13 Impaired aggregation response of *Grb2*$^{-/-}$ platelets in response to (hem)ITAM receptor agonists. Washed platelets from wt (black line) and *Grb2*$^{-/-}$ (gray line) mice were activated with the indicated concentrations of ADP, U46619, thrombin, collagen, CRP or rhodocytin and light transmission was recorded on a Fibrintimer 4-channel aggregometer. ADP measurements were performed in *platelet rich plasma* (prp), all other measurements were performed in buffer in the presence of 100 µg/ml human fibrinogen (except for thrombin). Representative aggregation traces of at least 3 individual experiments are depicted. (Dütting,* Vögtle* *et al.*, *Circ Res* 2013)[220]

Ligand binding to integrin αIIbβ3 triggers outside-in signaling, leading to cytoskeletal reorganization and platelet spreading.[13] It has been proposed that Grb2 plays a role in this process as well as in the formation of actin-rich protrusions.[114,221] To test this directly, *Grb2*$^{-/-}$ and wt platelets were allowed to spread on a fibrinogen-coated surface in the presence of low concentrations of thrombin. *Grb2*$^{-/-}$ and wt platelets formed filopodia and lamellipodia to the same extent with similar kinetics resulting in comparable numbers of fully spread platelets after 30 minutes (Figure 3-14 A). Likewise, no differences in spreading between wt and *Grb2*$^{-/-}$ platelets were observed when the experiments were performed in the presence of apyrase and indomethacin, to inhibit second wave mediators, in the presence as well as absence of thrombin (data not shown).

Another process that depends on integrin outside-in signaling is clot retraction.[222] Therefore, clot formation in prp was induced by addition of a high dose of thrombin (5 U/ml) and 20 mM $CaCl_2$. The subsequent clot retraction was monitored over time, but differences between wt and Grb2-deficient platelets were neither observed in the kinetics of the retraction process (Figure 3-14 B) nor in the volumes of the extruded fluid (wt: 94.4 ± 2.8% vs. *Grb2*$^{-/-}$: 90.7 ± 6.3% of initial volume).

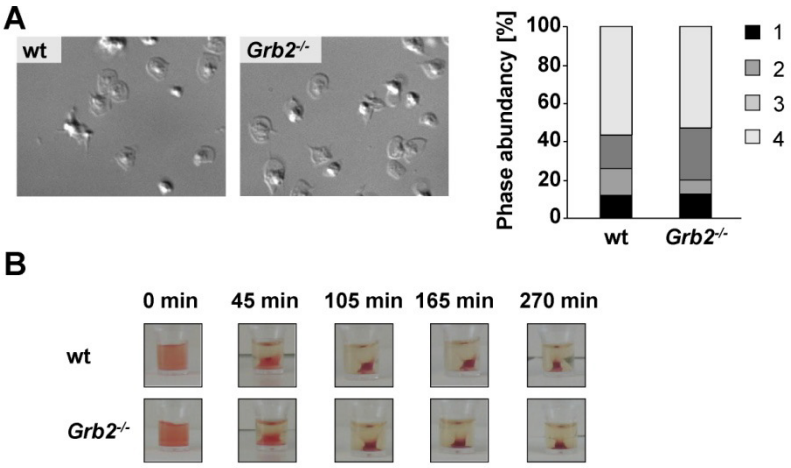

Figure 3-14 Unaltered integrin outside-in signaling in *Grb2*$^{-/-}$ platelets. (A) Washed platelets of wt and *Grb2*$^{-/-}$ mice were allowed to spread on fibrinogen (100 µg/ml) for 30 min after stimulation with 0.01 U/ml thrombin. Representative differential interference contrast images of 2 individual experiments (left) and statistical evaluation of the percentage of spread platelets at different spreading stages (right). 1: round, 2: only filopodia, 3: filopodia and lamellipodia, 4: fully spread. **(B)** Clot retraction of prp upon activation with 5 U/ml thrombin in the presence of 20 mM $CaCl_2$ at the indicated time points (n=3 for wt and n=7 for *Grb2*$^{-/-}$). (Dütting, Vögtle *et al.*, *Circ Res* 2013)[220]

In summary, the results from the clot retraction and spreading experiments indicated that Grb2 is not required for αIIbβ3 signaling processes.

3.2.3 Defective Ca^{2+} mobilization in *Grb2*$^{-/-}$ platelets in response to the GPVI agonist CRP

Agonist-induced platelet activation initiates signaling cascades that lead to PLC activity and subsequent IP_3 production. IP_3 in turn releases Ca^{2+} from intracellular stores, thereby triggering Ca^{2+} influx from the extracellular space inside the cell. This process, termed SOCE, is required for proper platelet activation (see introduction).

To investigate whether the observed GPVI signaling defect was based on impaired Ca^{2+} signaling, we studied agonist-induced changes in $[Ca^{2+}]_i$ fluormetrically.

Store release, measured as elevation in $[Ca^{2+}]_i$ in the absence of extracellular Ca^{2+} in response to thrombin was unaltered in *Grb2*$^{-/-}$ platelets as compared to wt controls (Figure 3-15 A and B). In line with this, Ca^{2+} influx in the presence of extracellular Ca^{2+} was also indistinguishable between wt and knock-out. In contrast, store release in *Grb2*$^{-/-}$ platelets upon stimulation with CRP was severely impaired (wt: 113 ± 9 nM vs. *Grb2*$^{-/-}$: 68 ± 15 nM; $p<0.01$). Similarly, the influx of Ca^{2+} in response to CRP was reduced in duration and amplitude (wt: 345 ± 48 nM vs. *Grb2*$^{-/-}$: 156 ± 55 nM; $p<0.05$; Figure 3-15 A, B). Notably, induction of SOCE by passive store depletion with the SERCA pump inhibitor *thapsigargin*

(TG) did not lead to any differences in the kinetics of Ca^{2+} mobilization between wt and *Grb2*$^{-/-}$ platelets (Figure 3-15 C and D). This demonstrated that the defects seen for CRP are due to GPVI signaling defects and not to alterations in the store content or changes in the SOCE machinery.

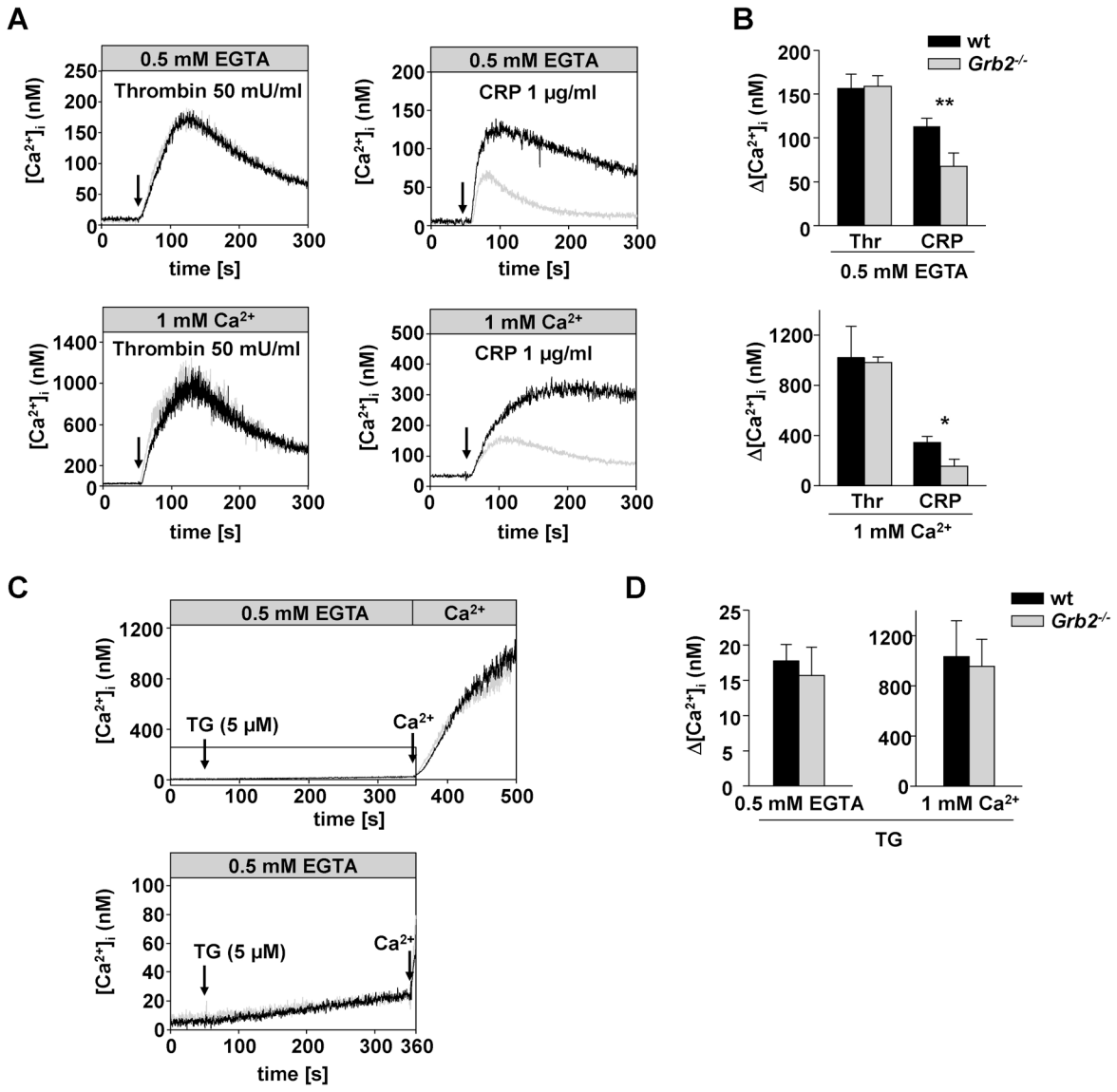

Figure 3-15 Defective GPVI-induced Ca^{2+} mobilization. (A) Time course of intracellular Ca^{2+} mobilization in wt (black line) and *Grb2*$^{-/-}$ platelets (gray line) in response to thrombin and CRP (addition indicated by an arrow). The experiment was performed in the absence (0.5 mM EGTA, upper panel) and in the presence (1 mM $CaCl_2$, lower panel) of extracellular Ca^{2+}. **(B)** Maximal increase of intracellular Ca^{2+} concentration ($\Delta[Ca^{2+}]_i$) of wt and *Grb2*$^{-/-}$ platelets after activation with the indicated agonists (thrombin 0.05 U/ml, CRP 1 µg/ml). **(C)** Time course of intracellular Ca^{2+} mobilization after treatment with thapsigargin (TG, upper panel). The measurement was started in Ca^{2+}-free medium and Ca^{2+} was added after 350 s of recording. The boxed area comprises the time frame prior to addition of extracellular Ca^{2+} and is shown magnified in the lower panel. **(D)** Maximal increase of $[Ca^{2+}]_i$ after treatment with TG in the presence and absence of extracellular Ca^{2+}.
The traces shown in **(A)** and **(C)** are representative of at least 3 individual experiments. Results in **(B)** and **(D)** are given as mean $\Delta[Ca^{2+}]_i$ (nM) ± SD, n=3-4 per group. * p<0.05 and ** p<0.01 (Dütting,* Vögtle* *et al.*, *Circ Res,* 2013)[220]

3.2.4 *Grb2*$^{-/-}$ platelets exhibit impaired procoagulant activity and defective aggregate formation on collagen under flow

Upon activation platelets expose negatively charged *phosphatidylserine* (PS) on their outer surface thereby providing a platform for key activators of the coagulation system. Since it is well established that this process requires prolonged high intracellular Ca^{2+} levels,[9] the impact of impaired Ca^{2+} mobilization in *Grb2*$^{-/-}$ platelets on procoagulant activity was investigated. To do so, wt and *Grb2*$^{-/-}$ platelets were stimulated with different agonists and PS exposure was measured by binding of DyLight-488 labeled annexin V in flow cytometry (Figure 3-16). Upon platelet stimulation with a combination of thrombin and CRP, as well as with a high dose of rhodocytin (1 µg/ml), the majority of wt platelets exposed PS on their surface. In sharp contrast, in Grb2-deficient platelets only partial responses were observed under these conditions (CRP + thrombin: wt: 90 ± 3% vs. *Grb2*$^{-/-}$: 37 ± 6% annexin V$^+$ platelets; p<0.001 rhodocytin: wt: 90 ± 3% vs. *Grb2*$^{-/-}$: 28 ± 9%; p<0.001). Furthermore *Grb2*$^{-/-}$ platelets displayed virtually abolished PS exposure in response to weaker stimuli which still produced a profound PS exposure in wt platelets.

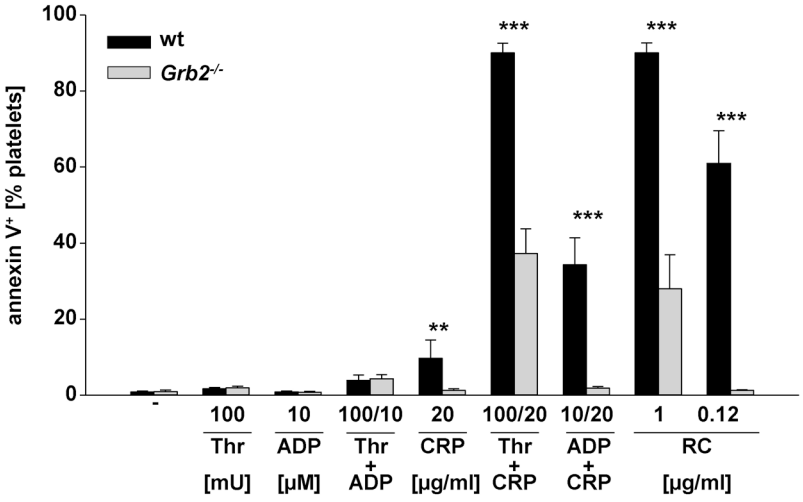

Figure 3-16 Defective procoagulant activity of *Grb2*$^{-/-}$ platelets. Flow cytometric analysis of PS exposure in response to the indicated agonists in wt and *Grb2*$^{-/-}$ platelets. Washed platelets were stimulated with the indicated agonists and stained with annexin V-DyLight-488 in the presence of Tyrode's buffer containing 2 mM Ca^{2+}. Results are percentage of annexin V positive platelets ± SD of 6 wt and 5 *Grb2*$^{-/-}$ mice and representative of 2 individual experiments. Thr, thrombin; RC, rhodocytin. ** p<0.01 and *** p<0.001. (Dütting,* Vögtle* *et al.*, *Circ Res,* 2013)[220]

In summary, these results demonstrated a prominent role for Grb2 in facilitating (hem)ITAM-induced coagulant activity in platelets.

So far, platelet function of Grb2 under static or stirring conditions was analyzed. At sites of vascular injury, however, platelet adhesion and aggregation are critically influenced by shear

forces. Furthermore, released second-wave mediators become rapidly diluted in flowing blood. Therefore, to address the function of Grb2 under more physiological conditions, platelet adhesion and thrombus formation on a collagen-coated surface under flow in an *ex vivo* whole blood perfusion system were analyzed. When blood from wt animals was perfused over immobilized collagen at a shear rate of 1000 s^{-1}, the platelets rapidly adhered and formed aggregates that grew into large three-dimensional thrombi within the 4 minutes observation period (Figure 3-17). In sharp contrast, adhesion of *Grb2*$^{-/-}$ platelets was markedly reduced, and the subsequent formation of stable three-dimensional aggregates was virtually abrogated. As a consequence, the surface area covered by platelets and the thrombus volume at the end of the perfusion period were reduced by approximately 94% in *Grb2*$^{-/-}$ platelets ($p<0.001$) compared to wt (Figure 3-17).

These results demonstrated that Grb2 is essential for *ex vivo* platelet adhesion and aggregate formation on collagen under flow conditions.

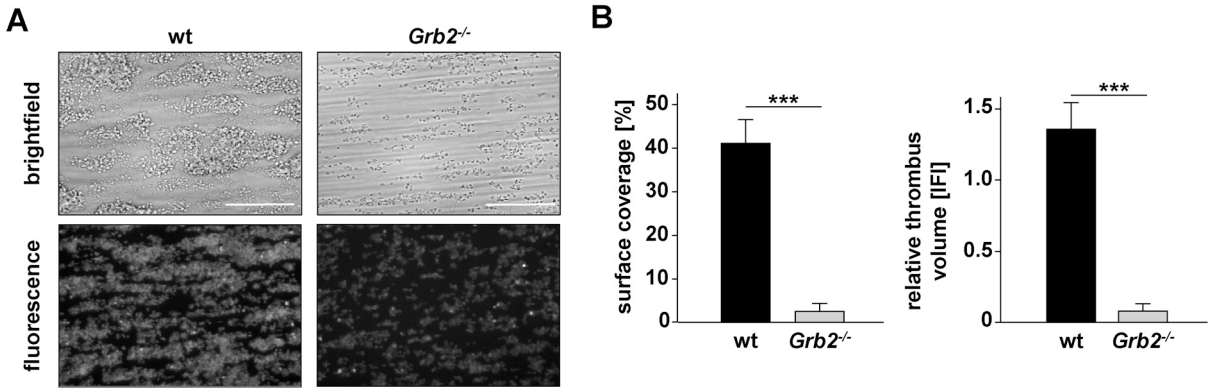

Figure 3-17 Impaired adhesion and defective aggregate formation of *Grb2*$^{-/-}$ platelets on collagen under flow. (A) Whole blood from wt or *Grb2*$^{-/-}$ mice was perfused over a collagen-coated surface (0.2 mg/ml) at a shear rate of 1000 s^{-1}. Representative phase contrast images (upper panel) and fluorescence images (lower panel) of aggregate formation on collagen after 4 min of perfusion time. Bar, 50 µm. **(B)** Means of surface coverage (left) and relative thrombus volume, expressed as *integrated fluorescence intensity* (IFI) (right) ± SD of 4 wt and 5 *Grb2*$^{-/-}$ mice. *** $p<0.001$ (Dütting,* Vögtle* *et al.*, *Circ Res,* 2013)[220]

3.2.5 Impaired hemostasis and partially defective arterial thrombus formation in *Grb2*$^{-/-}$ mice

To investigate the role of Grb2 in hemostasis, a tail bleeding time assay was performed. After cutting off a 1 mm segment of the tail tip, bleeding in wt animals usually ceased within 400 s and averaged at 197 ± 107 s (Figure 3-18). *Grb2*$^{-/-}$ mice, however, exhibited prolonged (381 ± 237 s; $p<0.001$) and highly variable bleeding times, suggesting thrombus instability. A similar phenotype has also been described for other mouse lines with defects in (hem)ITAM signaling, e.g. mice deficient in the adapter protein LAT.[88]

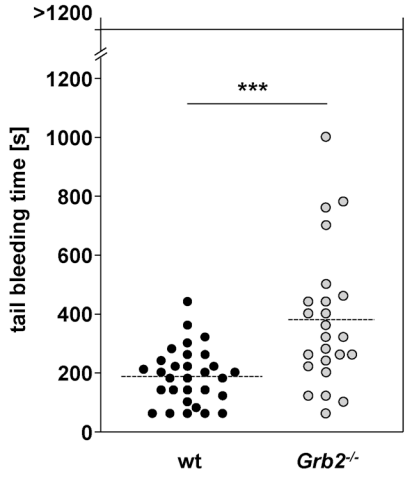

Figure 3-18 Impaired hemostasis in *Grb2*$^{-/-}$ mice. A 1 mm segment of the tail tip of anesthesized mice was cut off using a scalpel. Blood drops were absorbed every 20 s using a filter paper without touching the wound site until bleeding ceased. Each symbol represents the bleeding time of one animal. *** p<0.001. (Dütting,* Vögtle* *et al.*, *Circ Res,* 2013)[220]

In the next step, the requirement of Grb2 in platelets for thrombus formation *in vivo* was addressed by subjecting *Grb2*$^{-/-}$ mice to two different models of arterial thrombosis. These experiments were performed in collaboration with Martina Morowski in our laboratory. In the first model, the abdominal aorta was mechanically injured by firm compression with a forceps and blood flow was monitored with an ultrasonic Doppler flow probe. In this model thrombus formation occurs in a highly GPVI/PLCγ2-dependent manner, since GPVI-deficient mice do not occlude.[223] In the wt control group, 13 out of 14 animals formed vessel occluding thrombi within 10 minutes (mean occlusion time: 303 ± 101 s; Figure 3-19 A). Unexpectedly, *Grb2*$^{-/-}$ mice formed occlusive thrombi with similar kinetics and frequencies (occlusion in 11/12 animals; mean occlusion time: 351 ± 98 s). Comparable results were also obtained in the second model of arterial thrombosis, where mesenterial arterioles are chemically injured by topical application of $FeCl_3$ and thrombus formation is more dependent on soluble mediators.[224] Both wt and mutant animals formed thrombi within a similar time frame (mean occlusion time: wt: 16.14 ± 5.71 min vs. *Grb2*$^{-/-}$: 12.56 ± 1.94 min; Figure 3-19 B). These results argue against a prominent role of Grb2 in intravascular thrombus formation.

Ischemic stroke is the second leading cause of death and severe disability worldwide.[3] Platelets are critically involved in its pathogenesis by mechanisms involving GPIb and GPVI dependent platelet adhesion and activation,[225] but the exact underlying mechanisms remain unknown. To investigate how Grb2 deficiency impacts ischemic stroke, mice were challenged in the *transient middle cerebral artery occlusion* (tMCAO) model of experimental focal cerebral ischemia. These experiments were performed in close collaboration with Dr. Peter Kraft (research group of Prof. Dr. Guido Stoll; Department of Neurology, University of Würzburg)

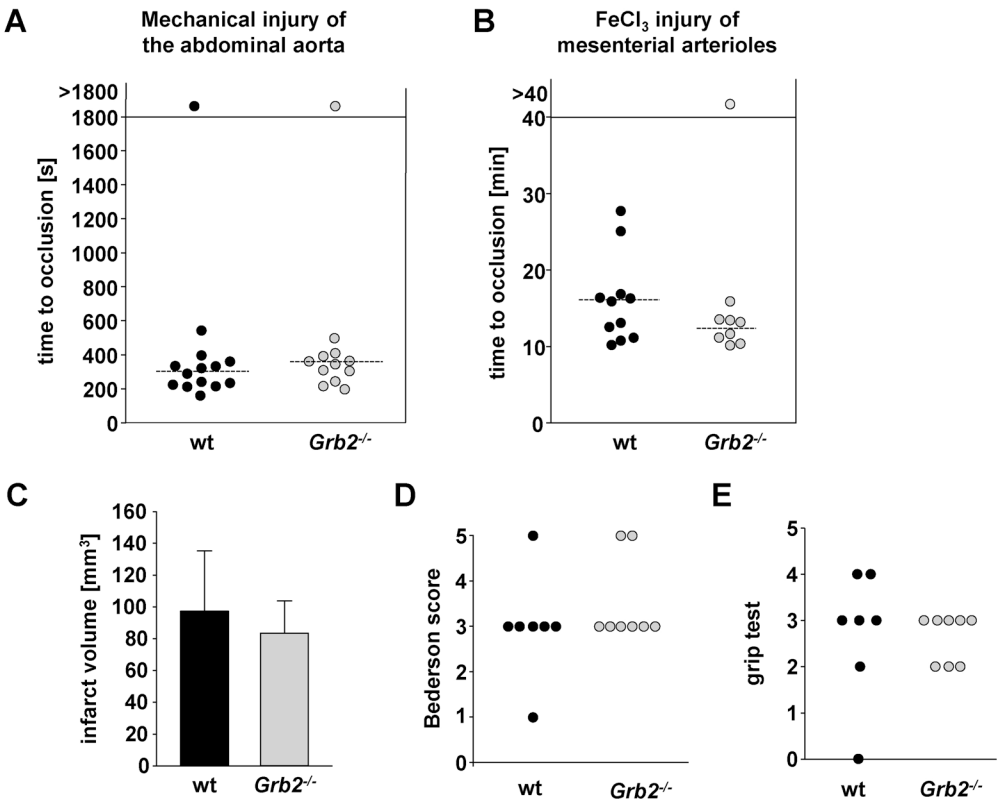

Figure 3-19 Unaltered thrombus formation and stroke outcome in *Grb2*$^{-/-}$ mice. (A, B) Time to stable vessel occlusion of wt and *Grb2*$^{-/-}$ mice upon vascular injury. **(A)** The abdominal aorta was injured by firm compression with a forceps and blood flow was monitored with an ultrasonic flow probe for 30 min or until full vessel occlusion. Each symbol represents one animal. **(B)** Small mesenteric arterioles were injured by topical application of $FeCl_3$ and thrombus formation of platelets (fluorescently labeled) was monitored using intravital microscopy. Each symbol represents one arteriole. **(C-E)** Consequences of cerebral ischemia induced by tMCAO. **(C)** The infarct volumes were determined by TTC staining of coronal brain sections 24 h after tMCAO. Bars represent mean infarct volumes ± SD of 7 wt vs. 8 *Grb2*$^{-/-}$ animals. **(D)** Bederson score and **(E)** grip test assessed 24 h after tMCAO. Each symbol represents one animal.

Transient cerebral ischemia in this model was induced by advancing a filament through the carotid artery into the middle cerebral artery. This reduces the cerebral blood flow by more than 90%. After 1 h the thread was withdrawn to allow reperfusion and mice were analyzed 24 h later.

The volume of the infacted area, apparent as white tissue in *2,3,5-triphenyltetrazolium chloride* (TTC) stained coronal brain sections, were comparable in wt and *Grb2*$^{-/-}$ mice (mean infarct volume: wt: 97 ± 38 mm^3 vs. *Grb2*$^{-/-}$: 83 ± 20 mm^3; p=0.41; Figure 3-19 C). In accordance with these results, wt and mutant mice were indistinguishable in their Bederson scores, assessing global neurological function and in the grip test, which assesses motor function and coordination of the mice (Figure 3-19 D, E). In conclusion, Grb2 is dispensable for ischemic brain infarction following tMCAO.

The absence of a protective effect of Grb2 deficiency in *in vivo* models of arterial thrombisis and ischemic brain infarction was surprising in face of the robust GPVI signaling defects of *Grb2*$^{-/-}$ platelets observed *in vitro* and *ex vivo*. As a possible explanation, defective GPVI signaling may be compensated *in vivo* by agonists that stimulate GPCR-dependent signaling pathways, for example by TxA_2, as shown previously.[226]

To test the importance of costimulatory signals on platelet activation, wt and *Grb2*$^{-/-}$ platelets were stimulated with an intermediate dose of CRP in combination with the GPCR agonist ADP or the stable TxA_2 analogue U46619 and analyzed for integrin activation and P-selectin exposure in flow cytometry. As depicted in Figure 3-20 A, ADP and U46619 alone only induced mild integrin activation and no P-selectin exposure in wt and mutant platelets. Consistent with the role of GPCR agonsits as amplifiers of platelet activation,[10] wt platelets treated with a GPCR agonist together with CRP exhibited strong integrin activation and P-selectin exposure. Detailed analysis revealed that the MFIs upon costimulation significantly exceeded the hypothetical values that would have been expected under the assumption of additive agonist effects (Figure 3-20 B, upper panel). Thus, this observation clearly points towards synergistic effects of GPCR and GPVI agonists. Strikingly, these synergistic effects were even more pronounced in *Grb2*$^{-/-}$ platelets (Figure 3-20). Despite the weak potency of CRP, U46619 or ADP to induce integrin activation or P-Selectin exposure in mutant platelets alone, combinations of CRP with U46619 or ADP resulted in robust responses. This became especially apparent upon costimulation with CRP and ADP, where the MFIs of *Grb2*$^{-/-}$ platelets reached values similar to those observed for wt platelets stimulated with CRP alone. However, the response of Grb2-deficient platelets to any CRP/GPCR agonist combination remained significantly weaker compared to the respective wt samples. Direct comparison of the measured MFIs to the hypothetical MFIs, that would have resulted from additive effects of the agonists, clearly revealed the strong synergistic effects of GPVI and GPCR agonists in Grb2-deficient platelets, that exceeded the additive effects by a factor up to 3. (Figure 3-20 B, lower panel)

In summary, these experiments demonstrated that (i) GPCR and GPVI signaling pathways synergize in platelet activation and (ii) that the residual signaling capacity of GPVI in Grb2-deficient platelets may be of functional relevance in the presence of other agonists.

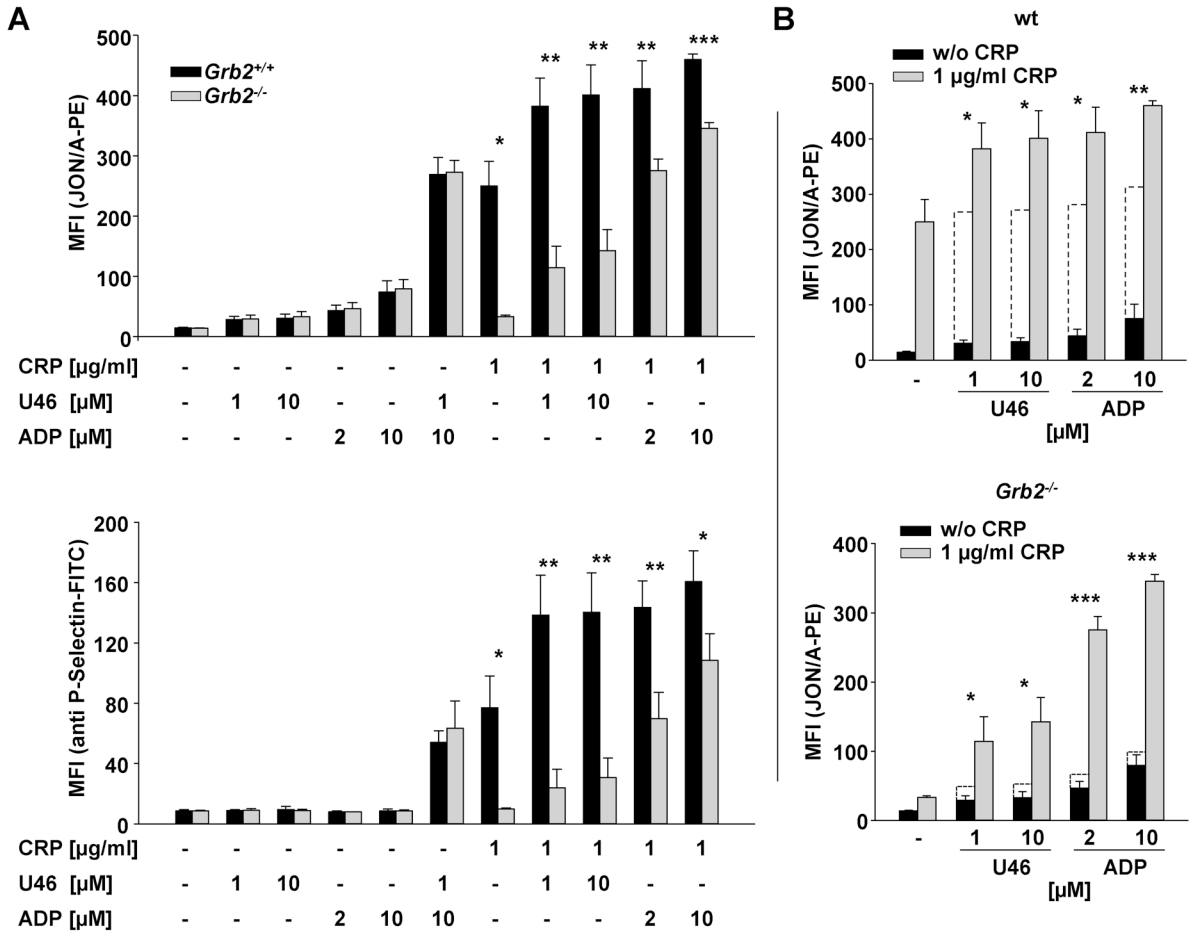

Figure 3-20 Costimulation of *Grb2*$^{-/-}$ platelets with CRP and GPCR agonists results in strong synergistic effects. (A) Flow cytometric analysis of integrin αIIbβ3 activation (upper panel) and degranulation-dependent P-selectin exposure (lower panel) in response to the indicated combinations of agonists in wt and *Grb2*$^{-/-}$ platelets. Results are MFI ± SD of 3-4 mice per group and representative of 2 individual experiments. U46, U46619. * p<0.05, ** p<0.01 and *** p<0.001 as compared to wt controls. **(B)** Alternative presentation of the data in A, upper panel, highlighting the synergistic effects. MFIs from GPCR stimulated platelets are opposed to the MFIs of platelets stimulated with the respective GPCR agonist in combination with 1 µg/ml CRP. Wt platelets are shown in the upper panel, *Grb2*$^{-/-}$ platelets in the lower. Dashed lines represent hypothetical values that would have resulted from sole additive effects of the GPCR agonist and CRP (MFI [GPCR agonist only] + (MFI [CRP only] – MFI [resting])). * p<0.05, ** p<0.01 and *** p<0.001 comparing values of costimulated platelets with the respective calculated value, assuming additive effects (dashed line).

The next goal was to collect evidence for a compensatory role of GPCR signaling *in vivo*. Therefore, it was intended to inhibit GPCR signaling *in vivo* and to investigate the outcome on thrombosis and hemostasis in wt and *Grb2*$^{-/-}$ mice. Clopidogrel and *acetylsalicylic acid* (ASA, or Aspirin®) are widely used antithrombotics, which interfere with GPCR signaling by blocking P2Y receptors or TxA_2 production, respectively. Clopidogrel, however, was not suitable for the planned studies, since previous experiments by others have demonstrated a severe impairment of thrombus formation in wt mice,[227] which would make it difficult to detect differences between wt and *Grb2*$^{-/-}$ mice. In contrast, treatment with ASA has only mild effects on hemostasis and thrombosis in wt mice[226,227] and furthermore TxA_2-induced

signaling has previously been shown to partially compensate for the loss of GPVI.[226] Therefore, mice received 1 mg/kg body weight ASA intravenously 10 minutes prior to experiments. This concentration resembles the dose recommended for primary prevention of cardiovascular disease.[228]

In a first set of experiments, platelets from wt and *Grb2*$^{-/-}$ mice treated with ASA were subjected to aggregometry and their ability to aggregate upon stimulation with collagen was compared to platelets of untreated mice. It is well established that under these conditions platelet aggregation is amplified by the release of second wave mediators, e.g. ADP and TxA_2.[32] As depicted in Figure 3-21, ASA treatment had little effect on the aggregation response of wt platelets. The light transmission traces of platelets from ASA treated animals reached comparable maximal aggregation values at all tested collagen concentrations, but a slight delay in aggregation onset was observed at lower agonist concentrations. This indicated a minor requirement for TxA_2-mediated amplification of the aggregation process in the presence of intact GPVI signaling. In contrast, ASA treatment of *Grb2*$^{-/-}$ mice led to impaired aggregation compared to untreated *Grb2*$^{-/-}$ mice at intermediate collagen concentrations. This became apparent especially at a collagen concentration of 3 µg/ml, at which the full aggregation response of Grb2-deficient animals was almost completely abolished upon pretreatment with ASA. As already mentioned, ASA pretreatment did not impair the response of wt platelets to the same collagen concentration (Figure 3-21).

In conclusion, these experiments revealed that TxA_2 can partially compensate for impaired GPVI signaling. Consequently, inhibition of TxA_2 production by a low dose of ASA raised the required concentration of the GPVI agonist collagen necessary to induce full platelet aggregation in *Grb2*$^{-/-}$ mice.

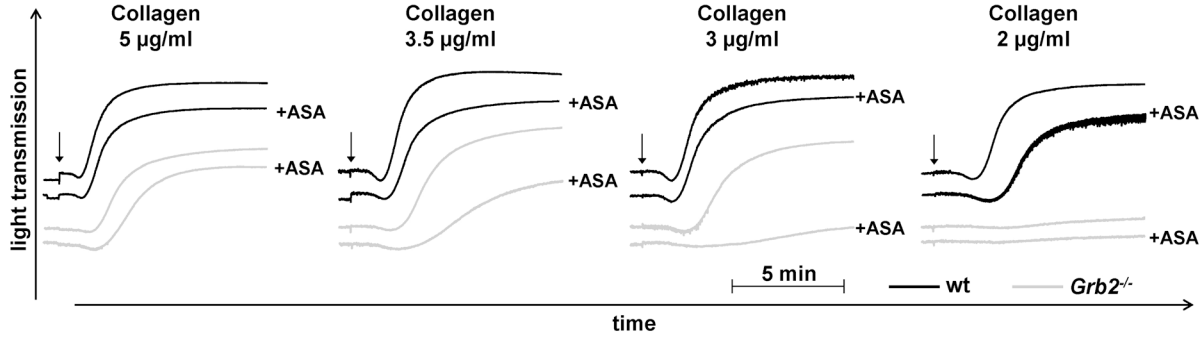

Figure 3-21 ASA treatment raises the threshold concentration required for thrombus formation in *Grb2*$^{-/-}$ mice. Washed platelets from wt (black lines) and *Grb2*$^{-/-}$ (gray lines) mice, treated or not with ASA (1 mg/kg i.v.) 10 min prior to bleeding, were activated with the indicated concentrations of collagen and light transmission was recorded on a Fibrintimer 4-channel aggregometer. The aggregation traces shown are representative of 2 measurements.

Having demonstrated the functional relevance of the inhibition of TxA_2 production *in vitro*, ASA treated animals were subjected to the tail bleeding time assay and the previously mentioned *in vivo* thrombosis models.

In the model of mechanical injury of the abdominal aorta, ASA treatment had no significant effect on thrombus formation in wt mice; vessel occlusion was observed in 14 of 15 animals (mean occlusion time: 296 ± 84 s, Figure 3-22 A). Strikingly, a strong effect was seen in the

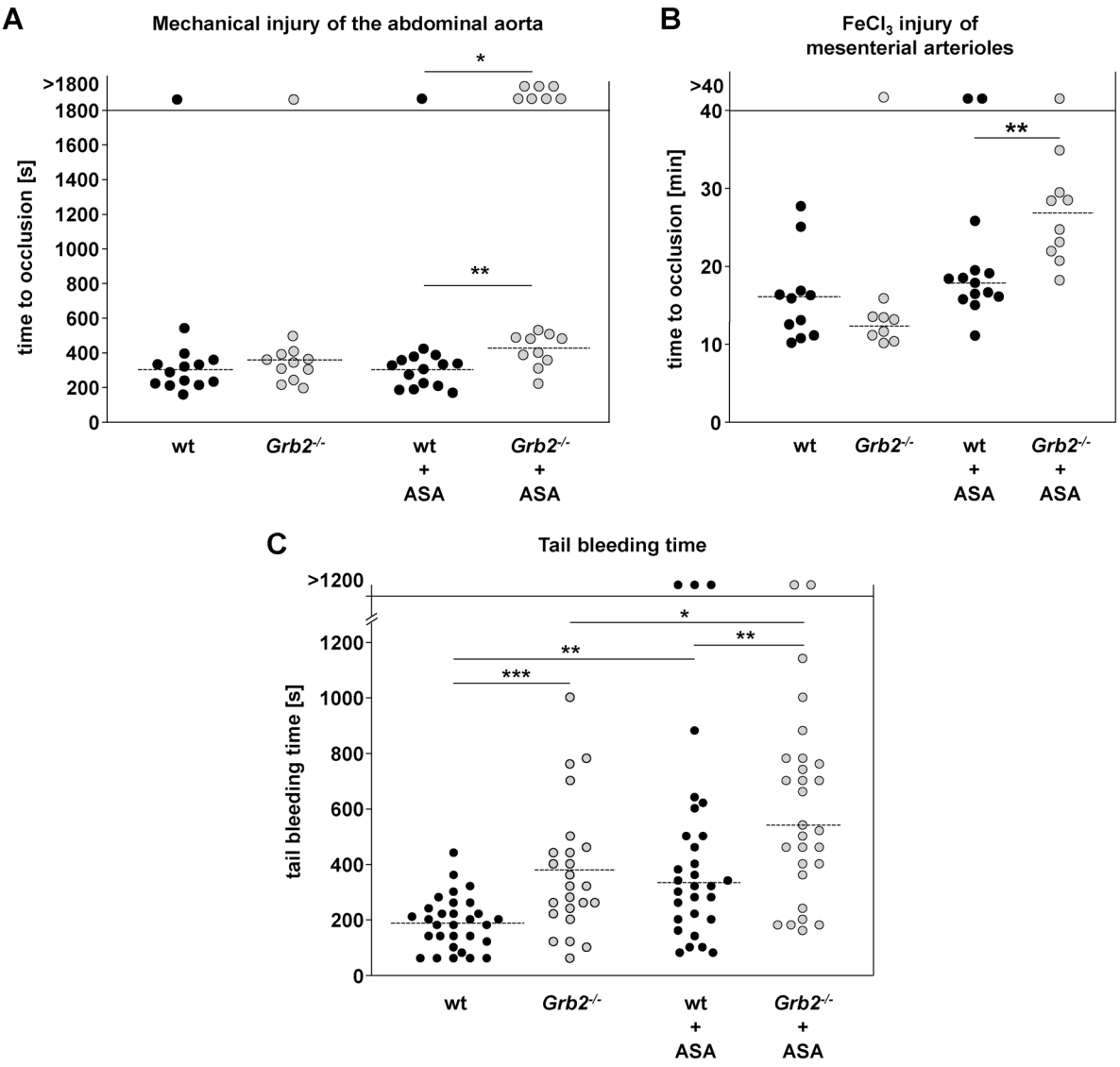

Figure 3-22 Impaired thrombus formation in *Grb2*$^{-/-}$ mice upon treatment with ASA. (A, B) Time to stable vessel occlusion of wt and *Grb2*$^{-/-}$ mice without or with ASA treatment (1 mg/kg i.v.) 10 min before the start of the experiment. **(A)** The abdominal aorta was injured by firm compression with a forceps and blood flow was monitored for up to 30 min. **(B)** Small mesenteric arterioles were injured by topical application of $FeCl_3$ and thrombus formation was investigated by intravital microscopy. **(C)** Tail bleeding times of wt and *Grb2*$^{-/-}$ mice without or with ASA treatment (1 mg/kg i.v.) 10 min before the start of the experiment. Each symbol represents one animal **(A, C)** or one arteriole **(B)**. * $p<0.05$, ** $p<0.01$ and *** $p<0.001$. The data for untreated animals is the same as shown in Figure 3-19 and Figure 3-18. (Dütting,* Vögtle* *et al.*, *Circ Res,* 2013)[220]

mutant mice where 7/17 vessels did not occlude ($p<0.05$), and occlusion times for the remaining vessels were increased compared to the wt group (419 ± 99 s; $p<0.01$).

Similar effects were observed in the model of $FeCl_3$-induced injury of mesenteric arterioles. Albeit treatment of *Grb2*$^{-/-}$ mice did not prevent vessel occlusion in this model, the mean time to occlusion was significantly prolonged compared to ASA-treated wt mice (wt: 17.89 ± 4.13 min vs. *Grb2*$^{-/-}$: 25.73 ± 5.20 min, $p<0.01$; Figure 3-22 B). These findings confirm that the GPVI signaling defect in these animals is at least in part compensated for by TxA_2-dependent activation pathways *in vivo*.

In contrast, ASA treatment prolonged tail bleeding times of wt and *Grb2*$^{-/-}$ mice to a similar extent (Figure 3-22 C).

3.2.6 Grb2 stabilizes the LAT signalosome

To characterize the molecular basis of Grb2 in transmitting (hem)ITAM-mediated signaling, signaling studies were performed. Grb2 was immunoprecipitated from lysates of untreated platelets or platelets stimulated with the GPVI agonist CVX and samples were analyzed using a pan anti-phospho-tyrosine (anti-pY) antibody (4G10). This antibody is extremely sensitive and thus can detect small amounts of co-immunoprecipitated proteins.

As depicted in Figure 3-23 A, few tyrosine phosphorylated proteins (approx. 38, 50, 95 and 150 kDa) were immunoprecipated from stimulated wt lysates, but not from *Grb2*$^{-/-}$ lysates, confirming the specificity of the system. Very prominent was the band at 38 kDa that most likely represents LAT since (i) this protein is well established to appear at this size in anti-pY blots,[26] (ii) LAT has been reported to interact with Grb2 (see introduction) and (iii) *immunoprecipitation* (IP) of LAT itself yielded a band at the same size (Figure 3-23 A).

Confirmation that the 38 kDa band corresponded to LAT came from the group of our collaboration partner, Prof. Dr. Steve Watson (University of Birmingham, UK). In their experiments, LAT was directly identified with a specific antibody in Grb2-IPs from lysates of wt mouse platelets stimulated with the GPVI agonist CRP or the CLEC-2 agonist rhodocytin (Figure 3-23 B). These results are in line with previous results obtained with human platelets[31] and demonstrated that Grb2 forms part of the LAT signalosome in mouse platelets upon induction of (hem)ITAM receptor signaling.

Comparison of the tyrosine phosphorylation patterns of whole cell lysates from wt and *Grb2*$^{-/-}$ platelets revealed no global impairment of tyrosine phosphorylation events in Grb2-deficient platelets (Figure 3-23 A, lanes WCL). Most of the bands coming up after stimulation with CVX had the same intensity in wt and *Grb2*$^{-/-}$ platelets with the prominent exception of two

bands comigrating with LAT (38 kDa) and PLCγ2 (approx. 150 kDa) that were weaker in the samples of mutant platelets. A possible explanation would be that signal transduction upon GPVI signaling is disrupted during transmission from the cell surface to the effector proteins.

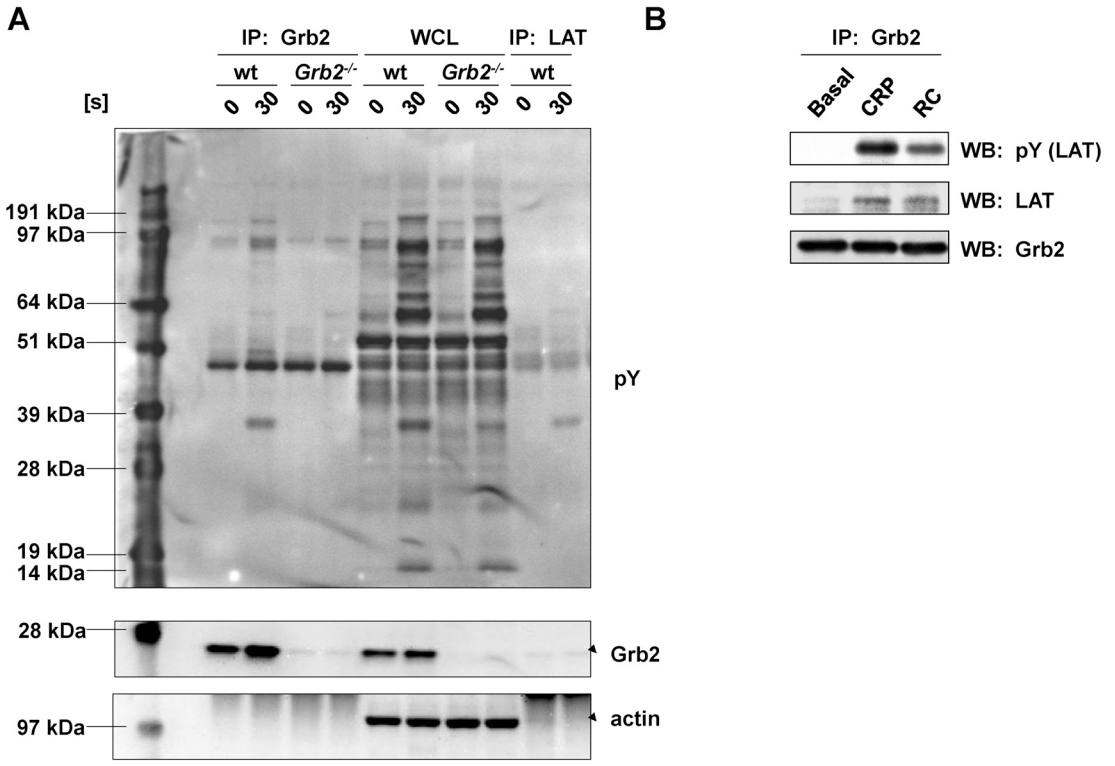

Figure 3-23 Grb2 interacts with LAT upon stimulation with (hem)ITAM receptor agonists. (A) Washed platelets (7x10^8/ml) from wt and *Grb2*$^{-/-}$ mice were stimulated with 0.5 µg/ml CVX in the presence of indomethacin (10 µM) and apyrase (2 U/ml) under stirring conditions for 30 s at 37°C. Grb2 and LAT were immunoprecitated, the proteins were separated by SDS-Page and transferred onto a PVDF membrane. The membrane was probed with an anti-pY mAb (4G10) and reprobed with anti-Grb2 and anti-actin antibodies. **(B)** Washed platelets (5x10^8/ml) were stimulated with 10 µg/ml CRP or 300 nM rhodocytin (RC) for 90 s and subsequently lysed with NP-40 detergent. Grb2 was immunoprecipitated and proteins were transferred onto a PVDF membrane. The membrane was probed with an anti-pY mAb (4G10), and reprobed with anti-LAT and anti-Grb2 antibodies. Figure **(B)** was kindly provided by Dr. Craig Hughes from the group of Prof. Dr. Steve Watson. WB, Western blotting; WCL, whole cell lysate. (Dütting,* Vögtle* *et al.*, *Circ Res,* 2013)[220]

To address this further, wt and *Grb2*$^{-/-}$ platelets were stimulated with the strong GPVI agonist CVX and changes in protein tyrosine phosphorylation of key components of the ITAM signaling cascade were further analyzed by Western blotting. Stimulation of GPVI induces Src-dependent phosphorylation of the FcR γ-chain ITAM, enabling the docking and activation of Syk. This tyrosine kinase initiates a downstream signaling cascade, that involves formation of a protein complex comprising LAT, SLP-76, Vav1/Vav3, Tec family kinases and PI3K and culminates in the activation of PLCγ2 (see introduction and [12]). Notably, Syk phosphorylation at Y519/520, which has been reported to reflect the kinase's activity,[229] was

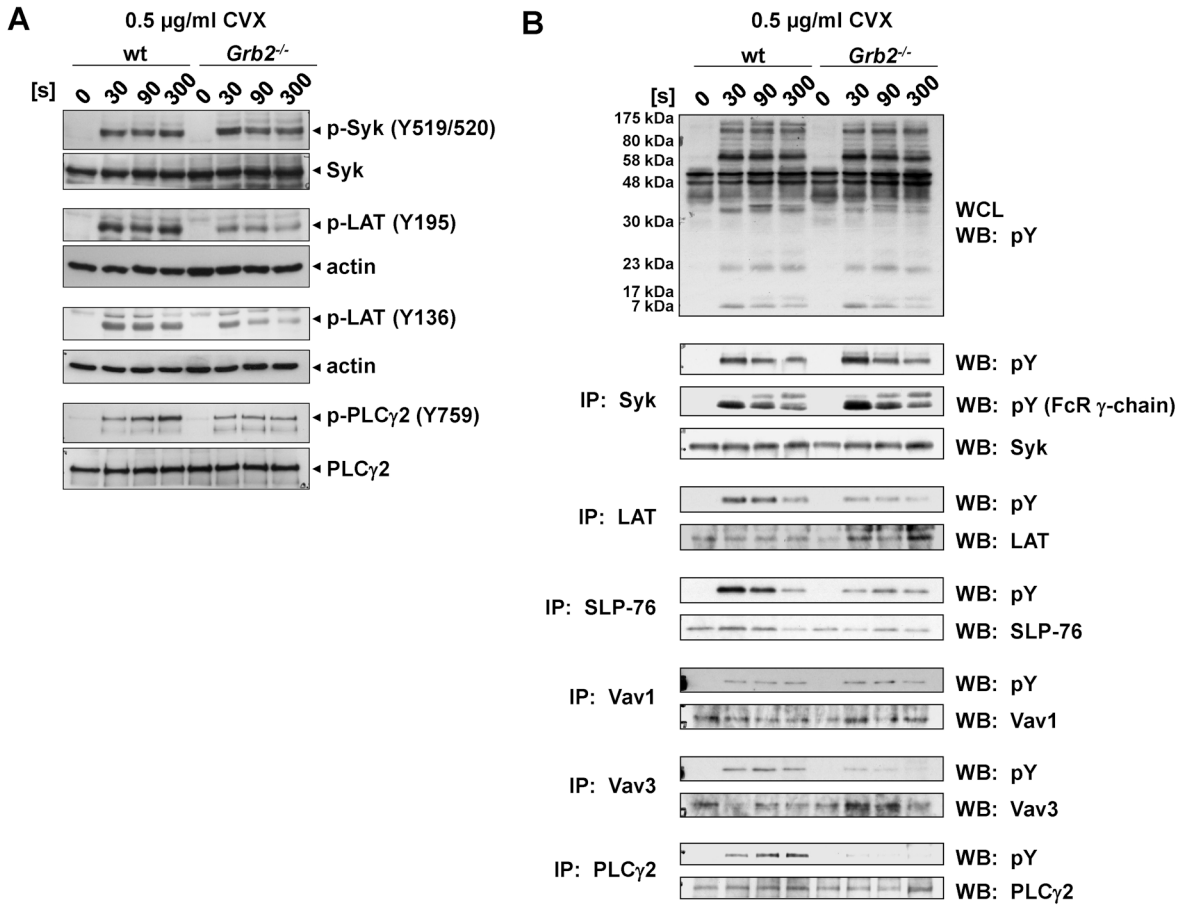

Figure 3-24 Defective ITAM-induced signaling in *Grb2*$^{-/-}$ platelets. (A) Washed platelets (7x10^8/ml) from wt and *Grb2*$^{-/-}$ mice were stimulated with 0.5 µg/ml CVX in the presence of indomethacin (10 µM) and apyrase (2 U/ml) under stirring conditions at 37°C. Aliquots were taken at the indicated time points and subsequently lysed with NP-40 detergent. Proteins were separated by reducing SDS-PAGE, blotted on a PVDF membrane, and stained using the indicated phospho-specific antibodies. Staining of the respective non-phosphorylated proteins or actin served as loading controls. The result shown is representative for three individual experiments. **(B)** Washed platelets (5x10^8/ml) were stimulated with 0.5 µg/ml CVX in the presence of indomethacin (10 µM) and apyrase (2 U/ml) for the indicated time points and subsequently lysed with NP-40 detergent. Syk, LAT, SLP-76, Vav1, Vav3, and PLCγ2, were immunoprecipitated and proteins were separated by SDS-PAGE and transferred to a PVDF membrane. The membrane was probed with an anti-pY mAb (4G10), and reprobed with anti-Syk, LAT, SLP-76, Vav1, Vav3, and PLCγ2 antibodies. WB, Western blotting; WCL, whole cell lysate (Dütting,* Vögtle* *et al.*, *Circ Res,* 2013)[220]

maintained in Grb2-deficient animals, indicating normal Syk activation (Figure 3-24 A). In contrast, phosphorylation of LAT at Y136 (corresponding to Y132 in human), the high affinity binding site for PLCγ2, and at Y195 (Y191 in human), which is bound by Grb2 and contributes to PLCγ2 activation,[79] was strongly reduced in Grb2-deficient platelets compared to wt platelets, resulting in reduced phosphorylation of PLCγ2 (Y759; Figure 3-24 A). These results were confirmed and further expanded by IP studies of our collaboration partners in Birmingham (Figure 3-24 B): Proteins upstream of the LAT signalosome, namely FcR γ-chain and Syk exhibited unaltered overall tyrosine phosphorylation in *Grb2*$^{-/-}$ platelets, while

phosphorylation of proteins within or downstream of the LAT signalosome, like SLP-76, LAT, Vav3 and PLCγ2, was strongly impaired. These results position Grb2 as a central adapter molecule within the LAT signalosome in platelets, stabilizing the protein complex by direct association, thereby enabling downstream signaling and platelet activation.

Analogous to the GPVI signaling studies, platelets were also stimulated with rhodocytin, an agonist of the hemITAM receptor CLEC-2, to analyze the role of Grb2 in the signaling pathway downstream of this receptor. Like for GPVI, phosphorylation of proteins located upstream of the LAT signalosome, most importantly CLEC-2 itself and Syk, was not affected in Grb2-deficient platelets, while phosphorylation of proteins within or downstream the LAT signalosome was reduced (Figure 3-25). Of note, although the decrease in LAT phosphorylation in *Grb2*$^{-/-}$ platelets appeared to be similar defective after GPVI or CLEC-2 stimulation, the effect of Grb2 deficiency on PLCγ2 phosphorylation was milder after CLEC-2 stimulation (Figure 3-24 vs. Figure 3-25).

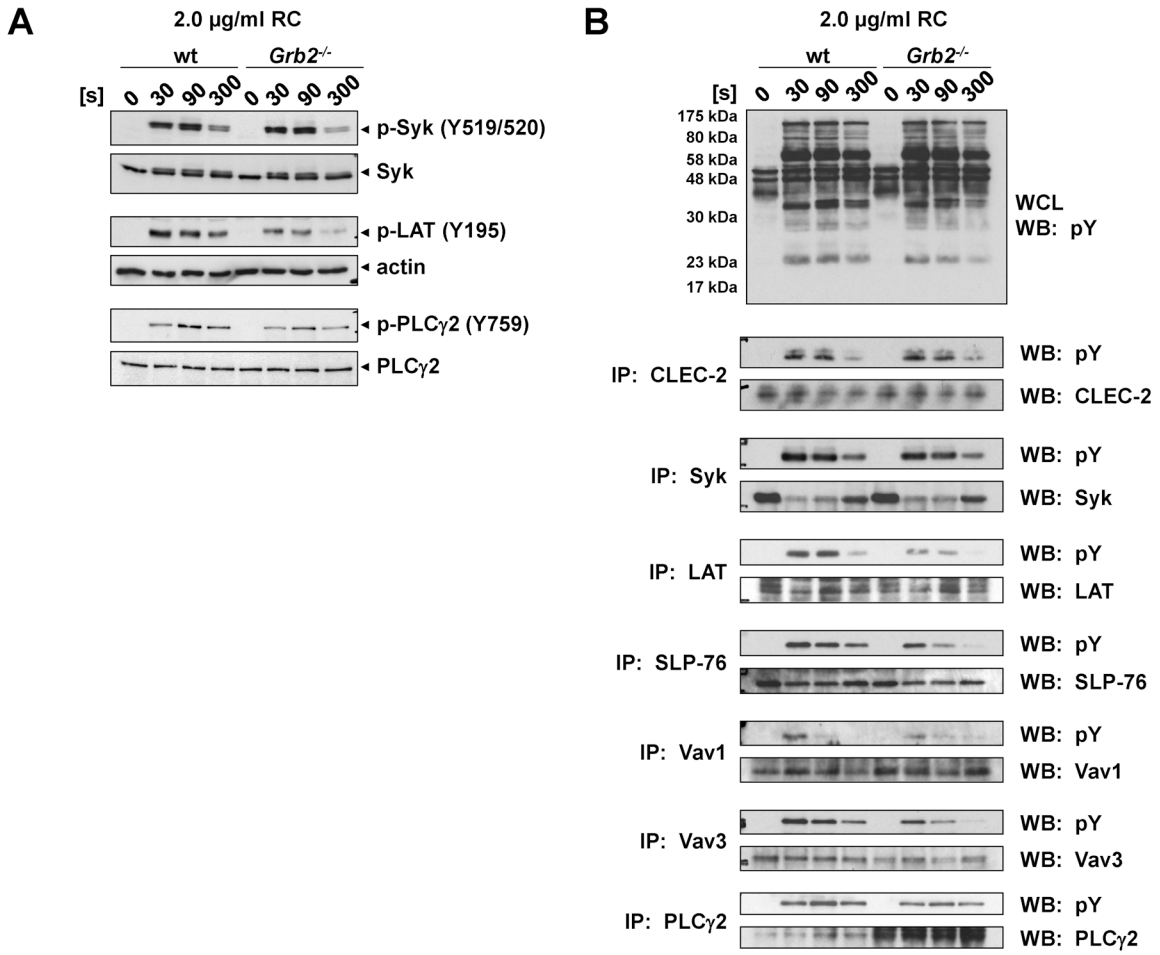

Figure 3-25 Impaired hemITAM signaling in *Grb2*$^{-/-}$ platelets. (A, B) Washed platelets (7x10^8/ml **(A)** or 5x10^8/ml **(B)**) from wt and *Grb2*$^{-/-}$ mice were stimulated with 2.0 µg/ml rhodocytin (RC) in the presence of indomethacin (10 µM) and apyrase (2 U/ml) under stirring conditions at 37°C. Aliquots were taken at the indicated time points and the sample were processed as in Figure 3-24. WB, Western blotting; WCL, whole cell lysate (Dütting,* Vögtle* *et al.*, *Circ Res,* 2013)[220]

Grb2 is an established mediator of Ras-*mitogen activated protein* (MAP) kinase signaling in receptor tyrosine kinase, as well as in BCR and TCR signaling. In platelets, the MAP kinases p38, JNK and ERK1/2 are activated upon stimulation with various agonists, but the knowledge about their function and signaling pathways is limited.[230] Therefore, MAP kinase signaling in Grb2-deficient platelets was investigated in collaboration with Carmen Schäfer from the group of Dr. Heike Hermanns (Rudolf Virchow Center for Experimental Biomedicine, Würzburg). Interestingly, Grb2-deficient platelets stimulated with CVX exhibited an impaired phosphorylation of ERK1/2 as compared to wt platelets, whereas phosphorylation of p38 was unaltered (Figure 3-26 A). Increased phosphorylation of JNK in response to platelet stimulation was observed neither in wt nor in *Grb2*$^{-/-}$ platelets. Of note, ERK1/2 phosphorylation was normal in Grb2-deficient platelets upon platelet stimulation with thrombin (data not shown).

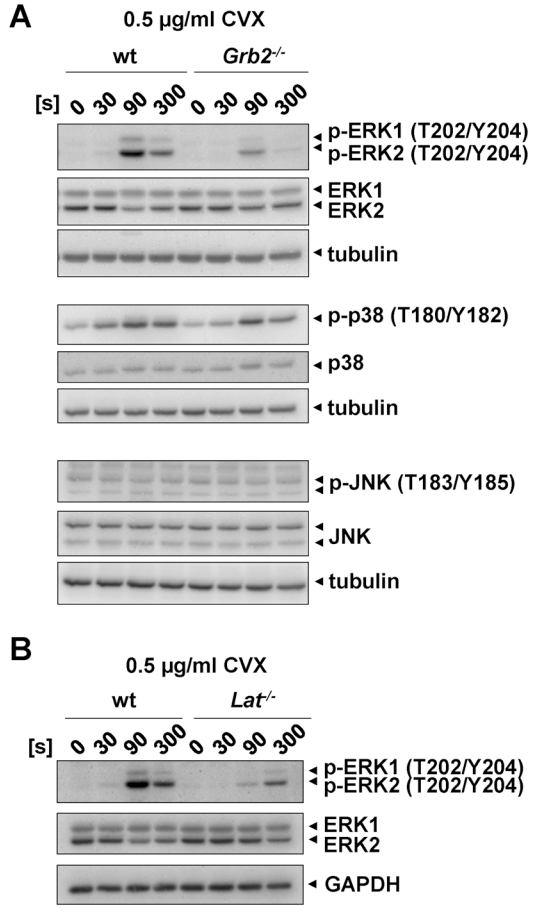

Figure 3-26 Defective ERK1/2 phosphorylation in Grb2- and LAT-deficient platelets. Washed platelets (7x10^8/ml) from *Grb2*$^{-/-}$ mice **(A)** or *Lat*$^{-/-}$ mice **(B)** with their respective wt control were stimulated with 0.5 µg/ml CVX in the presence of indomethacin (10 µM) and apyrase (2 U/ml) under stirring conditions at 37°C. Aliquots were taken at the indicated time points and subsequently lysed with NP-40 detergent. Samples were blotted on a PVDF membrane and stained using the indicated phospho-specific antibodies. Staining of the respective non-phosphorylated proteins, GAPDH or tubulin served as loading controls. The results shown are representative for three individual experiments. (Dütting,* Vögtle* *et al.*, *Circ Res,* 2013)[220]

To address a possible involvement of the LAT-Grb2 interaction in MAP kinase activation, ERK1/2 signaling was analyzed in LAT-deficient platelets. A similar reduction in ERK1/2 phosphorylation compared to *Grb2*$^{-/-}$ was seen in *Lat*$^{-/-}$ platelets (Figure 3-26 B), indicating

that Grb2-dependent recruitment of SOS1 to the LAT signalosome participates in ERK1/2 activation. Alternatively, impaired ERK1/2 phosphorylation may also be a result of impaired PKC-activity, as a consequence of reduced PLCγ2-mediated DAG production.[231]

3.3 Studies on the proteolytic regulation of CD84 receptor levels in platelets

Beside ITAM coupled receptors platelets also harbor receptors with ITIM or ITSM, with the SLAM family members CD150 and CD84 belonging to the latter group. CD84 is abundantly expressed on human and mouse platelets and has initially been supposed to strengthen platelet-platelet interactions upon platelet aggregation.[175]

Besides modulation of intracellular signaling pathways, regulation of receptor levels, either by internalization or intra- or extracellular proteolytic cleavage, represents another important mechanism to downregulate platelet reactivity. Extracellular cleavage by metalloproteinases, a process termed shedding, has already been demonstrated for several prominent platelet receptors. A proteomic approach provided the first evidence for CD84 cleavage from the surface of human platelets in a metalloproteinase-dependent manner, but details of this process remained elusive.[194] Therefore, the mechanisms underlying the regulation of CD84 receptor levels were studied in detail together with Dr. Sebastian Hofmann in our research group.[202]

3.3.1 CD84 is cleaved from the surface of human and mouse platelets

The starting point to investigate the proteolytic regulation of CD84 was a publication from Fong *et al.*, who identified soluble CD84 in the supernatant of activated human platelets using a mass spectrometric approach.[194] To study this process in more detail, washed human platelets were stimulated with thrombin or the GPVI agonist CRP and surface expression levels of CD84 were measured by flow cytometry (Figure 3-27). Indeed, substantial downregulation of CD84 surface levels in response to CRP and moderate downregulation in response to thrombin were detected. Importantly, these effects were inhibited in the presence of the broad range metalloproteinase inhibitor, GM6001. These data confirmed that CD84 surface expression in human platelets decreases in response to agonist stimulation in a metalloproteinase-dependent manner.

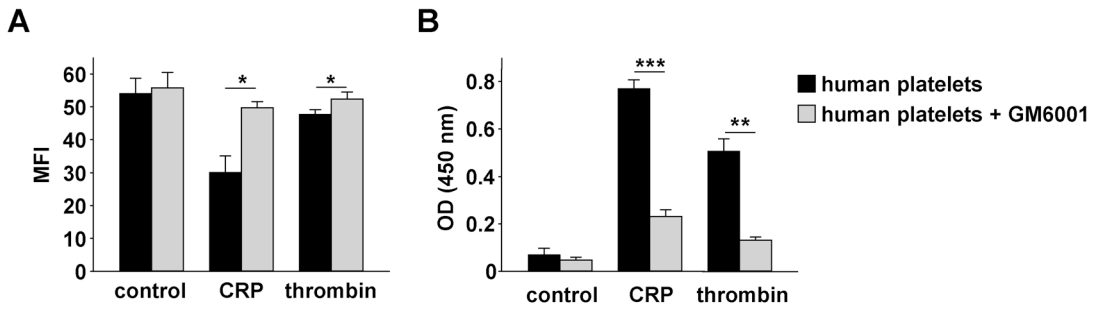

Figure 3-27 CD84 is cleaved from human platelets in a metalloproteinase dependent manner. Washed human platelets were stimulated with CRP (40 µg/ml) or thrombin (0.5 U/ml) for 1 h at 37°C in the presence or absence of the broad range metalloproteinase inhibitor GM6001 (100 µM). **(A)** Platelets were stained with the FITC-labeled anti-CD84 antibody for 15 min and analyzed directly by flow cytometry. **(B)** Alternatively, platelets were centrifuged and supernatants were applied on a MAX.3-coated ELISA plate and CD84 was detected using 2G7-biotin as described in the *Methods* section. Results are mean ± SD (n=3 individuals, representative of 2 individual experiments), * $p<0.05$; ** $p<0.01$ and *** $p<0.001$. (Hofmann,* Vögtle* *et al., J Thromb Haemost, 2012*)[202]

Total surface expression levels of CD84, as measured by flow cytometry, may also be influenced by internalization or exposure of additional CD84 proteins originating from intracellular pools. To circumvent this limitation, an ELISA system, using two monoclonal antibodies directed against distinct epitopes on the extracellular domain of human CD84 was established for direct measurements of *soluble CD84* (sCD84) in the platelet supernatant. As shown in Figure 3-27 B, the release of sCD84 from thrombin- and CRP-stimulated human platelets was confirmed by this technique.

Next, the regulation of CD84 was analyzed in mouse platelets, since genetic mouse models allow a deeper analysis of the underlying molecular mechanisms. In a first set of experiments, washed mouse platelets were activated with thrombin, the GPVI agonists CRP and CVX or the CLEC-2 activating snake venom protein rhodocytin. The release of sCD84 was determined with a newly established ELISA system, designed to detect the extracellular domain of mouse CD84. High levels of sCD84 were measured in the supernatant of wt platelets in response to stimulation with each of these agonists, compared to the untreated control (Figure 3-28 A). In contrast, virtually no sCD84 was detected when the experiments were performed in the presence of GM6001, strongly suggesting that CD84 cleavage was mediated by metalloproteinases. The specificity of the ELISA system was confirmed in experiments with supernatants from *CD84*$^{-/-}$ platelets, where only background signals were obtained (Figure 3-28 A).

Blocking platelet aggregation with inhibitors of integrin αIIbβ3 has previously been shown to influence CD40L[191], but not GPVI shedding.[186] To investigate whether CD84 shedding is influenced by αIIbβ3 signaling and aggregation, integrin αIIbβ3 binding to fibrinogen was

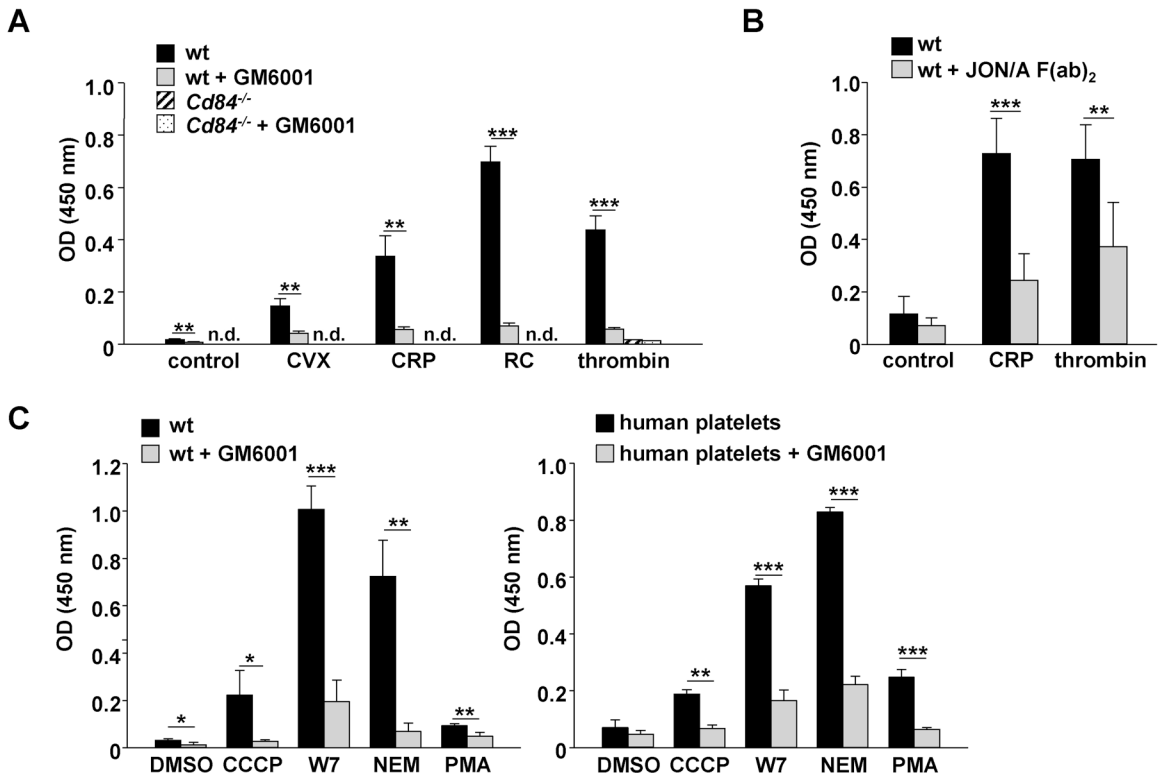

Figure 3-28 Metalloproteinase-dependent shedding of CD84 from mouse and human platelets. **(A)** Washed wt mouse platelets were incubated with CVX (1 µg/ml), CRP (40 µg/ml), rhodocytin (RC, 2 µg/ml) or thrombin (0.5 U/ml) for 1 hour at 37°C in the presence or absence of the broad range metalloproteinase inhibitor GM6001 (100 µM). Supernatants of platelets were applied on a JER1-coated ELISA plate and mouse CD84 was detected using mCD84.7-biotin as described in the *Methods* section. Platelet supernatants from CD84-deficient (*Cd84*$^{-/-}$) mice served as controls. n.d., not detectable. **(B)** Washed mouse platelets were incubated with CRP (40 µg/ml) or thrombin (0.1 U/ml) in the presence or absence of 25 µg/ml JON/A F(ab)$_2$ and ELISA was performed as described. **(C)** Washed mouse (left panel) or human platelets (right panel) were incubated with CCCP (100 µM) or W7 (150 µM) for 1 hour at 37°C, NEM (2 mM) for 20 min or PMA (50 ng/ml) for 15 min at 37°C in the presence or absence of GM6001. ELISA was performed as described. DMSO treatment served as control. Results of all experiments are mean ± SD (n=4 mice or 3 individuals per group, representative of 2-3 individual experiments). * p<0.05, ** p<0.01 and *** p<0.001 (Hofmann,* Vögtle* *et al., J Thromb Haemost, 2012*)[202]

blocked with F(ab)$_2$ fragments of the JON/A antibody.[204] Less sCD84 was detected after CRP and thrombin stimulation in the presence of JON/A F(ab)$_2$, indicating that cleavage of CD84 was, at least in part, dependent on platelet aggregation (Figure 3-28 B). Of note, addition of JON/A F(ab)$_2$ after the agonist incubation period did not reduce the sCD84 signal in ELISA, excluding that the F(ab)$_2$ interfered with the signal (data not shown). These results were confirmed with platelets from mice lacking the cytoskeletal protein talin1, which is required for inside-out activation of integrins (data not shown).

To further assess the mechanisms underlying CD84 ectodomain shedding, washed mouse platelets were treated with different agents known to induce shedding of multiple platelet

membrane receptors by distinct mechanisms[38] and cleavage of CD84 from the platelet surface was measured by sCD84 ELISA.

The calmodulin inhibitor W7 induces the disruption of calmodulin from receptors, thereby facilitating ectodomain shedding by ADAM10 and ADAM17. NEM is a thiol-modifying reagent which directly activates the metalloproteinases by acting on a cysteine switch within the proteases (see introduction). Both reagents induced marked ectodomain shedding of CD84 as revealed by detection of high levels of sCD84 in the platelet supernatant compared to the untreated control. This effect was virtually abolished in the presence of GM6001 (Figure 3-28 C). CCCP induces mitochondrial injury and triggers receptor shedding mainly in an ADAM17-dependent manner.[184,192] Compared to W7 and NEM, this agent induced only a mild GM6001-sensitive increase in sCD84 in the platelet supernatant. Similar results were obtained with human platelets for these three reagents (Figure 3-28 C). PMA is an activator of PKC, thereby inducing ectodomain shedding mainly by ADAM17.[184,188] PMA treatment of mouse platelets resulted only in weak metalloproteinase-dependent shedding of sCD84 as compared to untreated controls, while in human platelets, the increase in sCD84 levels in response to PMA was slightly more pronounced (Figure 3-28 C).

3.3.2 Dual regulation of CD84 by calpain and metalloproteinases

To gain deeper insights, the processing of CD84 in response to shedding inducing agents was analyzed by Western blotting, using two different antibodies: JER1 (anti-CD84$^{N\text{-}term}$), which also served as the capture antibody for the soluble fragment in ELISA experiments, and the polyclonal antibody, M-130, which has been raised against the intracellular C-terminal part of CD84 (anti-CD84$^{C\text{-}term}$).

The band of the full length murine CD84 protein appeared between 55 and 72 kDa under non-reducing conditions, much higher than the calculated molecular weight of approximately 37 kDa, because CD84 is highly glycosylated.[174] In unstimulated platelets, M-130 detected only the full length protein, while an additional band at a size of approximately 15 kDa appeared in NEM-treated platelets (Figure 3-29 A, lower left). As at the same time the band intensity of the full length protein decreased, it is conceivable that this 15 kDa band represents the C-terminal remnant of CD84, which is generated by shedding of the receptor ectodomain. This assumption was confirmed by the finding that GM6001 abrogated the appearance of this additional band in the lysate of NEM treated platelets. Also the band intensity of the full length protein recovered (Figure 3-29 A, lower left).

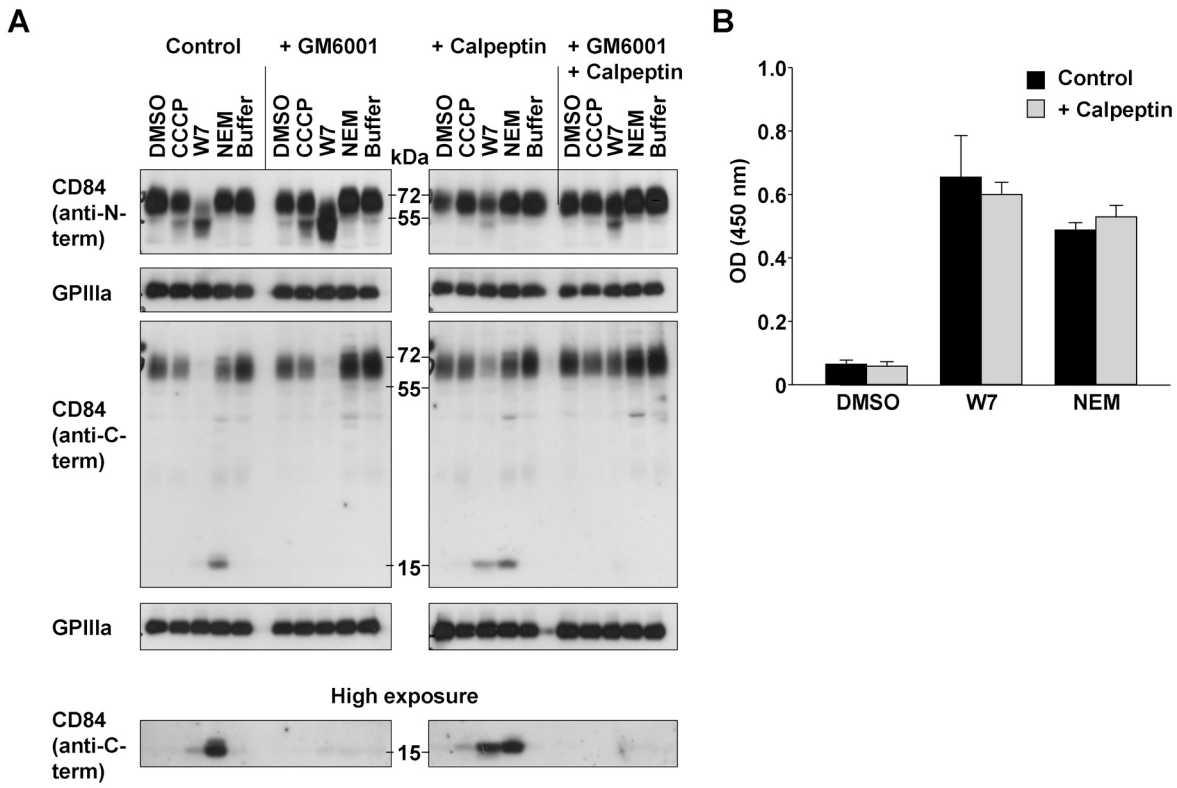

Figure 3-29 Calpain and metalloproteinases cleave CD84 independently. (A) Washed platelets from wt mice were preincubated at 37°C for 15 min in the presence or absence of GM6001 (100 µM), and/or calpeptin (5 µg/ml), an inhibitor of calpain. Shedding was induced with CCCP (100 µM, 1 h), W7 (150 µM, 1 h), and NEM (2 mM, 20 min). DMSO or buffer served as control. CD84 was detected by Western blotting with anti-CD84$^{N\text{-term}}$ antibody JER-1 and anti-CD84$^{C\text{-term}}$ antibody M-130. GPIIIa was used as a loading control (pooled platelets from 5 mice, representative of 3 individual experiments). **(B)** Washed platelets from wt mice were preincubated at 37°C for 15 min in the presence or absence calpeptin (5 µg/ml). Shedding was induced with W7 (150 µM, 1 h) or NEM (2 mM, 20 min). Soluble CD84 in the supernatant was detected by ELISA. Results are mean ± SD (n=4 mice per group, representative of 2 individual experiments). (Hofmann,* Vögtle* *et al., J Thromb Haemost, 2012*)[202]

Given the considerable GM6001-sensitve release of sCD84 into the supernatant upon platelet treatment with CCCP or W7 (Figure 3-28 C), which in case of W7 even exceeded the effect of NEM, it was surprising not to detect the C-terminal remnant in the respective lysates. Nevertheless, the band of the full length protein was clearly reduced in intensity after CCCP treatment compared to the untreated control or even absent after W7 treatment (Figure 3-29 A, lower left).

One possible explanation was that CD84, in addition to ectodomain shedding, may be cleaved in its intracellular C-terminus and that this cleavage interferes with binding of the anti-CD84$^{C\text{-term}}$ antibody, M-130. This assumption was further supported by the fact that a shift in molecular weight of CD84 was detectable with the anti-CD84$^{N\text{-term}}$ antibody in the lysates of platelets treated with W7 or CCCP, indicating a shortening of the protein.

Moreover, this shift as well as the lack of binding of the anti-CD84$^{C\text{-}term}$ antibody was not influenced by GM6001, excluding metalloproteinases as mediators of this process.

As a possible candidate enzyme for mediating this intracellular cleavage the cysteinyl protese calpain was identified, since (i) it has previously been recognized that shedding by metalloproteinases often occurs concomitantly with activation of calpains[38] and (ii) calmodulin-binding proteins are frequently substrates for calpains.[232] This hypothesis was further strengthened by bioinformatical analysis of the CD84 C-terminus with an online prediction tool (http://calpain.org).[233] The potential cleavage site with the highest score in the murine CD84 protein was found at an arginine residue at position 270, which is located between the two ITSMs (Figure 3-30). Of note, this arginine residue, as well as the biochemical properties of the adjacent amino acids, are highly conserved in mammals, implying a functional relevance of this sequence (Figure 3-30 B).

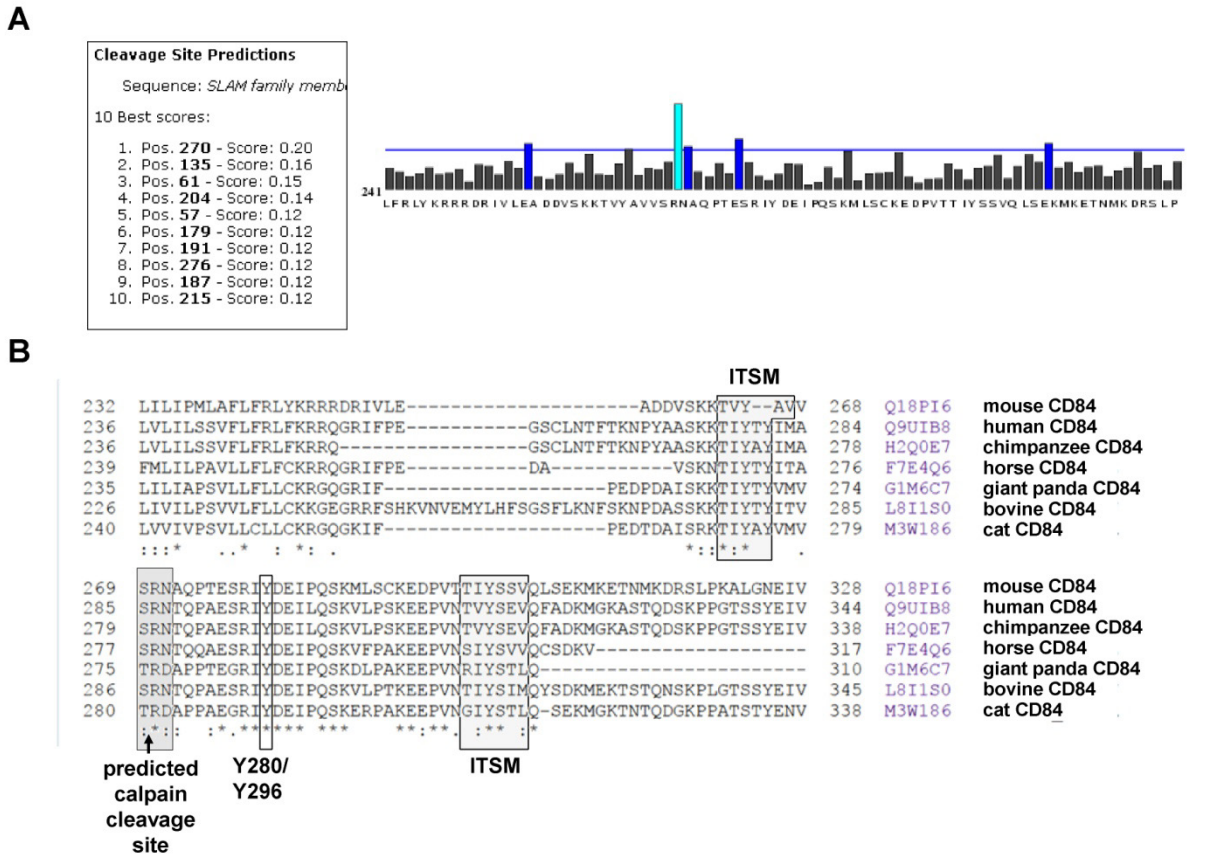

Figure 3-30 Bioinformatical information about cleavage of CD84 by calpain. (A) Predicted calpain cleavage within the murine CD84 protein as predicted by the online prediction tool http://calpain.org (SVM RBF kernel prediction model).[233] Top 10 cleavage site predictions are shown on the left, a graphical illustration of the results, ranging from amino acid 241 to 300, is shown on the right. **(B)** Sequence alignment of the C-terminal part of CD84 proteins form different species (www.uniprot.org, program: clustalO). Highlighted are the two ITSMs, the predicted calpain cleavage site and a tyrosine residue (Y280 and Y296 in mouse and human, respectively), that has been reported to become phosphorylated upon platelet aggregation.[175]

To collect experimental evidence for calpain-mediated cleavage of the CD84 C-terminus, the calpain-inhibitor calpeptin was used. Strikingly, preincubation of platelets with calpeptin abolished the shift in the molecular weight of CD84 seen in the lysates of W7 and CCCP treated platelets with the anti-CD84$^{N\text{-}term}$ antibody JER1 (Figure 3-29 A, upper right) and also allowed the detection of the C-terminal remnant with the anti-CD84$^{C\text{-}term}$ antibody M-130 (Figure 3-29 A, lower right). Moreover, also the binding of anti-CD84$^{C\text{-}term}$ antibody to the full length CD84 protein was enhanced. Together, these observations demonstrated that calpain can cleave both the full length CD84 protein as well as the remnant generated by metalloproteinases. The band intensity for this remnant was strong after W7 and NEM treatment and weak for lysates of CCCP-treated platelets, nicely correlating with the results obtained with the sCD84 ELISA system (Figure 3-28 C). Of note, no C-terminal remnant was detected upon platelet treatment with PMA (data not shown). Therefore, PMA was excluded from further Western blot analyses.

When platelets were preincubated with calpeptin and GM6001 in combination, the appearance of the 15 kDa remnant (detected by anti-CD84$^{C\text{-}term}$) as well as the shift in molecular weight and the decrease in band intensity (anti-CD84$^{N\text{-}term}$) were diminished, showing additive effects of the two inhibitors (Figure 3-29 A, right). Importantly, all bands detected by both antibodies in these studies were specific for CD84 as no signal was obtained when the experiments were performed with *Cd84*$^{-/-}$ platelets (data not shown). Since there had been concerns about the specificity of calpeptin,[234] two other membrane-permeable calpain inhibitors, MDL 28170 and ALLN were tested. Like calpeptin, these two inhibitors blocked the shift of the full length CD84 protein in anti-CD84$^{N\text{-}term}$ blots and rescued the detection of the C-terminal remnant with the anti-CD84$^{C\text{-}term}$ antibody upon W7 treatment, confirming the role for calpain in this process (data not shown).

In order to estimate whether inhibition of calpain activity interferes with CD84 ectodomain shedding by metalloproteinases, ELISA measurements were conducted. The levels for sCD84 were unaltered in the presence of calpeptin (Figure 3-29 B).

These results demonstrated that CD84 is proteolytically regulated by two independent mechanisms: extracellular ectodomain shedding by metalloproteinase(s) and intracellular cleavage by calpain. Apparently, shedding was functional under calpain-inhibiting conditions and *vice versa*. A summary of these results is shown schematically in Figure 4-1.

3.3.3 ADAM10 is critical for CD84 ectodomain cleavage in murine platelets

Having identified calpain as the protease for intracellular cleavage of CD84, it was sought to identify the metalloproteinase that is required for extracellular cleavage. Two possible candidates are ADAM10 and ADAM17, which are both GM6001-sensitive and expressed in platelets.[38] To test their individual contribution, platelets from *Adam17$^{ex/ex}$ bone marrow chimeric* (BMc) mice were studied. These mice exhibit a virtually complete loss of ADAM17 protein in hematopoietic cells, including platelets.[192,207] While parallel performed flow-cytometric control measurements showed absence of GPIb shedding in *Adam17$^{ex/ex}$* platelets in response to CCCP, W7, NEM and PMA (data not shown), levels of released sCD84, as

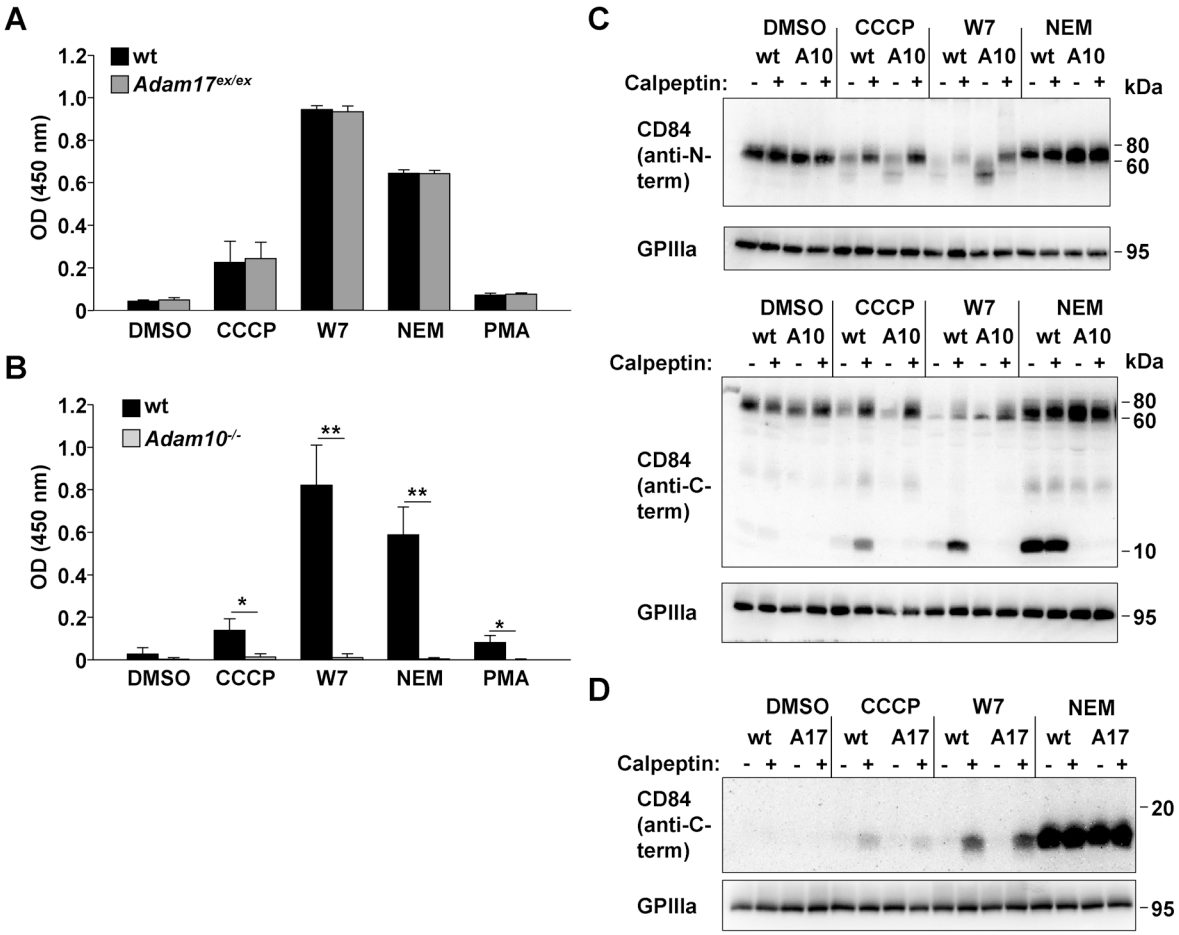

Figure 3-31 ADAM10 is essential for CD84 ectodomain shedding. Washed platelets from **(A)** *Adam17$^{ex/ex}$* bone marrow chimeric mice and **(B)** *Adam10$^{-/-}$* mice with their respective wt controls were treated with CCCP (100 µM, 1 h), W7 (150 µM, 1 h), NEM (2 mM, 20 min), PMA (50 ng/ml, 15 min) or DMSO as a vehicle control. sCD84 in the supernatants was detected by ELISA as described in *Methods*. Results are mean ± SD (n=4 mice per group, representative of 2 individual experiments). * $p<0.05$ and ** $p<0.01$ **(C, D)** Western blot detection of CD84 in lysates of platelets from mice with the indicated genotype. A10, *Adam10$^{-/-}$*; A17, *Adam17$^{ex/ex}$*; wt are the corresponding controls. Platelets were incubated with calpeptin (5 µg/ml, 37°C, 15 min) or vehicle control and shedding was induced as described above. (2 mice pooled per group, representative of 2-3 individual experiments). (Hofmann,* Vögtle* *et al., J Thromb Haemost, 2012*)[202]

determined by ELISA, were indistinguishable between wt and *Adam17*$^{ex/ex}$ platelets, excluding a major role of ADAM17 in CD84 ectodomain shedding under these experimental conditions (Figure 3-31 A).

To investigate the dependence of CD84 shedding on ADAM10, platelets from mice with a MK- and platelet-specific deficiency of ADAM10 (*Adam10*$^{fl/fl}$*/PF4-Cre*$^{+/-}$ mice, further on referred to as *Adam10*$^{-/-}$) were analyzed.[192] In sharp contrast to wt and *Adam17*$^{ex/ex}$ platelets treated with either agent, sCD84 was virtually not detectable in the supernatant of *Adam10*$^{-/-}$ treated platelets (Figure 3-31 B). These results were confirmed by Western blot analysis, where the band intensity of the C-terminal remnant in the lysates of *Adam17*$^{ex/ex}$ platelets was indistinguishable from that of wt platelets, but no C-terminal remnant was detectable in *Adam10*$^{-/-}$ platelets (Figure 3-31 C and D).

Taken together, these data established ADAM10 as the principal sheddase cleaving CD84 in mouse platelets, while ADAM17 is not significantly involved in this process.

In the next step, it was investigated whether ADAM10 is also the principal sheddase for CD84 cleavage in response to stimulation with platelet receptor agonists. Platelets from wt and *Adam10*$^{-/-}$ mice were stimulated with the GPVI agonists CRP and CVX, the CLEC-2 agonist rhodocytin and the GPCR-agonist thrombin. As illustrated in Figure 3-32 A, none of these agonists induced significant ectodomain shedding in the absence of ADAM10, as measured by ELISA.

To gather information on shedding kinetics and to investigate the intracellular cleavage by calpain, wt and *Adam10*$^{-/-}$ platelets were stimulated for different times in the presence or absence of calpeptin and lysates were subjected to Western blotting. Shedding, visualized by detection of the 15 kDa remnant with the anti-CD84$^{C\text{-}term}$ antibody M-130, occurred within 5 minutes in response to all agonists and the band intensity increased over time (Figure 3-32 B), revealing that CD84 shedding is a rather slow process. Remarkably, rhodocytin induced also strong activation of calpain, as indicated by the lack of binding of anti-CD84$^{C\text{-}term}$ in the absence of calpeptin, as well as by the shortened CD84 protein detected by the anti-CD84$^{N\text{-}term}$ antibody, in the absence of calpeptin. In contrast, the other agonists only moderately activated calpain. No C-terminal remnant was detected in lysates of platelets deficient in ADAM10, confirming the results from the ELISA. Calpain activity was unaffected by the absence of the metalloproteinase, as apparent in rhodocytin stimulated samples.

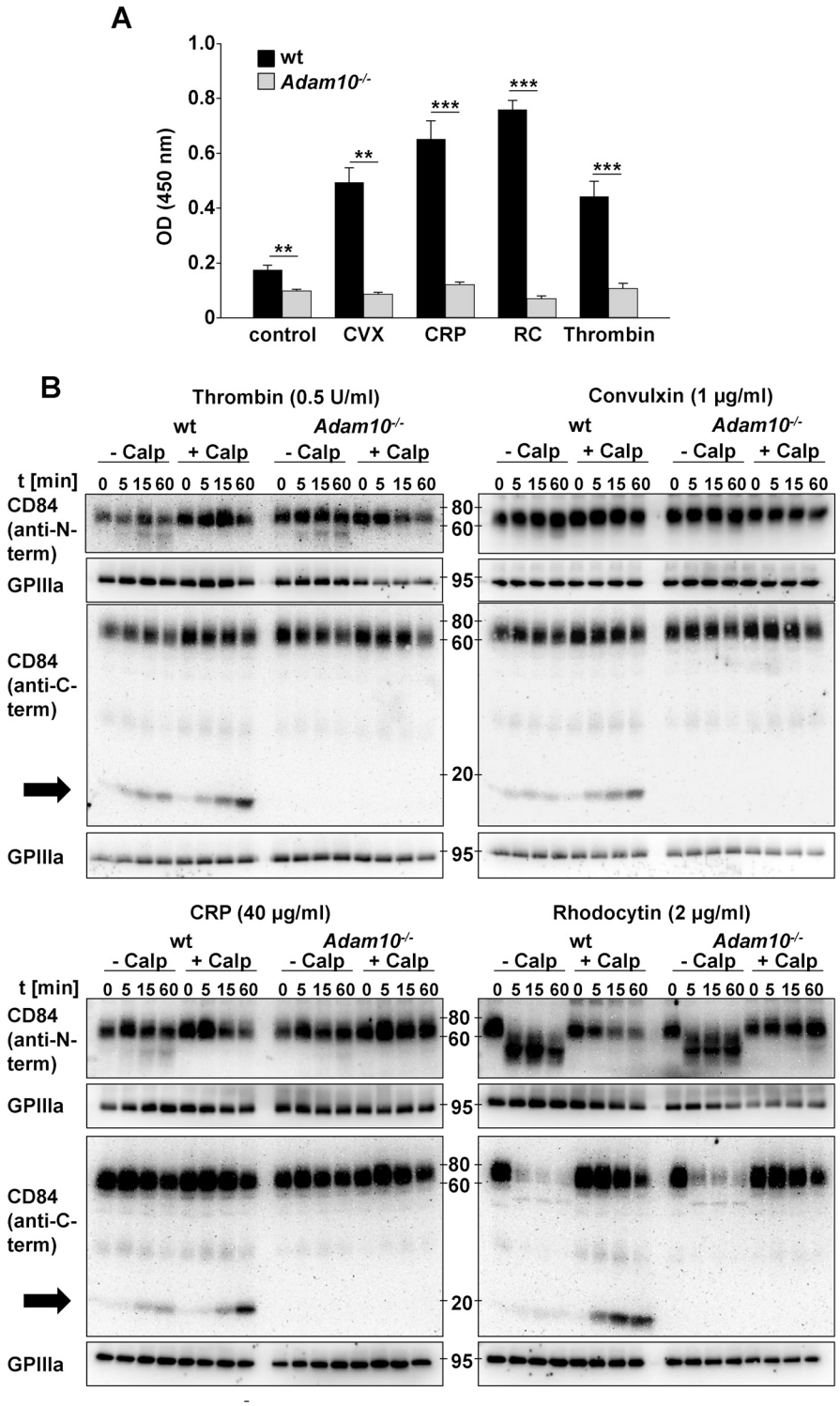

Figure 3-32 ADAM10 cleaves CD84 in response to platelet receptor stimulation. (A) Washed mouse platelets from wt and *Adam10*$^{-/-}$ mice were incubated with CVX (1 µg/ml), CRP (40 µg/ml), rhodocytin (RC, 2 µg/ml) or thrombin (0.5 U/ml) for 1 hour at 37°C. Soluble CD84 was detected by ELISA as described in *Methods*. Results are mean ± SD (n=4 mice per group, representative of 3 individual experiments). ** p<0.01 and *** p<0.001. **(B)** Washed platelets from wt and *Adam10*$^{-/-}$ mice were preincubated for 15 min at 37°C with calpeptin (5 µg/ml) or vehicle control, prior to stimulation for 5 min, 15 min or 1 h with the agonists described above. Platelet lysates were subjected to Western blotting. (4 mice pooled per group, representative of 3 individual experiments). (Hofmann,* Vögtle* *et al., J Thromb Haemost, 2012*)[202]

3.3.4 High concentrations of sCD84 in mouse plasma

To investigate whether CD84 shedding occurs *in vivo*, the levels of sCD84 in mouse plasma were determined by ELISA. Indeed, significant levels of sCD84 could be detected in the plasma of wt mice, while only background signals were obtained from plasma of *Cd84*$^{-/-}$ mice (Figure 3-33 A). Of note, sCD84 plasma levels in *Adam10*$^{-/-}$ mice were markedly reduced compared to wt mice, demonstrating that shedding by platelet ADAM10 occurs constitutively *in vivo* and accounts for approximately half of the total sCD84 protein found in the plasma of normal healthy mice. To investigate whether ADAM17 plays a role in CD84 shedding *in vivo*, sCD84 plasma levels of bone marrow chimeras with platelets double-deficient in ADAM10 and ADAM17 (*Adam10*$^{-/-}$/*Adam17*$^{ex/ex}$)[192] were measured. As depicted in Figure 3-33 A, the levels of sCD84 were not further reduced in plasma of double deficient bone marrow chimeras compared to ADAM10 single deficient mice. In line with this, plasma levels of wt and *Adam17*$^{ex/ex}$ bone marrow chimeras were indistinguishable (data not shown). Therefore, a role for ADAM17 in regulating plasma levels of sCD84 in healthy mice can be excluded.

In order to test whether CD84 shedding occurs during normal blood clotting, non-anticoagulated whole blood was allowed to clot *in vitro* and sCD84 levels were measured in the obtained serum. In wt mice, levels of sCD84 increased approximately two-fold in serum compared to the respective plasma samples (Figure 3-33 B). In contrast, sCD84 concentrations in the serum of *Adam10*$^{-/-}$ mice did not differ from those found in plasma, demonstrating that ADAM10 is the only protease that sheds CD84 during blood clotting.

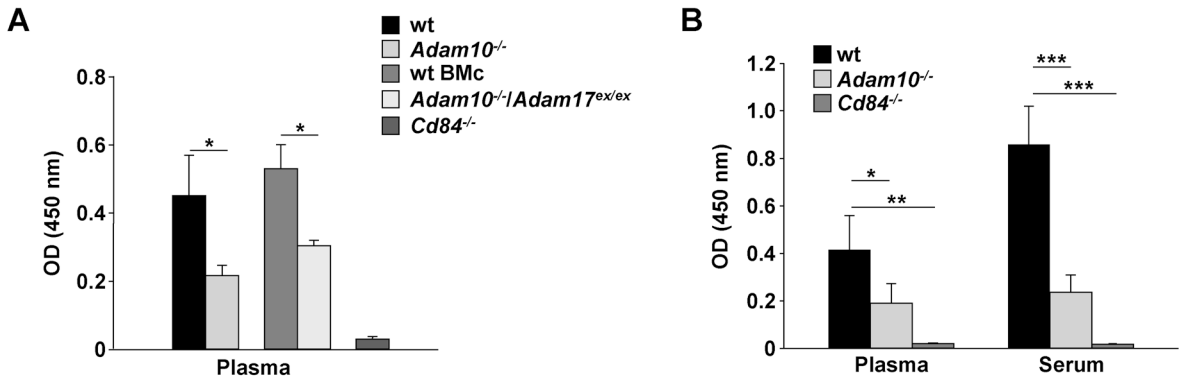

Figure 3-33 CD84 is constitutively shed from platelets and present in mouse plasma. (A) sCD84 levels in the plasma of *Adam10*$^{-/-}$ and *Adam10*$^{-/-}$/*Adam17*$^{ex/ex}$ mice, their respective wt controls and *Cd84*$^{-/-}$ mice were determined by ELISA. **(B)** sCD84 levels in the plasma and serum of wt, *Adam10*$^{-/-}$ and *Cd84*$^{-/-}$ mice were measured by ELISA. Serum and plasma samples were obtained from the same animals and analyzed within a single experiment. Bar graphs represent mean ± SD (n=4 mice per group representative of 2 individual experiments). * $p<0.05$, ** $p<0.01$ and *** $p<0.001$ (Hofmann,* Vögtle* *et al., J Thromb Haemost, 2012*)[202]

4 Discussion

4.1 Constitutive Ca^{2+} influx alters phosphorylation, but not activation of PLCγ1

STIM1 is established as an essential mediator of SOCE in lymphocytes[67] and platelets.[14] The *Stim1*$^{Sax/+}$ mouse is heterozygous for a gain of function mutation of the STIM1 protein and thus provides a model to investigate the impact of constitutive Ca^{2+} influx on T cell physiology and signaling pathways.[149] The data presented in this thesis reveal an altered phosphorylation pattern of the key enzyme PLCγ1 upon TCR stimulation in *Stim1*$^{Sax/+}$ T cells, which was, at least in part, a consequence of calcineurin activity. The enzymatic activity of PLCγ1 was, however, not altered and withdrawal of extracellular Ca^{2+} re-established the phosphorylation pattern of wt T cells. Additionally, a decreased production of Th2-type cytokines of *Stim1*$^{Sax/+}$ T cells was detected.

Ca^{2+} influx triggered by TCR stimulation results in the activation of the Ca^{2+}/calmodulin-dependent phosphatase calcineurin, which facilitates the translocation of NFAT from the cytoplasm into the nucleus, a critical event for T cell activation and proliferation.[68] In *Stim1*$^{Sax/+}$ T cells, NFAT was found in the nucleus independently of TCR stimulation, inidicating that calcineurin is constitutively active even in unstimulated cells (Figure 3-2). This assumption was confirmed by a direct measurement of calcineurin activity (Christoph Hintzen and Attila Braun, personal communication). Despite this observation, the T cell compartment was similar to wt in *Stim1*$^{Sax/+}$ mice (Figure 3-1) and no signs of hyperproliferation or autoimmune reactions were observed.[149] As suggested by Grosse *et al.*,[149] this may be explained by the different spatial and temporal features of the constantly elevated Ca^{2+} entry triggered by the *Stim1*^{Sax} mutation compared to the TCR-induced Ca^{2+} influx which involves a robust and sustained rise localized at the immunological synapse.[235,236] Another physiological consequence that one may have anticipated from constitutive nuclear NFAT localization is anergy, a state of unresponsiveness towards antigenic stimulation. In a current model, anergy is triggered by Ca^{2+}/calcineurin signaling in response to isolated stimulation of the TCR in the absence of costimulation, resulting in the activation of NFAT, but not of its interaction partner AP-1. In the absence of AP-1, NFAT is supposed to impose a genetic program of anergy that counters the cell activation program of the NFAT/AP-1 complex.[70,71] However, *Stim1*$^{Sax/+}$ T cells proliferated normally towards TCR stimulation *in vitro*[149] and produced reasonable amounts of cytokines (Figure 3-7). This result is similar to T cells from transgenic mice, which harbor a constitutively active form of calcineurin.[237] The absence of an anergic phenotype, may be explained by the difference of the low sustained rise of $[Ca^{2+}]_i$ in *Stim1*$^{Sax/+}$ T cells to the transient, but high increase of $[Ca^{2+}]_i$ of an anergy inducing

stimulus.[71] Additionally, the constitutively elevated $[Ca^{2+}]_i$ in *Stim1*$^{Sax/+}$ T cells may lead to an adaptation to elevated Ca^{2+} levels of the T cell already during T cell development, where calcineurin has been shown to play a role.[238] Independently of the underlying cause, the data demonstrates that nuclear NFAT localization does not necessarily lead to an anergic phenotype, at least upon stimulation *in vitro*. Whether *Stim1*$^{Sax/+}$ T cells preferentially differentiate into anergic cells in response to certain stimuli *in vivo*, as supposed for Golli-deficent T cells during EAE,[239] remains to be investigated.

Analysis of the more upstream signaling events revealed normal phosphorylation of the kinases Lck and Zap-70 upon TCR-complex ligation. Surprisingly, however, PLCγ1 phosphorylation at Y783 was completely abolished in *Stim1*$^{Sax/+}$ T cells when stimulated in the presence of extracellular Ca^{2+}. This (de)phosphorylation was regulated in a Ca^{2+}-dependent and highly dynamic manner, since withdrawal of extracellular Ca^{2+} rescued the phosphorylation at this residue (Figure 3-3). Phosphorylation of Y783 is carried out by Itk in T cells[240,241] and is reported to be required for the activation of the enzyme's lipase activity.[214,215] Similar to withdrawal of extracellular Ca^{2+}, treatment of *Stim1*$^{Sax/+}$ T cells with the calcineurin inhibitor CsA also recovered Y783 phosphorylation, demonstrating that calcineurin is involved in the loss of phosphorylation (Figure 3-4). A direct dephosphorylation of Y783 by calcineurin can, however, be excluded, since it is a serine/threonine phosphatase and thus phosphotyrosines are no proper substrates. Preliminary experiments in the group of Dr. Heike Hermanns point towards a participation of the tyrosine-specific protein phosphatase SHP-1 downstream of calcineurin (Christoph Hintzen and Heike Hermanns, personal communication). In addition, enhanced phosphorylation at Y771, a less well characterized PLCγ1 phosphorylation site, was identified in *Stim1*$^{Sax/+}$ T cells upon stimulation in the presence of extracellular Ca^{2+}. Withdrawal of extracellular Ca^{2+} reduced phosphorylation to normal levels (Figure 3-5). The molecules involved in this altered phosphorylation remain to be identified.

Despite this altered phosphorylation pattern, the lipase activity of PLCγ1 in *Stim1*$^{Sax/+}$ T cells was not different from wt T cells under all tested conditions (Figure 3-6). While a previous study reported that Y783 phosphorylation itself is not sufficient for PLCγ1 activation upon epidermal growth factor stimulation *in vitro*,[242] the results presented here indicate that Y783 may be even bypassed. Whether, and if yes to which extent, phosphorylation at Y771 can compensate for the loss of Y783 phosphorylation remains to be investigated. *In vitro* studies in heterologous cell systems reported a negligible role for Y771 phosphorylation in regulating PLCγ1 activity.[215,243] However, it has to be mentioned that Y771, similar to primary wt T cells (Figure 3-5), is hardly phosphorylated in cell lines[242] and that observations from *in vitro* cell

culture systems may not always directly apply to primary cells. Apart from that, a role of Y775 phosphorylation[215] and the recruitment of PLCγ1 accessory molecules such as coronin-1, whose absence dramatically impairs activity, but not phosphorylation of PLCγ1,[244] may also be considered. In conclusion, the altered phosphorylation pattern of PLCγ1 may reflect a piece of a cellular program that allows largely undisturbed signaling process in the presence of elevated $[Ca^{2+}]_i$. Whether other Ca^{2+}/calmodulin binding proteins, e.g. CamKII and IV participate,[72] remains to be investigated.

Upon TCR stimulation, naïve T cells can differentiate into different $CD4^+$ *T helper* (Th) cell subsets, which have distinct functions and secrete different effector cytokines (see introduction). Studies in STIM1- and Orai1-deficient mice revealed a critical role of SOCE for the function of all Th subsets (Th1, 2 and 17) with Th17 cells showing the greatest dependence on this Ca^{2+} entry pathway.[67,245] Measurements of cytokine levels after stimulation of T cells *in vitro* revealed an impaired secretion of the Th2-type cytokines IL-4, 5 and 13 and a tendency towards less IL-10 in *Stim1*$^{Sax/+}$ T cells. The level of the Th1 cytokine IFNγ was moderately, but not significantly elevated, while all other cytokines tested were released to a similar extent by wt and *Stim1*$^{Sax/+}$ T cells (Figure 3-7). When no polarizing cytokines are added to an *in vitro* culture, like in the illustrated experiment, Th1/Th2 differentiation is mainly controlled by the strength of TCR signaling. In general, weak signaling favors Th2 differentiation, while stronger signals result in Th1 differentiation and suppression of Th2 differentiation.[58,59] Therefore, these observations implicate that stimulation resulted in a stronger signal in *Stim1*$^{Sax/+}$ T cells than compared to their wt counterparts, what fits to the expectations of elevated $[Ca^{2+}]_i$. It will be interesting to determine if this reduced capability of Th2-type cytokine production is of functional relevance *in vivo*, e.g. in mouse models of Th2 cell-mediated immune disorders like allergic asthma.[246]

Stim1$^{Sax/+}$ animals showed increased frequencies and numbers of Tregs in the spleen (Figure 3-8). This was of particular interest since mice with a conditional deletion of both *Stim* genes exhibit a pronounced defect in Treg development and decreased Treg populations in thymus and secondary lymphoid organs.[163,247] However, Treg frequencies in the thymus, lymph nodes and blood were unaltered in *Stim1*$^{Sax/+}$ animals, indicating that an increased thymic output of Tregs is not responsible for the elevated numbers observed in spleen (Figure 3-8 and Figure 3-9). Also the proliferation of splenic Tregs was similar between wt and mutant mice, excluding an enhanced proliferation as the underlying cause (Figure 3-9). Alternatively, elevated Treg cell numbers may originate from enhanced differentiation of naïve T cells into Tregs in the periphery (see introduction).[57] Expression of Helios, a reported marker for Tregs of thymic, but not peripheral origin,[218] was, however, comparable within wt and *Stim1*$^{Sax/+}$ Treg populations (Figure 3-9). But since the utility of Helios to discriminate between thymic

and induced Tregs has been questioned in recent studies,[248,249] increased differentiation of naïve T cells into Tregs in *Stim1*$^{Sax/+}$ spleens cannot finally be excluded. Another explanation may be an increased survival of *Stim1*$^{Sax/+}$ Tregs. Indeed, a recent study demonstrated that Treg homeostasis is regulated by pro- and anti-apoptotic pathways in a highly dynamic manner.[250] It remains to be investigated whether *Stim1*$^{Sax/+}$ Tregs show an anti-apoptotic phenotype, but also why they preferentially accumulate in the spleen.

4.2 Grb2 stabilizes the LAT signalosome

Adapter proteins exert essential functions in signaling processes downstream of (hem)ITAM-coupled receptors in hematopoietic cells. In platelets, the formation of a signaling complex called the LAT signalosome, comprised of different adapter and effector proteins is central for proper signal transduction of the (hem)ITAM-coupled receptors GPVI and CLEC-2. The role of the adapter proteins Gads, SLP-76 and LAT in GPVI and CLEC-2 signaling has been addressed in previous studies by the use of knockout mice, but due to the lack of an appropriate animal model, the function of Grb2 in this process long remained unclear. In this study, a novel genetic mouse model with a MK/platelet-specific deletion of Grb2 was used to study the role of Grb2 in platelets *in vitro* and *in vivo*. Grb2-deficient platelets displayed severely impaired (hem)ITAM signaling, but unaltered GPCR function and integrin signaling. This highly specific defect resulted in impaired hemostasis and partially defective arterial thrombus formation.

Grb2 is widely expressed throughout the body and associates with a large variety of receptors and signaling pathways in different cell types.[74,94,96,98] Its physiological importance is highlighted by the early embryonic lethality of *Grb2*$^{-/-}$ mice due to defective differentiation of endodermal cells and formation of the epiblast.[105] Grb2 is also strongly expressed in the hematopoietic system and a role of the Grb2/SOS1/Ras/Raf-1/MEK pathway in thrombopoietin receptor (c-Mpl) induced ERK1/2 activation during MK differentiation was suggested.[251] However, platelet count and size (Figure 3-10) and bone marrow MK numbers (data not shown) were normal in mice with a MK-specific Grb2-deficiency demonstrating that Grb2 is dispensable for megakaryopoiesis and platelet production *in vivo*. This might at least partially be explained by compensatory alternative pathways downstream of c-Mpl leading to ERK1/2 activation, involving either the small GTPase Rap1[111] or PKC-mediated Raf1 activation, independently of Ras.[252,253]

A previous study also presumed a role for Grb2 in integrin outside-in signaling since an increased association between Grb2 and Dok-1 and Dok-3 upon activation of integrin αIIbβ3 was detected.[114] However, in this thesis unaltered platelet spreading on fibrinogen and

normal clot retraction in the absence of Grb2 was observed (Figure 3-14), excluding a major function of the adapter in integrin outside-in signaling. This might be explained by the fact that Dok-3 is not expressed in mouse platelets.[114] In addition, biochemical studies using phosphorylated β3 peptides initially suggested that Grb2 is recruited to a conserved tyrosine motif within the β3 cytoplasmic tail, which becomes phosphorylated upon platelet aggregation[254] and is required for processes like clot retraction.[255] However, a direct interaction of Grb2 to the β3 cytoplasmic tail upon aggregation has not been reported to date and further studies proposed other proteins (e.g. SHC, Dok2 and myosin) as main interaction partners of the β3 integrin.[256,257] The results presented here support this notion. Like Grb2, the adapter proteins Gads and LAT are also dispensable for spreading of mouse platelets.[31,86] In contrast SLP-76 is required for this process.[91,258] It is currently unknown how SLP-76 can serve this function independently of the other adapter proteins.[258]

Grb2 has been implicated in antigen receptor signaling in lymphocytes. Recent reports showed a prominent role of the adapter during B cell maturation by negatively regulating proximal BCR signaling[108,109] and an important function in thymic selection by amplifying TCR signaling.[106,107] Similar to the BCR and TCR complexes, the GPVI/FcR γ-chain complex and CLEC-2 in platelets use a (hem)ITAM signaling module to transduce extracellular signals, thereby mediating platelet activation, aggregation, and thrombus formation (see introduction). Previous studies in human platelets demonstrated that Grb2 binds to the membrane bound adapter molecule LAT[26] and that it is phosphorylated after GPVI-stimulation,[113] indicating a role of Grb2 in ITAM signaling in platelets. However, given the opposing effects of Grb2-deficiency in B and T cells, the exact function of the adapter in platelets was unclear.

In this study, Grb2-deficient platelets exhibited markedly impaired integrin αIIbβ3 activation, degranulation and aggregation in response to GPVI and CLEC-2 stimulation, while the response towards GPCR agonists was unaltered (Figure 3-11 and Figure 3-13). Animals heterozygous for Grb2 deletion, had reduced levels of Grb2 (Figure 3-10) and showed an intermediate phenotype of integrin activation (Figure 3-12). Thus, like in T cells Grb2 positively regulates platelet (hem)ITAM signaling in a quantitative manner.[106,107] The selective (hem)ITAM signaling defect of *Grb2*$^{-/-}$ platelets phenocopied the defects seen in LAT-deficient mice, although to a somewhat lesser extent, but is considerably more pronounced than in platelets lacking the Grb2-related adapter Gads.[31,77] The direct comparison of LAT and Grb2-deficient platelets for integrin αIIbβ3 activation by flow cytometry revealed only minor, but significant differences in response to CRP and a moderate difference in response to the more powerful GPVI agonist CVX (Figure 3-12). This result suggests that the disrupted Grb2-LAT interaction may be the main underlying cause for the GPVI signaling defect in

LAT-deficient mice. The difference between the two strains may be explained by the presence of the functional Grb2 homolog Gads, which also binds to LAT in response to CRP, but to a lesser extent than Grb2.[31] Interestingly, the hemITAM signaling defect was by far more pronounced in *Lat*$^{-/-}$ as compared to *Grb2*$^{-/-}$ platelets, in which the response to high doses of rhodocytin was only mildly impaired. Additionally, the phosphorylation defect of PLCγ2 in *Grb2*$^{-/-}$ platelets was less severe in response to CLEC-2 stimulation as compared to GPVI stimulation while the decrease in LAT phosphorylation was comparable (Figure 3-24 vs. Figure 3-25). These results implicate that the function of Grb2 downstream of CLEC-2 may be compensated for by an independent mechanism that requires LAT, but not necessarily LAT phosphorylation. A differential requirement for adapter proteins in GPVI versus CLEC-2 signaling has also been previously reported for SLP-76, whose lack can be overcome by high concentrations of rhodocytin,[39,44] but not of GPVI agonists.[76,85,86]

While in flow cytometry remarkable GPVI signaling defects were observed at high agonist concentrations, defects in the maximum aggregation response became apparent only at low and intermediate agonist concentrations (Figure 3-13). This difference to flow cytometry data is most likely a consequence of different experimental conditions: in aggregometry high concentrations of washed platelets are used, enabling platelets to amplify the activation process by the release of second wave mediators which signal via GPCRs.[32] In contrast, flow cytometric experiments are performed with diluted washed blood where the release of second wave mediators is less relevant. This was confirmed by measurements with platelets from mice treated with ASA, which blocks the generation of TxA_2. Under these conditions, *Grb2*$^{-/-}$ platelets showed aggregation defects at higher concentrations of collagen compared to untreated controls (Figure 3-21).

The GPVI signaling defect in *Grb2*$^{-/-}$ platelets translated into severely impaired platelet adhesion and aggregate formation on collagen under flow (Figure 3-17) and defective procoagulant activity *in vitro* (Figure 3-16). A similar phenotype has been reported in mice lacking LAT,[31,87] again indicating a prominent role for Grb2 in thrombus formation by linking signaling molecules within the LAT signalosome. Of note, platelet aggregation under flow has been reported to be unaltered in the absence of Gads.[31]

Comparable to immune receptor stimulation, agonist-induced platelet activation requires an increase in $[Ca^{2+}]_i$ that is mainly triggered by PLC-mediated IP_3 production, resulting in Ca^{2+} store release and subsequent Ca^{2+} entry.[14] The tyrosine phosphorylation cascade leading to PLCγ activation shows striking similarities between GPVI, the BCR, and the TCR, involving phosphorylation of accessory receptor chains, activity of Src and Syk family kinases and the scaffold function of various adapter proteins, like SLP-65/SLP-76 and LAT (see introduction

and Figure 1-3).[12,64,74] The presented findings clearly show that the Grb2 function in platelets resembles its function in TCR signaling in thymocytes, in that in both cell types deletion of Grb2 results in impaired Ca^{2+} signaling (Figure 3-15).[107] This is in contrast to B cells, where Ca^{2+} influx is enhanced in the absence of the adapter.[108,109] However, despite the same outcome, the mechanism by which Grb2 exerts its effect differs between thymocytes and platelets: In thymocytes, the signaling defect observed upon Grb2-deficiency was attributed to impaired activation of the Src-kinase Lck at the top end of the TCR signaling cascade, and may only partially, if at all, be caused by defects at the level of the LAT signalosome.[102,107] By contrast, Grb2 in platelets appears to act downstream of platelet GPVI solely at the level of the LAT signalosome. The results demonstrate that Grb2 interacts with LAT after (hem)ITAM stimulation (Figure 3-23) and that in the absence of Grb2 the tyrosine phosphorylation of LAT at Y136 and Y195 (corresponding to LAT Y132 and Y191 in human, respectively) is reduced (Figure 3-24 andFigure 3-25). Grb2 strongly associates via its SH2 domains with three phosphotyrosines of LAT (Y171, Y191, Y226),[78,99,100,259] whereas PLCγ preferentially binds at Y132.[99,259,260] Previous studies in T cell lines have shown that mutations of the Gads/Grb2 binding residues of LAT (Y171, Y191, Y226) result in reduced binding of PLCγ1 to LAT and attenuation of downstream signaling events including tyrosine phosphorylation of the phospholipase.[99,102,260,261] Therefore, a concept of cooperative binding among LAT-associated proteins that stabilize the signaling complex has been proposed.[79,102,262] In line with this, Grb2-deficient platelets displayed reduced tyrosine phosphorylation of the key downstream signaling molecules PLCγ2, SLP-76, and Vav3 after GPVI and CLEC-2 stimulation, whereas tyrosine phosphorylation of proteins that operate upstream of the LAT signalosome e.g. FcR γ-chain, CLEC-2, and Syk was maintained (Figure 3-24 and Figure 3-25). Taken together, the present observations emphasize that Grb2 is an important adapter protein of the LAT signalosome, which stabilizes this signaling complex by its direct association after (hem)ITAM-induced stimulation thereby enabling downstream signaling and platelet activation.

This conclusion is also supported by a platelet study using transgenic mice. Ragab *et al.* took advantage of a mouse line, where the three C-terminal tyrosine residues (Y171, Y191 and Y226), which are essential for Grb2 binding, were mutated to phenylalanine (LAT3YF mice).[263] This study demonstrated that these three tyrosine residues are required for membrane association and activation of PLCγ2 in response to platelet stimulation with CVX. Additionally, platelet aggregation, PLCγ2 phosphorylation and aggregation under flow were strongly impaired or abolished in these mice,[263] similar to *Lat*$^{-/-}$ mice.[31,86] However, from this study it could not be directly concluded to what extent defective Grb2 binding produces the phenotype, since also the Grb2 family member Gads binds to the same tyrosine residues

within the LAT protein.[99,100,259] Gads is a relative and a functional homolog of Grb2 and besides binding to LAT, both proteins can also bind and couple SLP-76 to LAT, albeit Gads seems to do this more efficiently.[104] Previous studies in DT40 B cell and Jurkat T cell lines have demonstrated that the recruitment of SLP-76 to the plasma membrane is essential for ITAM-signaling.[104,264] This seems to be also the case for platelets, since the expression of a membrane targeted SLP-76 mutant dramatically enhanced P-selectin exposure in response to CVX.[258] Because Gads binds to SLP-76 with higher affinity than Grb2,[103] and due to its established role in TCR signaling[81,92] it was anticipated that Gads, but not Grb2, is the main effector in GPVI signaling.[12] The role of Gads was, however, questioned in a study by Hughes *et al.* which showed a marked interaction of phosphorylated LAT with Grb2, but only weak interaction with Gads and in addition a very mild phenotype of *Gads*$^{-/-}$ platelets.[31] The results presented in this thesis clearly establish a dominant role of Grb2 in GPVI signaling as compared to Gads. Referring to the model discussed above, the stabilization of the LAT signalosome by Grb2 and possibly the Grb2/SOS1-mediated LAT-oligomerization[102] may serve as the structural basis required for retaining SLP-76 in the correct membrane compartment, thereby enabling downstream signaling and platelet activation.

The residual phosphorylation of LAT and PLCγ2 in the absence of Grb2 implicates that other proteins may partially compensate for its loss and, as mentioned above, the functional Grb2 homolog Gads is an obvious candidate. It will be very interesting to generate mice double deficient in Grb2 and Gads and to investigate whether their phenotype resembles LAT-deficient animals or whether double deficiency results in a complete block of GPVI activation, as observed for *Slp-76*$^{-/-}$ platelets.[76,85,86] In addition, these mice might also explain the less pronounced hem(ITAM) signaling defect in *Grb2*$^{-/-}$ mice compared to *Lat*$^{-/-}$ mice (Figure 3-12).

Besides LAT, further interaction partners of Grb2 in platelets are known (http://plateletweb.bioapps.biozentrum.uni-wuerzburg.de/plateletweb.php).[110] Therefore, it is feasible that Grb2 also exerts functions beyond LAT-dependent signaling. Subtle effects on other signaling pathways, however, may have been masked by the pronounced (hem)ITAM signaling defect that arose from the deletion of the protein. Comparison of LAT-deficient mice with mice double-deficient in LAT and Grb2 will be a useful approach to address this question. With regard to human platelets it is conceivable that Grb2 may contribute to the signaling pathway of the ITAM-bearing platelet Fc receptor, FcγRIIa.[265,266] Indeed, two studies in human platelets revealed that Grb2 associates to phosphorylated signaling molecules upon crosslinking of FcγRIIa.[267,268] However, FcγRIIa is not expressed in murine platelets, demonstrating a principal limitation of mouse studies. Certainly further investigations, e.g. by using FcγRIIa transgenic mice,[269] are required to address this issue.

Platelets express three different members of MAPK family: p38, JNK and ERK1/2.[230] Here it was found that Grb2 is a positive regulator of ERK1/2 signaling and that p38 was not affected by the loss of Grb2. Activation of JNK in wt platelets was not observed upon stimulation with CVX. Furthermore, the data demonstrated that Grb2 mediates ERK1/2 activation in a LAT-dependent manner, since LAT-deficiency resulted in a similar impairment of ERK1/2 activation (Figure 3-26). This can be explained by recruitment of SOS1 to the LAT-Grb2 complex which in turn activates the Ras-ERK1/2 signaling pathway.[270] The presence of SOS1 in platelets has been described.[267,268] ERK1/2, however, is also regulated downstream of PKC in platelets[231] and this would also be disrupted in Grb2-deficient platelets through impaired PLCγ2 activation. Regardless of the mechanism, the exact function of MAPKs in platelets is controversially discussed, possibly due to off-target effects of MAPK inhibitors, but increasing evidence suggests a role in promoting thrombus formation.[230] Interestingly, Mazharian *et al*. have previously shown that treatment of platelets with an ERK1/2 inhibitor results in decreased platelet adhesion to collagen under high shear flow.[271] Based on this observation, it appears possible that the impaired adhesion and thrombus formation of *Grb2*$^{-/-}$ platelets may in part be a consequence of impaired ERK1/2 signaling.

GPVI-deficient mice are protected from pathological thrombus formation, but display only very mildly prolonged bleeding times.[223] In contrast, while LAT-deficiency is also protective in experimental thrombosis models it additionally causes a significant hemostatic defect.[88] Here it was found that *Grb2*$^{-/-}$ mice, similar to *Lat*$^{-/-}$ mice,[88] display highly variable and overall prolonged bleeding times, indicating that Grb2 has an important functional role downstream of GPVI and CLEC-2 in normal hemostasis (Figure 3-18). Very surprisingly, however, Grb2-deficiency alone was not protective in models of arterial thrombosis (Figure 3-19), suggesting that other signaling pathways can fully compensate for the partial loss of (hem)ITAM signaling in this setting. Consistently, it was found that blocking TxA_2 generation by ASA treatment (1 mg/kg) markedly reduced or delayed occlusive thrombus formation in *Grb2*$^{-/-}$ mice, whereas it had no significant effect in wt mice (Figure 3-22). This effect may be explained by different mechanisms: First, a previous study from our group has demonstrated that abolished GPVI signaling can be compensated for by an alternative pathway involving TxA_2-mediated activation of integrin $\alpha2\beta1$ via G_q/G_{13}-induced signaling pathways, thereby enabling platelets to arrest on collagen and reinforce activation through outside-in signals.[226,272] In addition, the residual signaling capacity of *Grb2*$^{-/-}$ platelets in response to GPVI stimulation may become relevant under *in vivo* conditions in the presence of costimulatory GPCR agonists. Indeed, despite CRP had only a minor effect on integrin αIIbβ3 activation when applied on *Grb2*$^{-/-}$ platelets alone, it dramatically elevated integrin activation in the presence of the GPCR agonists ADP and the TxA_2 analogue U46619 *in*

vitro, resulting in a robust activation response (Figure 3-20). In accordance, aggregometry experiments with platelets from ASA treated mice confirmed a supportive role for TxA_2 production for aggregate formation of Grb2-deficient platelets *in vitro* (Figure 3-21). These observations are in line with a model in which the residual signaling capacity of Grb2-deficient platelets may be sufficient to trigger a self-amplifying loop that allows arterial thrombus formation *in vivo* and that administration of ASA interferes with this process, thereby constraining occlusive thrombus formation. The difference to LAT-deficient animals, which are protected in a model of laser-induced injury,[88] may consequently be a result of the weaker response of *Lat*$^{-/-}$ platelets to GPVI agonists (Figure 3-12) which has been shown to be accompanied by severely impaired or abolished release of second wave mediators.[86,273] Additionally, *Lat*$^{-/-}$ platelets displayed a much more pronounced impairment in the CLEC-2 signaling pathway (Figure 3-12), that has been shown to contribute to thrombus formation *in vivo*.[11,49] A completely different and quite speculative explanation for the lack of a protective phenotype of Grb2-deficient animals in thrombosis models would be that Grb2 has a function downstream of GPV, as the absence GPV can compensate for the loss of GPVI in different *in vivo* thrombosis models (David Stegner and Bernhard Nieswandt, personal communication).

Taken together, the presented data demonstrated that Grb2 is dispensable for platelet formation, but plays an important role in platelet activation in hemostasis and thrombosis by coordinating and stabilizing the formation of the LAT signalosome after GPVI/CLEC-2 receptor stimulation. This indicates that Grb2-dependent signaling in platelets may contribute to the pathogenesis of acute ischemic disease states.

4.3 Dual regulation of platelet CD84 by ADAM10 and calpain

Metalloproteinase-dependent cleavage of platelet receptors, shedding, is an established mechanism to regulate receptor surface expression and has been proposed to regulate platelet reactivity and cellular function, e.g. by modification of receptor signaling, adhesive properties of the platelet surface or the generation of bioactive fragments.[38,189,274] A recent proteomic approach identified several novel proteins which are proteolytically cleaved from the platelet surface, among them the ITSM-bearing type I transmembrane protein CD84.[194] The data presented in this thesis clearly confirm this initial finding in human and mouse platelets and provide further details of CD84 proteolysis. Using transgenic mice, ADAM10 was identified as the principal sheddase of CD84 in murine platelets and additionally calpain was found to cleave CD84 intracellularly. Thus, the data presented here reveal a dual regulation of CD84 by two distinct proteolytic mechanisms in platelets.

This study clearly established ADAM10 as the principal sheddase to mediate CD84 cleavage in mouse platelets in response to the GPCR agonist thrombin and the (hem)ITAM agonists rhodocytin, CVX and CRP, as well as upon platelet treatment with different shedding inducing agents. In contrast, ADAM17 plays no or only a very minor role in this process (Figure 3-31 and Figure 3-32). In this regard, CD84 seems to be unique, since prominent platelet receptors have been shown to be shed either exclusively by ADAM17 (GPIbα, semaphorin 4D)[184,189] or by ADAM10 and ADAM17, depending on the shedding-inducing stimulus (GPV, GPVI).[37,192] Importantly, ADAM10 also appears to be the only protease to mediate CD84 ectodomain shedding in clotting blood, as indicated by the unaltered sCD84 levels in the serum as compared to plasma of *Adam10*$^{-/-}$ mice (Figure 3-33). This suggests that even under conditions of maximal agonist receptor stimulation no other protease can cleave the receptor, at least in mouse platelets.

In contrast, Fong *et al.*[194] observed a significant reduction of CD84 shedding (about 44%) in human platelets in the presence of a selective ADAM17 inhibitor, but it was not analyzed in detail whether ADAM10 activity was also affected by this inhibitor. In addition, this effect was measured after platelet treatment with PMA, which hardly induced any shedding of CD84 in mouse and only moderate shedding in human platelets (Figure 3-28). Of note, the PMA concentration used in the other study is about 100-fold higher than the one used here and the incubation time was also prolonged (1 h vs. 15 min). Treatment of murine platelets for 1 h with PMA resulted in increased metalloproteinase-dependent shedding of CD84, similar to the effect of CCCP (data not shown). However, flow cytometric analysis revealed severely altered FSC/SSC characteristics which may be indicative for platelet disruption. This effect was absent after only 15 min of incubation, which was, however, still sufficient to shed GPIbα in control experiments (data not shown). Thus, the high doses of PMA and extended incubation in the experiments of Fong *et al.* may have additional effects besides PKC-mediated induction of metalloproteinase activity. It cannot be entirely excluded that minor differences in the substrate selectivity of ADAM family sheddases may exist between mouse and human. However, the comparable results between the species (Figure 3-28), including the moderate release of sCD84 by reagents acting mainly by activation of ADAM17 (PMA, CCCP) and the strong generation of sCD84 by reagents that activate both metalloproteinases (W7, NEM; see introduction), indicate that ADAM10 is also the dominant metalloproteinase for shedding of CD84 in human platelets. Additional studies are necessary to finally answer this question.

In addition to receptor stimulation a recent study has demonstrated that pathological shear triggers shedding of GPVI by a mechanism that is independent of aggregation and intracellular signaling.[275] Whether this also applies to CD84 remains to be elucidated.

Blocking of platelet aggregation by inhibition of integrin αIIbβ3 significantly reduced the release of sCD84 after platelet stimulation with CRP and thrombin. Similar observations have been made previously for CD40L shedding,[191] but not for GPVI shedding.[186] Interestingly, phosphorylation of CD84 in response to platelet activation is also markedly reduced by blocking platelet aggregation in human platelets.[175] Therefore, it is tempting to speculate that the aggregation-induced phosphorylation of CD84 may facilitate shedding of the receptor, e.g. by changing its conformation or by binding or dissociation of molecules. One example how molecules associated to the cytoplasmic tail can influence shedding of a receptor is calmodulin. The GPIb/V/IX complex and GPVI bind to calmodulin,[24,276] and its dissociation, e.g by treatment of platelets with the calmodulin inhibitor W7, induces receptor shedding.[186,188,192] Whether calmodulin interacts with CD84 was not directly addressed in this study. However, the finding that treatment of platelets with W7 induced strong shedding and calpain-dependent degradation of the C-terminal part of CD84 (Figure 3-28 and Figure 3-29) indicate that CD84 is a calmodulin-binding protein.[38,232] This is further supported by the presence of positively charged, membrane-proximal amino acid sequences in the human and mouse CD84 protein, similar to the calmodulin-binding sequences of GPVI and the GPIb/V/IX complex.[24,276]

The analysis of CD84 shedding by Western blot identified a second proteolytic cleavage of the protein that was carried out by the cysteinyl-proteinase calpain. Calpain-mediated intracellular cleavage of receptors in platelets has been described for PECAM-1,[198] the β3 integrin subunit[196] and for FcγRIIa, which becomes “de-ITAM-ized”.[197] The predicted calpain cleavage site within CD84 is located between the two ITSMs and upstream of the tyrosine that becomes phosphorylated upon ligation of CD84 and during platelet aggregation (Figure 3-30).[175] Thus, the calpain-mediated intracellular cleavage of the C-terminus may attenuate or terminate signaling, but further experimental evidence is required to prove this.

The data presented here show that CD84 is proteolytically cleaved by ADAM10 and calpain, which can operate simultaneously, but independently of each other (Figure 4-1). Calpain was able to cleave both the full length-protein and the C-terminal remnant which is generated by ADAM10 activity (Figure 3-29). It is well recognized that stimuli which induce extracellular shedding also have the potential to activate intracellular calpain cleavage.[38] This is nicely exemplified by a study of Gardiner *et al.*, investigating FcγRIIa and GPVI regulation in human platelets. Stimulation of either of these two receptors or treatment of platelets with W7 resulted in simultaneous calpain-induced proteolysis of FcγRIIa and metalloproteinase-mediated ectodomain shedding of GPVI.[197] In case of CD84 these two distinct proteolytic mechanisms act on one single protein, which appears to be unique for the proteolytic

regulation of platelet receptors. It is currently unclear why one receptor is targeted by two distinct proteolytic mechanisms, however, two different explanations are intruding: First, cleavage of the receptor by either protease may not directly terminate, but rather modify CD84 function. For example, calpain cleavage has been recently shown to switch the functional outcome of β3 integrin signaling from cell spreading to retraction.[199] Likewise, the shed extracellular domain of CD84 may be bioactive (see below). Second, ectodomain cleavage and intracellular calpain cleavage show different kinetics, with ectodomain shedding lagging behind (Figure 3-32). Therefore, CD84 cleavage maybe accelerated in certain settings, e.g. in the presence of CLEC-2 agonists, since the CLEC-2 agonist rhodocytin is the most powerful activator of calpain activity (Figure 3-32).

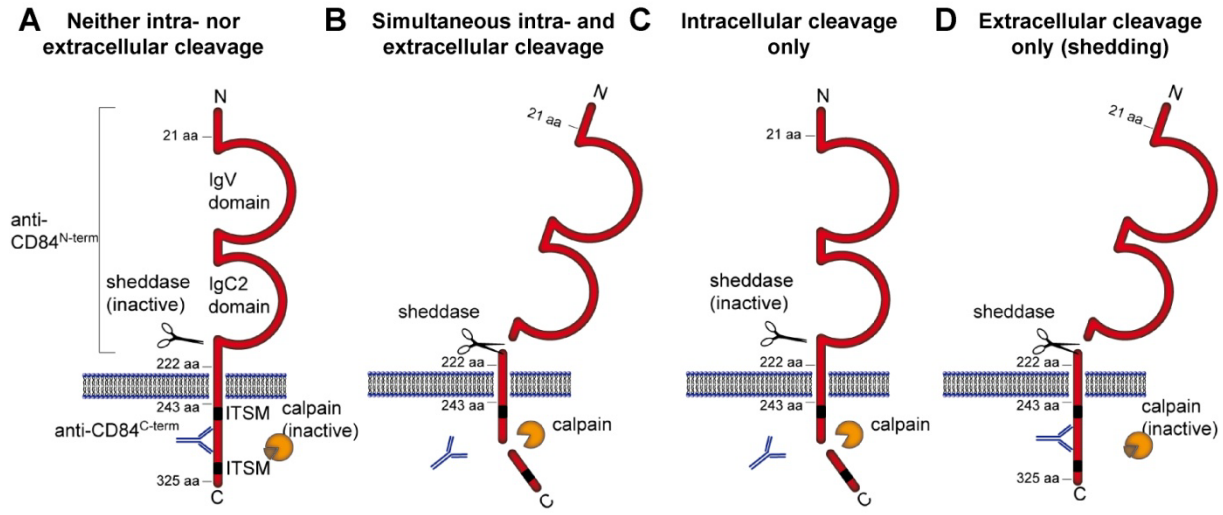

Figure 4-1 Schematic representation of the regulation of CD84 by intra- and extracellular cleavage. In the absence of sheddase and calpain activity, CD84 is intact and both antibodies detect the full length protein **(A)**. If intracellular cleavage occurs, the anti-CD84$^{C\text{-term}}$ antibody M-130 is unable to bind CD84 **(B and C)**. In addition to intracellular cleavage, ectodomain shedding by a metallo-proteinase may occur **(B)**. In the absence of shedding (e.g. W7 + GM6001 treatment), calpain-mediated cleavage can be visualized by detection of a shortened CD84 protein with the anti-CD84$^{N\text{-term}}$ antibody JER1 in Western blotting **(C)**. If shedding occurs in the absence of calpain activity (e.g. NEM treatment) a C-terminal remnant can be detected with anti-CD84$^{C\text{-term}}$ antibody **(D)**. Please note: the exact binding site of the anti-CD84$^{C\text{-term}}$ antibody is unknown, as are the cleavage sites for calpain and the sheddase; further degradation of the C-terminus may also occur. (Hofmann,* Vögtle* *et al., J Thromb Haemost, 2012*)[202]

Low amounts of sCD84 were consistently detected in the supernatant of unstimulated wt, but not of *Adam10*$^{-/-}$ or GM6001-treated wt platelets. Additionally, CD84 plasma levels in wt mice were elevated as compared to *Adam10*$^{-/-}$ mice. These two findings strongly suggest that CD84 is continuously released from the platelet surface by ADAM10, similar to constitutively shedding of GPIb by ADAM17.[37,184] The residual levels of sCD84 in *Adam10*$^{-/-}$ may originate from other cell types, such as leukocytes. Alternatively, cleavage may occur in *trans* with platelet CD84 being shed by ADAM10 present on other cell types, as it has been

demonstrated for ephrin cleavage in a heterologous cell system *in vitro*.[277] The high basal sCD84 levels in the plasma of healthy wt mice, which are about 50% of the levels measured after blood clotting in the serum, indicate that its use as a marker of thrombotic or inflammatory activity may be limited. Additional sCD84, which might be locally generated upon platelet activation *in vivo,* e.g. during thrombotic events, is not expected to reach sufficient amounts to result in a significant elevation in the systemic plasma concentration above the basal level. Glycocalicin, the shed extracellular fragment of GPIbα is another platelet receptor fragment that has likewise been detected in considerable amounts in plasma of normal healthy mice,[193] and is also not a sensitive marker of platelet activity.

The function of CD84 in platelet physiology is not well-explored, but one study reported that its C-terminus becomes tyrosine phosphorylated in response to platelet aggregation and upon antibody-mediated CD84-crosslinking.[175] Since the close proximity between platelets in aggregates enables contact-dependent signaling,[278] and because of the ability of CD84 to undergo homophilic interactions,[178] it has been suggested that CD84, similar to SLAM, may contribute to thrombus stability. Thus CD84 was proposed as a potential target for antithrombotic drug discovery.[175,279] Indeed, a role for CD84 in mediating cell-cell contacts has been recently demonstrated for lymphocytes where it facilitates prolonged B cell:T cell contact required for optimal germinal center formation.[180] Platelets can spread on the immobilized CD84 extracellular domain in a SAP-dependent manner, indicating a functional role of CD84,[175] however, a signaling or adhesive function of CD84 in platelet activation and aggregation has not been shown to date. Initial studies on *Cd84*$^{-/-}$ mice in our laboratory showed that the lack of CD84 in platelets does not affect classical platelet functions such as integrin activation or aggregation in response to major agonists. Also tail bleeding times are not prolonged in these animals, indicating that CD84 may not serve an essential function in hemostatic/thrombotic processes (Sebastian Hofmann, unpublished data). Besides platelets also many immune cell types abundantly express CD84[169,174,177] and the receptor undergoes homophilic interactions. Thus, CD84 may be of functional importance in mediating platelet-immune cell rather than platelet-platelet interactions. Shedding of CD84 from the platelet membrane may represent a novel mechanism to regulate such interactions e.g. by limiting the number of molecules available for adhesive contacts, thereby promoting the passification of the platelet surface. This may be of relevance in certain settings like leukocyte migration through the thrombus[280] or in the thrombo-inflammatory setting of ischemic stroke.[281] Further studies on platelet and immune cells are required to better understand the role of CD84 and its proteolytic cleavage in thrombotic, inflammatory and/or immunologic processes.

In addition, sCD84 may serve as a regulator of biological function, similar to the soluble fragments of CD40L and semaphorin 4D.[189,274] As shown recently, CD84 stabilizes B cell:T

cell interaction.[180] Therefore, it is tempting to speculate that sCD84 of platelet origin might have the potential to modulate immune cell interactions. This could be of relevance in distinct compartments where sCD84 can accumulate, e.g. in the joint fluid where platelet microparticles have been reported to contribute to disease progression of rheumatoid arthritis.[282] A very recent study reported CD84 to be a survival factor for *chronic lymphocytic leukemic* (CLL) B cells. Interestingly, the recombinantly expressed CD84 extracellular domain inhibits CCL cell survival *in vitro*, presumably by blocking homophilic interactions between these cells.[283] Whether and how sCD84 fragments also affect other cells, needs further investigation.

In summary, it was shown that CD84 is tightly regulated by two distinct proteolytic mechanisms in mouse platelets: the extracellular cleavage by ADAM10 and intracellular cleavage by calpain. In addition, it was demonstrated that shedding of CD84 is a constitutive process occurring *in vivo*.

4.4 Concluding remarks

In this thesis different aspects of cell receptor signaling and regulation in cells of the hematopoietic system were investigated by the use of transgenic mouse models and biochemical approaches. The major findings are:

Impact of the continuous Ca^{2+} influx on T cells:

- NFAT resides in the nucleus in unstimulated *Stim1*$^{Sax/+}$ T cells.
- Upon stimulation of *Stim1*$^{Sax/+}$ T cells, PLCγ1 shows an altered phosphorylation pattern in the presence, but not in the absence, of extracellular Ca^{2+}.
- Despite its aberrant phosphorylation, the enzymatic activity of PLCγ1 is not impaired.
- *Stim1*$^{Sax/+}$ T cells show a decreased production of Th2-type cytokines.

Function of Grb2 in platelets:

- Loss of Grb2 severely impairs (hem)ITAM signaling downstream of GPVI and CLEC-2.
- Grb2 is dispensable for GPCR signaling, integrin outside-in signaling and platelet production.
- The selective (hem)ITAM signaling defect impairs hemostasis, while thrombus formation *in vivo* can be compensated for by other signaling pathways.
- Grb2 facilitates (hem)ITAM signaling by stabilizing the LAT signalosome.

Proteolytic regulation of CD84:

- CD84 receptor levels on platelets are regulated by ADAM10-mediated ectodomain-shedding and intracellular cleavage by calpain.
- Both processes work simultaneously, but independently of each other.
- Shedding is a constitutive process occurring *in vivo* and soluble CD84 can be measured in mouse plasma.

4.5 Perspective

The molecular mechanisms of how *Stim1*$^{Sax/+}$ T cells maintain their function despite elevated $[Ca^{2+}]_i$ are still poorly understood. Furthermore, it remains to be investigated how the alternative phosphorylation pattern of PLCγ1 is established and if other proteins and signaling pathways are also affected by constitutive Ca^{2+} influx. Additionally, the function of *Stim1*$^{Sax/+}$ T cells in different mouse models of immunological disease has not yet been tested.

Grb2 was established as a critical adapter protein of the LAT signalosome. However, questions regarding the functional redundancies of adapter proteins like Grb2 and Gads and the different requirements of adapter proteins in ITAM, hemITAM and integrin signaling, as well as between platelets and immune remain to be answered. Further studies with mice double-deficient for known adapter proteins and the identification of new adapter proteins may answer some of these questions.

Owing to the limited knowledge about the function of CD84 in platelets, this study could not provide information about the physiological relevance of CD84 shedding and intracellular cleavage. Further studies on the function of CD84 in platelet and immune cells using *Cd84*$^{-/-}$ mice will help to better understand the role of this receptor in thrombotic, inflammatory, and/or immunologic processes and will ultimately provide novel insights into the significance of CD84 proteolysis on platelet function. In addition it remains to be elucidated whether or not CD84 can also be shed from cell types other than platelets.

5 References

1 Jackson SP. Arterial thrombosis--insidious, unpredictable and deadly. *Nat Med.* 2011; **17**: 1423-36

2 Nieswandt B, Pleines I, Bender M. Platelet adhesion and activation mechanisms in arterial thrombosis and ischaemic stroke. *J Thromb Haemost.* 2011; **9 Suppl 1**: 92-104

3 Lopez AD, Mathers CD, Ezzati M, Jamison DT, Murray CJ. Global and regional burden of disease and risk factors, 2001: systematic analysis of population health data. *Lancet.* 2006; **367**: 1747-57

4 Hagedorn I, Vogtle T, Nieswandt B. Arterial thrombus formation. Novel mechanisms and targets. *Hamostaseologie.* 2010; **30**: 127-35

5 Stegner D, Nieswandt B. Platelet receptor signaling in thrombus formation. *J Mol Med (Berl).* 2011; **89**: 109-21

6 Savage B, Saldivar E, Ruggeri ZM. Initiation of platelet adhesion by arrest onto fibrinogen or translocation on von Willebrand factor. *Cell.* 1996; **84**: 289-97

7 Nieswandt B, Brakebusch C, Bergmeier W, Schulte V, Bouvard D, Mokhtari-Nejad R, Lindhout T, Heemskerk JW, Zirngibl H, Fassler R. Glycoprotein VI but not alpha2beta1 integrin is essential for platelet interaction with collagen. *EMBO J.* 2001; **20**: 2120-30

8 Nieswandt B, Watson SP. Platelet-collagen interaction: is GPVI the central receptor? *Blood.* 2003; **102**: 449-61

9 Heemskerk JW, Mattheij NJ, Cosemans JM. Platelet-based coagulation: different populations, different functions. *J Thromb Haemost.* 2013; **11**: 2-16

10 Offermanns S. Activation of platelet function through G protein-coupled receptors. *Circ Res.* 2006; **99**: 1293-304

11 May F, Hagedorn I, Pleines I, Bender M, Vogtle T, Eble J, Elvers M, Nieswandt B. CLEC-2 is an essential platelet-activating receptor in hemostasis and thrombosis. *Blood.* 2009; **114**: 3464-72

12 Watson SP, Auger JM, McCarty OJ, Pearce AC. GPVI and integrin alphaIIb beta3 signaling in platelets. *J Thromb Haemost.* 2005; **3**: 1752-62

13 Ginsberg MH, Partridge A, Shattil SJ. Integrin regulation. *Curr Opin Cell Biol.* 2005; **17**: 509-16

14 Braun A, Vogtle T, Varga-Szabo D, Nieswandt B. STIM and Orai in hemostasis and thrombosis. *Front Biosci (Landmark Ed).* 2011; **16**: 2144-60

15 Suzuki-Inoue K, Inoue O, Ozaki Y. Novel platelet activation receptor CLEC-2: from discovery to prospects. *J Thromb Haemost.* 2011; **9 Suppl 1**: 44-55

16 Ramanathan G, Gupta S, Thielmann I, Pleines I, Varga-Szabo D, May F, Mannhalter C, Dietrich A, Nieswandt B, Braun A. Defective diacylglycerol-induced Ca2+ entry but normal agonist-induced activation responses in TRPC6-deficient mouse platelets. *J Thromb Haemost.* 2012; **10**: 419-29

17 Putney JW, Jr., Bird GS. The inositol phosphate-calcium signaling system in nonexcitable cells. *Endocr Rev.* 1993; **14**: 610-31

18 Putney JW. Capacitative calcium entry: from concept to molecules. *Immunol Rev.* 2009; **231**: 10-22

19 Reth M. Antigen receptor tail clue. *Nature.* 1989; **338**: 383-4

20 Nieswandt B, Schulte V, Bergmeier W, Mokhtari-Nejad R, Rackebrandt K, Cazenave JP, Ohlmann P, Gachet C, Zirngibl H. Long-term antithrombotic protection by in vivo depletion of platelet glycoprotein VI in mice. *J Exp Med.* 2001; **193**: 459-69

21 Auger JM, Kuijpers MJ, Senis YA, Watson SP, Heemskerk JW. Adhesion of human and mouse platelets to collagen under shear: a unifying model. *FASEB J.* 2005; **19**: 825-7

22 Clemetson JM, Polgar J, Magnenat E, Wells TN, Clemetson KJ. The platelet collagen receptor glycoprotein VI is a member of the immunoglobulin superfamily closely related to FcalphaR and the natural killer receptors. *J Biol Chem.* 1999; **274**: 29019-24

23 Dutting S, Bender M, Nieswandt B. Platelet GPVI: a target for antithrombotic therapy?! *Trends Pharmacol Sci.* 2012; **33**: 583-90

24 Andrews RK, Suzuki-Inoue K, Shen Y, Tulasne D, Watson SP, Berndt MC. Interaction of calmodulin with the cytoplasmic domain of platelet glycoprotein VI. *Blood.* 2002; **99**: 4219-21

25 Suzuki-Inoue K, Tulasne D, Shen Y, Bori-Sanz T, Inoue O, Jung SM, Moroi M, Andrews RK, Berndt MC, Watson SP. Association of Fyn and Lyn with the proline-rich domain of glycoprotein VI regulates intracellular signaling. *J Biol Chem.* 2002; **277**: 21561-6

26 Asazuma N, Wilde JI, Berlanga O, Leduc M, Leo A, Schweighoffer E, Tybulewicz V, Bon C, Liu SK, McGlade CJ, Schraven B, Watson SP. Interaction of linker for activation of T cells with multiple adapter proteins in platelets activated by the glycoprotein VI-selective ligand, convulxin. *J Biol Chem.* 2000; **275**: 33427-34

27 Batuwangala T, Leduc M, Gibbins JM, Bon C, Jones EY. Structure of the snake-venom toxin convulxin. *Acta Crystallogr D Biol Crystallogr.* 2004; **60**: 46-53

28 Gibbins J, Asselin J, Farndale R, Barnes M, Law CL, Watson SP. Tyrosine phosphorylation of the Fc receptor gamma-chain in collagen-stimulated platelets. *J Biol Chem.* 1996; **271**: 18095-9

29 Tsuji M, Ezumi Y, Arai M, Takayama H. A novel association of Fc receptor gamma-chain with glycoprotein VI and their co-expression as a collagen receptor in human platelets. *J Biol Chem.* 1997; **272**: 23528-31

30 Watson SP, Herbert JM, Pollitt AY. GPVI and CLEC-2 in hemostasis and vascular integrity. *J Thromb Haemost.* 2010; **8**: 1456-67

31 Hughes CE, Auger JM, McGlade J, Eble JA, Pearce AC, Watson SP. Differential roles for the adapters Gads and LAT in platelet activation by GPVI and CLEC-2. *J Thromb Haemost.* 2008; **6**: 2152-9

32 Pleines I, Elvers M, Strehl A, Pozgajova M, Varga-Szabo D, May F, Chrostek-Grashoff A, Brakebusch C, Nieswandt B. Rac1 is essential for phospholipase C-gamma2 activation in platelets. *Pflugers Arch.* 2009; **457**: 1173-85

33 Pearce AC, Senis YA, Billadeau DD, Turner M, Watson SP, Vigorito E. Vav1 and vav3 have critical but redundant roles in mediating platelet activation by collagen. *J Biol Chem.* 2004; **279**: 53955-62

34 Poole A, Gibbins JM, Turner M, van Vugt MJ, van de Winkel JG, Saito T, Tybulewicz VL, Watson SP. The Fc receptor gamma-chain and the tyrosine kinase Syk are essential for activation of mouse platelets by collagen. *EMBO J.* 1997; **16**: 2333-41

35 Quek LS, Pasquet JM, Hers I, Cornall R, Knight G, Barnes M, Hibbs ML, Dunn AR, Lowell CA, Watson SP. Fyn and Lyn phosphorylate the Fc receptor gamma chain downstream of glycoprotein VI in murine platelets, and Lyn regulates a novel feedback pathway. *Blood.* 2000; **96**: 4246-53

36 Andre P, Morooka T, Sim D, Abe K, Lowell C, Nanda N, Delaney S, Siu G, Yan Y, Hollenbach S, Pandey A, Gao H, Wang Y, Nakajima K, Parikh SA, Shi C, Phillips D, Owen W, Sinha U, Simon DI. Critical role for Syk in responses to vascular injury. *Blood.* 2011; **118**: 5000-10

37 Gardiner EE, Karunakaran D, Shen Y, Arthur JF, Andrews RK, Berndt MC. Controlled shedding of platelet glycoprotein (GP)VI and GPIb-IX-V by ADAM family metalloproteinases. *J Thromb Haemost.* 2007; **5**: 1530-7

38 Andrews RK, Karunakaran D, Gardiner EE, Berndt MC. Platelet receptor proteolysis: a mechanism for downregulating platelet reactivity. *Arterioscler Thromb Vasc Biol.* 2007; **27**: 1511-20

39 Suzuki-Inoue K, Fuller GL, Garcia A, Eble JA, Pohlmann S, Inoue O, Gartner TK, Hughan SC, Pearce AC, Laing GD, Theakston RD, Schweighoffer E, Zitzmann N, Morita T, Tybulewicz VL, Ozaki Y, Watson SP. A novel Syk-dependent mechanism of platelet activation by the C-type lectin receptor CLEC-2. *Blood.* 2006; **107**: 542-9

40 Senis YA, Tomlinson MG, Garcia A, Dumon S, Heath VL, Herbert J, Cobbold SP, Spalton JC, Ayman S, Antrobus R, Zitzmann N, Bicknell R, Frampton J, Authi KS, Martin A, Wakelam MJ, Watson SP. A comprehensive proteomics and genomics analysis reveals novel transmembrane proteins in human platelets and mouse megakaryocytes including G6b-B, a novel immunoreceptor tyrosine-based inhibitory motif protein. *Mol Cell Proteomics.* 2007; **6**: 548-64

41 Hughes CE, Pollitt AY, Mori J, Eble JA, Tomlinson MG, Hartwig JH, O'Callaghan CA, Futterer K, Watson SP. CLEC-2 activates Syk through dimerization. *Blood.* 2010; **115**: 2947-55

42 Watson AA, Christou CM, James JR, Fenton-May AE, Moncayo GE, Mistry AR, Davis SJ, Gilbert RJ, Chakera A, O'Callaghan CA. The platelet receptor CLEC-2 is active as a dimer. *Biochemistry.* 2009; **48**: 10988-96

43 Parguina AF, Alonso J, Rosa I, Velez P, Gonzalez-Lopez MJ, Guitian E, Eble JA, Loza MI, Garcia A. A detailed proteomic analysis of rhodocytin-activated platelets reveals novel clues on the CLEC-2 signalosome: implications for CLEC-2 signaling regulation. *Blood.* 2012; **120**: e117-26

44 Fuller GL, Williams JA, Tomlinson MG, Eble JA, Hanna SL, Pohlmann S, Suzuki-Inoue K, Ozaki Y, Watson SP, Pearce AC. The C-type lectin receptors CLEC-2 and Dectin-1, but not DC-SIGN, signal via a novel YXXL-dependent signaling cascade. *J Biol Chem.* 2007; **282**: 12397-409

45 Severin S, Pollitt AY, Navarro-Nunez L, Nash CA, Mourao-Sa D, Eble JA, Senis YA, Watson SP. Syk-dependent phosphorylation of CLEC-2: a novel mechanism of hem-immunoreceptor tyrosine-based activation motif signaling. *J Biol Chem.* 2011; **286**: 4107-16

46 Spalton JC, Mori J, Pollitt AY, Hughes CE, Eble JA, Watson SP. The novel Syk inhibitor R406 reveals mechanistic differences in the initiation of GPVI and CLEC-2 signaling in platelets. *J Thromb Haemost.* 2009; **7**: 1192-9

47 Navarro-Nunez L, Langan SA, Nash GB, Watson SP. The physiological and pathophysiological roles of platelet CLEC-2. *Thromb Haemost.* 2013; **109**: 991-8

48 Herzog BH, Fu J, Wilson SJ, Hess PR, Sen A, McDaniel JM, Pan Y, Sheng M, Yago T, Silasi-Mansat R, McGee S, May F, Nieswandt B, Morris AJ, Lupu F, Coughlin SR, McEver RP, Chen H, Kahn ML, Xia L. Podoplanin maintains high endothelial venule integrity by interacting with platelet CLEC-2. *Nature.* 2013; **502**: 105-9

49 Suzuki-Inoue K, Inoue O, Ding G, Nishimura S, Hokamura K, Eto K, Kashiwagi H, Tomiyama Y, Yatomi Y, Umemura K, Shin Y, Hirashima M, Ozaki Y. Essential in vivo roles of the C-type lectin receptor CLEC-2: embryonic/neonatal lethality of CLEC-2-deficient mice by blood/lymphatic misconnections and impaired thrombus formation of CLEC-2-deficient platelets. *J Biol Chem.* 2010; **285**: 24494-507

50 Bender M, May F, Lorenz V, Thielmann I, Hagedorn I, Finney BA, Vogtle T, Remer K, Braun A, Bosl M, Watson SP, Nieswandt B. Combined in vivo depletion of glycoprotein VI and C-type lectin-like receptor 2 severely compromises hemostasis and abrogates arterial thrombosis in mice. *Arterioscler Thromb Vasc Biol.* 2013; **33**: 926-34

51 Hughes CE, Navarro-Nunez L, Finney BA, Mourao-Sa D, Pollitt AY, Watson SP. CLEC-2 is not required for platelet aggregation at arteriolar shear. *J Thromb Haemost.* 2010; **8**: 2328-32

52 Daeron M, Jaeger S, Du Pasquier L, Vivier E. Immunoreceptor tyrosine-based inhibition motifs: a quest in the past and future. *Immunol Rev.* 2008; **224**: 11-43

53 Dhanjal TS, Ross EA, Auger JM, McCarty OJ, Hughes CE, Senis YA, Buckley CD, Watson SP. Minimal regulation of platelet activity by PECAM-1. *Platelets.* 2007; **18**: 56-67

54 Wong C, Liu Y, Yip J, Chand R, Wee JL, Oates L, Nieswandt B, Reheman A, Ni H, Beauchemin N, Jackson DE. CEACAM1 negatively regulates platelet-collagen interactions and thrombus growth in vitro and in vivo. *Blood.* 2009; **113**: 1818-28

55 Mazharian A, Wang YJ, Mori J, Bem D, Finney B, Heising S, Gissen P, White JG, Berndt MC, Gardiner EE, Nieswandt B, Douglas MR, Campbell RD, Watson SP, Senis YA. Mice lacking the ITIM-containing receptor G6b-B exhibit macrothrombocytopenia and aberrant platelet function. *Sci Signal.* 2012; **5**: ra78

56 Zhang W, Sommers CL, Burshtyn DN, Stebbins CC, DeJarnette JB, Trible RP, Grinberg A, Tsay HC, Jacobs HM, Kessler CM, Long EO, Love PE, Samelson LE. Essential role of LAT in T cell development. *Immunity.* 1999; **10**: 323-32

57 Sakaguchi S, Yamaguchi T, Nomura T, Ono M. Regulatory T cells and immune tolerance. *Cell.* 2008; **133**: 775-87

58 Zhu J, Yamane H, Paul WE. Differentiation of effector CD4 T cell populations (*). *Annu Rev Immunol.* 2010; **28**: 445-89

59 Constant SL, Bottomly K. Induction of Th1 and Th2 CD4+ T cell responses: the alternative approaches. *Annu Rev Immunol.* 1997; **15**: 297-322

60 Dong C. TH17 cells in development: an updated view of their molecular identity and genetic programming. *Nat Rev Immunol.* 2008; **8**: 337-48

61 Kuhns MS, Davis MM, Garcia KC. Deconstructing the form and function of the TCR/CD3 complex. *Immunity.* 2006; **24**: 133-9

62 Almeida AR, Rocha B, Freitas AA, Tanchot C. Homeostasis of T cell numbers: from thymus production to peripheral compartmentalization and the indexation of regulatory T cells. *Semin Immunol.* 2005; **17**: 239-49

63 Samelson LE. Immunoreceptor signaling. *Cold Spring Harb Perspect Biol.* 2011; **3**

64 Smith-Garvin JE, Koretzky GA, Jordan MS. T cell activation. *Annu Rev Immunol.* 2009; **27**: 591-619

65 Burkhardt JK, Carrizosa E, Shaffer MH. The actin cytoskeleton in T cell activation. *Annu Rev Immunol.* 2008; **26**: 233-59

66 Vallabhapurapu S, Karin M. Regulation and function of NF-kappaB transcription factors in the immune system. *Annu Rev Immunol.* 2009; **27**: 693-733

67 Shaw PJ, Feske S. Physiological and pathophysiological functions of SOCE in the immune system. *Front Biosci (Elite Ed).* 2012; **4**: 2253-68

68 Macian F. NFAT proteins: key regulators of T-cell development and function. *Nat Rev Immunol.* 2005; **5**: 472-84

69 Savignac M, Mellstrom B, Naranjo JR. Calcium-dependent transcription of cytokine genes in T lymphocytes. *Pflugers Arch.* 2007; **454**: 523-33

70 Baine I, Abe BT, Macian F. Regulation of T-cell tolerance by calcium/NFAT signaling. *Immunol Rev.* 2009; **231**: 225-40

71 Macian F, Garcia-Cozar F, Im SH, Horton HF, Byrne MC, Rao A. Transcriptional mechanisms underlying lymphocyte tolerance. *Cell.* 2002; **109**: 719-31

72 Liu JO. Calmodulin-dependent phosphatase, kinases, and transcriptional corepressors involved in T-cell activation. *Immunol Rev.* 2009; **228**: 184-98

73 Dolmetsch RE, Xu K, Lewis RS. Calcium oscillations increase the efficiency and specificity of gene expression. *Nature.* 1998; **392**: 933-6

74 Samelson LE. Signal transduction mediated by the T cell antigen receptor: the role of adapter proteins. *Annu Rev Immunol.* 2002; **20**: 371-94

75 Bubeck Wardenburg J, Fu C, Jackman JK, Flotow H, Wilkinson SE, Williams DH, Johnson R, Kong G, Chan AC, Findell PR. Phosphorylation of SLP-76 by the ZAP-70 protein-tyrosine kinase is required for T-cell receptor function. *J Biol Chem.* 1996; **271**: 19641-4

76 Gross BS, Lee JR, Clements JL, Turner M, Tybulewicz VL, Findell PR, Koretzky GA, Watson SP. Tyrosine phosphorylation of SLP-76 is downstream of Syk following stimulation of the collagen receptor in platelets. *J Biol Chem.* 1999; **274**: 5963-71

77 Pasquet JM, Gross B, Quek L, Asazuma N, Zhang W, Sommers CL, Schweighoffer E, Tybulewicz V, Judd B, Lee JR, Koretzky G, Love PE, Samelson LE, Watson SP. LAT is required for tyrosine phosphorylation of phospholipase cgamma2 and platelet activation by the collagen receptor GPVI. *Mol Cell Biol.* 1999; **19**: 8326-34

78 Zhang W, Sloan-Lancaster J, Kitchen J, Trible RP, Samelson LE. LAT: the ZAP-70 tyrosine kinase substrate that links T cell receptor to cellular activation. *Cell.* 1998; **92**: 83-92

79 Balagopalan L, Coussens NP, Sherman E, Samelson LE, Sommers CL. The LAT story: a tale of cooperativity, coordination, and choreography. *Cold Spring Harb Perspect Biol.* 2010; **2**: a005512

80 Koretzky GA, Abtahian F, Silverman MA. SLP76 and SLP65: complex regulation of signalling in lymphocytes and beyond. *Nat Rev Immunol.* 2006; **6**: 67-78

81 Liu SK, Fang N, Koretzky GA, McGlade CJ. The hematopoietic-specific adaptor protein gads functions in T-cell signaling via interactions with the SLP-76 and LAT adaptors. *Curr Biol.* 1999; **9**: 67-75

82 Clements JL, Yang B, Ross-Barta SE, Eliason SL, Hrstka RF, Williamson RA, Koretzky GA. Requirement for the leukocyte-specific adapter protein SLP-76 for normal T cell development. *Science.* 1998; **281**: 416-9

83 Pivniouk V, Tsitsikov E, Swinton P, Rathbun G, Alt FW, Geha RS. Impaired viability and profound block in thymocyte development in mice lacking the adaptor protein SLP-76. *Cell.* 1998; **94**: 229-38

84 Yablonski D, Kuhne MR, Kadlecek T, Weiss A. Uncoupling of nonreceptor tyrosine kinases from PLC-gamma1 in an SLP-76-deficient T cell. *Science.* 1998; **281**: 413-6

85 Clements JL, Lee JR, Gross B, Yang B, Olson JD, Sandra A, Watson SP, Lentz SR, Koretzky GA. Fetal hemorrhage and platelet dysfunction in SLP-76-deficient mice. *J Clin Invest.* 1999; **103**: 19-25

86 Judd BA, Myung PS, Obergfell A, Myers EE, Cheng AM, Watson SP, Pear WS, Allman D, Shattil SJ, Koretzky GA. Differential requirement for LAT and SLP-76 in GPVI versus T cell receptor signaling. *J Exp Med.* 2002; **195**: 705-17

87 Munnix IC, Strehl A, Kuijpers MJ, Auger JM, van der Meijden PE, van Zandvoort MA, oude Egbrink MG, Nieswandt B, Heemskerk JW. The glycoprotein VI-phospholipase Cgamma2 signaling pathway controls thrombus formation induced by collagen and tissue factor in vitro and in vivo. *Arterioscler Thromb Vasc Biol.* 2005; **25**: 2673-8

88 Kalia N, Auger JM, Atkinson B, Watson SP. Critical role of FcR gamma-chain, LAT, PLCgamma2 and thrombin in arteriolar thrombus formation upon mild, laser-induced endothelial injury in vivo. *Microcirculation.* 2008; **15**: 325-35

89 Bertozzi CC, Schmaier AA, Mericko P, Hess PR, Zou Z, Chen M, Chen CY, Xu B, Lu MM, Zhou D, Sebzda E, Santore MT, Merianos DJ, Stadtfeld M, Flake AW, Graf T, Skoda R, Maltzman JS, Koretzky GA, Kahn ML. Platelets regulate lymphatic vascular development through CLEC-2-SLP-76 signaling. *Blood.* 2010; **116**: 661-70

90 Abtahian F, Guerriero A, Sebzda E, Lu MM, Zhou R, Mocsai A, Myers EE, Huang B, Jackson DG, Ferrari VA, Tybulewicz V, Lowell CA, Lepore JJ, Koretzky GA, Kahn ML. Regulation of blood and lymphatic vascular separation by signaling proteins SLP-76 and Syk. *Science.* 2003; **299**: 247-51

91 Judd BA, Myung PS, Leng L, Obergfell A, Pear WS, Shattil SJ, Koretzky GA. Hematopoietic reconstitution of SLP-76 corrects hemostasis and platelet signaling through alpha IIb beta 3 and collagen receptors. *Proc Natl Acad Sci U S A.* 2000; **97**: 12056-61

92 Yoder J, Pham C, Iizuka YM, Kanagawa O, Liu SK, McGlade J, Cheng AM. Requirement for the SLP-76 adaptor GADS in T cell development. *Science.* 2001; **291**: 1987-91

93 Clark SG, Stern MJ, Horvitz HR. C. elegans cell-signalling gene sem-5 encodes a protein with SH2 and SH3 domains. *Nature.* 1992; **356**: 340-4

94 Lowenstein EJ, Daly RJ, Batzer AG, Li W, Margolis B, Lammers R, Ullrich A, Skolnik EY, Bar-Sagi D, Schlessinger J. The SH2 and SH3 domain-containing protein GRB2 links receptor tyrosine kinases to ras signaling. *Cell.* 1992; **70**: 431-42

95 Mayer BJ, Gupta R. Functions of SH2 and SH3 domains. *Curr Top Microbiol Immunol.* 1998; **228**: 1-22

96 Neumann K, Oellerich T, Urlaub H, Wienands J. The B-lymphoid Grb2 interaction code. *Immunol Rev.* 2009; **232**: 135-49

97 McCormick F. Signal transduction. How receptors turn Ras on. *Nature.* 1993; **363**: 15-6

98 Jang IK, Zhang J, Gu H. Grb2, a simple adapter with complex roles in lymphocyte development, function, and signaling. *Immunol Rev.* 2009; **232**: 150-9

99 Zhang W, Trible RP, Zhu M, Liu SK, McGlade CJ, Samelson LE. Association of Grb2, Gads, and phospholipase C-gamma 1 with phosphorylated LAT tyrosine residues. Effect of LAT tyrosine mutations on T cell angigen receptor-mediated signaling. *J Biol Chem.* 2000; **275**: 23355-61

100 Zhu M, Janssen E, Zhang W. Minimal requirement of tyrosine residues of linker for activation of T cells in TCR signaling and thymocyte development. *Journal of immunology.* 2003; **170**: 325-33

101 Buday L, Egan SE, Rodriguez Viciana P, Cantrell DA, Downward J. A complex of Grb2 adaptor protein, Sos exchange factor, and a 36-kDa membrane-bound tyrosine phosphoprotein is implicated in ras activation in T cells. *J Biol Chem.* 1994; **269**: 9019-23

102 Houtman JC, Yamaguchi H, Barda-Saad M, Braiman A, Bowden B, Appella E, Schuck P, Samelson LE. Oligomerization of signaling complexes by the multipoint binding of GRB2 to both LAT and SOS1. *Nat Struct Mol Biol.* 2006; **13**: 798-805

103 Berry DM, Nash P, Liu SK, Pawson T, McGlade CJ. A high-affinity Arg-X-X-Lys SH3 binding motif confers specificity for the interaction between Gads and SLP-76 in T cell signaling. *Curr Biol.* 2002; **12**: 1336-41

104 Ishiai M, Kurosaki M, Inabe K, Chan AC, Sugamura K, Kurosaki T. Involvement of LAT, Gads, and Grb2 in compartmentation of SLP-76 to the plasma membrane. *J Exp Med.* 2000; **192**: 847-56

105 Cheng AM, Saxton TM, Sakai R, Kulkarni S, Mbamalu G, Vogel W, Tortorice CG, Cardiff RD, Cross JC, Muller WJ, Pawson T. Mammalian Grb2 regulates multiple steps in embryonic development and malignant transformation. *Cell.* 1998; **95**: 793-803

106 Gong Q, Cheng AM, Akk AM, Alberola-Ila J, Gong G, Pawson T, Chan AC. Disruption of T cell signaling networks and development by Grb2 haploid insufficiency. *Nat Immunol.* 2001; **2**: 29-36

107 Jang IK, Zhang J, Chiang YJ, Kole HK, Cronshaw DG, Zou Y, Gu H. Grb2 functions at the top of the T-cell antigen receptor-induced tyrosine kinase cascade to control thymic selection. *Proc Natl Acad Sci U S A.* 2010; **107**: 10620-5

108 Ackermann JA, Radtke D, Maurberger A, Winkler TH, Nitschke L. Grb2 regulates B-cell maturation, B-cell memory responses and inhibits B-cell Ca2+ signalling. *EMBO J.* 2011; **30**: 1621-33

109 Jang IK, Cronshaw DG, Xie LK, Fang G, Zhang J, Oh H, Fu YX, Gu H, Zou Y. Growth-factor receptor-bound protein-2 (Grb2) signaling in B cells controls lymphoid follicle organization and germinal center reaction. *Proc Natl Acad Sci U S A.* 2011; **108**: 7926-31

110 Boyanova D, Nilla S, Birschmann I, Dandekar T, Dittrich M. PlateletWeb: a systems biologic analysis of signaling networks in human platelets. *Blood.* 2012; **119**: e22-34

111 Garcia J, de Gunzburg J, Eychene A, Gisselbrecht S, Porteu F. Thrombopoietin-mediated sustained activation of extracellular signal-regulated kinase in UT7-Mpl cells requires both Ras-Raf-1- and Rap1-B-Raf-dependent pathways. *Mol Cell Biol.* 2001; **21**: 2659-70

112 Matsumura I, Nakajima K, Wakao H, Hattori S, Hashimoto K, Sugahara H, Kato T, Miyazaki H, Hirano T, Kanakura Y. Involvement of prolonged ras activation in

thrombopoietin-induced megakaryocytic differentiation of a human factor-dependent hematopoietic cell line. *Mol Cell Biol.* 1998; **18**: 4282-90

113 Garcia A, Senis YA, Antrobus R, Hughes CE, Dwek RA, Watson SP, Zitzmann N. A global proteomics approach identifies novel phosphorylated signaling proteins in GPVI-activated platelets: involvement of G6f, a novel platelet Grb2-binding membrane adapter. *Proteomics.* 2006; **6**: 5332-43

114 Senis YA, Antrobus R, Severin S, Parguina AF, Rosa I, Zitzmann N, Watson SP, Garcia A. Proteomic analysis of integrin alphaIIbbeta3 outside-in signaling reveals Src-kinase-independent phosphorylation of Dok-1 and Dok-3 leading to SHIP-1 interactions. *J Thromb Haemost.* 2009; **7**: 1718-26

115 Berridge MJ, Bootman MD, Roderick HL. Calcium signalling: dynamics, homeostasis and remodelling. *Nat Rev Mol Cell Biol.* 2003; **4**: 517-29

116 Putney JW, Jr. A model for receptor-regulated calcium entry. *Cell Calcium.* 1986; **7**: 1-12

117 Hoth M, Penner R. Depletion of intracellular calcium stores activates a calcium current in mast cells. *Nature.* 1992; **355**: 353-6

118 Lewis RS, Cahalan MD. Mitogen-induced oscillations of cytosolic Ca2+ and transmembrane Ca2+ current in human leukemic T cells. *Cell Regul.* 1989; **1**: 99-112

119 Zweifach A, Lewis RS. Mitogen-regulated Ca2+ current of T lymphocytes is activated by depletion of intracellular Ca2+ stores. *Proc Natl Acad Sci U S A.* 1993; **90**: 6295-9

120 Parekh AB, Putney JW, Jr. Store-operated calcium channels. *Physiol Rev.* 2005; **85**: 757-810

121 Alonso MT, Alvarez J, Montero M, Sanchez A, Garcia-Sancho J. Agonist-induced Ca2+ influx into human platelets is secondary to the emptying of intracellular Ca2+ stores. *Biochem J.* 1991; **280 (Pt 3)**: 783-9

122 Sage SO, Reast R, Rink TJ. ADP evokes biphasic Ca2+ influx in fura-2-loaded human platelets. Evidence for Ca2+ entry regulated by the intracellular Ca2+ store. *Biochem J.* 1990; **265**: 675-80

123 Thastrup O, Foder B, Scharff O. The calcium mobilizing tumor promoting agent, thapsigargin elevates the platelet cytoplasmic free calcium concentration to a higher steady state level. A possible mechanism of action for the tumor promotion. *Biochem Biophys Res Commun.* 1987; **142**: 654-60

124 Feske S, Giltnane J, Dolmetsch R, Staudt LM, Rao A. Gene regulation mediated by calcium signals in T lymphocytes. *Nat Immunol.* 2001; **2**: 316-24

125 Feske S, Muller JM, Graf D, Kroczek RA, Drager R, Niemeyer C, Baeuerle PA, Peter HH, Schlesier M. Severe combined immunodeficiency due to defective binding of the nuclear factor of activated T cells in T lymphocytes of two male siblings. *Eur J Immunol.* 1996; **26**: 2119-26

126 Feske S, Prakriya M, Rao A, Lewis RS. A severe defect in CRAC Ca2+ channel activation and altered K+ channel gating in T cells from immunodeficient patients. *J Exp Med.* 2005; **202**: 651-62

127 Le Deist F, Hivroz C, Partiseti M, Thomas C, Buc HA, Oleastro M, Belohradsky B, Choquet D, Fischer A. A primary T-cell immunodeficiency associated with defective transmembrane calcium influx. *Blood.* 1995; **85**: 1053-62

128 Partiseti M, Le Deist F, Hivroz C, Fischer A, Korn H, Choquet D. The calcium current activated by T cell receptor and store depletion in human lymphocytes is absent in a primary immunodeficiency. *J Biol Chem.* 1994; **269**: 32327-35

129 Liou J, Kim ML, Heo WD, Jones JT, Myers JW, Ferrell JE, Jr., Meyer T. STIM is a Ca2+ sensor essential for Ca2+-store-depletion-triggered Ca2+ influx. *Curr Biol.* 2005; **15**: 1235-41

130 Roos J, DiGregorio PJ, Yeromin AV, Ohlsen K, Lioudyno M, Zhang S, Safrina O, Kozak JA, Wagner SL, Cahalan MD, Velicelebi G, Stauderman KA. STIM1, an essential and conserved component of store-operated Ca2+ channel function. *J Cell Biol.* 2005; **169**: 435-45

131 Wu MM, Buchanan J, Luik RM, Lewis RS. Ca2+ store depletion causes STIM1 to accumulate in ER regions closely associated with the plasma membrane. *J Cell Biol.* 2006; **174**: 803-13

132 Shaw PJ, Qu B, Hoth M, Feske S. Molecular regulation of CRAC channels and their role in lymphocyte function. *Cell Mol Life Sci.* 2013; **70**: 2637-56

133 Williams RT, Manji SS, Parker NJ, Hancock MS, Van Stekelenburg L, Eid JP, Senior PV, Kazenwadel JS, Shandala T, Saint R, Smith PJ, Dziadek MA. Identification and characterization of the STIM (stromal interaction molecule) gene family: coding for a novel class of transmembrane proteins. *Biochem J.* 2001; **357**: 673-85

134 Brandman O, Liou J, Park WS, Meyer T. STIM2 is a feedback regulator that stabilizes basal cytosolic and endoplasmic reticulum Ca2+ levels. *Cell.* 2007; **131**: 1327-39

135 Feske S, Gwack Y, Prakriya M, Srikanth S, Puppel SH, Tanasa B, Hogan PG, Lewis RS, Daly M, Rao A. A mutation in Orai1 causes immune deficiency by abrogating CRAC channel function. *Nature.* 2006; **441**: 179-85

136 Vig M, Peinelt C, Beck A, Koomoa DL, Rabah D, Koblan-Huberson M, Kraft S, Turner H, Fleig A, Penner R, Kinet JP. CRACM1 is a plasma membrane protein essential for store-operated Ca2+ entry. *Science.* 2006; **312**: 1220-3

137 Zhang SL, Yeromin AV, Zhang XH, Yu Y, Safrina O, Penna A, Roos J, Stauderman KA, Cahalan MD. Genome-wide RNAi screen of Ca(2+) influx identifies genes that regulate Ca(2+) release-activated Ca(2+) channel activity. *Proc Natl Acad Sci U S A.* 2006; **103**: 9357-62

138 Lis A, Peinelt C, Beck A, Parvez S, Monteilh-Zoller M, Fleig A, Penner R. CRACM1, CRACM2, and CRACM3 are store-operated Ca2+ channels with distinct functional properties. *Curr Biol.* 2007; **17**: 794-800

139 McNally BA, Prakriya M. Permeation, selectivity and gating in store-operated CRAC channels. *J Physiol.* 2012; **590**: 4179-91

140 Prakriya M, Feske S, Gwack Y, Srikanth S, Rao A, Hogan PG. Orai1 is an essential pore subunit of the CRAC channel. *Nature.* 2006; **443**: 230-3

141 Vig M, Beck A, Billingsley JM, Lis A, Parvez S, Peinelt C, Koomoa DL, Soboloff J, Gill DL, Fleig A, Kinet JP, Penner R. CRACM1 multimers form the ion-selective pore of the CRAC channel. *Curr Biol.* 2006; **16**: 2073-9

142 Yeromin AV, Zhang SL, Jiang W, Yu Y, Safrina O, Cahalan MD. Molecular identification of the CRAC channel by altered ion selectivity in a mutant of Orai. *Nature.* 2006; **443**: 226-9

143 Streb H, Irvine RF, Berridge MJ, Schulz I. Release of Ca2+ from a nonmitochondrial intracellular store in pancreatic acinar cells by inositol-1,4,5-trisphosphate. *Nature.* 1983; **306**: 67-9

144 Liou J, Fivaz M, Inoue T, Meyer T. Live-cell imaging reveals sequential oligomerization and local plasma membrane targeting of stromal interaction molecule 1 after Ca2+ store depletion. *Proc Natl Acad Sci U S A.* 2007; **104**: 9301-6

145 Luik RM, Wang B, Prakriya M, Wu MM, Lewis RS. Oligomerization of STIM1 couples ER calcium depletion to CRAC channel activation. *Nature.* 2008; **454**: 538-42

146 Luik RM, Wu MM, Buchanan J, Lewis RS. The elementary unit of store-operated Ca2+ entry: local activation of CRAC channels by STIM1 at ER-plasma membrane junctions. *J Cell Biol.* 2006; **174**: 815-25

147 Penna A, Demuro A, Yeromin AV, Zhang SL, Safrina O, Parker I, Cahalan MD. The CRAC channel consists of a tetramer formed by Stim-induced dimerization of Orai dimers. *Nature.* 2008; **456**: 116-20

148 Baba Y, Kurosaki T. Physiological function and molecular basis of STIM1-mediated calcium entry in immune cells. *Immunol Rev.* 2009; **231**: 174-88

149 Grosse J, Braun A, Varga-Szabo D, Beyersdorf N, Schneider B, Zeitlmann L, Hanke P, Schropp P, Muhlstedt S, Zorn C, Huber M, Schmittwolf C, Jagla W, Yu P, Kerkau T, Schulze H, Nehls M, Nieswandt B. An EF hand mutation in Stim1 causes premature platelet activation and bleeding in mice. *J Clin Invest.* 2007; **117**: 3540-50

150 Zhang SL, Yu Y, Roos J, Kozak JA, Deerinck TJ, Ellisman MH, Stauderman KA, Cahalan MD. STIM1 is a Ca2+ sensor that activates CRAC channels and migrates from the Ca2+ store to the plasma membrane. *Nature.* 2005; **437**: 902-5

151 Feske S. CRAC channelopathies. *Pflugers Arch.* 2010; **460**: 417-35

152 Bergmeier W, Oh-Hora M, McCarl CA, Roden RC, Bray PF, Feske S. R93W mutation in Orai1 causes impaired calcium influx in platelets. *Blood.* 2009; **113**: 675-8

153 Ahmad F, Boulaftali Y, Greene TK, Ouellette TD, Poncz M, Feske S, Bergmeier W. Relative contributions of stromal interaction molecule 1 and CalDAG-GEFI to calcium-dependent platelet activation and thrombosis. *J Thromb Haemost.* 2011; **9**: 2077-86

154 Braun A, Varga-Szabo D, Kleinschnitz C, Pleines I, Bender M, Austinat M, Bosl M, Stoll G, Nieswandt B. Orai1 (CRACM1) is the platelet SOC channel and essential for pathological thrombus formation. *Blood.* 2009; **113**: 2056-63

155 Varga-Szabo D, Braun A, Kleinschnitz C, Bender M, Pleines I, Pham M, Renne T, Stoll G, Nieswandt B. The calcium sensor STIM1 is an essential mediator of arterial thrombosis and ischemic brain infarction. *J Exp Med.* 2008; **205**: 1583-91

156 Gilio K, van Kruchten R, Braun A, Berna-Erro A, Feijge MA, Stegner D, van der Meijden PE, Kuijpers MJ, Varga-Szabo D, Heemskerk JW, Nieswandt B. Roles of platelet STIM1 and Orai1 in glycoprotein VI- and thrombin-dependent procoagulant activity and thrombus formation. *J Biol Chem.* 2010; **285**: 23629-38

157 McCarl CA, Picard C, Khalil S, Kawasaki T, Rother J, Papolos A, Kutok J, Hivroz C, Ledeist F, Plogmann K, Ehl S, Notheis G, Albert MH, Belohradsky BH, Kirschner J, Rao A, Fischer A, Feske S. ORAI1 deficiency and lack of store-operated Ca2+ entry cause immunodeficiency, myopathy, and ectodermal dysplasia. *J Allergy Clin Immunol.* 2009; **124**: 1311-8 e7

158 Feske S. Immunodeficiency due to defects in store-operated calcium entry. *Ann N Y Acad Sci.* 2011; **1238**: 74-90

159 Gwack Y, Srikanth S, Oh-Hora M, Hogan PG, Lamperti ED, Yamashita M, Gelinas C, Neems DS, Sasaki Y, Feske S, Prakriya M, Rajewsky K, Rao A. Hair loss and defective T- and B-cell function in mice lacking ORAI1. *Mol Cell Biol.* 2008; **28**: 5209-22

160 McCarl CA, Khalil S, Ma J, Oh-hora M, Yamashita M, Roether J, Kawasaki T, Jairaman A, Sasaki Y, Prakriya M, Feske S. Store-operated Ca2+ entry through

ORAI1 is critical for T cell-mediated autoimmunity and allograft rejection. *J Immunol.* 2010; **185**: 5845-58

161 Vig M, DeHaven WI, Bird GS, Billingsley JM, Wang H, Rao PE, Hutchings AB, Jouvin MH, Putney JW, Kinet JP. Defective mast cell effector functions in mice lacking the CRACM1 pore subunit of store-operated calcium release-activated calcium channels. *Nat Immunol.* 2008; **9**: 89-96

162 Beyersdorf N, Braun A, Vogtle T, Varga-Szabo D, Galdos RR, Kissler S, Kerkau T, Nieswandt B. STIM1-independent T cell development and effector function in vivo. *J Immunol.* 2009; **182**: 3390-7

163 Oh-Hora M, Yamashita M, Hogan PG, Sharma S, Lamperti E, Chung W, Prakriya M, Feske S, Rao A. Dual functions for the endoplasmic reticulum calcium sensors STIM1 and STIM2 in T cell activation and tolerance. *Nat Immunol.* 2008; **9**: 432-43

164 Ma J, McCarl CA, Khalil S, Luthy K, Feske S. T-cell-specific deletion of STIM1 and STIM2 protects mice from EAE by impairing the effector functions of Th1 and Th17 cells. *Eur J Immunol.* 2010; **40**: 3028-42

165 Schuhmann MK, Stegner D, Berna-Erro A, Bittner S, Braun A, Kleinschnitz C, Stoll G, Wiendl H, Meuth SG, Nieswandt B. Stromal interaction molecules 1 and 2 are key regulators of autoreactive T cell activation in murine autoimmune central nervous system inflammation. *J Immunol.* 2010; **184**: 1536-42

166 Byun M, Abhyankar A, Lelarge V, Plancoulaine S, Palanduz A, Telhan L, Boisson B, Picard C, Dewell S, Zhao C, Jouanguy E, Feske S, Abel L, Casanova JL. Whole-exome sequencing-based discovery of STIM1 deficiency in a child with fatal classic Kaposi sarcoma. *J Exp Med.* 2010; **207**: 2307-12

167 Fuchs S, Rensing-Ehl A, Speckmann C, Bengsch B, Schmitt-Graeff A, Bondzio I, Maul-Pavicic A, Bass T, Vraetz T, Strahm B, Ankermann T, Benson M, Caliebe A, Folster-Holst R, Kaiser P, Thimme R, Schamel WW, Schwarz K, Feske S, Ehl S. Antiviral and regulatory T cell immunity in a patient with stromal interaction molecule 1 deficiency. *J Immunol.* 2012; **188**: 1523-33

168 Picard C, McCarl CA, Papolos A, Khalil S, Luthy K, Hivroz C, LeDeist F, Rieux-Laucat F, Rechavi G, Rao A, Fischer A, Feske S. STIM1 mutation associated with a syndrome of immunodeficiency and autoimmunity. *N Engl J Med.* 2009; **360**: 1971-80

169 Cannons JL, Tangye SG, Schwartzberg PL. SLAM family receptors and SAP adaptors in immunity. *Annu Rev Immunol.* 2011; **29**: 665-705

170 Sidorenko SP, Clark EA. The dual-function CD150 receptor subfamily: the viral attraction. *Nat Immunol.* 2003; **4**: 19-24

171 Latour S, Gish G, Helgason CD, Humphries RK, Pawson T, Veillette A. Regulation of SLAM-mediated signal transduction by SAP, the X-linked lymphoproliferative gene product. *Nat Immunol.* 2001; **2**: 681-90

172 Tangye SG, Nichols KE, Hare NJ, van de Weerdt BC. Functional requirements for interactions between CD84 and Src homology 2 domain-containing proteins and their contribution to human T cell activation. *J Immunol.* 2003; **171**: 2485-95

173 Coffey AJ, Brooksbank RA, Brandau O, Oohashi T, Howell GR, Bye JM, Cahn AP, Durham J, Heath P, Wray P, Pavitt R, Wilkinson J, Leversha M, Huckle E, Shaw-Smith CJ, Dunham A, Rhodes S, Schuster V, Porta G, Yin L, Serafini P, Sylla B, Zollo M, Franco B, Bolino A, Seri M, Lanyi A, Davis JR, Webster D, Harris A, Lenoir G, de St Basile G, Jones A, Behloradsky BH, Achatz H, Murken J, Fassler R, Sumegi J, Romeo G, Vaudin M, Ross MT, Meindl A, Bentley DR. Host response to EBV

infection in X-linked lymphoproliferative disease results from mutations in an SH2-domain encoding gene. *Nat Genet.* 1998; **20**: 129-35

174 Krause SW, Rehli M, Heinz S, Ebner R, Andreesen R. Characterization of MAX.3 antigen, a glycoprotein expressed on mature macrophages, dendritic cells and blood platelets: identity with CD84. *Biochem J.* 2000; **346 Pt 3**: 729-36

175 Nanda N, Andre P, Bao M, Clauser K, Deguzman F, Howie D, Conley PB, Terhorst C, Phillips DR. Platelet aggregation induces platelet aggregate stability via SLAM family receptor signaling. *Blood.* 2005; **106**: 3028-34

176 de la Fuente MA, Pizcueta P, Nadal M, Bosch J, Engel P. CD84 leukocyte antigen is a new member of the Ig superfamily. *Blood.* 1997; **90**: 2398-405

177 Romero X, Benitez D, March S, Vilella R, Miralpeix M, Engel P. Differential expression of SAP and EAT-2-binding leukocyte cell-surface molecules CD84, CD150 (SLAM), CD229 (Ly9) and CD244 (2B4). *Tissue Antigens.* 2004; **64**: 132-44

178 Martin M, Romero X, de la Fuente MA, Tovar V, Zapater N, Esplugues E, Pizcueta P, Bosch J, Engel P. CD84 functions as a homophilic adhesion molecule and enhances IFN-gamma secretion: adhesion is mediated by Ig-like domain 1. *J Immunol.* 2001; **167**: 3668-76

179 Li C, Iosef C, Jia CY, Han VK, Li SS. Dual functional roles for the X-linked lymphoproliferative syndrome gene product SAP/SH2D1A in signaling through the signaling lymphocyte activation molecule (SLAM) family of immune receptors. *J Biol Chem.* 2003; **278**: 3852-9

180 Cannons JL, Qi H, Lu KT, Dutta M, Gomez-Rodriguez J, Cheng J, Wakeland EK, Germain RN, Schwartzberg PL. Optimal germinal center responses require a multistage T cell:B cell adhesion process involving integrins, SLAM-associated protein, and CD84. *Immunity.* 2010; **32**: 253-65

181 Tangye SG, van de Weerdt BC, Avery DT, Hodgkin PD. CD84 is up-regulated on a major population of human memory B cells and recruits the SH2 domain containing proteins SAP and EAT-2. *Eur J Immunol.* 2002; **32**: 1640-9

182 Morra M, Lu J, Poy F, Martin M, Sayos J, Calpe S, Gullo C, Howie D, Rietdijk S, Thompson A, Coyle AJ, Denny C, Yaffe MB, Engel P, Eck MJ, Terhorst C. Structural basis for the interaction of the free SH2 domain EAT-2 with SLAM receptors in hematopoietic cells. *EMBO J.* 2001; **20**: 5840-52

183 Rabie T, Varga-Szabo D, Bender M, Pozgaj R, Lanza F, Saito T, Watson SP, Nieswandt B. Diverging signaling events control the pathway of GPVI down-regulation in vivo. *Blood.* 2007; **110**: 529-35

184 Bergmeier W, Piffath CL, Cheng G, Dole VS, Zhang Y, von Andrian UH, Wagner DD. Tumor necrosis factor-alpha-converting enzyme (ADAM17) mediates GPIbalpha shedding from platelets in vitro and in vivo. *Circ Res.* 2004; **95**: 677-83

185 Bergmeier W, Rabie T, Strehl A, Piffath CL, Prostredna M, Wagner DD, Nieswandt B. GPVI down-regulation in murine platelets through metalloproteinase-dependent shedding. *Thromb Haemost.* 2004; **91**: 951-8

186 Gardiner EE, Arthur JF, Kahn ML, Berndt MC, Andrews RK. Regulation of platelet membrane levels of glycoprotein VI by a platelet-derived metalloproteinase. *Blood.* 2004; **104**: 3611-7

187 Aktas B, Pozgajova M, Bergmeier W, Sunnarborg S, Offermanns S, Lee D, Wagner DD, Nieswandt B. Aspirin induces platelet receptor shedding via ADAM17 (TACE). *J Biol Chem.* 2005; **280**: 39716-22

188 Rabie T, Strehl A, Ludwig A, Nieswandt B. Evidence for a role of ADAM17 (TACE) in the regulation of platelet glycoprotein V. *J Biol Chem.* 2005; **280**: 14462-8

189 Zhu L, Bergmeier W, Wu J, Jiang H, Stalker TJ, Cieslak M, Fan R, Boumsell L, Kumanogoh A, Kikutani H, Tamagnone L, Wagner DD, Milla ME, Brass LF. Regulated surface expression and shedding support a dual role for semaphorin 4D in platelet responses to vascular injury. *Proc Natl Acad Sci U S A.* 2007; **104**: 1621-6

190 Dole VS, Bergmeier W, Patten IS, Hirahashi J, Mayadas TN, Wagner DD. PSGL-1 regulates platelet P-selectin-mediated endothelial activation and shedding of P-selectin from activated platelets. *Thromb Haemost.* 2007; **98**: 806-12

191 Furman MI, Krueger LA, Linden MD, Barnard MR, Frelinger AL, 3rd, Michelson AD. Release of soluble CD40L from platelets is regulated by glycoprotein IIb/IIIa and actin polymerization. *J Am Coll Cardiol.* 2004; **43**: 2319-25

192 Bender M, Hofmann S, Stegner D, Chalaris A, Bosl M, Braun A, Scheller J, Rose-John S, Nieswandt B. Differentially regulated GPVI ectodomain shedding by multiple platelet-expressed proteinases. *Blood.* 2010; **116**: 3347-55

193 Bergmeier W, Rackebrandt K, Schroder W, Zirngibl H, Nieswandt B. Structural and functional characterization of the mouse von Willebrand factor receptor GPIb-IX with novel monoclonal antibodies. *Blood.* 2000; **95**: 886-93

194 Fong KP, Barry C, Tran AN, Traxler EA, Wannemacher KM, Tang HY, Speicher KD, Blair IA, Speicher DW, Grosser T, Brass LF. Deciphering the human platelet sheddome. *Blood.* 2011; **117**: e15-26

195 Goll DE, Thompson VF, Li H, Wei W, Cong J. The calpain system. *Physiol Rev.* 2003; **83**: 731-801

196 Du X, Saido TC, Tsubuki S, Indig FE, Williams MJ, Ginsberg MH. Calpain cleavage of the cytoplasmic domain of the integrin beta 3 subunit. *J Biol Chem.* 1995; **270**: 26146-51

197 Gardiner EE, Karunakaran D, Arthur JF, Mu FT, Powell MS, Baker RI, Hogarth PM, Kahn ML, Andrews RK, Berndt MC. Dual ITAM-mediated proteolytic pathways for irreversible inactivation of platelet receptors: de-ITAM-izing FcgammaRIIa. *Blood.* 2008; **111**: 165-74

198 Naganuma Y, Satoh K, Yi Q, Asazuma N, Yatomi Y, Ozaki Y. Cleavage of platelet endothelial cell adhesion molecule-1 (PECAM-1) in platelets exposed to high shear stress. *J Thromb Haemost.* 2004; **2**: 1998-2008

199 Flevaris P, Stojanovic A, Gong H, Chishti A, Welch E, Du X. A molecular switch that controls cell spreading and retraction. *J Cell Biol.* 2007; **179**: 553-65

200 Nieswandt B, Bergmeier W, Rackebrandt K, Gessner JE, Zirngibl H. Identification of critical antigen-specific mechanisms in the development of immune thrombocytopenic purpura in mice. *Blood.* 2000; **96**: 2520-7

201 Nieswandt B, Bergmeier W, Schulte V, Rackebrandt K, Gessner JE, Zirngibl H. Expression and function of the mouse collagen receptor glycoprotein VI is strictly dependent on its association with the FcRgamma chain. *J Biol Chem.* 2000; **275**: 23998-4002

202 Hofmann S, Vogtle T, Bender M, Rose-John S, Nieswandt B. The SLAM family member CD84 is regulated by ADAM10 and calpain in platelets. *J Thromb Haemost.* 2012; **10**: 2581-92

203 Unkeless JC. Characterization of a monoclonal antibody directed against mouse macrophage and lymphocyte Fc receptors. *J Exp Med.* 1979; **150**: 580-96

204 Bergmeier W, Schulte V, Brockhoff G, Bier U, Zirngibl H, Nieswandt B. Flow cytometric detection of activated mouse integrin alphaIIbbeta3 with a novel monoclonal antibody. *Cytometry.* 2002; **48**: 80-6

205 Andreesen R, Bross KJ, Osterholz J, Emmrich F. Human macrophage maturation and heterogeneity: analysis with a newly generated set of monoclonal antibodies to differentiation antigens. *Blood.* 1986; **67**: 1257-64

206 Tiedt R, Schomber T, Hao-Shen H, Skoda RC. Pf4-Cre transgenic mice allow the generation of lineage-restricted gene knockouts for studying megakaryocyte and platelet function in vivo. *Blood.* 2007; **109**: 1503-6

207 Chalaris A, Adam N, Sina C, Rosenstiel P, Lehmann-Koch J, Schirmacher P, Hartmann D, Cichy J, Gavrilova O, Schreiber S, Jostock T, Matthews V, Hasler R, Becker C, Neurath MF, Reiss K, Saftig P, Scheller J, Rose-John S. Critical role of the disintegrin metalloprotease ADAM17 for intestinal inflammation and regeneration in mice. *J Exp Med.* 2010; **207**: 1617-24

208 Nieswandt B, Moser M, Pleines I, Varga-Szabo D, Monkley S, Critchley D, Fassler R. Loss of talin1 in platelets abrogates integrin activation, platelet aggregation, and thrombus formation in vitro and in vivo. *J Exp Med.* 2007; **204**: 3113-8

209 Dirnagl U. Bench to bedside: the quest for quality in experimental stroke research. *J Cereb Blood Flow Metab.* 2006; **26**: 1465-78

210 Clark WM, Lessov NS, Dixon MP, Eckenstein F. Monofilament intraluminal middle cerebral artery occlusion in the mouse. *Neurol Res.* 1997; **19**: 641-8

211 Bederson JB, Pitts LH, Tsuji M, Nishimura MC, Davis RL, Bartkowski H. Rat middle cerebral artery occlusion: evaluation of the model and development of a neurologic examination. *Stroke.* 1986; **17**: 472-6

212 Moran PM, Higgins LS, Cordell B, Moser PC. Age-related learning deficits in transgenic mice expressing the 751-amino acid isoform of human beta-amyloid precursor protein. *Proc Natl Acad Sci U S A.* 1995; **92**: 5341-5

213 Swanson RA, Morton MT, Tsao-Wu G, Savalos RA, Davidson C, Sharp FR. A semiautomated method for measuring brain infarct volume. *J Cereb Blood Flow Metab.* 1990; **10**: 290-3

214 Kim HK, Kim JW, Zilberstein A, Margolis B, Kim JG, Schlessinger J, Rhee SG. PDGF stimulation of inositol phospholipid hydrolysis requires PLC-gamma 1 phosphorylation on tyrosine residues 783 and 1254. *Cell.* 1991; **65**: 435-41

215 Serrano CJ, Graham L, DeBell K, Rawat R, Veri MC, Bonvini E, Rellahan BL, Reischl IG. A new tyrosine phosphorylation site in PLC gamma 1: the role of tyrosine 775 in immune receptor signaling. *J Immunol.* 2005; **174**: 6233-7

216 Cao L, Yu K, Banh C, Nguyen V, Ritz A, Raphael BJ, Kawakami Y, Kawakami T, Salomon AR. Quantitative time-resolved phosphoproteomic analysis of mast cell signaling. *J Immunol.* 2007; **179**: 5864-76

217 Iwai LK, Benoist C, Mathis D, White FM. Quantitative phosphoproteomic analysis of T cell receptor signaling in diabetes prone and resistant mice. *J Proteome Res.* 2010; **9**: 3135-45

218 Thornton AM, Korty PE, Tran DQ, Wohlfert EA, Murray PE, Belkaid Y, Shevach EM. Expression of Helios, an Ikaros transcription factor family member, differentiates thymic-derived from peripherally induced Foxp3+ T regulatory cells. *J Immunol.* 2010; **184**: 3433-41

219 Gerdes J, Lemke H, Baisch H, Wacker HH, Schwab U, Stein H. Cell cycle analysis of a cell proliferation-associated human nuclear antigen defined by the monoclonal antibody Ki-67. *J Immunol.* 1984; **133**: 1710-5

220 Dutting S, Vogtle T, Morowski M, Schiessl S, Schafer CM, Watson SK, Hughes CE, Ackermann JA, Radtke D, Hermanns HM, Watson S, Nitschke L, Nieswandt B. Grb2 Contributes to (hem)ITAM-Mediated Signaling in Platelets. *Circ Res.* 2013

221 Mahankali M, Peng HJ, Cox D, Gomez-Cambronero J. The mechanism of cell membrane ruffling relies on a phospholipase D2 (PLD2), Grb2 and Rac2 association. *Cell Signal.* 2011; **23**: 1291-8

222 Morgenstern E, Ruf A, Patscheke H. Ultrastructure of the interaction between human platelets and polymerizing fibrin within the first minutes of clot formation. *Blood Coagul Fibrinolysis.* 1990; **1**: 543-6

223 Bender M, Hagedorn I, Nieswandt B. Genetic and antibody-induced glycoprotein VI deficiency equally protects mice from mechanically and FeCl(3) -induced thrombosis. *J Thromb Haemost.* 2011; **9**: 1423-6

224 Renne T, Pozgajova M, Gruner S, Schuh K, Pauer HU, Burfeind P, Gailani D, Nieswandt B. Defective thrombus formation in mice lacking coagulation factor XII. *J Exp Med.* 2005; **202**: 271-81

225 Kleinschnitz C, Pozgajova M, Pham M, Bendszus M, Nieswandt B, Stoll G. Targeting platelets in acute experimental stroke: impact of glycoprotein Ib, VI, and IIb/IIIa blockade on infarct size, functional outcome, and intracranial bleeding. *Circulation.* 2007; **115**: 2323-30

226 Gruner S, Prostredna M, Aktas B, Moers A, Schulte V, Krieg T, Offermanns S, Eckes B, Nieswandt B. Anti-glycoprotein VI treatment severely compromises hemostasis in mice with reduced alpha2beta1 levels or concomitant aspirin therapy. *Circulation.* 2004; **110**: 2946-51

227 Kawamura Y, Takahari Y, Tamura N, Eguchi Y, Urano T, Ishida H, Goto S. Imaging of structural changes in endothelial cells and thrombus formation at the site of FeCl(3)-induced injuries in mice cremasteric arteries. *J Atheroscler Thromb.* 2009; **16**: 807-14

228 Campbell CL, Smyth S, Montalescot G, Steinhubl SR. Aspirin dose for the prevention of cardiovascular disease: a systematic review. *JAMA.* 2007; **297**: 2018-24

229 Zhang J, Billingsley ML, Kincaid RL, Siraganian RP. Phosphorylation of Syk activation loop tyrosines is essential for Syk function. An in vivo study using a specific anti-Syk activation loop phosphotyrosine antibody. *J Biol Chem.* 2000; **275**: 35442-7

230 Adam F, Kauskot A, Rosa JP, Bryckaert M. Mitogen-activated protein kinases in hemostasis and thrombosis. *J Thromb Haemost.* 2008; **6**: 2007-16

231 Borsch-Haubold AG, Kramer RM, Watson SP. Cytosolic phospholipase A2 is phosphorylated in collagen- and thrombin-stimulated human platelets independent of protein kinase C and mitogen-activated protein kinase. *J Biol Chem.* 1995; **270**: 25885-92

232 Wang KK, Villalobo A, Roufogalis BD. Calmodulin-binding proteins as calpain substrates. *Biochem J.* 1989; **262**: 693-706

233 DuVerle DA, Ono Y, Sorimachi H, Mamitsuka H. Calpain cleavage prediction using multiple kernel learning. *PLoS One.* 2011; **6**: e19035

234 Schoenwaelder SM, Burridge K. Evidence for a calpeptin-sensitive protein-tyrosine phosphatase upstream of the small GTPase Rho. A novel role for the calpain inhibitor

calpeptin in the inhibition of protein-tyrosine phosphatases. *J Biol Chem.* 1999; **274**: 14359-67

235 Quintana A, Griesemer D, Schwarz EC, Hoth M. Calcium-dependent activation of T-lymphocytes. *Pflugers Arch.* 2005; **450**: 1-12

236 Quintana A, Pasche M, Junker C, Al-Ansary D, Rieger H, Kummerow C, Nunez L, Villalobos C, Meraner P, Becherer U, Rettig J, Niemeyer BA, Hoth M. Calcium microdomains at the immunological synapse: how ORAI channels, mitochondria and calcium pumps generate local calcium signals for efficient T-cell activation. *EMBO J.* 2011; **30**: 3895-912

237 Hayden-Martinez K, Kane LP, Hedrick SM. Effects of a constitutively active form of calcineurin on T cell activation and thymic selection. *J Immunol.* 2000; **165**: 3713-21

238 Gallo EM, Winslow MM, Cante-Barrett K, Radermacher AN, Ho L, McGinnis L, Iritani B, Neilson JR, Crabtree GR. Calcineurin sets the bandwidth for discrimination of signals during thymocyte development. *Nature.* 2007; **450**: 731-5

239 Feng JM, Hu YK, Xie LH, Colwell CS, Shao XM, Sun XP, Chen B, Tang H, Campagnoni AT. Golli protein negatively regulates store depletion-induced calcium influx in T cells. *Immunity.* 2006; **24**: 717-27

240 Bogin Y, Ainey C, Beach D, Yablonski D. SLP-76 mediates and maintains activation of the Tec family kinase ITK via the T cell antigen receptor-induced association between SLP-76 and ITK. *Proc Natl Acad Sci U S A.* 2007; **104**: 6638-43

241 Miller AT, Wilcox HM, Lai Z, Berg LJ. Signaling through Itk promotes T helper 2 differentiation via negative regulation of T-bet. *Immunity.* 2004; **21**: 67-80

242 Sekiya F, Poulin B, Kim YJ, Rhee SG. Mechanism of tyrosine phosphorylation and activation of phospholipase C-gamma 1. Tyrosine 783 phosphorylation is not sufficient for lipase activation. *J Biol Chem.* 2004; **279**: 32181-90

243 Poulin B, Sekiya F, Rhee SG. Intramolecular interaction between phosphorylated tyrosine-783 and the C-terminal Src homology 2 domain activates phospholipase C-gamma1. *Proc Natl Acad Sci U S A.* 2005; **102**: 4276-81

244 Mueller P, Massner J, Jayachandran R, Combaluzier B, Albrecht I, Gatfield J, Blum C, Ceredig R, Rodewald HR, Rolink AG, Pieters J. Regulation of T cell survival through coronin-1-mediated generation of inositol-1,4,5-trisphosphate and calcium mobilization after T cell receptor triggering. *Nat Immunol.* 2008; **9**: 424-31

245 Shaw PJ, Feske S. Regulation of lymphocyte function by ORAI and STIM proteins in infection and autoimmunity. *J Physiol.* 2012; **590**: 4157-67

246 Mowen KA, Glimcher LH. Signaling pathways in Th2 development. *Immunol Rev.* 2004; **202**: 203-22

247 Oh-Hora M, Komatsu N, Pishyareh M, Feske S, Hori S, Taniguchi M, Rao A, Takayanagi H. Agonist-selected T cell development requires strong T cell receptor signaling and store-operated calcium entry. *Immunity.* 2013; **38**: 881-95

248 Akimova T, Beier UH, Wang L, Levine MH, Hancock WW. Helios expression is a marker of T cell activation and proliferation. *PLoS One.* 2011; **6**: e24226

249 Gottschalk RA, Corse E, Allison JP. Expression of Helios in peripherally induced Foxp3+ regulatory T cells. *J Immunol.* 2012; **188**: 976-80

250 Pierson W, Cauwe B, Policheni A, Schlenner SM, Franckaert D, Berges J, Humblet-Baron S, Schonefeldt S, Herold MJ, Hildeman D, Strasser A, Bouillet P, Lu LF, Matthys P, Freitas AA, Luther RJ, Weaver CT, Dooley J, Gray DH, Liston A.

Antiapoptotic Mcl-1 is critical for the survival and niche-filling capacity of Foxp3(+) regulatory T cells. *Nat Immunol.* 2013; **14**: 959-65

251 Severin S, Ghevaert C, Mazharian A. The mitogen-activated protein kinase signaling pathways: role in megakaryocyte differentiation. *J Thromb Haemost.* 2010; **8**: 17-26

252 Marquardt B, Frith D, Stabel S. Signalling from TPA to MAP kinase requires protein kinase C, raf and MEK: reconstitution of the signalling pathway in vitro. *Oncogene.* 1994; **9**: 3213-8

253 Schonwasser DC, Marais RM, Marshall CJ, Parker PJ. Activation of the mitogen-activated protein kinase/extracellular signal-regulated kinase pathway by conventional, novel, and atypical protein kinase C isotypes. *Mol Cell Biol.* 1998; **18**: 790-8

254 Law DA, Nannizzi-Alaimo L, Phillips DR. Outside-in integrin signal transduction. Alpha IIb beta 3-(GP IIb IIIa) tyrosine phosphorylation induced by platelet aggregation. *J Biol Chem.* 1996; **271**: 10811-5

255 Law DA, DeGuzman FR, Heiser P, Ministri-Madrid K, Killeen N, Phillips DR. Integrin cytoplasmic tyrosine motif is required for outside-in alphaIIbbeta3 signalling and platelet function. *Nature.* 1999; **401**: 808-11

256 Cowan KJ, Law DA, Phillips DR. Identification of shc as the primary protein binding to the tyrosine-phosphorylated beta 3 subunit of alpha IIbbeta 3 during outside-in integrin platelet signaling. *J Biol Chem.* 2000; **275**: 36423-9

257 Jenkins AL, Nannizzi-Alaimo L, Silver D, Sellers JR, Ginsberg MH, Law DA, Phillips DR. Tyrosine phosphorylation of the beta3 cytoplasmic domain mediates integrin-cytoskeletal interactions. *J Biol Chem.* 1998; **273**: 13878-85

258 Abtahian F, Bezman N, Clemens R, Sebzda E, Cheng L, Shattil SJ, Kahn ML, Koretzky GA. Evidence for the requirement of ITAM domains but not SLP-76/Gads interaction for integrin signaling in hematopoietic cells. *Mol Cell Biol.* 2006; **26**: 6936-49

259 Houtman JC, Higashimoto Y, Dimasi N, Cho S, Yamaguchi H, Bowden B, Regan C, Malchiodi EL, Mariuzza R, Schuck P, Appella E, Samelson LE. Binding specificity of multiprotein signaling complexes is determined by both cooperative interactions and affinity preferences. *Biochemistry.* 2004; **43**: 4170-8

260 Paz PE, Wang S, Clarke H, Lu X, Stokoe D, Abo A. Mapping the Zap-70 phosphorylation sites on LAT (linker for activation of T cells) required for recruitment and activation of signalling proteins in T cells. *Biochem J.* 2001; **356**: 461-71

261 Hartgroves LC, Lin J, Langen H, Zech T, Weiss A, Harder T. Synergistic assembly of linker for activation of T cells signaling protein complexes in T cell plasma membrane domains. *J Biol Chem.* 2003; **278**: 20389-94

262 Lin J, Weiss A. Identification of the minimal tyrosine residues required for linker for activation of T cell function. *J Biol Chem.* 2001; **276**: 29588-95

263 Ragab A, Severin S, Gratacap MP, Aguado E, Malissen M, Jandrot-Perrus M, Malissen B, Ragab-Thomas J, Payrastre B. Roles of the C-terminal tyrosine residues of LAT in GPVI-induced platelet activation: insights into the mechanism of PLC gamma 2 activation. *Blood.* 2007; **110**: 2466-74

264 Boerth NJ, Sadler JJ, Bauer DE, Clements JL, Gheith SM, Koretzky GA. Recruitment of SLP-76 to the membrane and glycolipid-enriched membrane microdomains replaces the requirement for linker for activation of T cells in T cell receptor signaling. *J Exp Med.* 2000; **192**: 1047-58

265 Boylan B, Gao C, Rathore V, Gill JC, Newman DK, Newman PJ. Identification of FcgammaRIIa as the ITAM-bearing receptor mediating alphaIIbbeta3 outside-in integrin signaling in human platelets. *Blood.* 2008; **112**: 2780-6

266 Zhi H, Rauova L, Hayes V, Gao C, Boylan B, Newman DK, McKenzie SE, Cooley BC, Poncz M, Newman PJ. Cooperative integrin/ITAM signaling in platelets enhances thrombus formation in vitro and in vivo. *Blood.* 2013; **121**: 1858-67

267 Robinson A, Gibbins J, Rodriguez-Linares B, Finan PM, Wilson L, Kellie S, Findell P, Watson SP. Characterization of Grb2-binding proteins in human platelets activated by Fc gamma RIIA cross-linking. *Blood.* 1996; **88**: 522-30

268 Saci A, Liu WQ, Vidal M, Garbay C, Rendu F, Bachelot-Loza C. Differential effect of the inhibition of Grb2-SH3 interactions in platelet activation induced by thrombin and by Fc receptor engagement. *Biochem J.* 2002; **363**: 717-25

269 McKenzie SE, Taylor SM, Malladi P, Yuhan H, Cassel DL, Chien P, Schwartz E, Schreiber AD, Surrey S, Reilly MP. The role of the human Fc receptor Fc gamma RIIA in the immune clearance of platelets: a transgenic mouse model. *J Immunol.* 1999; **162**: 4311-8

270 Finco TS, Kadlecek T, Zhang W, Samelson LE, Weiss A. LAT is required for TCR-mediated activation of PLCgamma1 and the Ras pathway. *Immunity.* 1998; **9**: 617-26

271 Mazharian A, Roger S, Maurice P, Berrou E, Popoff MR, Hoylaerts MF, Fauvel-Lafeve F, Bonnefoy A, Bryckaert M. Differential Involvement of ERK2 and p38 in platelet adhesion to collagen. *J Biol Chem.* 2005; **280**: 26002-10

272 Inoue O, Suzuki-Inoue K, Dean WL, Frampton J, Watson SP. Integrin alpha2beta1 mediates outside-in regulation of platelet spreading on collagen through activation of Src kinases and PLCgamma2. *J Cell Biol.* 2003; **160**: 769-80

273 Cho MJ, Pestina TI, Steward SA, Jackson CW, Kent Gartner T. The roles of LAT in platelet signaling induced by collagen, TxA2, or ADP. *Biochem Biophys Res Commun.* 2002; **292**: 916-21

274 Andre P, Prasad KS, Denis CV, He M, Papalia JM, Hynes RO, Phillips DR, Wagner DD. CD40L stabilizes arterial thrombi by a beta3 integrin--dependent mechanism. *Nat Med.* 2002; **8**: 247-52

275 Al-Tamimi M, Tan CW, Qiao J, Pennings GJ, Javadzadegan A, Yong AS, Arthur JF, Davis AK, Jing J, Mu FT, Hamilton JR, Jackson SP, Ludwig A, Berndt MC, Ward CM, Kritharides L, Andrews RK, Gardiner EE. Pathologic shear triggers shedding of vascular receptors: a novel mechanism for down-regulation of platelet glycoprotein VI in stenosed coronary vessels. *Blood.* 2012; **119**: 4311-20

276 Andrews RK, Munday AD, Mitchell CA, Berndt MC. Interaction of calmodulin with the cytoplasmic domain of the platelet membrane glycoprotein Ib-IX-V complex. *Blood.* 2001; **98**: 681-7

277 Janes PW, Saha N, Barton WA, Kolev MV, Wimmer-Kleikamp SH, Nievergall E, Blobel CP, Himanen JP, Lackmann M, Nikolov DB. Adam meets Eph: an ADAM substrate recognition module acts as a molecular switch for ephrin cleavage in trans. *Cell.* 2005; **123**: 291-304

278 Brass LF, Zhu L, Stalker TJ. Minding the gaps to promote thrombus growth and stability. *J Clin Invest.* 2005; **115**: 3385-92

279 Nanda N, Phillips DR. Novel targets for antithrombotic drug discovery. *Blood Cells Mol Dis.* 2006; **36**: 228-31

280 Ghasemzadeh M, Kaplan ZS, Alwis I, Schoenwaelder SM, Ashworth KJ, Westein E, Hosseini E, Salem HH, Slattery R, McColl SR, Hickey MJ, Ruggeri ZM, Yuan Y, Jackson SP. The CXCR1/2 ligand NAP-2 promotes directed intravascular leukocyte migration through platelet thrombi. *Blood.* 2013; **121**: 4555-66

281 Stoll G, Kleinschnitz C, Nieswandt B. Combating innate inflammation: a new paradigm for acute treatment of stroke? *Ann N Y Acad Sci.* 2010; **1207**: 149-54

282 Boilard E, Nigrovic PA, Larabee K, Watts GF, Coblyn JS, Weinblatt ME, Massarotti EM, Remold-O'Donnell E, Farndale RW, Ware J, Lee DM. Platelets amplify inflammation in arthritis via collagen-dependent microparticle production. *Science.* 2010; **327**: 580-3

283 Binsky-Ehrenreich I, Marom A, Sobotta MC, Shvidel L, Berrebi A, Hazan-Halevy I, Kay S, Aloshin A, Sagi I, Goldenberg DM, Leng L, Bucala R, Herishanu Y, Haran M, Shachar I. CD84 is a survival receptor for CLL cells. *Oncogene.* 2013

6 Appendix

6.1 Abbreviations

aa	amino acid
ab	antibody
ASA	acetylsalicylic acid
ACK	ammonium-chloride-potassium
ADAM	a disintegrin and metalloproteinase
ADP	adenosine diphosphate
AP-1	activator protein 1
ATP	adenosine triphosphate
BCR	B cell receptor
BMc	bone marrow chimeric
bp	base pairs
BSA	bovine serum albumin
Btk	Bruton's tyrosine kinase
$[Ca^{2+}]_i$	intracellular calcium level $[Ca^{2+}]_i$
Ca^{2+}	calcium
CC	coiled coil
CCCP	carbonyl cyanide m-chlorophenylhydrazone
CD	cluster of differentiation
CLEC-2	C-type lectin-like receptor 2
CRAC	Ca^{2+}-release-activated Ca^{2+}
CRP	collagen-related peptide
CsA	cyclosporin A
CTLA-4	cytotoxic T lymphocyte antigen 4
CVX	convulxin
DAG	diacylglycerol
DIC	differential interference contrast
DMEM	Dulbecco's modified Eagle's medium
DMSO	dimethyl sulfoxide
Dok	downstream of tyrosine kinase
EAT-2	Ewing's sarcoma activated transcript 2
ECM	extracellular matrix
EDTA	ethylenediaminetetraacetic acid
ER	endoplasmic reticulum
ERK	extracellular-signal-regulated kinase
FACS	fluorescence-activated cell sorting
f.c.	final concentration
FcR	Fc receptor
FCS	fetal calf serum
FITC	fluorescein isothiocyanate
FSC	forward scatter
Foxp3	forkhead box P3
Gads	Grb2-related adapter downstream of Shc
GDP	guanosine diphosphate
GEF	guanine nucleotide exchange factor

GP	glycoprotein
GPCR	G protein-coupled receptors
Grb2	growth factor receptor-bound protein 2
GTP	guanosine trisphosphate
h	hour(s)
HEPES	4-(2-hydroxyethyl)-1-piperazineethanesulfonic acid
HRP	horseradish peroxidase
IFN	interferon
Ig	immunoglobulin
IL	interleukin
IP	immunoprecipitation
IP_3	inositol-1,4,5-trisphosphate
ITAM	immunoreceptor tyrosine-based activation motif
ITIM	immunoreceptor tyrosine-based inhibition motif
Itk	IL-2-induced tyrosine kinase
ITSM	immunoreceptor tyrosine-based switch motif
JNK	c-Jun N-terminal kinase
kDa	kilo Dalton
LAT	linker for activation of T cells
M	molar
mAb	monoclonal antibody
MAP	mitogen-activated protein
MEK	mitogen-activated protein kinase/ERK kinase
MFI	mean fluorescence intensity
MHC	major histocompatibility complex
min	minute(s)
MK	megakaryocyte
MOPS	3-(N-morpholino) propanesulfonic acid
MPV	mean platelet volume
NEM	N-ethylmaleimide
NFAT	nuclear factor of activated T cells
PCR	polymerase chain reaction
PECAM-1	platelet-endothelial cell adhesion molecule-1
PE	phycoerythrin
PF4	platelet factor 4
PGI_2	prostacyclin
PI3K	phosphoinositide-3-kinase
PIP_2	phosphatidylinositol-4,5-bisphosphate
PKC	protein kinase C
PLC	phospholipase C
PMA	phorbol 12-myristate 13-acetate
prp	platelet-rich plasma
PS	phosphatidylserine
PVDF	polyvinylidene difluoride
RasGRP	Ras guanyl nucleotide-releasing protein
RC	rhodocytin
rpm	rotations per minute
RPMI	Roswell Park Memorial Institute

RT	room temperature
SAM	sterile α-motif
s	second(s)
sCD84	soluble CD84
SD	standard deviation
SDS	sodium dodecyl sulfate
SDS-PAGE	sodium dodecyl sulfate polyacrylamide gel electrophoresis
SERCA	sarco/endoplasmic reticulum Ca^{2+}-ATPase
SH2	Src homology 2
SHIP	SH2 domain-containing inositol-5-phosphatase
SHP	SH2 domain-containing protein-tyrosine phosphatase
SAP	SLAM-associated protein
SLAM	signaling lymphocytic activation molecule
SLP-76	SH2 domain-containing leukocyte protein of 76 kDa
SOCE	store-operated calcium entry
Sos1	son of sevenless homolog 1
SSC	side scatter
STIM	stromal interaction molecule
Syk	spleen tyrosine kinase
TAE	TRIS acetate EDTA
TBS	TRIS-buffered saline
TBS-T	TRIS-buffered saline containing Tween
TCR	T cell receptor
TF	tissue factor
TG	thapsigargin
TGF	transforming growth factor
Th	T helper
tMCAO	transient middle cerebral artery occlusion
TNF	tumor necrosis factor
Treg	regulatory T cell
TRIS	tris(hydroxymethyl)aminomethane
TRPC	transient receptor potential channel
TTC	2,3,5-triphenyltetrazolium chloride
TxA_2	thromboxane A_2
vWF	von Willebrand factor
w/o	without
wt	wildtype
XLP	X-linked lymphoproliferative syndrome

6.2 Acknowledgements

The work presented here was accomplished at the Chair of Experimental Biomedicine, University Hospital Würzburg and the Rudolf Virchow Center for Experimental Biomedicine, University of Würzburg in the group of Prof. Dr. Bernhard Nieswandt.

During the period of my PhD work (October 2008 - January 2014), many people helped and supported me. I would like to thank the following people:

- Prof. Dr. Bernhard Nieswandt for the opportunity to work in his laboratory and for his support, patience, encouragement and useful advice. Also I would like to thank him for allowing me to present my work at various international conferences.
- Prof. Dr. Thomas Dandekar and Prof. Dr. Stephan Kissler for helpful scientific discussions and for reviewing my thesis.
- Dr. Sebastian Dütting for the joint analysis of Grb2-deficient mice and for his great sacrifice during the Ca^{2+} measurements.
- Dr. Sebastian Hofmann for great teamwork and Dr. Markus Bender for advice and mice in the CD84 “Shedding!” project
- Dr. Attila Braun, Dr. Christoph Hintzen, Carmen Schäfer and especially Dr. Heike Hermanns for the efforts and support in the *Stim1*^{Sax} project and the latter two also for their contribution to the Grb2 project.
- Martina Morowski for performing the *in vivo* experiments.
- All of the technical assistants, especially Sylvia Hengst, for their kind help and for providing an excellent working basis.
- Prof. Dr. Guido Stoll, Dr. Peter Kraft and their team for performing the stroke experiments.
- Prof. Dr. Lars Nitschke for providing Grb2-floxed mice.
- Prof. Dr. Steve Watson, Dr. Craig Hughes and Stephanie Watson for the fruitful collaboration in the Grb2 project.
- The animal caretakers for running the animal facility.
- The *Graduate School of Life Sciences* (GSLS) for organizing the transferable skill courses and for the financial support of congress participations.
- All volunteers who donated blood for the CD84 project.

- All proofreaders of this thesis; especially Deya Cherpokova, Judith van Eeuwijk and Sarah Schießl.
- All former and present members of the Nieswandt lab, who have not been mentioned by name, for support, useful discussions and the nice working atmosphere.
- Finally, I would like to thank my parents, brother, grandparents and friends for continuous support, encouragement and patience.

6.3 Curriculum vitae

6.4 Publications

6.4.1 Original articles

1. Dütting S,* **Vögtle T,*** Morowski M, Schiessl S, Schafer CM, Watson SK, Hughes CE, Ackermann JA, Radtke D, Hermanns HM, Watson S, Nitschke L, Nieswandt B. Grb2 contributes to (hem)ITAM-Mediated signaling in platelets. *Circ Res.* 2013

2. Morowski M, **Vögtle T**, Kraft P, Kleinschnitz C, Stoll G, Nieswandt B. Only severe thrombocytopenia results in bleeding and defective thrombus formation in mice. *Blood.* 2013; 121: 4938-47

3. Deppermann C, Cherpokova D, Nurden P, Schulz JN, Thielmann I, Kraft P, **Vögtle T**, Kleinschnitz C, Dutting S, Krohne G, Eming SA, Nurden AT, Eckes B, Stoll G, Stegner D, Nieswandt B. Gray platelet syndrome and defective thrombo-inflammation in Nbeal2-deficient mice. *J Clin Invest.* 2013

4. Bender M, May F, Lorenz V, Thielmann I, Hagedorn I, Finney BA, **Vögtle T**, Remer K, Braun A, Bosl M, Watson SP, Nieswandt B. Combined in vivo depletion of glycoprotein VI and C-type lectin-like receptor 2 severely compromises hemostasis and abrogates arterial thrombosis in mice. *Arterioscler Thromb Vasc Biol.* 2013; 33: 926-34

5. Hofmann S,* **Vögtle T,*** Bender M, Rose-John S, Nieswandt B. The SLAM family member CD84 is regulated by ADAM10 and calpain in platelets. *J Thromb Haemost.* 2012; 10: 2581-92

6. Dramane G, Abdoul-Azize S, Hichami A, **Vögtle T**, Akpona S, Chouabe C, Sadou H, Nieswandt B, Besnard P, Khan NA. STIM1 regulates calcium signaling in taste bud cells and preference for fat in mice. *J Clin Invest.* 2012; 122: 2267-82

7. May F, Hagedorn I, Pleines I, Bender M, **Vögtle T**, Eble J, Elvers M, Nieswandt B. CLEC-2 is an essential platelet-activating receptor in hemostasis and thrombosis. *Blood.* 2009; 114: 3464-72

8. Braun A,* Gessner JE,* Varga-Szabo D, Syed SN, Konrad S, Stegner D, **Vögtle T**, Schmidt RE, Nieswandt B. STIM1 is essential for Fcgamma receptor activation and autoimmune inflammation. *Blood.* 2009; 113: 1097-104

9. Beyersdorf N,* Braun A,* **Vögtle T**, Varga-Szabo D, Galdos RR, Kissler S, Kerkau T, Nieswandt B. STIM1-independent T cell development and effector function in vivo. *J Immunol.* 2009; 182: 3390-7

6.4.2 Reviews

1. Braun A, **Vögtle T**, Varga-Szabo D, Nieswandt B. STIM and Orai in hemostasis and thrombosis. *Front Biosci (Landmark Ed)*. 2011; 16: 2144-60
2. Hagedorn I, **Vögtle T**, Nieswandt B. Arterial thrombus formation. Novel mechanisms and targets. *Hamostaseologie.* 2010; 30: 127-35

6.4.3 Talks

5th International Symposium of the Graduate School of Life Sciences, Würzburg, Germany, October 2010. “Store-operated calcium entry in T cell signaling and activation”

XXIVth Congress of the International Society on Thrombosis and Hemostasis, Amsterdam, The Netherlands, July 2013. ““Shedding” light on platelet CD84”
Winner of the **Young Investigator Award** (prize money: 500 €).

6.4.4 Poster

International Symposium of the Sonderforschungsbereich (SFB) 487, Würzburg, Germany, July 2011. “Stromal Interaction Molecule 1 (STIM1) is essential for proper immune cell proliferation and activation”

17th International Vascular Biology Meeting (IVBM), Wiesbaden, Germany, June 2012. “Dual regulation of CD84 by ADAM10 and calpain in platelets”

Joint Symposium of the SFB 688 and the Comprehensive Heart failure Center Würzburg, Würzburg, Germany, June 2012. “Grb2 is essential for GPVI-mediated platelet activation”

7th International Symposium of the Graduate School of Life Sciences, Würzburg, Germany, October 2012. “Grb2 is essential for GPVI-mediated platelet activation”

6.5 Affidavit

I hereby confirm that my thesis entitled “Studies on receptor signaling and regulation in platelets and T cells from genetically modified mice” is the result of my own work. I did not receive any help or support from commercial consultants. All sources and/or materials applied are listed and specified in the thesis.

Furthermore, I confirm that this thesis has not yet been submitted as part of another examination process neither in identical nor in similar form.

Würzburg, January 2014 _____

6.6 Eidesstattliche Erklärung

Hiermit erkläre ich an Eides statt, die Dissertation „Studien zur Signaltransduktion und Regulierung von Rezeptoren in Thrombozyten und T-Zellen genetisch veränderter Mäuse“ eigenständig, d.h. insbesondere selbständig und ohne Hilfe eines kommerziellen Promotionsberaters, angefertigt und keine anderen als die von mir angegebenen Quellen und Hilfsmittel verwendet zu haben.

Ich erkläre außerdem, dass die Dissertation weder in gleicher noch in ähnlicher Form bereits in einem anderen Prüfungsverfahren vorgelegen hat.

Würzburg, Januar 2014 _____